THE UNIVERSITY *of* EDINBURGH

Characterisation of a mouse model of chronic cerebral hypoperfusion and its application to investigating the impact of hypoperfusion on the development of Alzheimer's disease

Robin Bruce Coltman BSc (Hons)

Doctor of Philosophy
The University of Edinburgh
2011

Table of Contents

Acknowledgements

I would like to begin by thanking my supervisors, Dr Karen Horsburgh and Dr Jill Fowler for their continued guidance and support over the last three and a half years. I would also like to thank Prof Jim McCulloch for always being available and willing to offer advice when requested. Additionally I would like to extend my thanks to the other academic and technical staff at the University of Edinburgh who have helped with this project.

During my Ph.D. I have been very fortunate to have met and worked with some wonderful people within the Horsburgh and McCulloch groups. It would be impossible to list all of these people here; however, certain individuals deserve a special mention. Firstly Dr Aisling Spain who has been my partner in Ph.D. studentship, secondly Dr Philip Holland was always willing to help and single handedly proof read the majority of my thesis and finally Darren Downing for offering moral support in the form of beer when required.

As well as the above I would like to thank my family; Mum, Dad, David, Kirstin and the wee ones and also all my wonderful friends who have kept me sane during what has been a particularly challenging time. Especially the guys I train with and also Steve Farquhar and Jonathan Gregson. I would also like to thank my wife Jill whose strength and determination have been a real source of inspiration.

Whilst the majority of the work described within this thesis was conducted by the author for clarity, I would also like to thank the following people for their various contributions as outlined below.

Dr. Karen Horsburgh: For all surgeries with the exception of those described in chapter 3 and for analysis of dMBP sections as described in chapter 4 and appendix A1

Dr. Cath Gliddon (Post Doc): For surgeries described in chapter 3.

Mrs. Fiona Scott (Histology Lab Manager) and Mr. Tommy Dingwall (Histology Technician): For assistance with cutting and immunostaining (MAG and APP) of sections described in chapter 3 (specifically from the 7, 14 and 28 day cohorts) and also assistance with immunostaining of sections from cohorts 2 and 3 (MAG, dMBP, APP and Iba-1) as described in chapter 4. Additionally for assistance with cutting and staining of sections described in chapter 5 (0.18mm coil cohort: MAG, Iba-1; 0.16mm coil cohort: MAG, Iba-1) and also the immunostaining of sections from aged animals as described in chapter 6 (MAG and Iba-1).

Dr. Aisling Spain (PhD Student at time of conducting experiments): For assistance with running the spatial reference memory watermaze task and radial arm maze task described in chapter 4 and also for running the trials to criterion task described in the same chapter.

Miss. Jess Smith (Technician): For running the trials to criterion task.

Miss Yanina Tsenkina (PhD Student): For assistance with the radial arm maze task and for running the trials to criterion task. Also for assistance with analysis of sections from cohort 3 as described in chapter 4.

Declaration

I declare that this thesis comprises my own original work and has not been submitted previously for any degree. The work comprising this thesis was carried out by myself, except where acknowledged in the text. All sources of data and information have been specifically referenced.

Robin Coltman

Table of Figures

Table of tables

Abstract

The integrity of brain white matter is vital for the interneuronal signalling between distinct brain regions required for normal cognitive function. White matter integrity is compromised with ageing and could contribute to age-related cognitive decline. Chronic cerebral hypoperfusion is thought to underlie the development of white matter pathology and cognitive changes, often seen in the elderly. Additionally, the development of regional hypoperfusion and white matter damage are thought to be early events in Alzheimer's disease (AD) pathogenesis. This thesis set out to test the hypothesis that chronic cerebral hypoperfusion underlies the development of white matter pathology and cognitive decline and also that chronic cerebral hypoperfusion causes the development of Aβ pathology in AD.

The first aim was to investigate the impact of hypoperfusion on the development of white matter damage and different aspects of cognition in a mouse model of chronic cerebral hypoperfusion. Two studies were undertaken to address this. The first study examined the temporal development of pathology following hypoperfusion induced by bilateral carotid artery stenosis (BCAS) using microcoils Hypoperfusion was induced in wild type (WT) mice and the pathological changes examined at one week, two weeks, one month and two months. Hypoperfused animals developed a diffuse and widespread white matter pathology, present from one week, which occurred predominantly in the myelin component of white matter; this was accompanied by minimal axonal damage. A second study examined the impact of hypoperfusion on different aspects of spatial memory and further investigated pathological changes in the model at one and two months. Behavioural testing revealed a significant impairment in spatial working memory but not episodic

memory or spatial reference memory in hypoperfused animals. In the same mice, pathological assessment indicated that there was a significant increase in levels of myelin damage and elevated levels of microglial activation as compared to shams. These results demonstrate that modest reductions in cerebral blood flow are sufficient to cause the development of white matter damage and the development of cognitive deficits.

The second aim was to investigate the impact of hypoperfusion on the development of white matter and amyloid pathology in a mouse model (3xTg-AD) of AD. To address this, using 2 different sizes of microcoils (0.18mm and 0.16mm internal diameter) BCAS of varying severities was induced in 3xTg-AD mice and white matter and Aβ pathology were assessed at one month. Circle of Willis (CoW) architecture was also compared between WT and 3xTg-AD mice. Overall white matter pathology was not exacerbated in experimental 3xTg-AD mice with BCAS induced by 0.18mm coils. However with a greater level of stenosis (0.16mm coil) ischaemic damage to neuronal perikarya was present in most experimental animals. In addition to ischaemic damage, localised areas of severe white matter pathology were also observed in conjunction with subtle changes to white matter Aβ levels. Hypoperfusion did not impact on the development of intraneuronal Aβ pathology, other than in the presence of ischaemic damage when levels were reduced. Comparison of CoW architecture between WT and 3xTg-AD mice revealed strain specific differences in the presence and morphology of the posterior communicating artery which may explain the lack of pathology in 3xTg-AD mice as compared to WT following BCAS induced using 0.18mm dia. microcoils.

The third aim was to investigate whether white matter protein composition changed with age and also whether ageing conferred increased vulnerability to hypoperfusion. To address this, white matter protein levels were compared between young (3-4 months) and old (12-13 months) 3xTg-AD mice. White matter pathology was compared between sham and hypoperfused animals in the aged cohort. Levels of myelin basic protein and 2', 3'-cyclic nucleotide 3'-phosphodiesterase were found to be significantly increased whilst levels of myelin associated glycoprotein were significantly reduced with ageing. These results suggest that changes in myelin protein composition may contribute to the development of age related white matter pathology. White matter pathology was not exacerbated in aged hypoperfused animals following one month of hypoperfusion as compared to shams.

The results presented within the thesis demonstrate that chronic cerebral hypoperfusion precipitates the development of selective white matter damage and impacts on cognition. Also it has been shown that where hypoperfusion is severe enough to cause ischaemic damage to neuronal perikarya and localised areas of severe white matter pathology, alterations in white matter Aβ levels can occur. Hypoperfusion does not impact on APP processing or on intraneuronal levels of APP or Aβ, other than in the presence of ischaemic damage to neuronal perikarya, when levels are reduced. These findings highlight the importance of early intervention strategies in the treatment of vascular risk factors which can lead to hypoperfusion and the development of white matter damage and a decline in cognitive function in later life. These findings also suggest that repair or prevention of white matter damage may be an appropriate strategy for the attenuation of cognitive decline

following onset of hypoperfusion. This thesis also highlights some of the limitations of animal models of human disease.

List of abbreviations

2VO	2 vessel occlusion
Aβ	β amyloid protein
AD	Alzheimer's disease
ANOVA	analysis of variance
SEM	standard error of the mean
APOE4	apolipoprotein E 4
APP	amyloid precursor protein
BACE-1	β amyloid cleavage enzyme 1
BBB	blood brain barrier
BCAS	bilateral carotid artery stenosis
BCCAO	bilateral common carotid artery occlusion
CAA	cerebral amyloid angiopathy
CBF	cerebral blood flow
CC	corpus callosum
CNPase	2' 3' cyclic nucleotide 3' phosphodiesterase
CNS	central nervous system
CT	computed tomography
dMBP	degraded myelin basic protein
EC	external capsule
EM	electron microscopy
FH	hippocampal fimbria
fMRI	functional magnetic resonance imaging

FTDP17	fronto temporal dementia with parkinsonism linked to chromosome 17
GSK3-β	glycogen synthase kinase 3β
H&E	haematoxylin and eosin
IC	internal capsule
kDa	kilo Dalton
L-MAG	large myelin associated glycoprotein
LRP1	low density lipoprotein receptor related protein
LTP	long term potentiation
MAG	myelin associated glycoprotein
MAP	microtubule associated protein
MBP	myelin basic protein
MCI	mild cognitive impairment
MEOX2	mesenchyme homeobox 2
MRI	magnetic resonance imaging
NCAM	neural cell adhesion molecule
OEF	oxygen extraction fraction
OT	optic tract
PBS	phosphate buffered saline
PcomA	posterior communicating artery
PET	positron emission tomography
PLP	proteolipid protein
PS1	presenilin 1
PS2	presenilin 2

PVDF	polyvinylidene fluoride
ROD	relative optical density
sAPPα	soluble extracellular APP domain
SDS-PAGE	sodium decyl polyacrylamide gel electrophoresis
S-MAG	small myelin associated glycoprotein
SOD	super oxide dismutase
SPECT	single photon emission computed tomography
SHRSP	stroke prone spontaneously hypertensive rat
SRM	spatial reference memory
St	striatum
SWM	spatial working memory
TTC	trials to criterion

Chapter 1: Introduction

The term chronic cerebral hypoperfusion, is used to describe a subtle, chronic reduction in cerebral blood flow (CBF), which in humans, is thought to occur due to a loss of vascular integrity (Iadecola, 2010; Gorelick et al., 2011). Unlike in stroke, where CBF reduction is acute and often fatal, these reductions have been shown to develop over prolonged periods in line with normal ageing (Leenders et al., 1990). The findings of several studies e.g. (Breteler et al., 1994; Wakita et al., 1994; Shibata et al., 2004; Fernando et al., 2006; Farkas et al., 2007) conducted in both human and animal cohorts suggest that chronic cerebral hypoperfusion impacts detrimentally on the integrity of brain white matter, which is critical for normal cognitive function. The presence of white matter damage is a common feature in the brains of elderly individuals and is thought to be linked to the development of age related cognitive decline.

Hypoperfusion has also been shown to be one of the earliest features of Alzheimer's disease (AD), occurring in temporo parietal regions, in some cases, up to decades prior to onset of clinical AD symptoms. Whilst a considerable body of evidence exists which demonstrates links between hypoperfusion, white matter damage and cognitive decline, it is impossible to define in the human brain the underlying mechanisms involved due to the presence of multiple confounding factors e.g. hypertension, diabetes, and arteriosclerosis.

The overarching aim of this thesis is to investigate the links between chronic cerebral hypoperfusion, the development of white matter pathology and how this may impact on cognition. The impact of hypoperfusion on amyloid and the influence of ageing will also be investigated. Central to the aims of the thesis is the

development and characterisation of a mouse model of chronic cerebral hypoperfusion.

1.1 White matter

White matter is found ubiquitously throughout the central nervous system (CNS) of all vertebrates. In humans (Fig 1.1a), brain white matter volume accounts for over half of total brain volume, this is a far greater fraction than is seen in other animals (Fields, 2008) e.g. the mouse, where brain white matter volume accounts for approximately only 25% of total brain volume. Despite this, the functional role of white matter has been over looked by researchers until only relatively recently.

When white matter was first described by Virchow in 1846 it was assumed to be some form of connective tissue, a belief which endured for almost a century until the pathologists Ramon y Cajal and Rio Hortega characterised the three major cell types of which white matter is comprised. Namely oligodendrocytes, astrocytes and microglia. As well as these cellular components, white matter is also comprised of blood vessels and axons which are the physical connection between nerve cells. Axons extend from neuronal cell bodies situated within grey matter regions and facilitate the flow of electrical information over long distances as cells communicate with one another.

1.1.1 *Components of white matter*

In order to understand the functional role of white matter it is necessary to describe its vascular network and cellular components; oligodendrocytes, astrocytes and microglia (Fig. 1.1b).

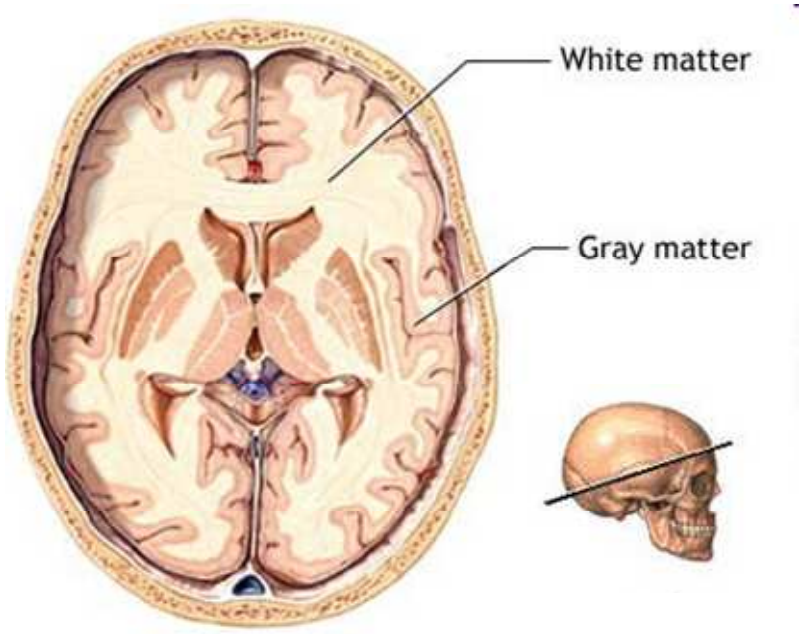

Figure 1.1a Location of white and grey matter in the brain
Schematic of a horizontal section of a human brain showing location of grey and white matter. (Image from American Accreditation HealthCare Commission (www.urac.org))

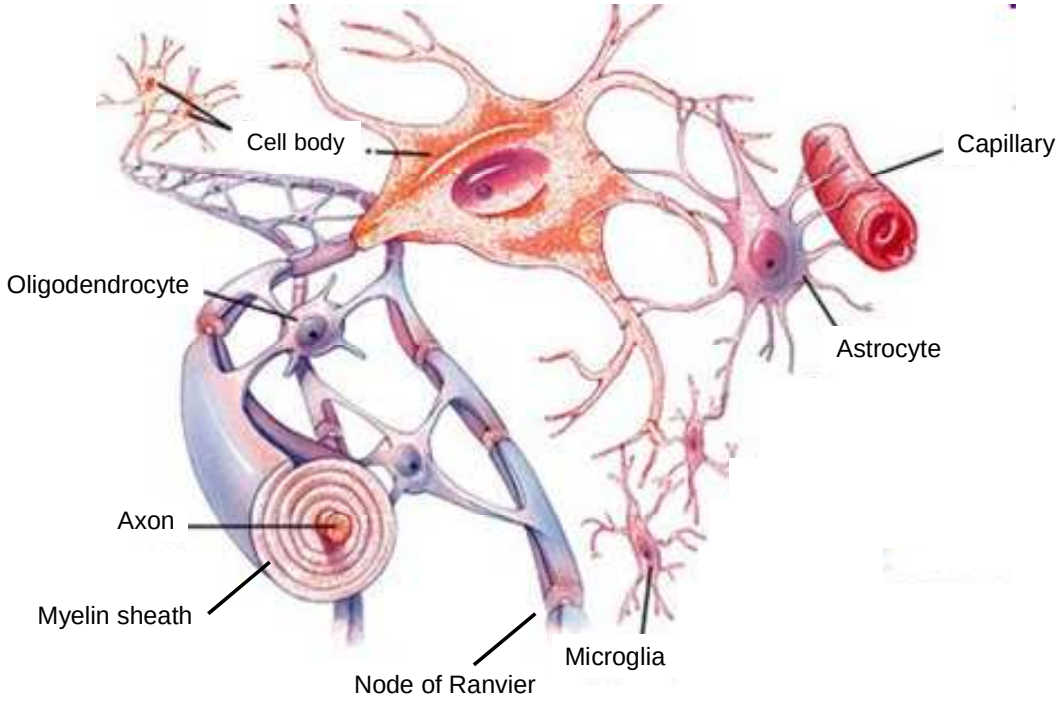

Figure 1.1b Components of white and grey matter
Components of grey matter (cell bodies) and white matter (oligodendrocytes, astroglia, microglia and axons). Capillaries comprise the cerebrovascular network which delivers essential nutrients to the brain. (Image adapted from The McGraw-Hill Company inc. (www.mcgraw-hill.co.uk))

1.1.1.1 *Oligodendrocytes*

The most abundant cell type found in white matter, and arguably the most functionally significant is the oligodendrocyte. Oligodendrocytes are the cells which produce myelin, a fatty, whitish substance comprised of lipids and proteins (70% lipid/ 30% protein (Quarles, 2006*)* which gives the white matter its colour. In the CNS oligodendrocytes extend processes composed of myelin which make contact with and ensheath neighbouring axons, wrapping around them, forming an insulating coating which increases the conduction velocity of nerve impulses, or axon potentials, by up to 100 times as compared to unmyelinated axons (Fields, 2008). An appropriate analogy is to imagine the axons as the copper wire in a household electrical cable whilst the myelin is the insulating plastic coating. The three main advantages conferred by myelin to the CNS, are high speed conduction of nerve impulses, fidelity of transfer signalling between distinct brain regions (often over long distances) and space economy (Baumann and Pham-Dinh, 2001).

During the process of myelination, each oligodendrocyte may extend processes to as many as 40 different axons, such that on the same axon adjacent myelin segments originate from different oligodendrocytes (Peters, 1991). These segments of myelin are referred to as internodes and are separated by short unmyelinated regions called 'The Nodes of Ranvier'. Internodes are between 100-1700μm in length (depending upon species/ location) whilst the length of Nodes of Ranvier is approximately 1μm (Edgar and Nave, 2009). Voltage gated sodium channels are concentrated in the axonal membrane at the Nodes of Ranvier, thus the insulating effect of myelin facilitates saltatory conduction of action potentials along the axon as the current 'leaps' from one node to the next (Fig 1.1b).

Oligodendrocytes may be morphologically divided into four different subtypes based upon the thickness of their myelin sheath. This is related to the calibre of the axon they ensheath. Type I cells typically myelinate between 15-30 small diameter axons, type II and III cells myelinate larger intermediate diameter axons whilst type IV cells form long, thick myelin sheaths around only 1-3 large diameter axons (Butt et al., 1995). This heterogeneity is important as, in order to achieve maximum conduction velocity the thickness of the myelin sheath must be proportional to the diameter of the axon around which it is wrapped. This optimal ratio, termed the g ratio (axon diameter/ total fibre diameter) has been calculated as 0.65 (Fields, 2008; Franklin and ffrench-Constant, 2008).

1.1.1.2 *Astrocytes*

Astrocytes are the second most abundant cell type found in white matter. There are three distinct types of astrocytes; fibrous, protoplasmic and radial. Astrocytes in white matter are mainly the fibrous subtype (Miller and Raff, 1984). They are a functionally diverse cell type with contributing roles in white matter structure, synapse maintenance, blood brain barrier function, extracellular ion concentration homeostasis, intercellular signalling and injury repair. Astrocytes also provide trophic support to the myelin sheath and play a role in initiating myelination (Franklin and ffrench-Constant, 2008).

1.1.1.3 *Microglia*

Microglia are the main form of immune defence in the CNS. In the normal healthy brain they are present in what is described as their ‘resting’ state which is characterised by a small cell body in conjunction with short outwards extending

processes. However, in response to CNS injury, onset of ischaemia or the presence of inflammatory stimuli, they quickly adopt their activated phenotype which is associated with cell proliferation and migration to the site of injury, as well as phagocytosis of dead and dying cells. Activation also results in the release of inflammatory mediators which recruit more microglia to the site of injury and also immuno modulatory cells from the blood stream (Garden and Möller, 2006). Once the activating stimulus begins to diminish, microglia also play a role in the down regulation of the inflammatory response. An increased level of microglial activation is a common feature of normal ageing (Von Bernhardi et al., 2010) and also many neurodegenerative diseases, where they act to phagocytose abnormal accumulations of pathological proteins. The best documented case of this is in Alzheimer's disease (Rogers et al., 2002; Perry et al., 2010). In addition to neurodegenerative disease, upregulated microglial activation is also commonly observed in the brains of individuals at risk of developing vascular disorders (Von Bernhardi et al., 2010) and also following vascular insults, such as stroke (Danton and Dietrich, 2003).

1.1.1.4 *Blood vessels*

In addition to the cellular components outlined above, white matter also contains blood vessels which comprise the vascular network delivering oxygen and glucose required for normal cellular function. Blood supply to the deep sub cortical white matter is facilitated through penetrating arterioles which stem from the pial network on the surface of the brain. Penetrating arteries branch off at right angles from the subarachnoid vessels and run down through the cortex into the white matter (Van Den Bergh et al., 1968). These arteries do not furcate but instead, give off

short branches (distributing vessels) which supply discrete areas of the white matter (metabolic units) (Rowbotham and Little, 1965).

1.1.2 *The protein architecture of myelin*

The insulating properties of the myelin sheath are largely due to its unique lipid: protein ratio. Myelin is exceptionally lipid rich and for this reason has very low water content (~40% as compared to ~70% in grey matter). The specific glycolipid and protein constituents of myelin are formed by the oligodendrocyte.

The majority of the proteins which comprise the myelin sheath are specific to oligodendrocytes (Campagnoni and Macklin, 1988). In the CNS the major myelin proteins which constitute ~80% of its protein content are myelin basic protein (MBP) and proteolipid protein (PLP). Other protein constituents include the Wolfgram family of proteins of which 2',3'- Cyclic Nucleotide 3'- Phosphodiesterase (CNPase) is a member and also the glycoproteins which include the myelin associated glycoprotein (MAG).

1.1.2.1 *Myelin Basic Protein (MBP)*

MBP is not one, but a family of proteins. There are several isoforms which are differentially expressed in both the immature and mature oligodendrocyte. In the adult human the four major isoforms are 21.5, 20.2, 18.5 and 17.2kDa and in the mouse they are 21.5, 18.5, 17 and 14kDa (Campagnoni and Macklin, 1988). These isoforms are readily separated using SDS-PAGE gel electrophoresis (see chapter 2). The most abundant isoforms in humans are the 18.5 and 17.2kDa isoforms whilst in the mouse the most abundant isoforms are the 18.5 and 14kDa isoforms (Staugaitis et al., 1990). The MBP gene is comprised of 7 exons. Isoforms containing exon 2

(20.2 and 21.5kDa in the human and 17 and 21.5kDa in the mouse) have been identified as being expressed earlier during development and also in chronic lesions in MS where their expression correlates with the onset of remyelination (Capello et al., 1997). Exon 2 containing isoforms are distributed diffusely throughout the cytoplasm and have been shown to be translocated to cell nuclei via active transport. Their distribution, taken together with their expression profile has led to the conclusion that these isoforms play a regulatory role in the myelination process (Pedraza et al., 1997). Expression of the more abundant non-exon 2 containing isoforms occurs later in development and their cellular location is confined to the plasma membrane where they play a role in myelin compaction (Roach et al., 1985). Deficiency in MBP has been shown to cause myelin disruption (Privat et al., 1979).

1.1.2.2 *2',3'- Cyclic Nucleotide 3'- Phosphodiesterase (CNPase)*

CNPase is the third most abundant protein in CNS myelin constituting ~4% of total myelin protein composition (Kurihara and Tsukada, 1967). CNPase consists of 2 different isoforms which may be visualised using SDS-PAGE gel electrophoresis. They are named CNP1 and CNP2 and are 48-55kDa (species dependent). In the mouse they are 46kDa and 48kDa respectively. The role of CNPase lies in the hydrolysation of 2'3'-cyclic nucleotides into their 2' derivative however the relevance of CNPase to myelin is unclear as the presence of 2'3'-cyclic nucleotides has never been demonstrated in oligodendrocytes (Vogel and Thompson, 1988; Hinman et al., 2008).

The cellular location of CNPase has been shown to be within the cytoplasm of non compacted myelin and also the paranodal loops which are located at the edge of the myelin internode at the nodes of Ranvier (Trapp et al., 1988). In light of the

lack of CNPase substrates present in myelin a role for CNPase has been proposed in a lipid raft –mediated signalling cascade which regulates interactions between myelin and axonal cytoskeletal components (Hinman et al., 2008). This is based on evidence from studies which have shown that a large proportion of CNPase is associated with lipid rafts in the plasma membrane (Kim and Pfeiffer, 1999). CNPase also meets the criteria for classification as a microtubule associated protein (MAP) (Bifulco et al., 1993). Deficiency, and also CNPase over expression, has been shown to cause abnormalities in the myelin sheath which are detectable at the ultrastructural level (Gravel et al., 1996; Rasband et al., 2005).

1.1.2.3 *Myelin associated glycoprotein (MAG)*

MAG is a 100kDa transmembrane glycoprotein which is found localised periaxonally. As a protein constituent of myelin, it is relatively minor, comprising only 1% of total myelin in the CNS (Quarles et al., 1973). There are two distinct MAG isoforms both of which have similar homology to members of the neural cell adhesion molecule (NCAM) family. The isoforms are identical to one another, other than differences within their cytoplasmic domains (Salzer et al., 1987). Prior to post translational modification, the isoforms are 72kDa and 67kDa large MAG (L-MAG) and small MAG (S-MAG) respectively. These isoforms have a distinct chronological pattern of expression during development, however, exist in approximately equimolar concentrations in the adult CNS. Each isoform is thought to have a functionally discrete role in the development and maintenance of the myelin sheath. L-MAG is thought to play a role in axon/ glia or glia/ glia signal transduction and adhesion whilst S-MAG is involved in myelin maintenance and

stabilisation of paranodal loops (Erb et al., 2006). MAG is also known to play a role in inhibition of neurite outgrowth during myelination (McKerracher et al., 1994).

Studies investigating the impact of ischaemia on white matter have identified MAG as one of the most vulnerable proteins (Aboul-Enein et al., 2003). Studies utilising MAG null mice have demonstrated that MAG deficiency leads to the development of myelin sheath abnormalities in later life and also a 'dying back oligodendrogliopathy' of the myelin sheath (Lassmann et al., 1997).

1.1.3 *White matter and cognition*

The person credited with first describing white matter changes associated with cognitive decline is Swiss psychiatrist and neurologist Otto Binswanger. At autopsy, Binswanger described a marked atrophy of the cerebral white matter (amongst other pathological changes) in a syphilitic patient who had displayed a marked deterioration in cognitive ability and motor function prior to his death (Blass et al., 1991). The advent of sophisticated neuroimaging techniques such as computed tomography (CT) and various magnetic resonance imaging (MRI) scanning techniques has provided further evidence which shows a clear correlation between loss of white matter integrity and the development of detrimental changes in cognition (Rosenberg et al., 1979; Breteler et al., 1994; Deary, 2003; Bucur et al., 2008).

White matter integrity is critical for normal brain function. The insulating properties of myelin result in saltatory conduction which greatly increases the speed of nerve impulses along the axon. This ability to increase the speed of information and also the ability to integrate this information as it flows between distinct brain regions is the underlying feature of higher cognitive function (Bartzokis, 2004).

Furthermore, increased conduction velocity also allows the temporal coding of information in the form of high frequency bursts of signalling between cells. This means that even modest damage to the myelin sheath can lead to slower conduction speed and a disruption in inter-cellular signalling, essentially leading to a disconnection of brain regions (Peters and Sethares, 2002).

As well as a decline in normal cognitive function a decline in white matter integrity has been recognised as a key feature in many neurological and psychiatric disorders e.g. dyslexia, post-traumatic stress disorder, multiple sclerosis and Alzheimer's disease to name a few (Fields, 2008). Furthermore, polymorphisms in several of the genes encoding myelin proteins have been linked to the development of mental illnesses such as schizophrenia (Hakak et al., 2001) and major depression (Tkachev et al., 2003).

1.1.4 *The impact of ageing on white matter integrity*

In the absence of neurological disease the greatest risk factor which has been linked to a loss of myelin integrity and the development of cognitive deficits is ageing. Myelination in the human brain occurs in a heterochronological pattern (Bartzokis, 2004). At birth myelin is only found in a few brain regions. Myelination occurs in developmental spurts in a posterior to anterior pattern with axons in the prefrontal cortical areas and the temporal and parietal lobes myelinating last (as late as the 5^{th} decade) (Bartzokis, 2004). Studies utilising various methods have shown that it is myelinated fibres within these later myelinating regions which are lost first with ageing (Marner et al., 2003).

Some of the most compelling evidence linking the development of age-related cognitive deficits and a loss of white matter integrity comes from large, long-

term epidemiological studies (e.g. The Rotterdam Study, The Honolulu-Asia Ageing and The Lothian Birth Cohort 1936). Studies such as these have utilised neuroimaging to investigate how white matter changes with age in large human cohorts. Their findings indicate that the development of white matter lesions, which are visible as hyperintensities on MRI scans (Fig 1.2), are a common feature of the normal ageing process and are present in the brains of upwards of 50% of individuals over the age of 65 (Enzinger et al., 2006). They have also shown that the number of these hyperintensities correlates with levels of cognitive ability in aged individuals (Deary et al., 2006; Bucur et al., 2008; Kennedy and Raz, 2009).

Further evidence which supports these findings comes from stereological studies conducted in aged human brains (Tang et al., 1997; Pakkenberg et al., 2003) and in the brains of aged non-human primates (O'Donnell et al., 1999; Peters, 2002). For example, results published by Tang et. al. (1997) indicate that the total volume of white matter is reduced in young (mean age 37.4 +/-14.8 years) as compared to old (mean age 74+/-11 years) subjects. Additionally the total calculated end to end length of myelinated fibres was found to be reduced (86,000km versus 114,000km) in old as compared to young individuals. This was attributed to a loss of small myelinated fibres. MRI data from studies performed on humans (Guttmann et al., 1998) and non-human primates (Lai et. al. 1995) support these findings. A loss of white matter integrity in older individuals, as demonstrated using MRI has also been associated with impaired performance on behavioural tasks (O'Sullivan et al., 2001; Deary, 2003). Electron microscopy (EM) studies have confirmed that, at the ultrastructural level, abnormalities of the myelin sheath are a common feature in brain tissue from aged humans and non human primates and that the frequency of these abnormalities increases with age (Peters, 2002, 2009).

Whilst it is unclear what pathological mechanisms underlie a loss of white matter integrity and the development of white matter damage with ageing, a large body of evidence strongly implicates chronic cerebral hypoperfusion as a causative factor.

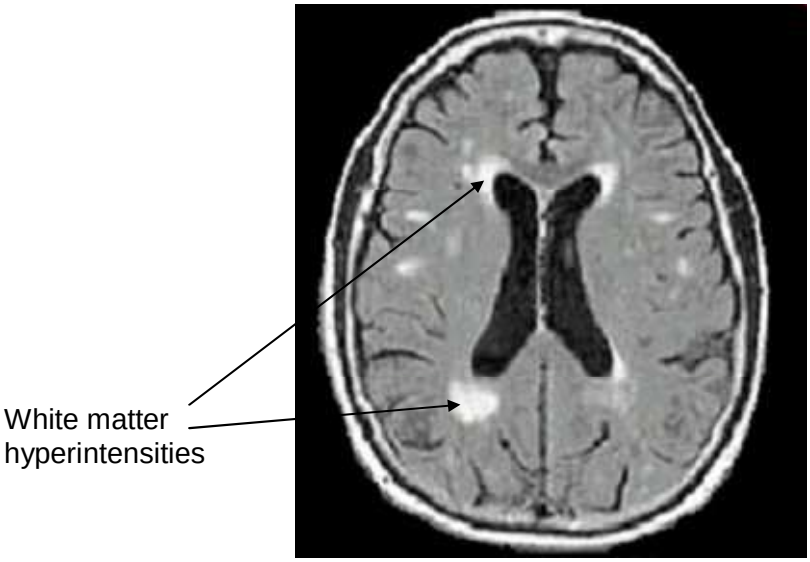

Figure 1.2 CT scan of a human brain

Image of a CT scan of a human brain displaying evidence of white matter hyperintensities. (Image courtesy of Centre for Human Genetic Research J. Philip Kistler Stroke Research Centre, Dept. of Neurology, Massachusettes General Hospital (http://www.strokegenomics.org))

1.2 Chronic cerebral hypoperfusion

1.2.1 *Cerebral blood flow and its regulation*

The brain is critically dependent on a steady uninterrupted blood supply for normal function. In higher mammals blood supply to the brain is facilitated by the internal carotid arteries which supply the forebrain and the basilar artery which supplies the hind brain. Each of these arteries feeds into an anatomical structure named the Circle of Willis (Fig. 1.3). The Circle of Willis is vital to maintaining CBF uniformity throughout the brain. The circular structure of the Circle of Willis means that if an artery becomes occluded then the distal arteries which it supplies, may receive blood from another artery, this is termed collateral circulation (Liebeskind, 2003). Put simply, an example of collateral circulation would be a situation where blood supply to the forebrain is reduced, say due to the presence of atherosclerotic plaques in the internal carotid arteries, which is then compensated for via recruitment of blood flow from the basilar artery. The Circle of Willis is complete in most mammals, one notable exception being the gerbil (discussed below).

To highlight how crucial uninterrupted CBF actually is, it is worth considering the ratio of tissue weight in the CNS to the volume of oxygen/glucose use compared to the rest of the body (table 1.1). However, unlike the peripheral organs (e.g. lungs, heart, liver kidneys), the brain has no glucose or oxygen reserves, meaning that any interruption or reduction in CBF may result in disastrous and potentially fatal consequences; an acute example of this being stroke.

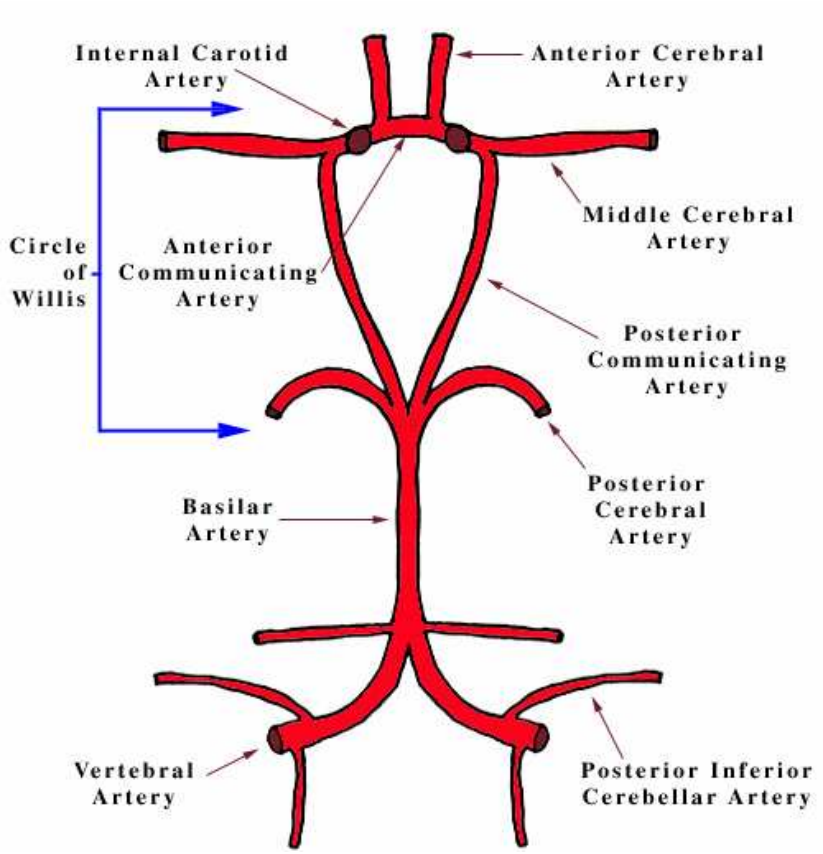

Figure 1.3 Circle of Willis anatomy

Schematic drawing of Circle of Willis anatomy. Blood is supplied to the forebrain via the internal carotid artery and to the hind brain by the basilar artery. Because these two distinct supplies are linked (blue arrow) via the posterior communicating artery any reduction in flow through one may be compensated for by the other. (Image taken from http://vetsci.wordpress.com)

Table 1.1 Oxygen/ glucose use of the CNS
(Edvinson, et. al (1993)

The Central Nervous System	
Accounts for	• *2-3% of body weight*
Requires	• *15% of cardiac output* • *20% oxygen* • *25% glucose*

Average CBF in humans is 50ml/ 100g of brain tissue/ min. (Brain, 1993). CBF is regulated (under normal physiological conditions) by the brain's metabolic needs due to neuronal activity i.e. as a region becomes functionally active, its demand for oxygen and glucose will increase. In order to meet this increased demand CBF must also increase. This is termed flow-metabolism coupling, or, functional hyperaemia. Functional hyperaemia is achieved via vasodilatory responses of the arterioles e.g. if metabolic demand increases then arterioles will dilate, cerebral blood volume will increase and metabolic demand will be met (Edvznsson, 1993).

Uninterrupted CBF is maintained via a combination of cerebral perfusion pressure and vascular resistance. In other words, in order to maintain a constant CBF, the cerebrovasculature must compensate for fluctuations in perfusion pressure via vasodilatory responses e.g. as perfusion pressure falls then vascular resistance must also fall (via vessel dilation) this leads to an increase in cerebral blood volume and therefore steady state CBF. Under normal physiological conditions this is facilitated by a mechanism which is dependent upon myogenic, neurogenic, endothelial derived, metabolic and chemical/ hormonal factors (Farkas and Luiten,

2001) known as autoregulation. Normally, autoregulation is able to maintain a constant CBF provided that blood pressure remains within the range of 60-160mmHg.

Autoregulation and the ability to compensate for transient changes in cerebral perfusion pressure are due to what is termed the vascular reserve. Once this reserve is used up i.e. when arterioles are fully dilated and cerebral blood volume has reached its maximal point, if metabolic demand increases or perfusion pressure drops, then autoregulation fails, rendering the brain vulnerable to ischaemia. Under these conditions, the brain enters a phase known as misery perfusion, also termed oligaemia, or, cerebral hypoperfusion, where it attempts to extract more oxygen from the blood (Brain, 1993). Normally the brain extracts 40% oxygen from the blood (Leenders et al., 1990); this figure is termed the oxygen extraction fraction (OEF). Misery perfusion is synonymous with an increased OEF as measured using positron emission tomography (PET) scanning (Gibbs et al., 1984). Eventually the OEF reaches its limit and CBF is no longer able to meet the brains metabolic demands. This is defined as ischaemia (Derdeyn et al., 2002).

In addition to failure of autoregulation, chronic cerebral hypoperfusion may occur as a result of changes in blood flow dynamics. For example the development of local areas of microturbulent flow in the microvasculature, as a result of vascular alterations associated with either ageing or a vascular risk factor such as atherosclerosis, can alter detrimentally the transport of nutrients across the blood brain barrier (BBB) (Farkas and Luiten, 2001). This may lead to the development of microenvironments throughout the vasculature where cerebral metabolism is impaired. Blood viscosity is a second rheological factor which may impact negatively on cerebral metabolism. Haematocrit value (Harrison, 1989) and

erythrocyte aggregation (Schmid-SchÃ¶nbein, 1983) have been identified as two features which impact on blood viscosity. In particular, haematocrit value has been shown to increase in conjunction with carotid artery occlusion, leading to increased blood viscosity and in turn lower CBF (Harrison, 1989). Furthermore, studies in both humans (Thomas et al., 1977) and animals (Lin et al., 1995) have shown that a lower haematocrit value correlates with reduced blood viscosity and improved CBF.

Following the development of chronic cerebral hypoperfusion, it is the brain regions where CBF is lowest which are rendered most at risk (de Reuck, 1971; Pantoni and Garcia, 1997).

Chronic cerebral hypoperfusion is most often observed in the elderly, where CBF, cerebral blood volume and the cerebral metabolic rate of oxygen has been shown to reduce by approximately 0.5% per year (Leenders et al., 1990) in conjunction with age related changes to cerebrovasculature, in particular the microvasculature (Farkas and Luiten, 2001). These changes are detrimental to vascular integrity and include increased arteriolar tortuosity, fibrohyalinosis, vascular wall thickening and arteriosclerosis (often as a result of hypertension) (Farkas et al., 2006). Chronic cerebral hypoperfusion may also occur as a secondary condition linked to a primary disease state, for example heart failure.

1.2.2 *The impact of chronic cerebral hypoperfusion on white matter integrity*

White matter has been shown to be particularly vulnerable to reductions in cerebral blood flow (Pantoni et al., 1996), with large scale epidemiological studies highlighting the link between vascular disorders and risk factors for cerebrovascular disease, reduced CBF and the development of white matter damage. This has been achieved through the application of neuroimaging technology such as CT and MRI

scanning in conjunction with *post-mortem* studies (Breteler et al., 1994; van Dijk et al., 2004). This approach has confirmed that hyperintensities on scans correlate with areas of white matter damage (characterised histologically by demyelination, loss of oligodendrocytes and vacuolation (Brun and Englund, 1986; Brown and Thore, 2011) and increased expression of hypoxia related proteins. Further support for the role of hypoperfusion in the development of white matter damage comes from studies utilising animal models (see below) where components of white matter have been shown to be lost prior to the development of ischaemic damage to neuronal perikarya (Wakita et al., 1994; Shibata et al., 2004).

1.2.3 *Vascular architecture of the cerebral white matter*

The likely reason for the heightened sensitivity of white matter to CBF reduction lies in its vascular architecture. It is the pattern of this vascular network which is thought to leave white matter particularly vulnerable to reductions in CBF (Pantoni and Garcia, 1997). As outlined in section 1.1.1.4, the penetrating arterioles in the deep sub-cortical white matter do not arborise but instead give off short branches which create metabolic units. Around these metabolic units border zones are created, in other words, because each metabolic unit is fed by only one branch from one penetrating artery, this means there are no other surrounding vessels which may compensate for a reduction in nutrient delivery should CBF in the branch servicing that metabolic unit be reduced (Rowbotham and Little, 1965). Essentially, as far as blood supply is concerned, white matter is the end of the line.

1.2.4 *Animal models of hypoperfusion*

A wide range of conditions may lead to the onset of chronic cerebral hypoperfusion in humans and these often occur concomitantly and have overlapping

pathologies. For this reason, the most appropriate way to examine the pathological impact of hypoperfusion on brain white matter and how this in turn affects cognition, in isolation, is through the utilisation of animal models.

The first animal model of cerebrovascular disease was the stroke prone spontaneously hypertensive rat (SHRSP) (Okamoto, 1973). These rats develop abnormally high blood pressure by age 4-5 months and neurological deficits at approximately 6 months and their average life span is greatly reduced (approximately 12 months). Pathological studies conducted on this strain have revealed that fibrinoid necrosis occurs in intracerebral arterial walls in conjunction with rarefaction of the white matter and the neuropil (Ogata et al., 1982). Since the SHRSP, a wide range of cerebrovascular disease models, including models of cerebral hypoperfusion have been developed using several different species including rodent, cat, dog and non-human primate. Of these, the most consistently used has been rodent (rat, gerbil and mouse), due to economic and ethical acceptability issues (Sarti et al., 2002).

The most often used and well characterised animal model of hypoperfusion is the bilateral common carotid artery occlusion (BCCAO) or 2 vessel occlusion (2VO) model in the rat. Following ligation of the bilateral common carotid arteries an immediate reduction in CBF (to as low as 25% of baseline levels) is seen in the forebrain (Farkas and Luiten, 2007). Over a period of months CBF in experimental animals returns to normal, initially due to collateral stabilisation (Liebeskind, 2003) which is then followed by a period of vascular remodelling (Choy et al., 2006). This is accompanied by progressive neuronal cell loss, particularly in the striatum and CA1 region of the hippocampus and also moderate to severe white matter rarefaction and gliosis. White matter regions most affected are the corpus callosum and the

optic tract (Wakita et al., 1994). Cognitive testing in this model has revealed a number of cognitive deficits which become more pronounced over time; including visiospatial learning, fear conditioning and other aspects of non-spatial memory (Farkas et al., 2007). Whilst it is clear that white matter damage occurs following 2VO in the rat, it has not been possible to conclude that white matter damage alone is responsible for the observed changes in cognition. This is due to the fact that ischaemic damage to neuronal perikarya is often observed and secondly because the most vulnerable region to CBF reduction is the optic tract which raises questions as to the validity of results from tests which rely on visual cues.

The gerbil has also been used in an attempt investigate the impact of hypoperfusion on white matter. In this model, coiled clips termed microcoils, were used to induce hypoperfusion. The main advantage of using microcoils to induce hypoperfusion is that they cause a stenosis of the vessel to which they are attached as opposed to a complete ligation as seen in the 2VO rat model, thus causing a more modest CBF reduction (Kato and Kogure, 1990). A further advantage of microcoils is that the pitch and diameter of the coils may be modulated to permit more or less blood to flow along the artery allowing conditions of varying severity to be modelled. A disadvantage of the gerbil as a species for this type of study is its inability to tolerate CBF reductions due to species variability in its cerebrovascular architecture. Unlike other rodents, the gerbil has an incomplete Circle of Willis owing to the absence of a posterior communicating artery; consequently there is no collateral circulation available to compensate for sudden CBF reductions, therefore damage caused by bilateral carotid artery stenosis (BCAS) is severe (global ischaemia) (Hattori et al., 1992).

More recently microcoils have been used to develop a mouse model of hypoperfusion (Shibata et al., 2004) using C57Bl/6J mice. The C57Bl/6J strain is considered particularly suited to studies investigating cerebral hypoperfusion because of its cerebrovascular architecture, where collateral flow within the Circle of Willis is compromised due to underdevelopment of the posterior communicating artery (Kitagawa et al., 1998; Shibata et al., 2004). It is also the most commonly used inbred strain of laboratory mouse when generating transgenic mouse models of human disease. Optimisation of this model was conducted such that the diameter of microcoils used was sufficient to induce wide spread damage exclusively to white matter. Using 0.18mm diameter coils, modest damage was apparent in hypoperfused mice 14 days following induction of hypoperfusion; this had become severe by the 30 day time point. This occurred in conjunction with initial reductions in CBF, measured at two hours to 67.3 ± 18.5% baseline levels, a considerably more modest reduction than that seen in the 2VO model. CBF was still significantly lower than baseline at day 14 and was approximately 10-15% below baseline at 30 days (Fig 1.4) (Shibata et al., 2004; Shibata et al., 2007). Behavioural testing in this model revealed a deficit in working memory 8 weeks following hypoperfusion in the absence of any changes in spatial reference memory. No other behavioural deficits were observed (Shibata et.al. 2007).

The mouse model of hypoperfusion described above represents an excellent tool with which to study hypoperfusion induced white matter pathology in detail and also how hypoperfusion may impact on cognition. It may also be applied to transgenic mouse strains in an effort to understand how chronic hypoperfusion may influence the pathogenesis of disease.

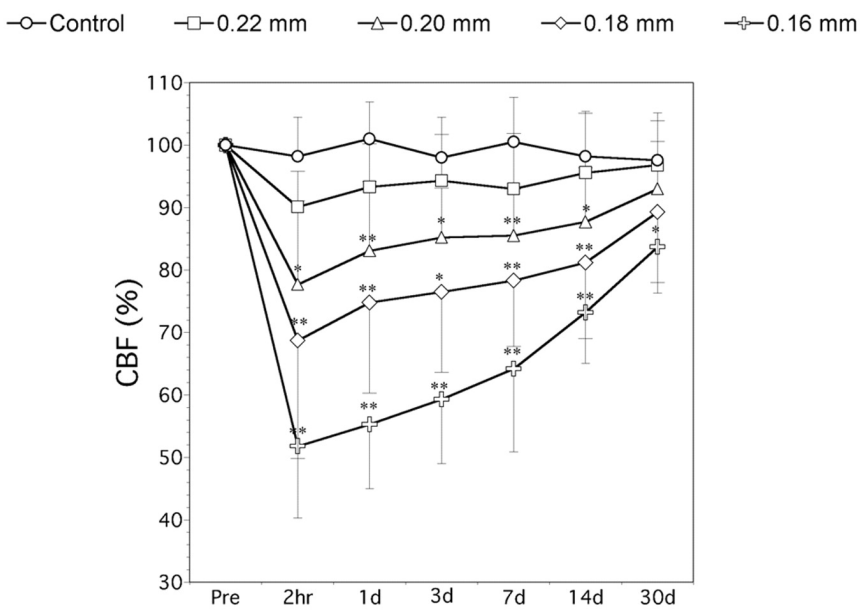

Figure 1.4 CBF reductions in the mouse following microcoil application
Using a 0.18mm microcoil (diamond symbol) CBF reductions are initially reduced to ~70% of baseline and recover to ~90% of baseline by 30 days. Data shown published by Shibata et al. 2004.

1.3 Alzheimer's disease

Alzheimer's disease (AD) is a neurodegenerative disease and is the most frequently diagnosed form of dementia in the elderly in the developed world. It is estimated that currently 35 million people are affected by AD worldwide (Querfurth and LaFerla, 2010) and that this figure is set to double every 20 years as average life expectancy increases (Qiu, 2007). In the UK it is estimated that there are currently over 750,000 dementia sufferers and that by 2025 this number will have risen to over 2 million. The current financial cost of dementia to the UK is over £20 billion annually (Jonsson and Wimo, 2009). The single most important risk factor for the development of AD is age (Bartzokis, 2004); people over the age of 65 are much more likely to display clinical symptoms. The incidence of the disease increases with age, doubling every 5 years after age 65, until by age 85, more than one in three individuals receive a clinical diagnosis (Querfurth and LaFerla, 2010).

1.3.1 *The clinical and pathological characterisation of AD*

Clinically, AD is characterised in its earliest stages by the development of deficits in episodic memory, followed by a noticeable deterioration in other elements of cognition. Onset of these symptoms may occur up to 2-3 years prior to AD diagnosis (Fox et al., 1998). Mean survival time is 6-8 years following diagnosis. The latter stages of the disease are characterised by behavioural changes, manifest as depression and aggressive behaviour and eventually a loss of language and motor skills and finally death (Hope et al., 1997). A point of note is that AD itself does not cause death. IIn AD patients death occurs most often due to an underlying or co-existing condition such as an opportunistic infection e.g. pneumonia or due to choking, or due to malnutrition and/ or dehydration (Castellani et. al. 2010;

AD diagnosis may only be confirmed *post-mortem* although regional hypoperfusion on brain imaging scans has been identified as a strong predictor of disease development (Luckhaus et al., 2008) (discussed later). Pathologically AD is characterised by the abnormal accumulation of Aβ protein sequestered within extracellular amyloid plaques and the presence of intraneuronal neurofibrillary tangles comprised of hyperphosphorylated tau protein (Selkoe and Podlisny, 2002). These plaques and tangles are predominantly found in regions that play important roles in learning and memory formation such as the hippocampus, frontal cortex, amygdala and entorhinal cortex. Other key features of the disease include widespread neuronal cell loss and atrophy in affected brain regions, inflammation and oxidative stress (Castellani et al., 2010).

1.3.2 *Generation of Aβ*

Amyloid precursor protein (APP) is a transmembrane protein with three major isoforms (695kDa, 751kDa and 770kDa) (Turner et al., 2003) which are expressed throughout the body in different tissue specific, isoform ratios (Selkoe et al., 1988). Within the brain the most abundant APP isoform is 695kDa. The functional role of APP is unknown however various studies have implicated a role for APP in axonal transport, cell adhesion, cholesterol metabolism, gene transcription, synaptic plasticity and synaptogenesis (Turner et al., 2003; Gralle and Ferreira, 2007).

Generation of Aβ is achieved via sequential cleavage of full length APP (Glenner and Wong, 1984a, 1984b) by a series of enzymes or enzyme complexes (α–, β– and γ– secretases). Cleavage of APP by α–secretase results in non-pathological, or, non-amyloidogenic processing of APP as cleavage of APP occurs

within the region containing β– amyloid. Two fragments are generated, a C-terminal fragment 83 amino acids long (C83) and a large N-terminal fragment; sAPPα. sAPPα is secreted extracellularly whilst C83 undergoes further cleavage by γ–secretase to produce a short fragment termed p3. Pathological or, amyloidogenic processing of APP occurs when the APP parent protein is cleaved by β–secretase (BACE-1) in the first instance, generating fragments sAPPβ and the c-terminal fragment C99. C99 undergoes further cleavage by γ–secretase resulting in the production of the 4kDa Aβ protein (Fig. 1.5) (LaFerla et al., 2007a). Under normal physiological conditions it is estimated that the majority of Aβ protein produced is 40 amino acids ($A\beta_{1–40}$) in length whilst approximately 10% is 42 residues in length ($A\beta_{1–42}$). $A\beta_{1–42}$ is more hydrophobic and more prone to aggregation and fibril (insoluble species) formation and is also the principal form found in extracellular plaques whilst the vascular deposits of Aβ seen in cerebral amyloid angiopathy (CAA) are comprised mainly of $A\beta_{1–40}$ (Jarrett et al., 1993). Changes in the APP processing pathway, leading to increased Aβ production and also changes in the $A\beta_{1–40}$: $A\beta_{1–42}$ ratio, are known to underlie the development of Aβ pathology in AD (for review see (Pimplikar, 2009).

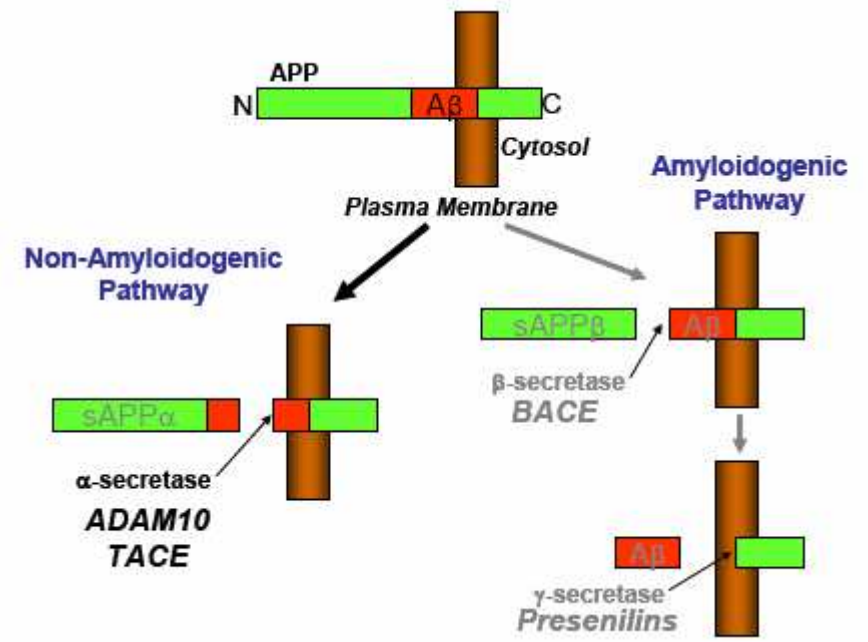

Figure 1.5 The APP processing pathway

APP is cleaved via either the non-amyloidogenic pathway (left) or the Aβ forming, amyloidogenic pathway (right). (Image from http://www.fbs.leeds.ac.uk/staff/Hooper_N/alzheimers.htm)

1.3.3 Assembly states of Aβ protein and the amyloid cascade hypothesis

The biggest advance in the field of AD research in nearly 100 years was the identification of Aβ as the major protein component of amyloid plaques and the discovery that it was the proteolytically derived product of APP cleavage (Glenner and Wong, 1984a, 1984b). The subsequent cloning of the APP gene (Kang et al., 1987) led to the identification of several mutations linked to the development of familial AD (Levy et al., 1990; Goate et al., 1991; St George-Hyslop, 2000) and the formulation of the amyloid cascade hypothesis (Hardy and Allsop, 1991; Selkoe, 1991) which states that 'accumulation of Aβ in the brain is the primary influence driving AD pathogenesis' and that 'the rest of the disease process, including formation of neurofibrillary tangles containing tau protein, results from an imbalance between Aβ production and Aβ clearance' (Hardy and Selkoe, 2002). Significant weight was lent to the amyloid cascade hypothesis with the discovery of mutations in the genes Presenelin 1 (PS1) (Sherrington et al., 1995) and Presenelin 2 (PS2) (Rogaev et al., 1995; Levy-Lahad et al., 1995a; Levy-Lahad et al., 1995b) which form part of the γ-secretase complex in the APP processing pathway. These mutations have been demonstrated to cause increased production and oligomerisation of $A\beta_{1-42}$ (Scheuner et al., 1996; Xia et al., 1997). A major criticism of the amyloid cascade hypothesis however, is that plaque load is known not to correlate well with severity of dementia (Giannakopoulos et al., 2003). This has led to various studies examining the neurotoxicity of different Aβ species.

Following amyloidogenic cleavage of APP, the Aβ protein is prone to aggregation and may exist in a number of different assembly states. These include monomers, oligomers, protofibrils and fibrils (Fig. 1.6). Monomers, oligomers and

protofibrils are soluble species whilst fibrils, which aggregate to form extracellular plaques, are insoluble (Walsh et al., 2002).

Studies examining the toxicity of the various species of Aβ indicate that it is the intermediate species which are most harmful, particularly oligomers (Lesne et al., 2006; Shankar et al., 2008). These are thought to cause synaptic dysfunction, which may be the cause of early cognitive deficits observed in both animal models and humans (Oddo et al., 2003b; LaFerla et al., 2007b). It has also been suggested that oligomeric Aβ causes neuronal cell death (Cizas et al., 2010); the method by which this occurs however, is unknown. Several mechanisms of Aβ toxicity have been proposed. These include Aβ induced mitochondrial dysfunction, production of reactive oxygen species and oxidative stress, impairment of synaptic transmission, membrane disruption, upregulation of the inflammatory response, calcium dysregulation and also direct activation of the apoptotic pathway (Cotman and Anderson, 1995; Griffin et al., 1995; Huang et al., 1998; Billings et al., 2005; Caspersen et al., 2005; Lau et al., 2006).

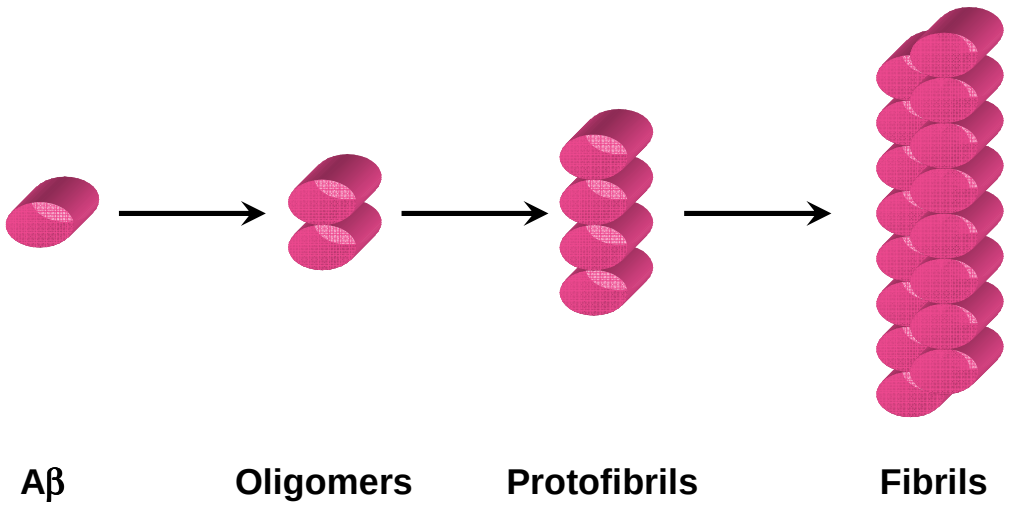

Figure 1.6 Assembly states of Aβ
Studies examining Aβ have found that it aggregates readily to form a number of soluble and insoluble species, monomers, oligomers (toxic), protofibrils and fibrils. (Image based on Laferla (2007))

1.3.4 Tau protein and neurofibrillary tangle pathology in AD

Tau is a microtubule associated protein found within neurons of the CNS. Its primary role is the stabilisation of microtubules, this is achieved via differential isoform expression (tau has six isoforms which differ from one another in the number of tubulin binding repeats they contain and also the amino acid sequence of their N-terminal domain) and also tau phosphorylation (Ballatore et al., 2007). In AD, tau becomes hyperphosphorylated which causes its detachment from microtubules. Hyperphosphorylated tau is functionally inactive however it can cause the disassembly of microtubules; this is thought to occur due to its competing with tubulin for the binding of normal tau. This is because hyperphosphorylated tau acts as a nucleation centre to which normal tau binds, causing aggregation and the development of neurofibrillary tangles within neurons (Alonso et al., 2001).

Hyperphosphorylated tau has been shown to be neurotoxic and unlike extracellular plaque load, the number of neurofibrillary tangles present in AD brains has been shown to correlate with severity of cognitive decline observed in patients (Arriagada et al., 1992). Proposed mechanisms of tau toxicity in AD include disruption of axonal transport leading to synaptic dysfunction and ultimately neurodegeneration (Roy et al., 2005), or potentially, a toxic gain of function where the neurofibrillary tangles become large enough to pose a physical barrier to normal cellular functioning (Ballatore et al., 2007).

Results from studies conducted in animal models have shown that a relationship between Aβ and tau exists and that this is in agreement with the relationship predicted by the amyloid cascade hypothesis to some degree. Tau transgenic mice do not develop Aβ pathology however; introduction of $A\beta_{1-42}$ fibrils into the brains of tau overexpressing transgenic mice has been shown to cause a 5-

fold increase in levels of neurofibrillary tangles (Gotz et al., 2001). Also when tau transgenic mice (JNPL3) are crossed with APP overexpressing mice (Tg2576), their offspring have higher levels of neurofibrillary tangle pathology as compared to JNPL3/ JNPL3 mice (Lewis et al., 2001). The mechanism by which Aβ influences the development of neurofibrillary tangles is unknown, however several studies have shown that in the presence of Aβ, tau phosphorylation is modulated. This is thought to be either via the upregulation of tau kinases (e.g. GSK-3β or CDK-5) or the down regulation of protein phosphatases which regulate tau phosphorylation (e.g. PP2A) (Iqbal and Grundke-Iqbal, 2008) or, indirectly via upregulation of the inflammatory response (Metcalfe and Figueiredo-Pereira, 2010).

Much work has been conducted to characterise amyloid and tau pathology in AD and their impact on brain function. More recently however, the research focus within the AD field has shifted away from the characteristic disease pathology and more towards early events in the AD brain and what potentially may underlie these.

1.3.5 *Risk factors for the development of AD*

Despite a significant research effort, both clinical and basic, the underlying causes of AD remain unknown. Mutations in the three key genes outlined in section 1.3.3, namely Amyloid Precursor Protein (APP) and Presenilins 1 & 2 (PS1, PS2) have been identified as the cause of early onset AD, or familial AD as it is known (due to its heritability as an autosomal dominant condition), however, this form of the disease accounts for less than 1% of clinical diagnoses (Hardy, 2009). Several risk factors have been implicated in the development of late onset (also known as sporadic) AD.

For many years the only known major genetic risk factor for the development of late onset AD was to be a carrier of the APOE4 allele of the Apolipoprotein E gene (Strittmatter et al., 1993; Hardy, 2009). Carriers homozygous for the APOE4 allele have an increased risk of up to 30 times as compared to those not carrying the APOE4 allele of developing AD in later life. More recently however, a number of other genes have been identified which are thought to confer increased risk of developing sporadic AD. These include, but are not limited to, SORL1 (Rogaeva et al., 2007), A2M (Dodel et al., 2000), GSTO1 (Li et al., 2003), Clusterin (Lambert et al., 2009).

In addition to the aforementioned genes, several environmental and lifestyle risk factors have been linked via epidemiological studies with the development of AD in later life. These include traumatic brain injury (Lye and Shores, 2000) and severe cerebrovascular challenges such as stroke (Scheinberg, 1988). As well as stroke, numerous other factors which lead to a more subtle, long term reduction in cerebral perfusion are thought to contribute towards AD development. Many of these are associated with ageing and have a vascular component e.g. smoking, poor diet, lack of exercise, atherosclerosis, arteriosclerosis, hypertension, heart failure (for review see (de la Torre, 2004)). Furthermore, specific patterns of cerebral hypometabolism and hypoperfusion have been identified as being a reliable indicator as to whether an individual develops AD in later life and these may be detected decades prior to the onset of clinical symptoms (Matsuda, 2007).

1.3.6 *Hypoperfusion in Alzheimer's disease*

Regional cerebral hypoperfusion has been recognised as a feature of AD for some time. Initially there was some debate as to whether this was a contributing factor to disease development or as a result of disease related brain atrophy.

Early blood flow studies, conducted in AD patients, utilising the ^{133}Xe inhalation CT scanning method identified significant reductions in whole brain perfusion in AD patients as compared to healthy age matched controls and also disease specific reductions within the temporoparietal cortex (Prohovnik et al., 1988). These findings were recapitulated using more sophisticated and less invasive neuroimaging methods e.g. arterial spin labelling MRI and single photon emission CT (SPECT) scanning, which were also able to identify specific patterns of regional hypoperfusion which strongly indicated that AD development in later life was likely (Hirao et al., 2005; Matsuda, 2007). Many studies conducted to examine the correlation between regional hypoperfusion and degree of cognitive decline in AD patients, have shown that a strong proportional relationship exists (Farkas and Luiten, 2001).

Functional MRI (fMRI) studies have shown that task associated increases in CBF are delayed in patients with mild cognitive impairment (MCI) during performance of episodic memory tasks and that these delays become more prominent in AD patients (Rombouts et al., 2005). This is of particular importance as MCI is thought to be a transitional condition between normal health and the development of AD thus implying hypoperfusion and altered CBF regulation are early events in AD as opposed to a result of brain atrophy following disease progression.

Several hypotheses have been proposed to account for reductions in CBF during AD pathogenesis. These include observed atherosclerotic changes to vessels

within the Circle of Willis (Kalback, 2004), or, disease associated microvascular pathology e.g. arteriole and capillary atrophy, microvascular collagen deposition, the presence of endothelial cell abnormalities and damage, reduced microvascular density and altered basement membrane composition (Kalaria and Pax, 1995; Berzin et al., 2000; Farkas and Luiten, 2001; Grammas, 2002). CBF reductions in AD have also been attributed to a loss or dysfunction of cholinergic innervation (Bell et al., 2006). It is well established that a loss of cholinergic neurotransmission due to the loss or shrinkage of cholinergic neurons in the basal forebrain is an early event in AD pathogenesis. These neurons have been shown to project to the microvasculature of the frontoparietal cortex where they act to cause acetylcholine (ACh) mediated vessel dilation, thus their loss in AD has a pathophysiological impact on CBF (Farkas and Luiten, 2001).

A more recent study conducted by (Wu et al., 2005) has shown that in AD patients, endothelial expression of the MEOX2 gene is significantly lower than in age-matched healthy controls. MEOX2 has been identified as being important for vascular differentiation, further more it has also been shown to mediate expression of the LRP1 receptor which plays a prominent role in Aβ clearance (Tanzi et al., 2004). This has led researchers to hypothesise that its down regulation in AD may lead to aberrant angiogenesis and hence reductions in CBF as well as impaired Aβ clearance. A further cause of hypoperfusion in AD is the presence of CAA which is present in >80% of AD patients (Bell and Zlokovic, 2009). Imaging studies have shown that patients with CAA display significantly reduced levels of CBF in brain regions where pathology is present as compared to age matched controls (Chung et al., 2009).

Whilst much of the work discussed above refers to neuroimaging studies conducted in conjunction with *post-mortem* studies in humans, evidence has also been gathered from studies utilising ex-vivo and in-vivo animal models which supports a role for altered CBF in AD. Interestingly, this work has demonstrated that $A\beta_{1-40}$ in particular impacts detrimentally on neurovascular CBF regulation.

The first study implicating a role for Aβ in cerebrovascular dysfunction was conducted in 1996 (Thomas et al., 1996). In this study, conducted ex-vivo, it was shown that Aβ caused damage to vascular endothelial cells and that this impacted on vasoactivity. A number of in-vivo studies soon followed. In 1999 Iadecola et al. showed that endothelial vascular regulation was attenuated in APP transgenic mice (Iadecola et al., 1999) and in 2000, Niwa et al. showed that somatosensory induced functional hyperaemia was impaired in a transgenic mouse model of AD as compared to non transgenic controls and that this impairment correlated with total levels of brain Aβ (Niwa et al., 2000). They also produced a similar effect in wild type mice by addition of exogenous $A\beta_{1-40}$ to the cortex. In a separate study (Niwa et al., 2001) it was shown that addition of exogenous Aβ to the brains of wild type mice was sufficient to cause regional reductions in resting CBF. In all of these studies the Aβ induced CBF alterations were rescued by the superoxide scavenging enzyme superoxide dismutase (SOD) thus implicating a role for superoxide radicals and oxidative stress in AD related vascular alterations.

Higher levels of the vasoconstrictor endothelin-1 in the AD brain have also been suggested as a potential candidate underlying CBF reduction (Palmer et al., 2009; Palmer et al., 2010). It is well established that endothelin converting enzymes 1 and 2 (ECE-1, ECE-2), in addition to cleaving endothelin to produce endothelin-1

(ET-1), also degrade Aβ (Eckman et al., 2001). Higher levels of ET-1 have been shown to be present in the human AD brain and also in mice over-expressing mutant human APP. Furthermore in ECE-2 null mice, and in ECE-1 heterozygotes, levels of endogenous Aβ were found to be higher than in litter mate controls (Eckman et al., 2003). Preserved endothelial function has been demonstrated in the presence Aβ following administration of an ET-1 antagonist (Elesber et al., 2006) thus demonstrating a potential role for ET-1 in endothelial cell dysfunction in AD which may underlie CBF reductions associated with the early stages of the disease (Palmer et al., 2010).

In addition to the impact of Aβ on CBF regulation, other work utilising APP transgenic mice has shown that as well as regional reductions in brain metabolism APP transgenics are more susceptible to ischaemic damage (Zhang et al., 1997). More recently, through the use of both autoradiography (Niwa et al., 2002) and more sophisticated MRI techniques (Wu et al., 2004; Weidensteiner et al., 2009) regional alterations in CBF have been identified in various APP over-expressing transgenic animals. The fact that these alterations occur prior to overt CAA or amyloid plaque pathology in these models lends significant weight to the argument that altered CBF is an early rather than late event in AD pathogenesis.

1.3.7 *White matter integrity and Alzheimer's disease*

Given the large number of vascular risk factors linked to the development of AD and also the identification of hypoperfusion as an early feature in AD development, it could be argued that, it is of little surprise a prominent feature of the AD brain is the presence of white matter abnormalities (Brun and Englund, 1986; Bartzokis et al., 2003; Riekse et al., 2004). Increasingly, changes to brain white

matter are being recognised as an early event in AD (de la Monte, 1989) prior to the development of characteristic plaque and tangle pathology, this has been shown in humans (Stokin et al., 2005; deToledo-Morrell et al., 2007) and animal models (Wirths et al., 2007; Desai et al., 2009). Furthermore as many as 66% of AD brains exhibit evidence of white matter pathology *post-mortem* in addition to plaques and tangles (Roher et al., 2002).

Neuroimaging is being used with increasing frequency to detect early changes to brain white matter in AD. Many studies have been conducted examining individuals with MCI prior to AD conversion (DeCarli et al., 2001) and also in individuals exhibiting clinical symptoms of AD (Stout et al., 1996), where white matter abnormalities are found to be present with even greater frequency. A number of these studies have identified the splenium of the corpus callosum and the frontal and temporal lobes as being the initial areas where white matter damage is detected in AD (Duan et al., 2006; Naggara et al., 2006; Ukmar et al., 2008), and that this damage becomes more severe with disease progression (Duan et al., 2006; Di Paola et al., 2010).

Evidence from pathology studies has also been used to demonstrate that white matter changes are an early feature of AD. De la Monte (1989) reported that regional white matter shrinkage, in the absence of cortical pathology was a common feature observed in the pre clinical AD brain. In an earlier, more detailed study, Brun and Englund (1986) described pathological changes to white matter in AD. These were characterised by myelin loss, axonal degeneration and damage to oligodendrocytes and also activation of inflammatory cells, all in conjunction with microvascular pathology. Interestingly the authors hypothesised that this damage was due to hypoperfusion due to the fact that many of the subjects exhibited signs of

cardiovascular disease coupled with hypotension. Other white matter changes occurring in AD include abnormalities of the myelin sheath, detectable at the ultra structural level and also disruption of the axonal cytoskeleton and in turn axonal transport (Stokin et al., 2005; Wirths et al., 2006).

Why white matter pathology is exacerbated in AD is unknown, however, Aβ has been shown to be toxic to oligodendrocytes (Guela et al., 1998; Xu et al., 2001; Roth et al., 2005) and Aβ toxicity is known to be exacerbated with ageing (Guela et al., 1998). Interestingly oligodendrocytes *in-vitro* have recently been identified as a source of Aβ (Skaper et al., 2009). Several studies have hypothesised that Aβ toxicity is via the production of reactive oxygen species due to mitochondrial dysfunction which in turn leads to the activation of the sphingomyelinase-ceramide pathway and apoptosis (Lee et al., 2004; Hsu et al., 2010). Abnormally phosphorylated tau protein has also been shown to be neurotoxic. The hyperphosphorylation of tau is thought to cause destabilisation of the axonal cytoskeleton (Roy et al., 2005) which in turn may lead to disruption of axonal transport. However, whilst disruption of axonal transport in AD is known to occur early in the disease process, whether this is a cause or a consequence of the disease remains to be elucidated (Stolin et. al. 2005).

1.3.8 *Animal models of AD*

Numerous transgenic mouse models of AD have been created since the identification of mutations in three genes (APP, PS1 and PS2) which are linked to the development of familial AD. A large number of models now exist which recapitulate a range of AD related pathologies. Despite the fact that none of the models fully replicates the disease they have been extremely useful in determining

how Aβ and tau pathology develop and also how these pathologies interact and how they impact on normal brain function.

The most commonly utilised method by which transgenic mice are created is via pronuclear injection (Elder et al., 2010), where foreign DNA (transgene of interest) coupled to a promoter which drives expression is injected into a freshly fertilised embryo. The transgene is then integrated (randomly and often at multiple sites) into the mouse genome. This technique is efficient, ~80% of mice created in this manner are true transgenics (every cell has a copy of the transgene) however due to the random nature of transgene integration different founder mice display different levels of protein expression (Evans, 1994). Almost all transgenic mice created in this manner are hemizygous for the gene of interest; also because the promoters used to drive transgene expression are typically strong, the transgenic protein tends to be expressed at much higher levels than would be present physiologically (Elder et al., 2010).

The earliest successful transgenic models of AD were based on over expression of human APP transgenes containing mutations identified as underlying early onset AD e.g. the PDAPP (Games et al., 1995) and the Tg2576 (Hsiao et al., 1996) mouse strains. These mice develop extracellular plaque pathology, synaptic dysfunction and cognitive deficits in an age dependent manner. Around the same time transgenic mice over-expressing human PS1 genes containing AD related mutations were also created (Duff et al., 1996). Whilst endogenous $A\beta_{1-42}$ levels were increased in these PS1 transgenic animals, extracellular pathology was lacking, this has been attributed to the fact that endogenous mouse Aβ is less prone to aggregation than human Aβ (Jankowsky et al., 2007). However, when these mice

were crossed with plaque forming APP over-expressing animals, earlier and more extensive plaque formation occurred (Holcomb et al., 1998).

One of the major issues facing researchers attempting to model AD in mice has been that despite the evidence of overt Aβ pathology in many of the transgenic lines created, neurofibrillary tangle pathology is almost always absent. This has been overcome by the discovery of a mutation in the human tau gene (P301L) (Hutton et al., 1998) which underlies the development of another distinct type of dementia, known as frontotemporal dementia and parkinsonism linked to chromosome 17 (FTDP-17). Mice transgenic for human P301L tau readily develop neurofibrillary tangle pathology which correlates with levels of cognitive decline (Lewis et al., 2000).

The first transgenic line to successfully model both plaque and tangle pathology was created in 2001 by Lewis et al. (Lewis et al., 2001). This was achieved by crossing APP_{Swe} over-expressing APP Tg2576 mice with JNPL3 transgenic mice expressing mutant P301L tau. Shortly after this in 2003, Oddo et al derived a triple transgenic (3xTg-AD) mouse strain by utilising a novel co microinjection technique where two transgenes (APP_{Swe} and tau_{P301L}) were injected into single cell embryos from homozygous $PS1_{M146V}$ knockin mice (Oddo et al., 2003b). The resulting 3xTg-AD strain was suggested by many to be the most accurate mouse model of human AD as cognitive changes occur prior to the development of overt AD pathology and also the emergence of amyloid and tau pathology follow a similar temporal pattern to that seen in the human form of the disease.

In 3xTg-AD mice Oddo et al. initially reported that intraneuronal Aβ was present from 3-4 months of age in the cortex and by 6 months in the hippocampus,

this was followed by the development of extracellular cortical Aβ deposits in some animals from 6 months which became readily visible and also evident in the hippocampus by 12 months of age in all animals. Tau pathology was first apparent in the hippocampus at 12 months and progressed to cortical structures with age. Hyperphosphorylated forms of tau were evident in neurons from 12-15 months. This pathology was accompanied by deficits in synaptic dysfunction and long term potentiation (LTP) from six months onwards (Oddo et al., 2003b).

Other work utilising 3xTg-AD mice has shown that in addition to deficits in LTP and synaptic function these animals develop cognitive deficits in accordance with the emergence of intraneuronal (oligomeric) Aβ pathology; furthermore these cognitive changes are rescued by Aβ immunotherapy which causes a reduction in intraneuronal Aβ levels. Following this, re-emergence of intraneuronal Aβ pathology again leads to cognitive deficits (Billings et al., 2005). This finding was key in establishing a role in toxicity for oligomeric Aβ species. Another interesting finding from a separate study utilising immunotherapy in 3xTg-AD mice has shown that clearance of Aβ leads to a reduction in levels of early forming hyperphosphorylated tau aggregates thus providing further support for the amyloid cascade hypothesis (Oddo et al., 2004).

More recently, work employing the 3xTg-AD model has provided further evidence for white matter changes as an early event in the pathogenesis of AD. In animals where intraneuronal pathology but not plaque or tangle pathology was present regional reductions in white matter protein levels (MBP and CNPase) and alterations in the myelin sheath at the ultra structural level were observed in conjunction with a reduction in levels of oligodendrocyte markers (Desai et al., 2009;

Desai et al., 2010). In addition to the 3xTg-AD model, white matter damage has been identified as being present in other AD models. Wirths et al. (2006) reported the presence of progressive axonal damage in APP/PS1 transgenic mice whilst other groups have utilised diffusion tensor imaging to identify axonal and myelin damage in APP transgenic strains (Song et al., 2004; Sun et al., 2005).

Despite the identification of a number of vascular risk factors which underlie the development of both white matter damage and AD, and also the identification of reduced CBF and white matter damage in several AD models, few studies have been conducted utilising animal models to investigate how these may be linked to AD pathogenesis.

1.4 Aims of thesis

The creation of a mouse model of chronic cerebral hypoperfusion, which allows CBF to be modulated such that selective white matter damage may be induced, has provided a powerful tool which can be used to investigate how white matter damage impacts on cognition in the absence of other confounding factors. This model may also be utilised in 3xTg-AD mice to investigate how hypoperfusion impacts on the development of Aβ pathology. This thesis set out to test the hypothesis that chronic cerebral hypoperfusion underlies the development of white matter pathology and cognitive decline and additionally that chronic cerebral hypoperfusion causes the development of Aβ pathology in AD.

The specific aims of this thesis were-

1. To investigate the temporal evolution of white and grey matter pathology in a mouse model of chronic cerebral hypoperfusion.

2. To characterise in detail which components of white matter are selectively damaged following hypoperfusion and to investigate the impact of hypoperfusion induced white matter damage on different elements of cognition.
3. To investigate how varying severities of hypoperfusion may impact on the development of white matter and intraneuronal Aβ pathology in 3xTg-AD mice.
4. To investigate how ageing may impact on white matter protein composition and also how ageing may confer increased vulnerability of white matter to hypoperfusion in 3xTg-AD mice.

Chapter 2: Materials and Methods

2.1 Mice

All animals used in studies reported were housed in the animal housing unit within The Centre for Cognitive and Neural Systems (CCNS), University of Edinburgh. The unit was on a 12h light/dark cycle with a regulated environment (temperature, humidity). All mice were given access to food and water *ad libitum* upon arrival in the facility. All experiments were conducted under a project and personal licence issued by the UK Home Office under the Animals (Scientific Procedures) Act 1986.

2.1.1 *C57Bl/6J Mice*

C57Bl/6J male mice weighing 25-30g were purchased from Charles River UK.

2.1.2 *3xTg-AD Mice*

The 3xTg-AD mouse strain used in studies reported in this thesis was originally generated by Oddo et al. in 2003 (Oddo et al., 2003a). Briefly, single cell embryos were harvested from homozygous mutant $PS1_{M146V}$ knockin mice (PS1-KI). The PS1-KI mice were created on a C57/Bl6J/ SV-129 mixed background by exchanging a homologous exon from the mouse PS-1 gene with one which encoded an AD-linked PS-1 mutation (Guo et al 1999). Two human transgenes were comicroinjected into the embryos (human APP_{Swe} and human tau_{P301L}). See Fig 2.1.

Both transgenes were under transcriptional control of the mouse Thy1.2 regulatory element which drives transgene expression specifically within the CNS from early in post natal development through to adulthood (Caroni, 1997). Founder

lines harbouring all three transgenes were identified and back crossed to PS1-KI mice to maintain the M146V mutation. Subsequent analysis of transgene inheritance pattern showed that both the mutant human transgenes were inherited with 100% frequency suggesting that both had co-integrated at the same locus and would be consequently passed onto offspring as a pair at a single genetic locus (Oddo et al., 2003b).

Breeding pairs of 3xTg-AD mice were obtained via a collaboration with Frank LaFerla and a homozygous colony established and maintained. Transgene expression was initially determined via PCR genotyping. All 3xTg mice utilised in studies described in later chapters were male.

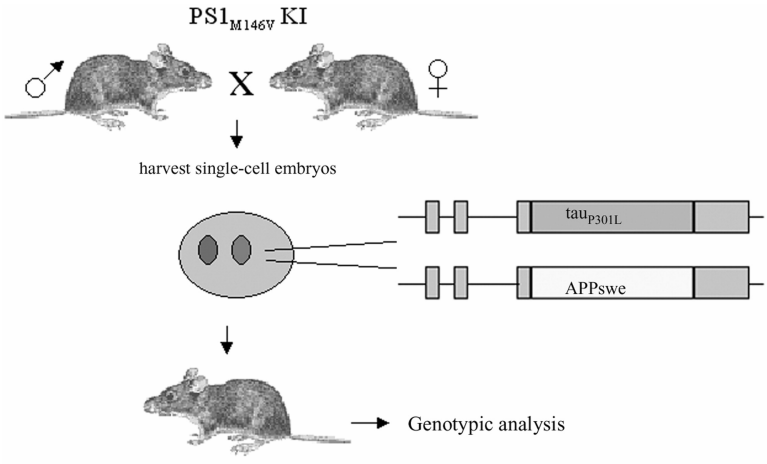

Figure 2.1 Generation of 3xTg-AD mice
3xTg-AD mice were generated via comicroinjection of transgenes into single cell embryos. (Image adapted from Oddo (2003)).

2.2 Surgery

2.2.1 *Induction of Hypoperfusion*

Hypoperfusion was induced via the placement of microcoils around the common carotid arteries of mice (Fig 2.2). 0.18mm and 0.16mm diameter microcoils, constructed from piano wire were obtained from the Sawane Spring Co., Japan. All surgery relating to studies reported in this thesis was performed by Dr Karen Horsburgh with the exception of the initial investigation into temporal pathological changes in response to hypoperfusion (Chapter 3) where surgery was performed by Dr Catherine Gliddon.

Surgery was performed as follows. Animals were anaesthetised with isoflurane and their common carotid arteries (CCA) exposed via midline cervical incision. Microcoils were applied to each CCA. A period of 30 mins was left between the insertion of each coil. Post surgery, animals were given soft food and closely monitored for the following 48hrs, and then twice daily for the following 5 days.

Any mice displaying a poor recovery from surgery were culled, notably, an ischaemic phenotype (spontaneous circling) which was often accompanied by a poor appetite and severe weight loss (greater than 20% pre surgical weight). Sham animals underwent an identical procedure except that microcoils were not applied to each CCA.

2.3 Behavioural testing

Prior to undergoing surgery all animals which were selected for behavioural testing were handled for 5 mins per day for 5 days in order to minimise stress caused by handling during experiments.

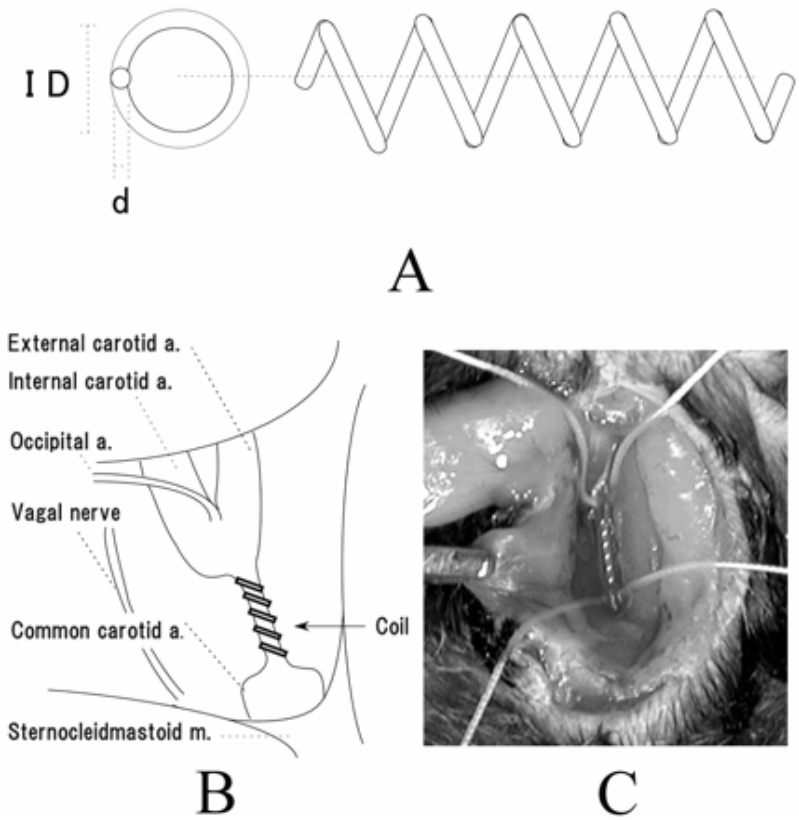

Figure 2.2 Induction of hypoperfusion

A. Schematic of microcoil (ID-internal diameter, d-wire diameter of 0.18 mm) B. Schematic of coil in place around common carotid artery below the carotid bifurcation C. Image of microcoil in situ, note sutures are placed at the proximal and distal end of the CCA and used to gently lift the artery to enable application of the coil. (Adapted from Shibata et al (2004)).

2.3.1 *Morris water maze*

All water maze testing was carried out in a 2m diameter fibre glass pool filled with water (Fig 2.3). Liquid latex was added to render the water opaque to prevent the use of pool features for navigation (e.g. outlet pipe). Water was maintained at a temperature of 25 ± 1°C. A camera fixed directly above the pool allowed monitoring of the animals' swimming behaviour (latency to platform, swim patterns) by a Water maze video tracking system (ActiMetrics Software, v 2.6, Willmet, IL, U.S.A.). 3D and 2D extramaze visual cues were placed around the room to allow spatial navigation.

2.3.1.1 *Cued version of the water maze*

In order to ensure animals were able to swim and that they did not exhibit an abnormal stress response, training was conducted on a cued version of the water maze task prior to animals undergoing surgery. Upon entering the pool animals were placed facing the wall and allowed to swim until finding the cued platform or until 90 secs had elapsed. Any animals unable to complete the task were excluded at this time. Following surgery, animals were allowed a period of 7 days to recover. Cued training on the water maze task was undertaken for a period of 4 days to ensure no visual or motor deficits had arisen as a result of surgery.

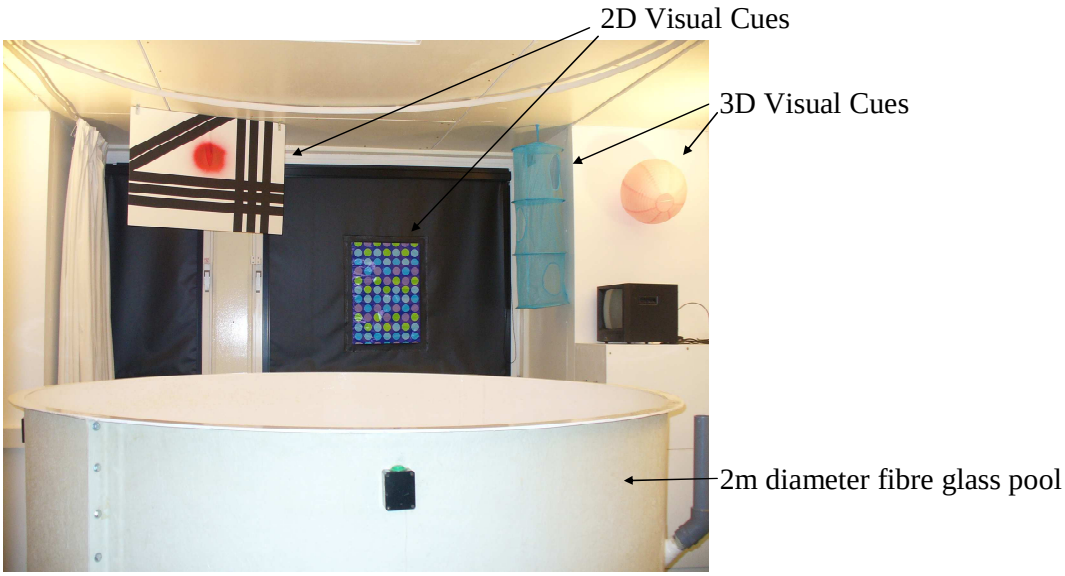

Figure 2.3 The Morris Watermaze
Image of water maze with 2D and 3D extramaze cues highlighted.

Each animal underwent 4 trials per day with a period of 20 mins between trials. To prevent the use of extramaze cues in finding the platform a white curtain was drawn around the pool, the platform (20cm diameter) was made visible by placement of a 20cm high cue at its location. The quadrant in which the platform was located was changed each day of training. For each trial the start position was changed (north, south, east or west) so that no start position was repeated in any one day.

2.3.1.2 *Spatial reference learning and memory testing*

Training in the spatial reference memory task was initiated 3 days after completion of the cued platform task. In this task the platform (13cm diameter) was submerged 1cm below the surface of the water and was not cued. Training lasted 5 days and 4 trials were undertaken per day with a period of 20 mins between each trial. As in the cued task starting positions were different for each trial however throughout the trial the location of the platform did not change for each animal. Platform locations and start positions were counter balanced across groups. In this task the use of extra maze cues was allowed.

2.3.1.3 *Serial spatial reference learning and memory testing*

A trials to criterion protocol was utilised to test serial spatial reference learning and memory, also termed episodic memory, as previously described (Chen et al., 2000). Testing commenced 3 days after the end of the cued water maze task. In this task animals were required to learn a series of hidden platform locations. Each animal was trained for up to eight trials per day (inter trial interval was 10 mins) up to a maximum of 32 trials (with the exception of the first trial where the maximum no. of trial allowed was 40), until a performance criterion of three

successive trials with an escape latency of less than 20s was reached. Once criterion or the maximum no. of trials was reached, training ended and probe tests were conducted to assess memory for the platform location at 10 mins and 3 hours as outlined in section 2.3.1.3. The following day training on a new platform location began. Animals were tested for a minimum of ten days or until 5 platform locations were learned. Counterbalancing of platform locations and start positions was employed across groups.

2.3.1.4 *Probe testing in the water maze*

Probe testing was conducted at 10 mins and 24 hours after the final trial of the spatial reference learning and memory task and at 10 mins and 3 hours following animals reaching criterion in the serial spatial learning and memory task. Probe tests were conducted to test spatial reference memory retention. During probe trials the platform was fully submerged at the bottom of the pool. Animals were allowed to search for the platform for a period of 60 secs, during which, time spent in each quadrant was recorded. After 60 secs the platform was made accessible at its former location in the preceding training period and animals were allowed a further 30 seconds in which to locate it, in order to preserve platform finding behaviour.

2.3.2 *Radial arm maze*

All radial arm maze testing was conducted in an 8 arm radial arm maze constructed of white plastic with 20cm high transparent Plexiglas walls (Stoelting Co. Europe, Dublin, Ireland), (Fig.2.4). The maze consisted of an octagonal centre platform (20cm in diameter) with arms (47cm long, 7cm wide) leading off and a plastic food well (3.5cm diameter, 2cm deep) situated at the distal end of each arm.

Gates leading to each arm in the maze were controlled by a remote computer using the Any-Maze software package (Stoelting Co. Europe, Dublin, Ireland). A camera fixed directly above the maze and connected to the remote computer allowed monitoring of the animals' behaviour (arm choices) within the maze and automatic control of gate opening/ closing based on animals' position. A remote operator also manually recorded arm choices. 3D and 2D extramaze visual cues were placed around the room to allow spatial navigation.

2.3.2.1 *Radial arm maze pretraining*

Animals were food deprived beginning four weeks after surgery to reduce their initial body weight by 10-15%, once this weight was reached feeding remained restricted until the end of testing in order to maintain this. In order to habituate animals to the maze, and the task, two days of pretraining were undertaken. On day 1, mice were placed on the central platform and allowed to explore the maze consuming food pellets (Bio-Serv, Frenchtown, NJ, U.S.A.) scattered throughout for a period of 5 mins. On day 2 each arm was baited with a single food pellet. Gates were used to control access to arms, only one arm was open at any one time; subsequent arms were opened only after the food pellet had been retrieved.

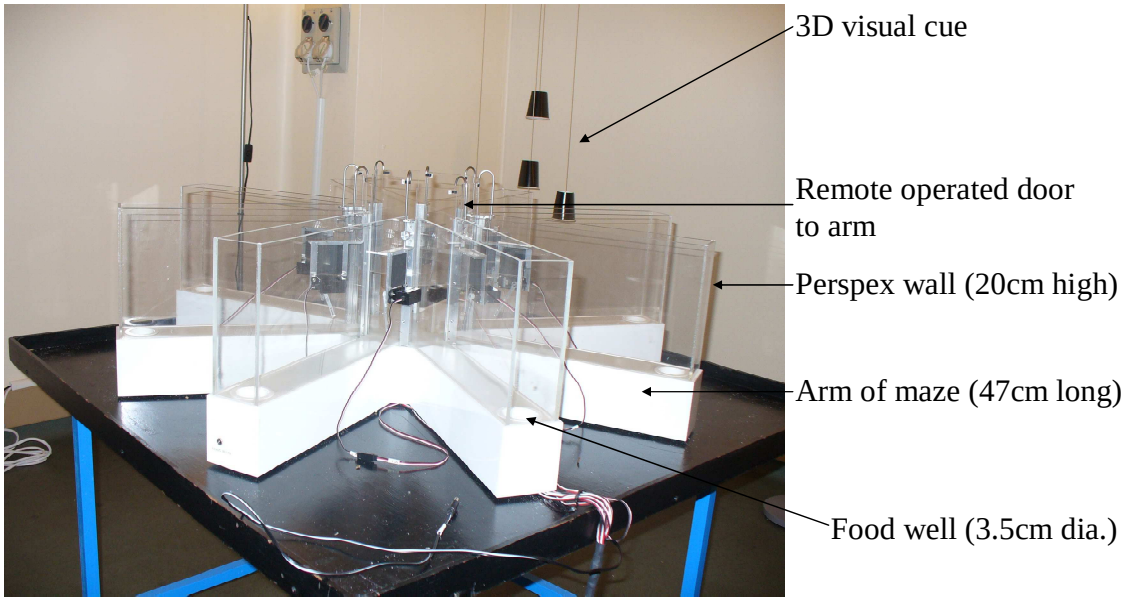

Figure 2.4 The 8 Arm radial arm maze
The maze was situated on a raised platform (1m from the floor)

2.3.2.2 *Spatial working memory testing in the radial arm maze*

Each animal undertook one trial per day for 20 days. Prior to starting the trial each arm of the maze was baited with one food pellet. At the start the trial animals were placed on the central platform and all gates were open allowing animals to make any arm choice. An arm choice was recorded when the animal had proceeded 5cm into an arm (as tracked by the Any-Maze software). Following entry into an arm, gates on the other 7 arms closed automatically. When an animal subsequently left the arm, the remaining door closed and the animal was restricted to the central platform for a period of 5 secs, following the 5 secs delay all gates opened and the animal was allowed to make another arm choice. Trials were halted immediately after the successful retrieval of all 8 pellets or after a period of 25 mins. had elapsed. The number of correct (novel) arm entries in the first eight visits, the total number of revisiting (working memory) errors and length of time to task completion were recorded for each trial.

2.4 Generation of tissue and tissue processing

2.4.1 *Perfusion fixation*

Mice were weighed and then deeply anaesthetised with 5% isoflurane in oxygen (30%). A midline incision was made and a sternotomy performed to expose the heart, 20ml of heparinised (0.9%) saline was perfused through the left ventricle and an incision was made in the right atria to allow blood to flow out. Following removal of blood, tissue fixation was achieved by perfusion of a further 20ml of 4% paraformaldehyde (PAM) (Sigma Aldrich Company, Gillingham, U.K.) in phosphate buffered solution (pH 7.4) through the vasculature. Stiffening of the extremities, forelimbs, hind limbs and tail, was taken as an indication that adequate perfusion had

been achieved. Subsequent to perfusion mice were decapitated and the brain left in the skull and post fixed in PAM for a period of 24 hours, after which brains were removed from skulls and immersed in PAM for a further 24 hours. Where hemi brains were taken for biochemical analysis, brains were immediately removed from skulls following saline perfusion and bisected along the longitudinal fissure. The right hemibrain was taken for immunohistochemistry and post fixed in PAM for a period of 48 hours and the left brain was dissected. The cerebellum and olfactory bulb were removed and the remaining portion divided coronally, into two equal parts, forebrain and hind brain. Brain portions were placed in 1.5ml Eppendorf tubes and snap frozen in liquid nitrogen immediately, before being transferred to a –80oC storage facility for long term storage until required.

2.4.2 *Paraffin processing and embedding*

Following fixation in PAM brains were coronally dissected into 3 x 3mm slices, striatal, hippocampal and hindbrain (Fig. 2.5) using a mouse brain matrix. Sliced brains/ hemi brains were placed into labelled plastic embedding cassettes and washed in running water for 30 minutes prior to being dehydrated through a series of alcohols and liquid paraffin (table 2.1). Following processing, each 3mm slice was embedded in fresh paraffin and left to set prior to cutting.

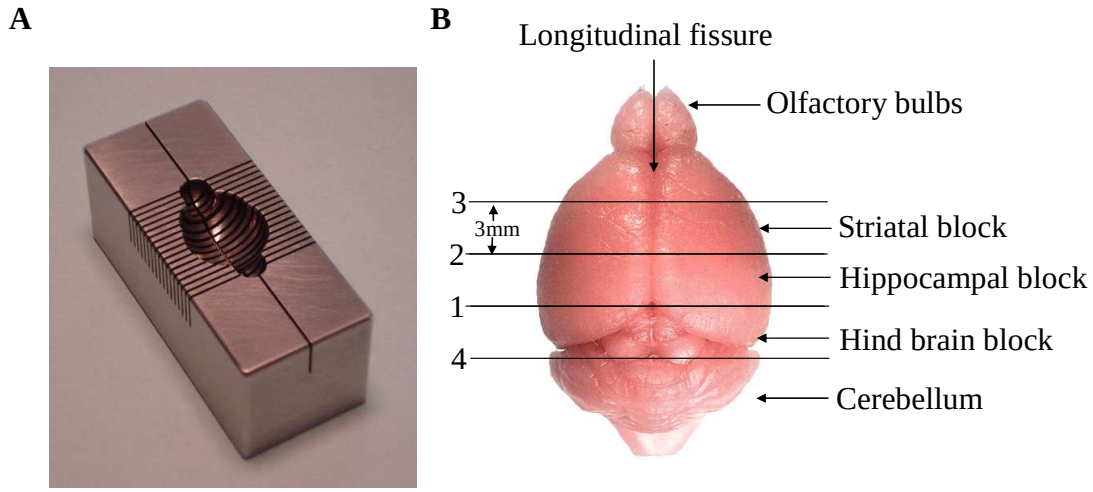

Figure 2.5 Brain dissection

A. Mouse brain matrix used for dissection of tissue, channels for coronal slicing are situated at 1mm intervals. Image provided courtesy of www.zivic-miller.com. B. Diagram illustrating dissection procedure. Numbers on the left indicate order of blade insertion. Where hemi brains were taken for biochemistry brains were bisected along the longitudinal fissure. Image adapted from (Airey et al., 2001).

Table 2.1 Tissue processing prior to paraffin embedding

Sequence of solutions brains were processed through prior to paraffin embedding.

Stage	Solution	Temperature	Time in Solution
1	Running water	~ 15^{o}C	30 mins
2	70% Ethanol	Room Temp.	30 mins.
3	70% Ethanol	Room Temp.	30 mins.
4	90% Ethanol	Room Temp.	30 mins.
5	90% Ethanol	Room Temp.	30 mins.
6	100% Ethanol	Room Temp.	30 mins.
7	100% Ethanol	Room Temp.	30 mins.
8	Xylene	Room Temp.	30 mins.
9	Xylene	Room Temp.	30 mins.
10	Liquid paraffin	65^{o}C	30 mins.
11	Liquid paraffin	65^{o}C	30 mins.
12	Liquid paraffin	65^{o}C	30 mins.
13	Liquid paraffin	65^{o}C	Overnight

2.4.3 *Cutting*

Serial sections (6μm) were cut from paraffin blocks at the level of the striatum and the hippocampus at the level of the lateral habenula on a microtome. Levels were defined as corresponding to 0.38mm and -1.70mm from bregma according to Franklin and Paxinos (1997). Sections were floated on a water bath maintained at 40^{o}C to remove any creases and then mounted on poly-l-lysine coated slides (WVR International, Lutterworth, U.K.). To ensure lateral and ventro-dorsal symmetry fresh cut sections were examined using a light microscope. Sections were dried on a hotplate (80^{o}C) and then stored in slide storage boxes until required.

2.5 Histology

Haematoxylin and eosin (H&E) staining was used to identify areas of ischaemic damage to neuronal perikarya. H&E was also used to assess quality of tissue fixation/ processing.

2.5.1 *Haematoxylin and Eosin staining*

Sections mounted on poly-l-lysine slides were heated in an oven maintained at 60^{o}C for 30 mins then de-waxed in xylene for 15 mins before being rehydrated through a series of alcohols, 100% (2 x 5 mins) > 90% (2 mins) > 70% (2 mins), and running tap water (5 mins). Sections were immersed in a water based haematoxylin solution (Thermo Scientific, Loughborough, U.K.) for 35 secs and then quickly washed in running tap water. To achieve differentiation, sections were immersed in acid alcohol solution (1%HCl in 70% EtOH) for 8 secs. Following differentiation sections were rinsed in running tap water for 2 mins prior to 'blueing' in Scott's tap water (2% $MgSO_4$, 0.35% $NaHCO_3$) for 2 mins and then a further 2 min wash in

running tap water. At this point slides were assessed to ensure adequate nuclear staining had been achieved using a light microscope, where staining was too dark sections were re-immersed in acid alcohol, and where to light haematoxylin. Slides were then submerged in undiluted alcoholic Eosin Y solution (Surgipath, Cambridgeshire, UK) for 2 mins followed by a rinse in running tap water and then dehydrated through a series of alcohols, 70% (2 mins) > 90% (2 mins) > 100% (2 x 5 mins) and xylene (15 mins) before being mounted with coverslips using DPX.

2.5.2 *Counterstaining with haematoxylin*

Where immunostained sections were counterstained with haematoxylin to aid delineation of anatomical features following DAB visualisation, sections were rinsed for 10 mins and then immersed in haematoxylin, differentiated and 'blued', then dehydrated through alcohols and xylene and mounted with coverslips using DPX as above.

2.5.3 *Identification of areas of ischaemic damage to neuronal perikarya*

Areas of ischaemic damage were identified within H&E sections as regions where loss of staining and vacuolation of the neuropil had occurred in conjunction with changes in neuronal cell morphology (shrunken pyknotic nuclei and eosinophilic cytoplasm) and/or the presence of eosinophilic ghost cells (a dead cell where the outline remains identifiable in the neuropil but the nucleus or cytoplasmic structures are not stained by haematoxylin). These were easily delineated from undamaged tissue where neuropil remained intact and uniformly stained and neuronal cell morphology was consistent with the presence of healthy cells; large round nuclei and cell bodies and visible cytoplasmic structures.

2.6 Immunohistochemistry

All sections used for immunostaining were adjacent to those which had undergone histological analysis. All immunostaining was conducted by the author unless otherwise stated.

2.6.1 *General principle*

Immunohistochemistry is a commonly used technique to investigate cell structure and organisation of tissue. It exploits the basic principles of immunology i.e. the specific interaction of an antibody with its antigen, to allow the visualisation of specific cell or tissue constituents. All immunohistochemistry conducted in studies reported in this thesis utilised the immunoperoxidase method of staining.

2.6.1.1 *Avidin-biotin-peroxidase Complex (ABC) immunostaining*

The ABC method of staining was used for all immunohistochemistry experiments reported in this thesis. The method was first reported by Hsu et al. in 1981 (Hsu et al., 1981) and is based on the high affinity of the protein avidin to bind biotin. Briefly, sections are incubated with a primary antibody to the antigen of interest. A secondary biotin-conjugated antibody is then introduced which binds the primary antibody and causes the localisation of many biotin molecules to the site of the antigen. Following this, an avidin/ biotinylated peroxidase complex is added to the section which binds to the biotinylated secondary antibody thus amplifying the signal. Finally a chromogen (diaminobenzidene) is added to the section which reacts with the peroxidase forming a brown deposit which is readily visible via light microscopy.

2.6.1.2 *Immunohistochemistry method*

Day1: Sections were heated in an oven maintained at 60^{o}C for 30 mins then dewaxed in xylene for 10 mins followed by submersion in 100% alcohol (2 x 5 mins). Sections were then immersed in 3% H_2O_2 methanol solution for 30 mins to block any endogenous peroxidase activity then washed in running water for 10 mins. Where heat mediated or formic acid mediated antigen retrieval was performed sections were microwaved on full power (2 x 5 mins) in pH 6 citric acid buffer or submerged in 80% formic acid for a period of 10 mins. Slides were then rinsed in PBS and blocking of non-specific binding sites was achieved by incubation for 1 hour at room temp with 10% normal serum and 0.5% bovine serum albumin in PBS. The appropriate concentration of primary antibody solution (made in blocking solution) was added to sections which were then incubated overnight at 4^{o}C.

Day 2: Sections were washed in PBS (2 x 10 mins) and then incubated with biotinylated secondary antibody (1:100) for one hour at room temp. Following this, sections were washed in PBS and then incubated with an avidin-biotin-peroxidase complex solution (Vector Laboratories, UK) at room temp for a period of one hour. Sections were washed in PBS (2 x 10 mins) and then incubated with 3'3'-diaminobenzidene solution to visualise antibody binding. The colour reaction was stopped after 3 mins by immersion of sections in running water (10 mins). Sections were then dehydrated through a series of alcohols; 70% (2 mins), 90% (2 mins.), 100% (2 x 5 mins) and then xylene (10 mins) before being mounted and cover slipped in DPX.

2.6.1.3 *Optimisation of antibodies*

Prior to conducting immunostaining on full studies a dilution curve was set up to establish the optimal concentration for each antibody and also to establish whether heat mediated, or in the case of Aβ, formic acid mediated retrieval was required. Secondary antibodies against the species in which the primary antibody was raised were used; these in turn determined the species of normal sera which was added to the blocking solution. All immunohistochemistry experiments conducted included a negative control which received identical treatment with the exception of addition of primary antibody. This ruled out the possibility of non-specific binding causing the generation of false positive results. When setting up the dilution curves in C57Bl/6 tissue, positive control tissue was also included. Tissue obtained from a pilot study utilising microcoil induced hypoperfusion (conducted by Dr. Karen Horsburgh) was used. Additionally, tissue from a previous study investigating the impact of global ischaemia on white matter (conducted by Dr. Jill Fowler) was also utilised. Tissue from 6 month old sham operated 3xTg animals was used to construct dilution curves for antibodies described in chapters 5 and 6, tissue from the 0.18mm diameter coil cohort was included as a positive control.

Table 2.2 Antibodies used for immunohistochemistry experiments

Primary antibody	Species, Type	Secondary Sera	Clone	Source	Dilution used
APP	Mouse	10% Horse serum, 0.5% BSA in PBS	22C11	Millipore	1:1000
Aβ	Mouse	10% Horse serum, 0.5% BSA in PBS	4G8	Chemicon (Millipore)	1:1000
MAG	Goat	10% Horse serum, 0.5% BSA in PBS	Polyclonal	Santa Cruz Biotechnology	1:250
MBP	Rat	10% Rabbit serum, 0.5% BSA in PBS	12	Chemicon (Millipore)	1:10000
dMBP	Rabbit	10% Goat serum, 0.5% BSA in PBS	Polyclonal	Millipore	1:300
Iba-1	Rabbit	10% Goat serum, 0.5% BSA in PBS	Polyclonal	A. Menarini	1:500

2.6.2 *Quantification of immunohistochemistry*

All analysis of immunohistochemistry was conducted by a blinded observer (the author unless otherwise stated). Sections were examined by conventional light microscopy. All analysis (grading and cell counting) was conducted over two days, sections were scored on both days. To ensure reproducibility, scores for each region were compared and the Kappa coefficient calculated (Haley and Osberg, 1989; Holland et al., 2010). This was done for each antibody in a different cohort. For each antibody in all regions $\kappa \geq 0.77$ which may be interpreted as excellent reproducibility (Landis, 1977).

Where grading scores were different regions were scored again on day three. For cell counts, where regional counts differed by greater than 10% between days one and two, a third count was conducted on day three.

2.6.2.1 *Quantification of intraneuronal APP expression and intraneuronal Aβ levels in the hippocampus and cortex*

Intraneuronal Aβ and APP deposits were identified based on the typical morphology observed. In the case of APP this constituted large intracellular deposits of immunoreactive material in pyramidal cells within the cortex and hippocampus, Aβ was visible as granular deposits of immunoreactive material, also visible within cortical and hippocampal pyramidal cells. Photomicrographs were taken of immunostained sections using MCID imaging software (MCID, Cambridge, UK) attached to a Leica microscope (Leica Microsystems (UK) Ltd., Milton Keynes, UK). For analysis of immunostaining in the CA1 hippocampal subregion, 4 consecutive images at 400x magnification were taken from each section. For cortical immunostaining analysis 8 consecutive images at 200x magnification were

taken. Using ImageJ software (V1.41), images were converted to greyscale and cropped to size for analysis (200 x 800 pixels for hippocampal images and 250 x 900 pixels for cortical images), mean gray values for each image were measured and then averaged to give a mean gray value per section for each region. Mean gray values were converted to relative optical density (Lazic, 2009) for comparison of sham and hypoperfused groups. Relative optical density levels were used as an index of levels of immunostaining.

In order to ensure reliable reproducibility slides from three animals were chosen at random from each group of animals to be examined and analysed as described three times. The measure was deemed reproducible when the 3 measurements fell within 10% of the median value.

2.6.2.2 *Quantification of MAG immunohistochemistry*

Loss of myelin integrity in response to hypoperfusion was assessed via MAG immunostaining. A semi quantitative grading scale (0-3) was devised for analysis of MAG immunohistochemistry. The scale was as follows; normal (grade 0), minimal myelin debris, vacuolation, and disorganisation of fibres (grade 1), modest myelin debris, vacuolation, and disorganisation of fibres (grade 2), and extensive myelin debris, vacuolation, and disorganisation of fibres (grade 3) (See Fig 2.6).

2.6.2.3 *Quantification of APP immunohistochemistry in white matter*

Axonal damage was visualised using anti amyloid precursor protein (APP) antibody which is a well established marker for axonal damage (McKenzie et al., 1996). Axonal damage is visualised by the presence of APP stained axonal bulbs. Using this marker a semi quantitative grading scale was devised for analysis of levels

of APP staining as an index of axonal pathology (see Fig. 2.7). Axonal damage was identified as intense APP immunoreactivity in swollen or bulbous axons and graded as normal (grade 0), minimal axonal damage (grade 1), moderate areas of axonal damage (grade 2) and extensive areas of axonal damage (grade 3).

2.6.2.4 *Quantification of Iba-1 immunohistochemistry*

Ionized calcium binding adaptor molecule 1 (Iba-1) is the protein product of upregulation of the Aif1 gene (allograft inhibitory factor) and is specifically expressed in brain tissue by microglia following their activation. Activated microglia were quantified in chapter 4, by placing a box grid of defined size in randomly selected fields within each region of interest and then calculating the number of activated microglial cells per mm^2. In chapters 5 & 6 activated microglial were quantified using a grading scale (Fig. 2.9) which was as follows. Grade 0- no activated microglia, grade 1- modest microglial activation, grade 2- moderate microglial activation, and grade 3- extensive microglial activation.

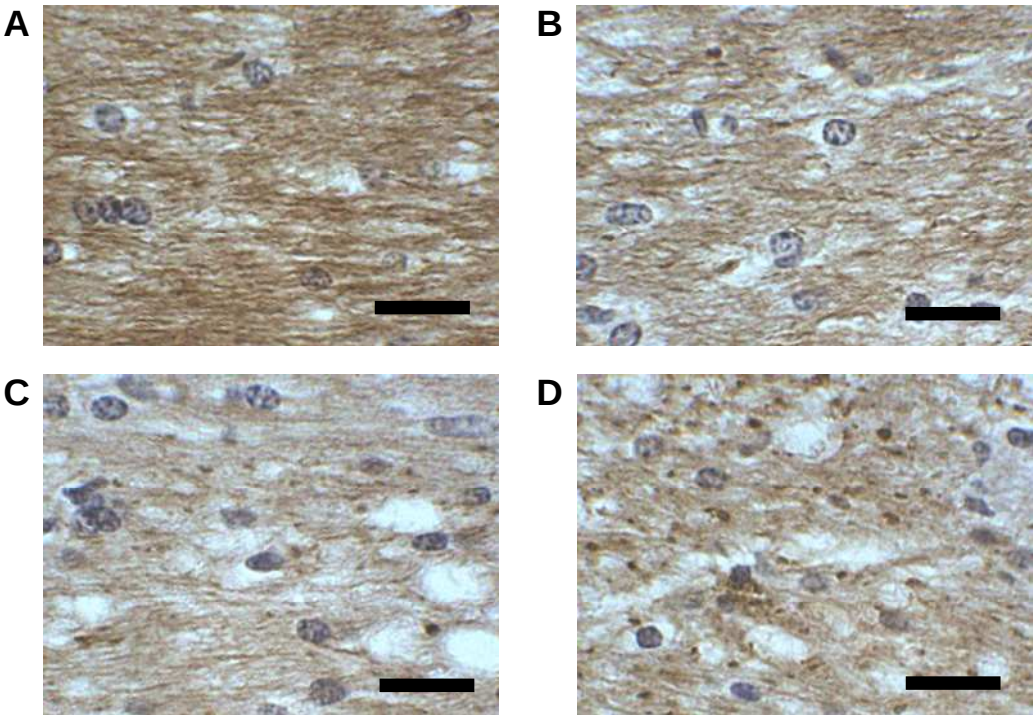

Figure 2.6 MAG immunostaining grading scale

Individual brain regions were scored as (A) normal (grade 0), (B) minimal myelin debris, vacuolation, and disorganisation of fibres (grade 1), (C) modest myelin debris, vacuolation, and disorganisation of fibres (grade 2), (D) extensive myelin debris, vacuolation, and disorganisation of fibres (grade 3). All images taken from the optic tract at 200x magnification. Scale bar = 25μm.

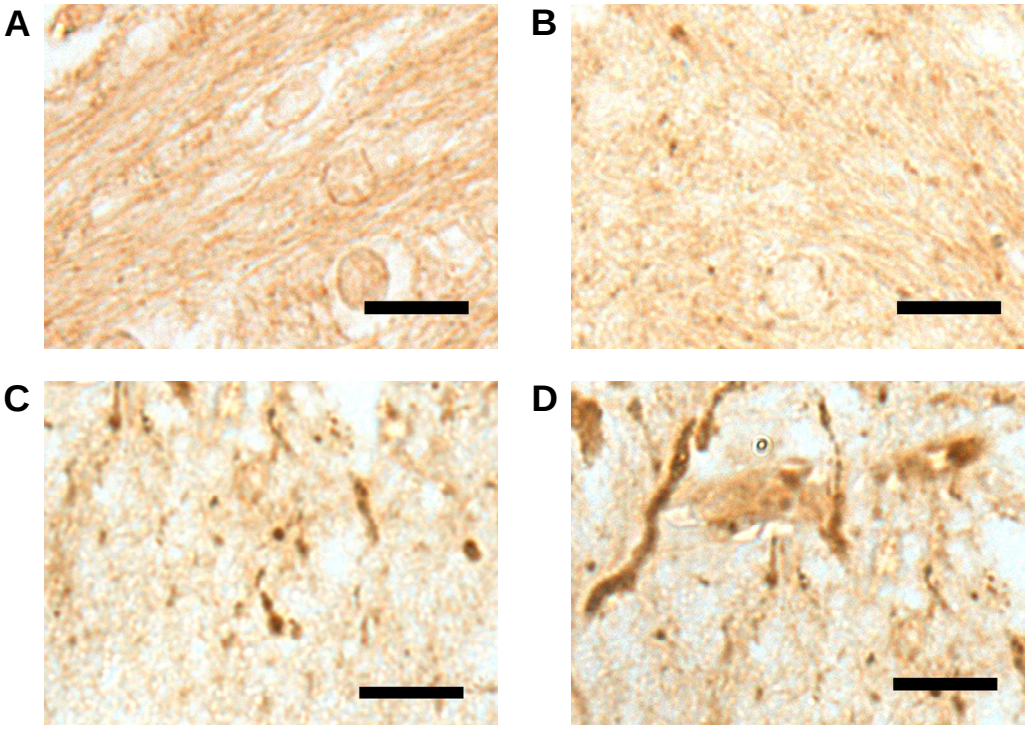

Figure 2.7 APP immunostaining grading scale

Individual brain regions were scored as (A) normal, grade (0), (B) minimal axonal damage (grade 1), (C) moderate areas of axonal damage (grade 2), (D) extensive areas of axonal damage (grade 3). All images taken from the internal capsule x400 mag. Scale bar = 12.5μm.

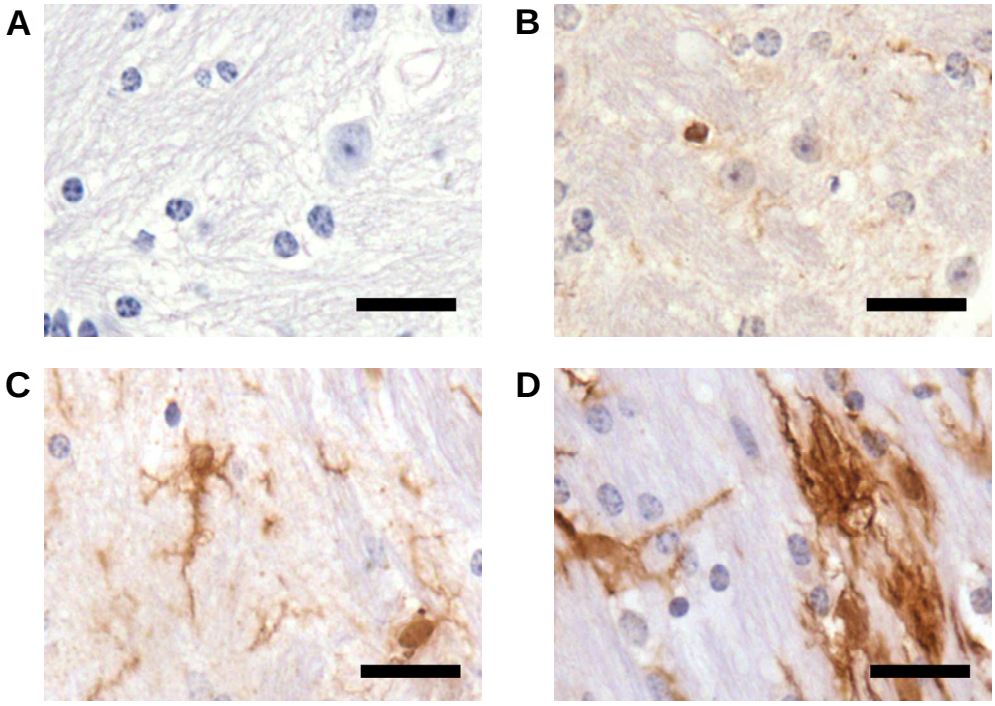

Figure 2.8 Iba-1 immunostaining grading scale

Individual brain regions were scored as (A) no microglial activation (grade 0); (B) minimal microglial activation (grade 1); (C) moderate microglial activation (grade 2); (D) extensive microglial activation (grade 3). Images taken from the internal capsule. Scale bar = 25μm.

2.7 Western Blotting

2.7.1 *Antibodies and optimisation*

Western blot analysis was utilised to investigate protein levels in whole brain homogenate. For a list of antibodies and the concentration at which they were used see table 2.3. Prior to running studies blots were conducted in control tissue (male 3xTg 10 months of age) to ascertain optimal antibody concentration and also to ascertain antibody specificity. Negative controls were also run, where blots received the same treatment in every aspect with the exception of the addition of primary antibody.

Whilst Western blotting may be considered a relatively cheap, reliable and time economic method of protein quantification a potential caveat which must be taken into considertation and one which can prove problematic when attempting to interpret results, is the presence of non-specific binding (N.S.B.). This can lead to false positive results and also issues with blot quantification. This highlights the importance of negative controls. It also highlights the importance of incubation with an appropriate blocking buffer following protein transfer (section 2.7.5).

An advantage of using the Western blotting method utilised in this thesis lies in the quantification of blots. Previously Western blotting was only considered sensitive enough to detect changes in protein levels of > 20%. However the Odyssey infra red imaging system and Odyssey imaging software V3.0 (Li-Cor Biotechnology UK Ltd., Cambridge, UK) is able to detect changes in protein levels as small as 2-3%.

Table 2.3 Antibodies used for Western blot experiments

Primary antibody	Species Type	Clone	Source	Dilution used	Secondary antibody
APP	Mouse	22C11	Millipore	1:1000	Goat anti-mouse 680
APP-CT20	Rabbit	Polyclonal	Merck	1:1000	Goat anti-rabbit 680
MAG	Goat	Polyclonal	Santa Cruz Biotechnology	1:500	Donkey anti-goat 680
MBP	Rat	12	Chemicon (Millipore)	1:10000	Donkey anti-rat 680
CNPase	Mouse	11-5B	Abcam	1:5000	Goat anti-mouse 680
GAPDH	Mouse	GAPDH 71.1	Sigma-Aldrich	1:100000	Goat anti-mouse 800
GAPDH	Rabbit	Polyclonal	Sigma-Aldrich	1:100000	Goat anti-rabbit 800

2.7.2 *Tissue homogenisation and preparation*

Hemi brain sections (3 mm) taken at the level of the hippocampus as described in section 2.4.2 were removed from -80^{o}C storage, weighed and kept on dry ice. Homogenisation was conducted in 10x volume (e.g. 750µl in 75mg) of total homogenisation buffer (250mM sucrose, 20mM tris base, 1mM EDTA, 1mM EGTA) to which protease and phosphatase inhibitors had been added (Merck, Nottingham, UK). Tissue was homogenised in a 1ml glass-glass Dounce hand held homogeniser using 15 strokes of the pestle and then pulse spun (the centrifuge was allowed to reach full speed and then stopped) in a bench top centrifuge. Supernatant was aspirated off, transferred to a fresh 1.5ml Eppendorf tube and refrozen at -80^{o}C.

2.7.3 *Assessment of protein concentration of samples*

Protein concentration of samples was determined using the bicinchoninic acid (BCA) protein assay method (Thermo Scientific, Loughborough, UK). This assay is

based on the reduction of Cu^{2+} ions to Cu^{+} by protein in an alkaline medium (known as the biuret reaction) and the subsequent reaction of the reduced copper cation with BCA to produce a quantifiable colourimetric reaction. The colour intensity may be measured via spectrophotometry (wavelength 562nm); colour intensity is proportional to protein concentration allowing accurate determination of sample protein concentration between a range of 20 to 2000 μg/ml.

The BCA assay was conducted in a 96 well plate. A series of protein (bovine serum albumin (BSA)) standards 25-2000 μg/ml were made from 2000 μg/ml stock diluted in total homogenisation buffer. 1:15 dilutions of total homogenate were prepared, 50 parts of BCA reagent A (Sodium carbonate, sodium bicarbonate, bicinchoninic acid and sodium tartrate in 0.1M sodium hydroxide) was added to 1 part BCA reagent B (4% cupric sulphate) to form the BCA working reagent. 10μl of diluted total homogenate sample was added to the microplate in triplicate, 200μl of BCA working reagent was then added to each well and plates were covered and incubated at 37^{0}C. Plates were read on a plate reader (Dynex Technologies, Worthing, UK) and results recorded. Triplicates were examined and any values greater than +/- 10% were excluded, the value for each sample was taken as the average of each triplicate (or duplicate where a value had been excluded). A standard curve was constructed from the values of the known standards and then the protein content of samples was determined via linear regression analysis (Fig. 2.9).

2.7.4 *SDS-Page electrophoresis*

Sodium dodecyl sulphate polyacrylamide gel electrophoresis (SDS-PAGE) separates polypeptides based on their electrophoretic mobility. SDS binds proteins denaturing their polypeptide back bone and causes the dissociation of hydrogen

bonds which results in an unfolding of tertiary and secondary structures, SDS also confers an overall net negative charge on proteins meaning that they are separated solely on size. Samples are prepared in Laemeli buffer which contains 2-mercaptoethanol, dithiothreitol (DTT), bromophenol blue and glycerol. 2-mercaptoethanol and DTT are reducing agents which reduce inter and intramolecular di-sulphide bonds ensuring proteins remain as linear structures, bromophenol blue is added as an indicator dye allowing observation of protein migration through the gel, it also makes gel loading easier, glycerol is added to increase the density of the sample ensuring it will sink to the bottom of the well when loaded. All SDS-Page electrophoresis and Western blotting in studies reported in this thesis were conducted using the XCell Surelock mini gel system (Invitrogen, Paisley, UK).

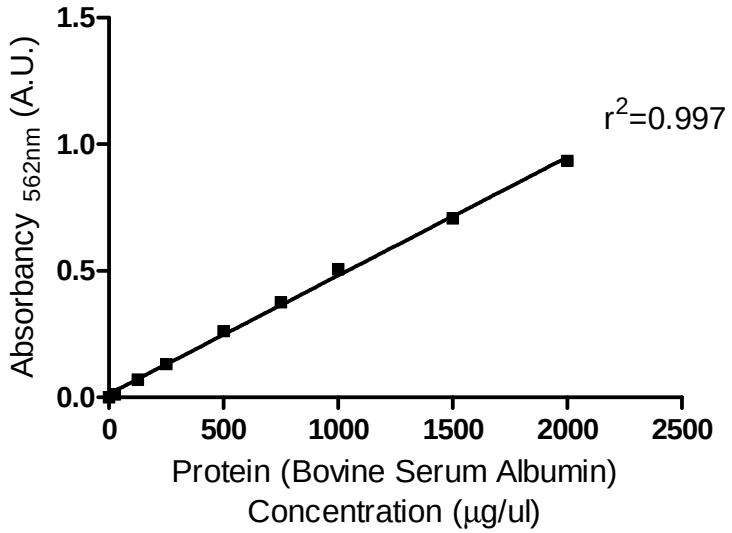

Figure 2.9 Example of standard curve for determining protein concentration
The relative absorbancy of BSA standards at 562nm increases with increasing concentration of BSA. Linear regression was used to calculate the protein concentration of samples of total homogenate utilised for Western blotting experiments.

Following determination of protein concentration of homogenates, samples containing equal amounts of protein were prepared for Western blot analysis. 4x laemmli buffer and distilled water were added to each sample to make up to the required volume (for 10 well gels this was 25µl and for 15 well gels 10µl). Samples were heated at 70^{o}C in a water bath for 10 mins to denature proteins and then vortexed prior to gel loading. Protein was separated by SDS-polyacrylamide gel electrophoresis on 4-12% Bis/ Tris gels using 2-(N-morpholino)ethanesulfonic acid (MES) running buffer (Invitrogen, Paisley, UK), gels were run for 1.5 – 2 hours at 150V unless otherwise stated.

2.7.5 *Protein transfer*

Following separation of proteins, gels were removed from chambers and opened ready for protein transfer. The section of the gel containing stacking gel and wells was trimmed off and a sheet of blotting paper (6cm x 4cm) soaked in transfer buffer placed over the gel. Gels were then flipped over and polyvinylidene fluoride (PVDF) membrane (6cm x 4cm) (GE Healthcare, Amersham, UK) which had previously been activated in 100% methanol for 5 mins then rinsed in dH2O was placed over the gel and another piece of blotting paper placed on top. Blotting paper, gel and membrane 'sandwiches' (Fig 2.10) were placed into XCell Surelock blot modules (Invitrogen, Paisley, UK) between sponges soaked in transfer buffer (see appendix 1). Where possible two transfers were conducted per blot module, in the event of an odd number of gels, extra sponges were added to the blot modules to ensure flow of current between electrodes. Following securing of the blot module with the gel tension wedge blot modules were filled with transfer buffer, the chamber

around the blot module was filled with dH2O. Protein transfer was conducted at 30V for a period of 1.5 hours.

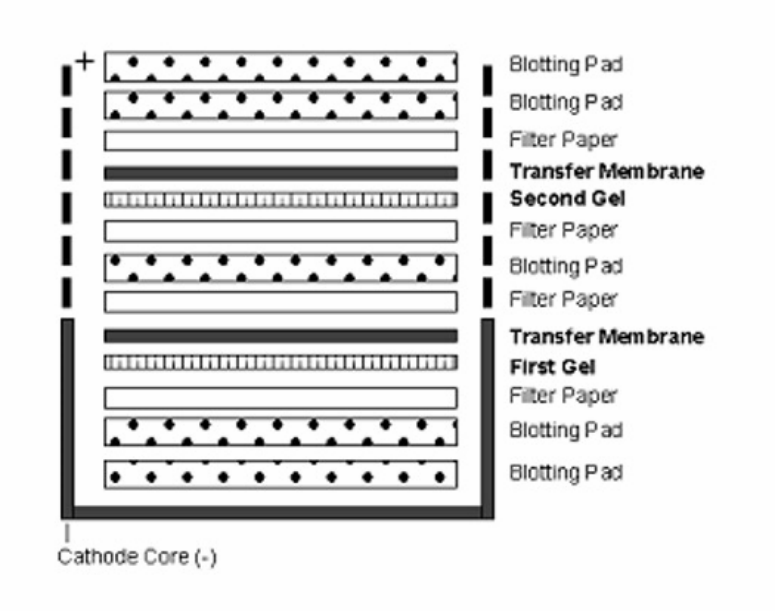

Figure 2.10 Protein transfer
Schematic of a blotting paper, gel and membrane 'sandwich'. These were placed between sponges soaked in transfer buffer and into a blot module, a current was then passed through to facilitate protein transfer. Image adapted from www.invitrogen.com

Following protein transfer, membranes were incubated in Ponceau S solution (Sigma Aldrich Company Ltd., Dorset, UK) to ensure equal loading of protein. Membranes were then blocked in 10ml Odyssey blocking buffer (Li-Cor Biotechnology UK Ltd., Cambridge, UK) / PBS (1:1) in a light proof box at room temp for a period of one hour. Membranes were incubated with primary antibody in blocking buffer/PBS (1:1), 0.1% Tween20 (Sigma Aldrich Company Ltd., Dorset, UK) solution (10ml) overnight at 4^{o}C. In all Western blotting experiments Glyceraldehyde 3-phosphate dehydrogenase (GAPDH) (1:100000, Sigma Aldrich Company Ltd., Dorset, UK) was used as a loading control. On day two membranes were washed 6 times in PBS 0.1% Tween solution for 5 mins each wash, then incubated with appropriate secondary fluorescent antibody (1:3000 Li-Cor Biotechnology UK Ltd., Cambridge, UK) in blocking buffer/ PBS (1:1), 0.1% Tween20, 0.01%SDS solution for 45 mins at room temp. Following incubation membranes were washed 6 times in PBS 0.1% Tween20 solution for 5 mins per wash and then twice for 2 mins in PBS solution. Membranes were then allowed to dry prior to quantification of protein levels.

2.7.6 *Coomassie blue staining*

Coomassie blue staining was used to assess whether protein transfer had been successful. Following western blotting gels were incubated in coomassie blue stain (Biorad, Herts., UK) at room temp for a period of one hour then washed in dH_2O for 6 x 5 min washes.

2.7.7 *Quantification of protein levels*

Once dry, blots were scanned using an Odyssey infra red imaging system and protein levels quantified using Odyssey imaging software V3.0 (Li-Cor Biotechnology UK Ltd., Cambridge, UK). GAPDH was utilised as a loading control for all Western blotting experiments. The intensity value (measured in arbitrary units (A.U.)) for the protein of interest was expressed as a ratio of the intensity value of GAPDH for each lane on each gel. In most cases each Western blot was run twice and the values from each gel were averaged for analysis. To ensure reproducibility of gels, images of blots and protein concentration values were compared by eye.

To ensure the suitability of GAPDH as a loading control and that GAPDH levels were not affected by either hypoperfusion or ageing, GAPDH values were compared for each group i.e. sham vs hypoperfused, or, young vs old. In all cases GAPDH levels did not change in response to either hypoperfusion or ageing ($p > 0.05$) (Fig. 2.12).

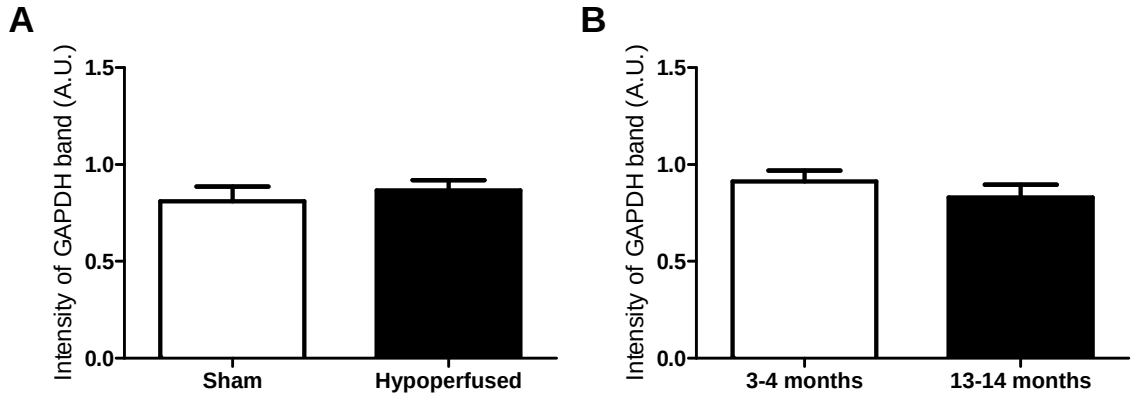

Figure 2.11 GAPDH is unaffected by hypoperfusion or ageing

Data are expressed as GAPDH intensity value ± SEM. A. Comparison of GAPDH levels in sham (n = 7) and hypoperfused animals (n = 8) where hypoperfusion was induced using 0.16mm dia microcoils (p=0.557). B. Comparison of GAPDH levels in young (n = 6) and aged animals (n = 12 p=0.352). In each case GAPDH levels were unchanged. Two-way Student's t-test.

2.8 Comparison of Circle of Willis anatomy

Circle of Willis anatomy was compared between adult male C57Bl/6J and adult 3xTg-AD mice. Mice were transcardially perfused with 0.9% saline solution in PB as outlined in section 2.4.1. Following this, 5ml of Carbon Black ink were perfused at the same rate. Animals were taken to be adequately perfused when their extremities turned black. Animals were decapitated and the brains removed from skulls. Circle of Willis anatomy was visualised using a dissecting microscope (magnification x10). Circle of Willis anatomy was scored as either complete or incomplete, based on the presence or absence of both posterior communicating arteries. Brains were then frozen and scored for a second time by an independent blinded observer.

2.9 Statistical analysis

2.9.1 *Behaviour*

Behavioural data were analysed using 2-way ANOVA with the Greenhouse-Geisser correction. Student's t-test with Bonferroni adjustment for multiple comparisons was used *post hoc*.

2.9.2 *Pathology*

Loss of myelin integrity, levels of degraded myelin and axonal damage were compared between sham and hypoperfused animals. The statistical design employed, initially determined whether the probability of damage ocurring to the aforementioned white matter components was higher following hypoperfusion. This was tested using Fisher's exact test. Latterly a Mann-Whitney U test was employed to assess whether levels of damage were higher in animals following hypoperfusion

as compared to shams. The grading score for regions of interest were summated to give an overall score per animal and then scores were compared. Microglial activation was compared using Student's t-test unless otherwise stated. Number of activated microglia in regions of interest were summated to give the number of activated microglia/animal/mm^2. Relative optical density values obtained via image analysis were compared using Student's t-test.

2.9.3 *Western blot analysis*

All Western blot data are presented as mean of two blots unless otherwise stated. Order of samples on gels was changed between run 1 and run 2 to ensure loading pattern had no impact on results. All data are expressed as mean protein of interest/ GAPDH ± SEM. Groups were compared using Student's t-test.

2.9.4 *Statistical analysis package*

Statistical analysis of data from all studies was performed using Graph Pad Prism v5.0 (Graphpad Software Inc. El Camino Real, U.S.A.).

Chapter 3: The temporal development of pathology following hypoperfusion in C57Bl/6J mice

3.1 Introduction

Chronic reductions in cerebral blood flow may impact on the integrity of brain white matter and could underlie the development of cognitive deficits (Kawamura et al., 1991; Breteler, 2000; Raz et al., 2007). To date several experimental animal models have been developed to investigate this (Kudo et al., 1993; Farkas et al., 2007). The most often used and well characterised is the 2VO rat model where CBF is attenuated via ligation of the common carotid arteries resulting in reductions of CBF of up to ~35% of baseline levels (Farkas et al., 2007). Whist this model has proven useful, one of its major drawbacks is the development of ischaemic damage to neuronal perikarya in many experimental animals, making it impossible to differentiate the independent role of white matter disruption in any cognitive deficit observed during behavioural testing.

More recently a mouse model of chronic cerebral hypoperfusion has been developed, in which CBF is attenuated via the application of microcoils of a fixed diameter to the common carotid artery (Shibata et al., 2004). The ability to vary the internal diameter of the coils means that more modest reductions in CBF may be induced.

This mouse model provides a powerful tool to examine the impact of hypoperfusion on the development of white and grey matter pathology and also how different types of pathology may impact on different cognitive domains. However, prior to conducting behavioural testing to investigate cognitive changes, a necessity arises to establish firstly, when following induction of hypoperfusion pathology becomes detectable and secondly what the extent and severity of this pathology is.

This study will test the hypothesis that hypoperfusion will cause a temporal progression of white and grey matter pathology.

3.1.1 *Aims of study*

This study sought to investigate the temporal development of white matter pathology following chronic cerebral hypoperfusion at, 7, 14, 28 and 56 days post surgery, in C57Bl/6J wild type mice.

3.2 Methods

3.2.1 *Animals and group sizes*

In four cohorts of C57Bl/6J male mice (aged 3-4 months; table 3.1) hypoperfusion was induced as described in section 2.2 using 0.18mm diameter microcoils.

To investigate the development of pathological changes to white matter following hypoperfusion, animals were culled via perfusion fixation as outlined in section 2.4 at 7, 14, 28 and 56 days post surgery. All surgeries conducted on animals described in this chapter were performed by Dr. Cath Gliddon.

Table 3.1 Initial cohort sizes

Treatment / Time point	Sham	Hypoperfusion
7 days	n=6	n=17
14 days	n=6	n=12
28 days	n=6	n=16
56 days	n=5	n=8

3.2.2 *Histology*

Haematoxylin and eosin (H&E) staining, as described in section 2.5, was used to identify areas of ischaemic damage to neuronal perikarya.

3.2.3 *Immunostaining*

MAG immunostaining was used to investigate changes in myelin integrity in response to hypoperfusion. APP immunostaining was used to investigate the development of axonal pathology in response to hypoperfusion. Immunostaining and quantification was conducted as described in section 2.6. Initially Fisher's exact test was used to determine whether the probability of damage ocurring to white matter components was increased following hypoperfusion. Mann-Whitney U tests were used to compare loss of myelin integrity and levels of axonal pathology between sham and hypoperfused animals.

3.2.4 *Regions of interest*

In this study hemi brain sections were stained and analysed (the other hemi brains were utilised in a biochemical study not reported in this body of work). White matter regions of interest examined were external capsule, internal capsule, hippocampal fimbria, optic tract and white matter fibre bundles of the striatum (Fig. 3.1). Initial attempts were made to analyse myelin/ axonal integrity in the corpus callosum however this was not possible due to the presence of artefacts in the tissue in all animals examined. The likely cause of these is the shrinking back of hydrophobic white matter during tissue processing. This may be considered a weakness of attempting to conduct both immunohistochemical and biochemical studies using tissue from the same animals.

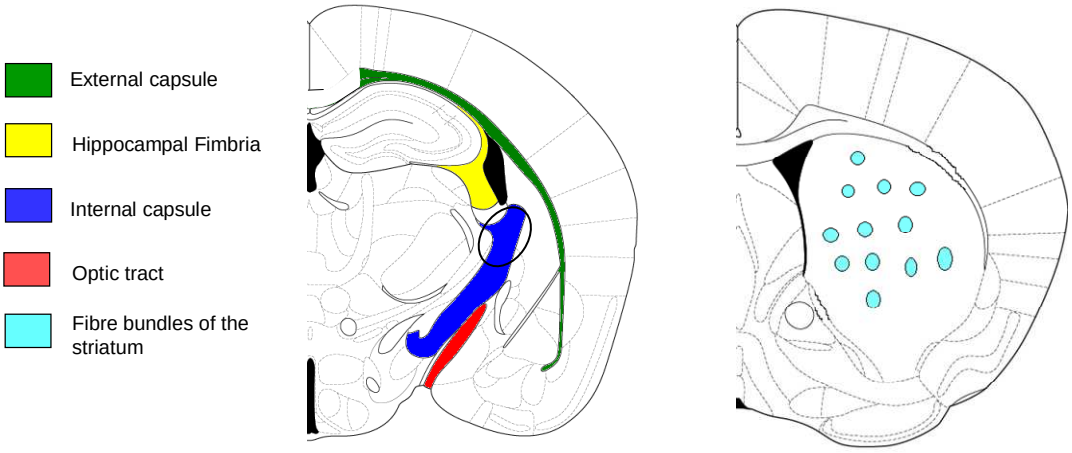

Figure 3.1 White matter regions of interest

Pathology was examined in the external capsule, internal capsule (area assessed circled), hippocampal fimbria, optic tract and white matter fibre bundles of the striatum. Images adapted from Franklin and Paxinos (1997).

3.3 Results

3.3.1 *Recovery after surgery*

All animals recovered well from surgery with the exception of two hypoperfused animals from the 28 day cohort which were culled due to poor recovery. This gave final group numbers for this cohort of n = 6 sham and n = 14 hypoperfusion.

3.3.2 *Pathology*

3.3.2.1 *Histological examination of grey matter following hypoperfusion*

There was no evidence of ischaemic damage (as described in section 2.5.3) to neuronal perikarya in any brain region in any of the sham operated animals. Ischaemic neuronal perikaryal damage was seen in 5 out of 17 hypoperfused animals in the 7 day cohort, in 4 out of 12 hypoperfused animals in the 14 day cohort, in 4 out of 14 hypoperfused animals in the 28 day cohort and 3 out of 8 animals in the 56 day cohort. Areas where ischaemic damage was observed were striatum, hippocampus and cortex, (table 3.2 & Fig. 3.2), severity of damage varied between animals.

Table 3.2 Animals displaying evidence of ischaemic damage

Cohort	Total no. of animals with ischaemic damage	No. of animals with ischaemic damage in Striatum	No. of animals with ischaemic damage in Hippocampus	No. of animals with ischaemic damage in Cortex
7 days	5/17	5	4	4
14 days	4/12	3	4	3
28 days	4/14	4	3	3
56 days	3/8	3	1	1

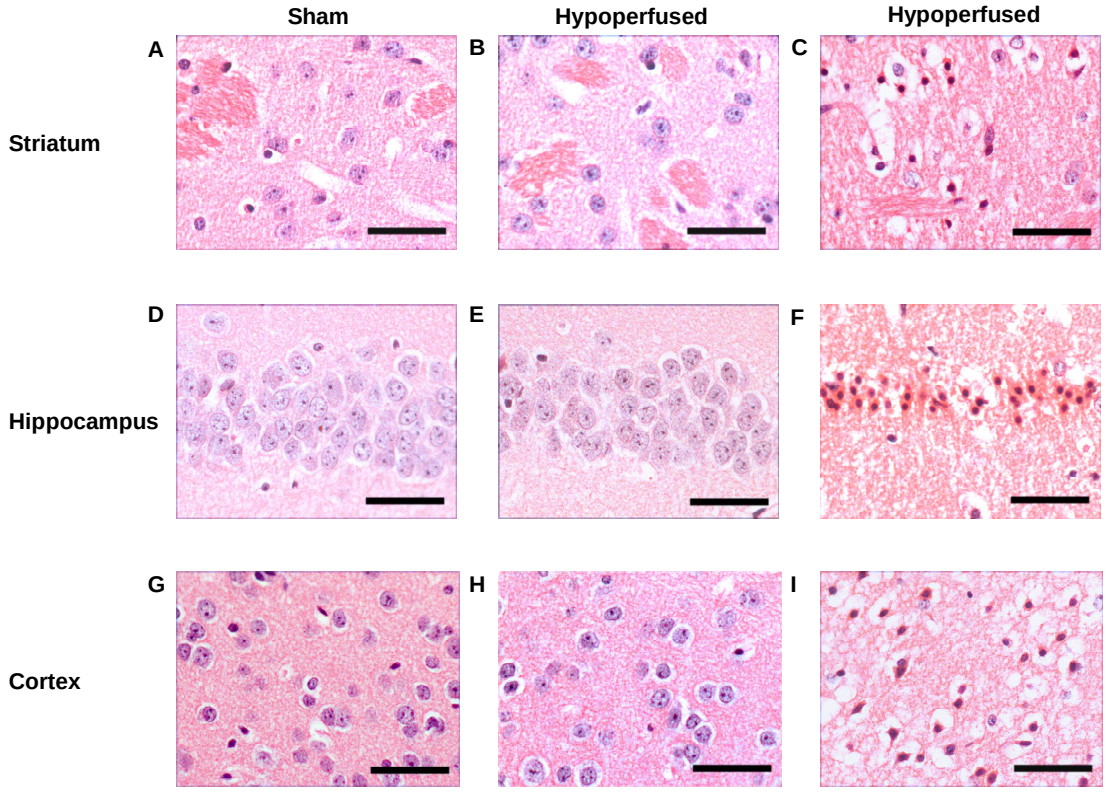

Figure 3.2 H&E staining to assess ischaemic damage

Images from the striatum (A-C), the hippocampus (D-F) and the cortex (G-I) in sham (A, D, G), hypoperfused animals where no evidence of ischaemic damage was seen (B, E, H) and hypoperfused animals displaying evidence of ischaemic damage to neuronal perikarya (C, F, I). Scale bar = 50μm.

3.3.2.2 *Analysis of MAG immunostaining*

The probability of myelin damage occurring following hypoperfusion was increased (7 days, $p = 0.003$, 14 days $p = 0.004$, 28 days $p<0.001$, 56 days $p<0.001$), Fisher's exact test. The majority of sham animals displayed no evidence of damage to myelinated fibres (Fig. 3.43). One sham animal from each of the 7, 14 and 28 day cohorts displayed minimal evidence of myelin pathology (grading score of 1 in regions affected). Myelin damage was present in hypoperfused animals (Fig. 3.3B) from 7 days and was significantly increased as compared to shams at all 4 time points; 7 days ($p = 0.004$), 14 days ($p = 0.003$), 28 days ($p < 0.001$), 56 days ($p = 0.004$) (Mann Whitney U Test; Fig. 3.4). Myelin damage was anatomically widespread and present in all regions examined in the majority of animals. There was no evidence to support a temporal evolution of pathology across the time points. Variability within the 4 cohorts of hypoperfused animals was similar.

In animals where ischaemic damage to neuronal perikarya had occurred myelin damage was markedly more severe across all regions (Figs. 3.3C and 3.4).

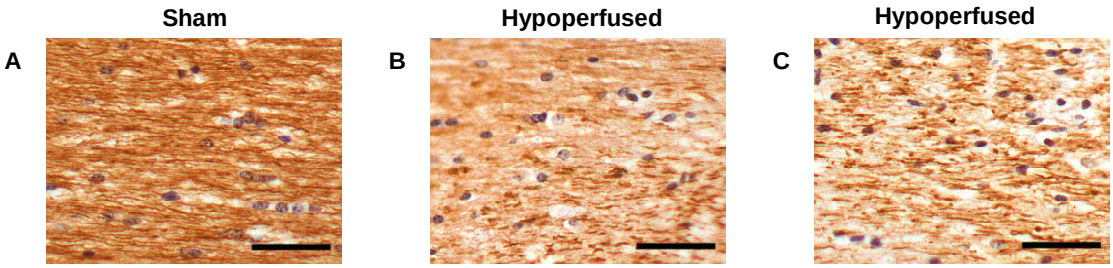

Figure 3.3 MAG immunostaining

Representative images of MAG staining in the optic tract in sham (A), hypoperfused animals where no ischaemic damage to neuronal perikarya was evident (B) and hypoperfused animals where ischaemic damage was evident (C). Scale bar = 50μm

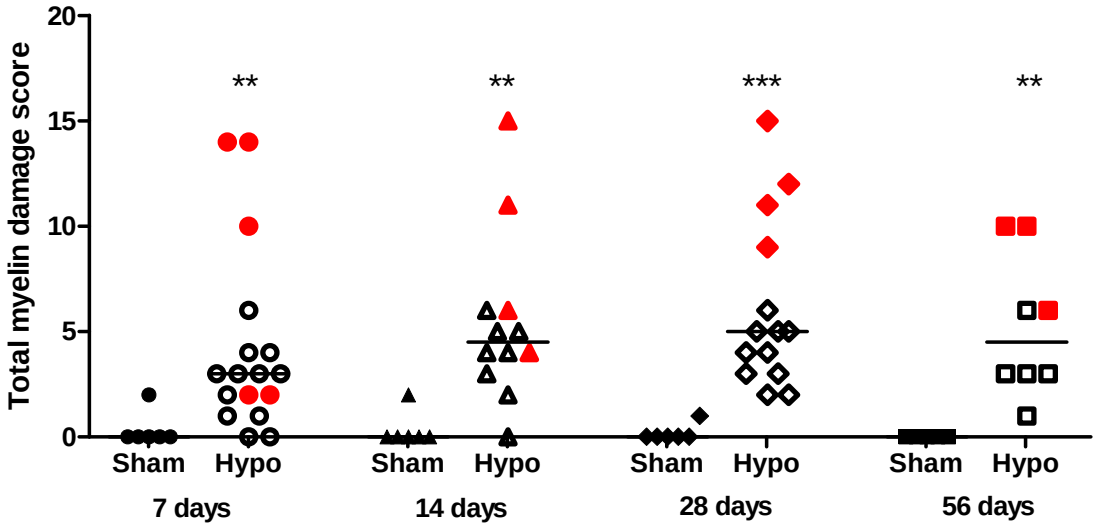

Figure 3.4 Assessment of myelin damage

The probability of observing myelin damage following hypoperfusion was increased (7 days, n= 6 sham, 17 hypoperfused; p = 0.003, 14 days, n= 6 sham, 12 hypoperfused; p = 0.004, 28 days n= 6 sham, 16 hypoperfused; p<0.001, 56 days, n= 5 sham, 8 hypoperfused; p<0.001), Fisher's exact test. Myelin damage was increased in hypoperfused animals at all time points as compared to shams, median value for sham animals in all 4 cohorts was 0; 7 days (p=0.004, median value=3.0), 14 days (p=0.003, median value=4.5), 28 days (p<0.001, median value=5.0), 56 days (p=0.004, median value=4.5). Mann-Whitney test. A similar level of variability was present in each experimental group. All animals were included in analyses. In animals where ischaemic damage to neuronal perikarya had occurred (highlighted in red), myelin pathology was markedly more severe.

3.3.2.3 *Analysis of APP immunostaining*

The probability of axonal damage occurring following hypoperfusion was not increased at 7 days, (p = 0.124), 28 days (p = 0.052*)* or 56 days (p = 0.231*)* but was increased at 14 days, (p = 0.009) Fisher's exact test. There was no axonal pathology present in any brain region of any sham animal (Fig. 3.5A). Axonal pathology was increased in some but not all hypoperfused mice (Fig. 3.5B). At 7 days axonal pathology was present in 7 out of 17 hypoperfused mice, at 14 days axonal pathology was present in 9 out of 12 mice, at 28 days axonal pathology was present in 7 out of 14 mice and at 56 days axonal pathology was present in 3 out of 8 mice. The increase in pathology was significant at 14 days (p = 0.023) but not at 7 days (p = 0.404), 28 days (p = 0.223) or 56 days (p = 0.739) (Mann Whitney U test; Fig 3.6).

Notably, the presence of axonal damage was more prominent in mice where there was evidence of ischaemic neuronal damage (Fig. 3.5C and 3.6).

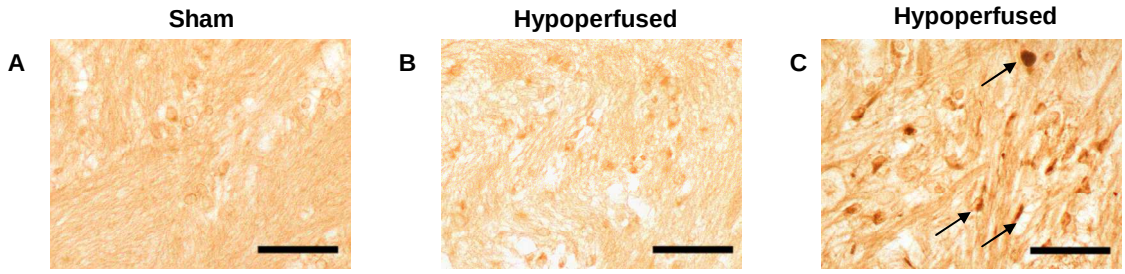

Figure 3.5 APP immunostaining

Representative images of APP staining in the internal capsule in sham (A), hypoperfused animals where no ischaemic damage to neuronal perikarya was evident (B) and hypoperfused animals where ischaemic damage was evident (C). Arrows denote accumulations of APP, indicative of axonal damage. Scale bar = 50μm

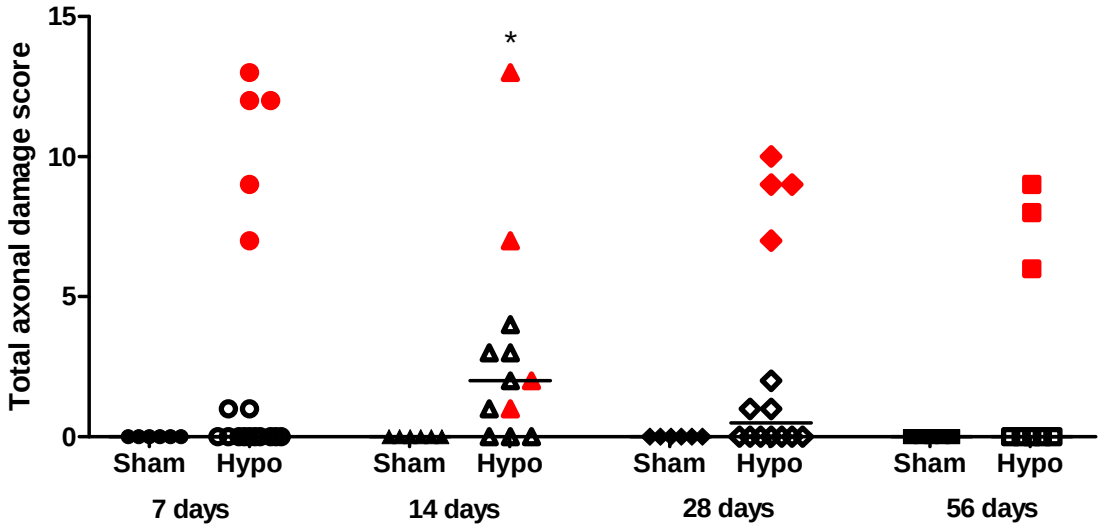

Figure 3.6 Assessment of axonal damage

The probability of axonal damage occurring following hypoperfusion was not increased at 7 days, (n=6 sham, 17 hypoperfused; p = 0.124), 28 days (n= 6 sham, 16 hypoperfused; p = 0.052) or 56 days (n= 5 sham, 8 hypoperfused; p = 0.231) but was increased at 14 days, (n= 6 sham, 12 hypoperfused; p = 0.009) Fisher's exact test. . Axonal pathology was increased in hypoperfused animals at 14 days as compared to shams (p=0.023, median value 2.0). There was no difference in levels of axonal pathology between sham and hypoperfused animals at any of the other three time points examined; 7 days (p=0.0.404, median value 0), 28 days (p=0.223, median value 0.5) or 56 days (p=0.739, median value 0). Mann Whitney U test. All animals were included in analyses. The median value for sham animals in all 4 cohorts was 0. In animals where ischaemic damage was observed (highlighted red), axonal pathology was markedly increased. Variability was similar within each experimental group.

3.4 Discussion

The results from the study presented in this chapter demonstrate that chronic cerebral hypoperfusion as induced by 0.18mm microcoils in C57Bl/6J mice results in the development of both white and grey matter pathology which is present from 7 days. Contrary to the initial hypothesis there was no clear temporal evolution of pathology.

Previously, (Shibata et al., 2004) conducted a study to characterise pathology in the same model of hypoperfusion as described in this chapter. They reported that white matter rarefaction had occurred and was apparent from 14 days, becoming more severe by 30 days. This was in the absence of any ischaemic damage to grey matter. In the present study, ischaemic damage to neuronal perikarya was present in approximately one third of hypoperfused animals thus demonstrating one of the biggest disparities between results presented here and those of Shibata et al (2004). In both studies ischaemic damage was assessed in the same manner, thus ruling out methodological differences in quantification as a reason for this discrepancy. One possible explanation for this difference may be due to the fact that different surgeons were used in each study. Whilst it would be unfair to question the competency of the surgeons the fact that this model was novel to our lab cannot be dismissed. This may have led to surgery taking longer and so the increased likelihood of the development of more severe damage or, alternatively the overall reduction in CBF may have been greater in hypoperfused animals. As CBF was not measured this is speculative but must be considered as a possible explanation.

Other reasons as to why there was a higher incidence of ischaemic damage reported in the present study may be due to differences in animal housing facilities. For example, both basic and clinical studies have demonstrated that lower

temperatures have been shown to confer neuroprotection against ischaemia (Little, 1959), hence had the animals utilised in the study by Shibata et al. been housed in a unit with a lower ambient temperature this may have influenced outcome after surgery. A further factor which may have influenced the development of ischaemic damage is behavioural stress. In experimental studies investigating the impact of behavioural stress, increased psychosocial stress has been associated with hypertension, cardiac arrhythmias and sudden death in both humans and animals (Lane et al., 2005; Trudel et al., 2010). Several experimental studies have shown that sensory contact with aggressive mice is associated with an increased stress response (Pardon et al., 2004). In the present study animals were housed 5 or 6 to a cage, whilst it is unknown how animals from the Shibata study were housed, had they been housed in isolation, then cage aggression and therefore increased psychosocial stress would have been avoided potentially lowering the likelihood of any stress induced ischaemia.

A further and arguably more pertinent reason why more ischaemic damage to neuronal perikarya was observed in the current study as compared to Shibata et. al. (2004) may be due to the different types of anaesthesia utilised during surgery. In the study undertaken by Shibata et. al. mice were anaesthetised using sodium pentobarbital (50 mg/kg, intraperitoneal injection), whilst in the present study inhalational anaesthesia (isoflurane) was used. Several studies have been conducted which have reported anaesthesia as having a general neuroprotective effect (Kitano et al., 2006; Clarkson, 2007; Lasarzik et al., 2011). Recovery time following inhalational anaesthesia is considerably faster than when anaesthesia is induced via injection, thus the animals in the study conducted by Shibata et. al. may have had a

prolonged period of neuroprotection conferred upon them compared to those described in the present study.

In addition to increased levels of ischaemic damage in hypoperfused animals, another notable difference between the study by Shibata et al (2004) and the one presented here is the finding that myelin pathology was evident from 7 days. One reason for this temporal difference may be due to the sensitivity of the different markers used in each study. Luxol fast blue (used by Shibata et al) is a general histological stain which binds several different myelin components, including phospholipids (Kluver and Barrera, 1953; Salthouse, 1962; Lycette et al., 1970) which comprise ~70% of myelin. For this reason Luxol fast blue may be considered a suitable marker to identify where damage to white matter has occurred, however, it does not provide insight into specifically which components of white matter are altered, due to lack sensitivity. The immunostaining method utilised by the present study is much more precise and confers an advantage over Luxol fast blue in that it allows specific targeting of selective myelin components. This is highlighted by the use of MAG as a marker for myelin integrity. As stated in chapter 1, MAG comprises < 1% of total myelin however as demonstrated by the results above, following hypoperfusion, clear cellular redistribution of MAG may be observed in white matter tracts as early as seven days. Attempts to investigate the impact of hypoperfusion on other protein constituents of myelin at 30 days, MBP, PLP and CNPase, conducted as part of an earlier immunohistochemical study within the Horsburgh group, demonstrated no detectable changes to these protein constituents in response to hypoperfusion at this time point.

The fact that changes in MAG are observed at an early time point, prior to gross myelin changes or changes in other myelin components, highlights the

possibility that MAG is one of the myelin proteins most vulnerable to hypoperfusion. This hypothesis is supported by previous work (Aboul-Enein et al., 2003) which demonstrated that preferential loss of MAG is observed in hypoxia related tissue injury prior to the loss of other myelin proteins and oligodendrocyte apoptosis. Given the cellular location of MAG (Fig 3.7) and its function in maintaining the axo-glial connection (Quarles, 2007) this finding suggests that a loss of normal axo-glial integrity/ function is an early event following onset of hypoperfusion. Further work which supports this has been conducted within the Horsburgh group where changes in MAG protein levels were evident as early as three days following onset of hypoperfusion (Reimer et. al, manuscript in preparation).

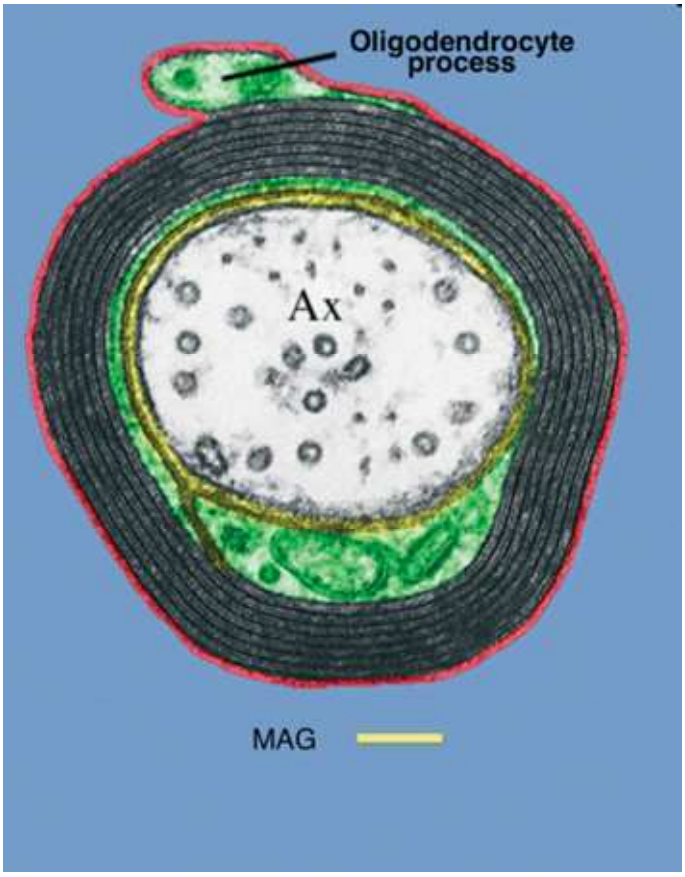

Figure 3.7 Cellular location of MAG

Electron micrograph coloured to show the cellular location of MAG. MAG is located periaxonally (coloured yellow). Ax = axon. Image adapted from Quarles (2007).

In addition to the identification of MAG as being particularly vulnerable to hypoperfusion another feature of the model identified via immunostaining is that axonal pathology is minimal. The relative lack of axonal pathology observed in the present study may be representative of differences in the ability of oligodendrocytes and neurons to tolerate reductions in CBF. Several reasons have been suggested as to why this may be the case; oligodendrocytes have high intracellular iron levels which renders them particularly vulnerable to oxidative stress, they also have a very large surface area to volume ratio (Bartzokis, 2004) coupled with a relatively low metabolic rate as compared to other cell types and, as discussed in chapter one, blood supply to white matter is relatively limited as compared to grey matter (Pantoni and Garcia, 1997).

Previously the most widely used and well characterised model of hypoperfusion was the 2VO rat model, where hypoperfusion is induced via complete ligation of the bilateral common carotid artery (Farkas et al., 2007). An advantage of the BCAS mouse model described in this thesis is that attenuation of CBF may be modulated by varying the internal diameter of the microcoils. This means that more modest reductions in CBF may be induced as compared to the 2VO rat model. This allows investigation of how levels of hypoperfusion, comparable with those observed in human ageing may impact on cognition in isolation (see next chapter). A further advantage of the BCAS mouse model, is that it may be applied with relative ease to any number of transgenic mouse lines to investigate the role hypoperfusion may contribute to a number of neurodegenerative disorders. This is demonstrated later in this thesis.

Whilst the study presented in this chapter and by others clearly demonstrates that an early, prominent pathological feature of this model is damage to white matter,

more specifically myelin, the mechanisms underlying this pathology remain to be elucidated.

In the mouse model of hypoperfusion described above, using 0.18mm microcoils, CBF is reduced to approximately 70% of baseline values immediately after surgery and returns to between 10-15% below baseline by 30 days (Shibata et al., 2004). This reduction in itself is too modest to cause ischaemic damage to neuronal perikarya (Jones et al., 1981) and should be able to be compensated for via auto regulation (Brain, 1993). However it must be noted that Shibata et al. used laser Doppler flowmetery to quantify CBF which measures cortical blood flow and not that of the subcortical white matter where flow is known to be lower (Pantoni et al., 1996). Furthermore, the brain is less able to compensate for reductions in blood flow in white matter due to the pattern of the white matter vascular network (Pantoni and Garcia, 1997). Hence, whilst cortical flow may be reduced by up to 30% initially, the flow reduction in white matter may be even greater and as such, sufficient to cause damage. Alternatively the degree of stenosis caused by microcoil placement on the carotid arteries (greater than 50%) (Shibata et al., 2004) may be sufficient to cause alterations in rheological factors such as blood viscosity, or the development of microturbulent flow (Brain, 1993). Each of these factors alone or a combination of them may lead to the development of chronic cerebral hypoperfusion (Farkas and Luiten, 2001). However, as yet, no evidence exists to support these speculations.

Other work, which has provided insight into the potential mechanisms underlying the development of white matter damage associated with hypoperfusion, in the same model utilised by the present study, has implicated a role for matrix metalloproteinases (MMPs), specifically MMP2, which was shown to be upregulated

in response to hypoperfusion (Nakaji et al., 2006). Furthermore, inflammation and severity of white matter rarefaction was shown to be attenuated in MMP2 KO mice (Nakaji et al., 2006). MMPs belong to a group of endopeptidases which are able to degrade numerous pericellular substrates, including the majority of components which comprise the extracellular matrix (Sternlicht and Werb, 2001). MMP2 has been shown to be upregulated in the white matter lesions of patients with vascular dementia (Rosenberg et al., 2001) and is also known to be particularly efficient at digesting myelin (Chandler et al., 1995) as well as being implicated in BBB dysfunction and the subsequent initiation of inflammation (Caplan, 2005).

A recent study conducted within the Horsburgh group which utilised Collagen IV immunohistochemistry to measure vessel diameter in cortical and hippocampal vessels, has shown that vessel diameter is increased following 1-2 months of hypoperfusion (Scullion, unpublished data). In this study lumen diameter was not measured, therefore it is not possible to ascertain whether enlarged vessel diameter was due to increased collagen deposition and basement membrane thickening or, vessel dilation. Nonetheless, changes in vascular diameter are known to impact on vascular resistance and in turn CBF (Brain, 1993). If the observed changes were due to increased collagen deposition, this may indicate the emergence of vascular pathology in response to hypoperfusion, alternatively were it due to vessel dilation then this may indicate that vascular reserve has become impaired i.e. in response to a reduction in perfusion pressure due to the induction of hypoperfusion, the arterioles may have dilated in order to increase cerebral blood volume and regulate cerebral blood pressure (autoregulation). If vascular reserve has been used up then this would render the brain vulnerable to any additional transient

changes in perfusion pressure. To confirm of reject either of these hypotheses further work is required.

There are several pathologic features which have been described as characterising white matter lesions in the brains of elderly individuals. These include, damage to myelinated fibres and myelin loss, ranging from modest to severe, varying severities of axonal damage, infiltration of glial cells (microglia and astrocytes), the upregulation of markers of hypoxia e.g. HIF1-α and also blood brain barrier dysfunction (Akiguchi et al., 2004; Fernando et al., 2004; Simpson et al., 2007a; Simpson et al., 2007b). Selective damage to white matter observed, in the majority of animals in the present study, following hypoperfusion was mild and limited mainly to the myelin component. Axonal pathology following hypoperfusion was minimal and only present in regions where myelin pathology was severe. This lack of axonal pathology suggests that the mouse model of chronic cerebral hypoperfusion described above may model most accurately early changes observed in the pathogenesis of white matter lesions. The next stage in model characterisation will be to investigate pathological changes to white matter in more detail and also whether hypoperfusion is associated with cognitive changes.

Chapter 4: Characterisation of cognitive deficits in a mouse model of chronic cerebral hypoperfusion

4.1 Introduction

In addition to the development of white matter pathology (Kawamura et al., 1991; Fernando et al., 2006), chronic cerebral hypoperfusion has also been associated with the development of cognitive deficits in the elderly (Ruitenberg et al., 2005; Tiehuis et al., 2008). Moreover, it has been hypothesised that white matter pathology underlies these changes (Junque et al., 1990; Breteler et al., 1994). Several studies conducted in cohorts of aged individuals have demonstrated a correlation between deficits in different aspects of cognition, including processing speed, executive function, episodic memory and levels of white matter damage (Deary, 2003; Bucur et al., 2008; Kennedy and Raz, 2009).

A major confounding factor of human studies attempting to investigate how chronic cerebral hypoperfusion, white matter pathology and the development of cognitive deficits may be linked, is the presence of multiple vascular risk factors, each of which may impact detrimentally on white matter integrity e.g. atherosclerosis, hypertension or diabetes, thus preventing any observed changes to white matter or cognition being attributed solely to hypoperfusion.

The development of animal models of hypoperfusion has gone some way to address this issue. Following on from the preceding chapter, the aim of the present study was to further examine pathological changes and also investigate the impact of hypoperfusion on different aspects of cognition in the mouse model previously described. Similar work has already been conducted (Shibata et al., 2007) however; the use of separate cohorts for the analysis of pathology and behaviour in this study prevent the definite attribution of the observed cognitive changes solely to changes in

white matter. This point is of particular relevance given the findings presented in chapter 3 where a spectrum of white and grey matter pathology was observed in animals following hypoperfusion. This caveat will be overcome by the present study where parallel analysis of pathology and behaviour will be conducted. This will permit the exclusion of hypoperfused animals displaying any evidence of obvious ischaemic damage to grey matter (as described in chapter 3), thus allowing more definite conclusions being drawn as to the role of white matter pathology in the development of cognitive deficits.

This study tests the hypothesis that in addition to precipitating damage to the myelin component of white matter, chronic cerebral hypoperfusion will impact detrimentally on cognition.

4.1.1 *Aims of study*

This study sought to further investigate and characterise the selective components of white matter which are damaged in response to chronic cerebral hypoperfusion in a mouse model and also to investigate how chronic cerebral hypoperfusion may impact on different aspects of spatial learning and memory.

4.2 Methods

4.2.1 Animals, group sizes and experimental design

For this study three cohorts of C57Bl/6J mice (aged 3-4 months) were set up (table 4.1) and hypoperfusion was induced as described in section 2.2. In cohort 1, cued learning and spatial reference memory were assessed using a water maze task (Schenk and Morris, 1985); behavioural testing ended and analysis of pathology was undertaken at 1 month post surgery. In cohort 2, cued learning and serial spatial

learning and memory (as a measure of episodic memory) were assessed using a trials to criterion task (Chen et al., 2000), also in the water maze, behavioural testing ended and analysis of pathology was undertaken at two months post surgery. In cohort 3 spatial working memory was assessed using an 8-arm radial arm maze (Shibata et al., 2007), behavioural testing ended and analysis of pathology was undertaken at two months post surgery. All surgery conducted on animals described in this chapter was performed by Dr. Karen Horsburgh.

Table 4.1 Initial cohort sizes

Treatment / Cohort/ Task	Sham	Hypoperfusion
1 (Spatial reference memory)	n=12	n=14
2 (Trials to criterion)	n=12	n=18
3 (Spatial working memory)	n=10	n=16

4.2.2 *Pathological analysis*

4.2.2.1 *Histological assessment of gray matter pathology*

Haematoxylin and eosin (H&E) staining, as described in section 2.5, was used to identify areas of ischaemic damage to neuronal perikarya. Staining of cohort 1 was conducted by the author, staining of cohorts 2 and 3 were conducted by Miss Jess Smith and Miss Yanina Tsenkina. Assessment of histological staining in cohorts 1 and 2 was undertaken by the author. In cohort 3 this was performed by Miss Yanina Tsenkina.

4.2.2.2 *Immunohistochemical assessment of white matter pathology*

MAG immunostaining was used to investigate changes in myelin integrity in response to hypoperfusion. dMBP immunostaining was used to investigate levels of degraded myelin following hypoperfusion. APP immunostaining was used to investigate the presence of axonal pathology in response to hypoperfusion. Iba-1 immunostaining was used to investigate microglial upregulation in response to hypoperfusion. Immunostaining and quantification was conducted as described in section 2.6 where damage was assessed using a grading score (MAG, dMBP and APP) regions were scored bilaterally; for quantification of microglial activation, cell counts from each hemisphere were averaged. Immunostsaining of sections from cohort 1 was undertaken by the author, sections from cohorts 2 and 3 were immunostained by Mrs Fiona Scott and Mr Tommy Dingwall. Analysis of sections from cohorts 1 and 2 was undertaken by the author. Immunostained sections from cohort 3 were analysed by Miss Yanina Tsenkina.

4.2.2.3 *Regions of interest*

Sections adjacent to those used for histological staining were selected for immunohistochemical staining. White matter structures quantified in these sections, were, corpus callosum, external capsule, internal capsule, hippocampal fimbria, optic tract and the white matter fibre bundles of the striatum (Fig. 4.1).

4.2.3 *Behaviour: Assessment of spatial reference learning and memory, serial spatial learning and memory and spatial working memory*

For full details of behavioural testing see section 2.3. The spatial reference memory task was conducted by the author and Miss Aisling Spain. The trials to criterion task was conducted by Miss Aisling Spain, Miss Yanina Tsenkina and Miss Jess Smith. The radial arm maze task was conducted by the author, Miss Aisling Spain and Miss Yanina Tsenkina.

4.2.4 *Statistics*

Statistical analysis of behavioural data and data obtained from analysis of pathology was conducted as outlined in section 2.9.2. Pathology was examined as follows, initially Fisher's exact test was used to determine whether the probability of damage ocurring to white matter components was increased following hypoperfusion. Mann-Whitney U tests were used to compare loss of myelin integrity, levels of axonal pathology and levels of degraded myelin between sham and hypoperfused animals. All data were analysed by the author.

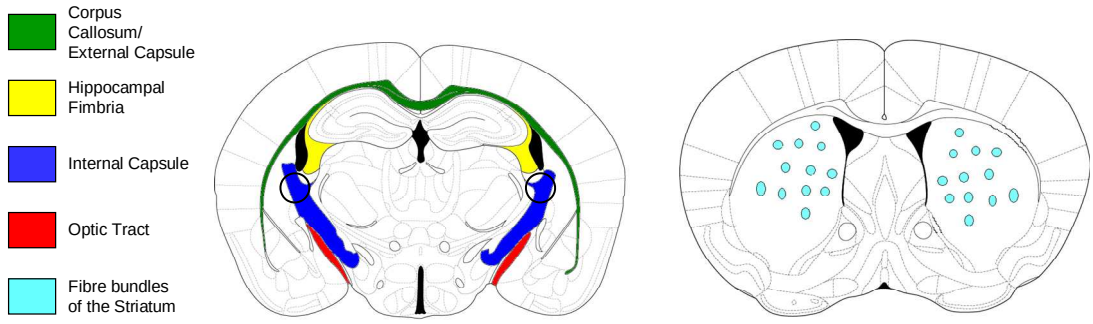

Figure 4.1 White matter regions of interest

Pathology was examined in the corpus callosum, external capsule, internal capsule (area assessed circled), hippocampal fimbria, optic tract and the white matter fibre bundles of the striatum. Images adapted from Franklin and Paxinos (1997).

4.3 Results

4.3.1 Recovery after surgery

All animals recovered well from surgery except two hypoperfused animals from cohort 1, three hypoperfused animals from cohort 2 and four hypoperfused animals from cohort 3 which were culled due to poor recovery. See table 4.2 for cohrt sizes following surgery.

Table 4.2 Cohort sizes following surgery

Treatment / Cohort	Sham	Hypoperfusion
1 (Spatial reference memory)	n=12	n=12
2 (Trials to criterion)	n=12	n=15
3 (Spatial working memory)	n=10	n=12

4.3.2 *Exclusion criteria*

The specific purpose of this study was to examine the impact of hypoperfusion on white matter pathology and how hypoperfusion may impact on cognition. For this reason, prior to analysing data from behavioural testing and analysis of pathology, exclusion criteria were set.

4.3.2.1 *Exclusion criteria- pathology*

Animals from all three cohorts, where evidence of overt ischaemic damage to neuronal perikarya was observed in H&E sections, were excluded from analysis of behavioural data and further analysis of white matter pathology.

4.3.2.2 *Exclusion criteria- behavioural testing*

In cohorts 1 & 2, which were subject to behavioural testing in the water maze, animals exhibiting floating behaviour were excluded. Floating behaviour was defined as floating persistently on consecutive trials over consecutive days. Animals exhibiting floating behaviour were also omitted from analysis of pathology. See table 4.3 for excluded animals and final cohort sizes for further pathological and behavioural analysis.

Table 4.3 Animals excluded on the basis of exclusion criteria

Cohort	No. of animals starting study **(sham/ hypoperfused)**	No. of animals displaying floating behaviour **(sham/ hypoperfused)**	No. of animals with evidence of overt ischaemic damage **(sham/ hypoperfused)**	Final no. of animals included in analysis **(sham/ hypoperfused)**
1 (Spatial reference memory)	Sham=12 Hypo=12	Sham=3 Hypo=1	Sham=0 Hypo=2	Sham=9 Hypo=9
2 (Trials to criterion)	Sham=12 Hypo=15	Sham=1 Hypo=1	Sham=0 Hypo=4	Sham=11 Hypo=10
3 (Spatial working memory)	Sham=10 Hypo=12	n/a	Sham=0 Hypo=9	Sham=10 Hypo=3

4.3.3 *Pathology*

4.3.3.1 *Histological examination of grey matter following hypoperfusion*

There was no evidence of ischaemic damage (as defined in section 2.5.3) to neuronal perikarya in any sham animals. In cohort one, 2 of 12 hypoperfused animals displayed evidence of overt ischaemic damage to neuronal perikarya in the hippocampus and striatum. In cohort two, 4 of 15 hypoperfused animals displayed evidence of overt ischaemic damage to neuronal perikarya in the hippocampus and striatum. One of these animals also displayed evidence of a cortical infarction. In

cohort three, 9 of 12 animals displayed evidence of overt ischaemic damage to neuronal perikarya in the hippocampus and striatum. As stated above, animals displaying evidence of ischaemic damage to neuronal perikarya were initially excluded from further analysis (table 4.3).

4.3.3.2 *Detailed analysis of white matter following hypoperfusion*

Detailed analysis of white matter pathology was conducted in cohorts 1, 2, and 3 following behavioural testing, at one and two months following induction of hypoperfusion. There was no difference in the extent of white matter damage between the three cohorts ($p < 0.05$; Kruksal-Wallis; Coltman et al (2010)). All pathology data presented in this chapter are from analysis of pathology in cohort 1.

4.3.3.3 *Assessment of myelin integrity following hypoperfusion*

The probability of a loss of myelin integrity following hypoperfusion was increased ($p = 0.015$; Fig 4.2B , F, I), Fisher's exact test. In sham operated animals, the majority of animals displayed no evidence of myelin damage as assessed by MAG immunostaining (Fig. 4.2B). In the sham animal where a disruption of myelin integrity was observed, this was minimal (grading score 1). In hypoperfused animals, a spectrum of myelin damage was observed, from modest to severe (Fig. 4.2F). Disruption of myelin integrity was widespread and apparent in most regions of most animals. Myelin damage was significantly increased in hypoperfused animals as compared to shams ($p = 0.004$; Fig 4.2I) Mann-Whitney-U test.

4.3.3.4 *Assessment of dMBP immunostaining following hypoperfusion*

dMBP immunostaining was conducted to assess levels of degraded myelin (Fig. A2, B). The probability of myelin damage occurring following hypoperfusion was increased ($p < 0.001$; Fig A1 A,B,C), Fisher's exact test. In one out of nine sham animals where degraded myelin was observed, this was at low levels. Degraded myelin was present in all hypoperfused mice. There was a significant increase in levels of degraded myelin in hypoperfused mice as compared to shams (Fig. A1 C; $p < 0.001$) Mann Whitney-U test.

4.3.3.5 *Assessment of axonal integrity following hypoperfusion*

Axonal damage was assessed via APP immunostaining. The probability of axonal damage occurring following hypoperfusion was not increased ($p = 0.082$; Fig 4.2C, G, J), Fisher's exact test. No sham animals displayed any evidence of axonal pathology in any region examined (Fig. 4.2C). Minimal axonal pathology was evident in four out of nine hypoperfused animals (Fig. 4.2G). Axonal pathology was not increased in hypoperfused animals as compared to shams ($p = 0.094$; Fig. 4.2J) Mann Whitney-U test.

4.3.3.6 *Assessment of microglial activation following hypoperfusion*

Activated microglia were present to varying degrees in all regions assessed in all animals, both sham and hypoperfused. Hypoperfused animals displayed elevated levels of microglial activation as compared to shams, although this difference was not significant ($p = 0.509$; Fig. 4.2 D, H, K) Student's t-test.

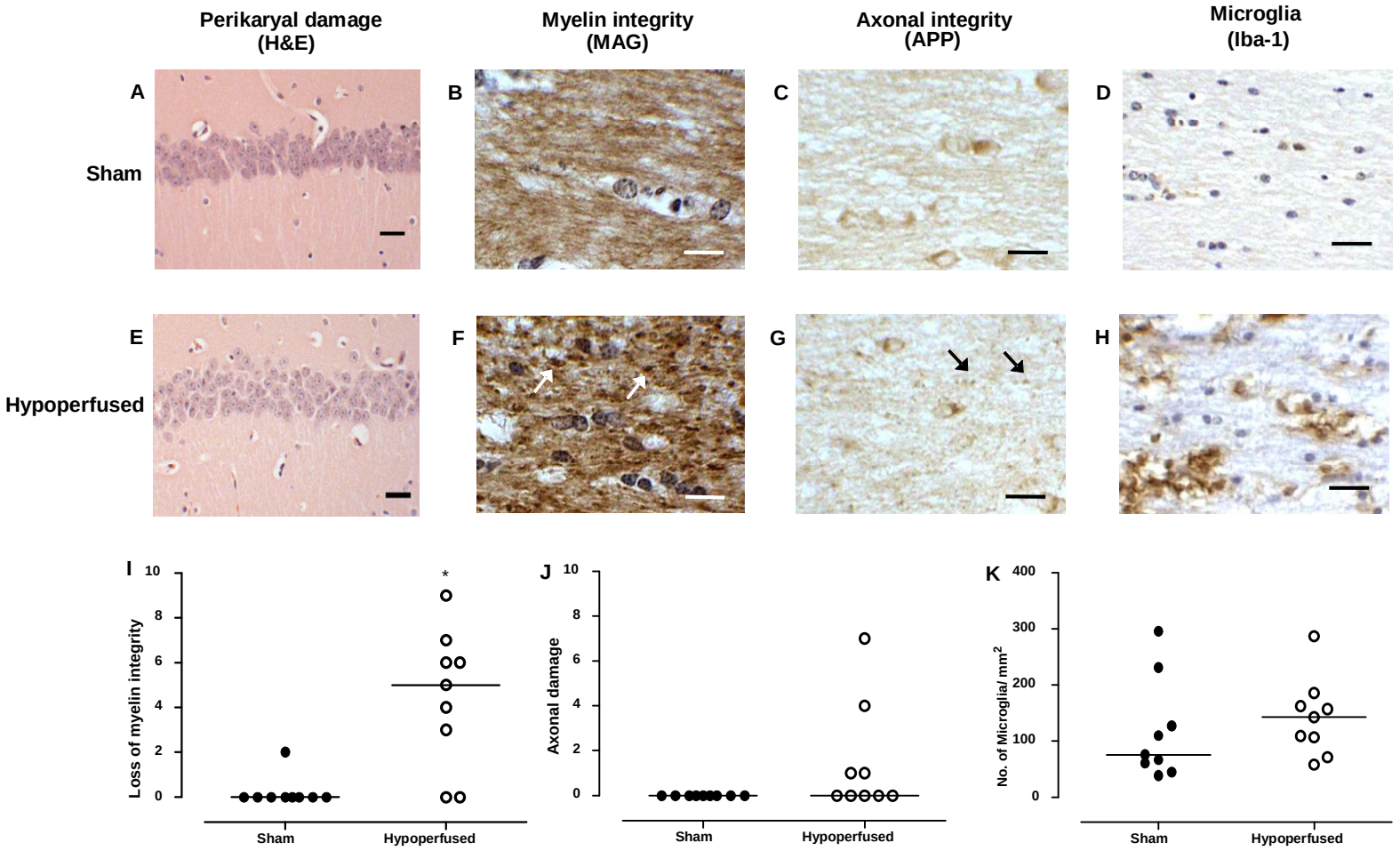

Figure 4.2 Assessment of pathology following hypoperfusion

Representative images of pathology following hypoperfusion. Neuronal cell bodies in the CA1 were intact in most hypoperfused animals (A, E) Scale bar = 30μm. The probability of myelin disruption occurring following hypoperfusion induced using 0.18mm diameter microcoils was significantly increased (I; p=0.015). The probability of axonal pathology occurring following hypoperfusion was not increased (J; p= 0.082) Fisher's exact test. Disruption of myelin (white arrows) was significantly increased in hypoperfused animals as compared to shams (B, F, I; p=0.004; median values- sham 0, hypoperfused 5). There was no significant difference in levels of axonal pathology (black arrows) between sham and hypoperfused animals following one month of hypoperfusion (C, G, J; p=0.094; median values- sham 0, hypoperfused 0) Mann Whitney-U test. Microglial activation was noticeably, but not significantly upregulated in hypoperfused mice (D, H, K; p=0.509; mean values- sham 116.8 ± 29.78 , hypoperfused 142.2 ± 22.97 activated microglia mm^2). Two tailed Student's t-test. n=9 sham, 9 hypoperfused. Images of white matter pathology taken from the optic tract. Scale bar = 15μm.

4.3.4 *Behaviour*

4.3.4.1 *Assessment of spatial reference learning and memory in the watermaze following hypoperfusion*

Of the 24 (n=12 sham/ 12 hypoperfused) animals in cohort one which underwent behavioural testing, 6 animals in total were excluded from analysis of behaviour based on the exclusion criteria described in section 4.3.2 (n = 3 sham/3 hypoperfusion). This gave final group numbers of n = 9 sham/9 hypoperfusion.

4.3.4.2 *Cued task*

All mice were able to complete the cued navigation task. Average swim speed for sham animals was 26.41 ± 0.97cms (average ± SEM) whilst hypoperfused animals averaged 26.44 ± 0.93 cms. Swim speeds did not differ significantly between sham and hypoperfused animals $|t| = 0.024$, df = 16, $p = 0.981$ (Fig. 4.6A). A repeated measures ANOVA of the latency to reach the platform across days for sham and hypoperfused animals revealed a significant difference over days [$F(5,80) = 21.961$, $p < 0.001$], but no significant difference between groups [$F(1,16) = 0.002$, $p = 0.97$] (Fig. 4.6B), neither was there a significant interaction [$F(5, 80) = 1.333$, $p = 0.273$]. By the last day of the task following surgery (day 5), escape latencies averaged less than 10 seconds for animals from both groups.

4.3.4.3 *Spatial reference learning*

A repeated measures ANOVA conducted to compare escape latencies over the five training days showed a significant effect of day [$F(4,64) = 10.327$, $p < 0.001$], but no significant effect of group [$F(1,16) = 0.206$, $p = 0.66$] (Fig. 4.5C)

neither was there a significant group x day interaction [F(4, 64) = 0.412, p = 0.80]. These data show that the performance of sham and hypoperfused animals improved significantly throughout the duration of the task and that hypoperfusion had no impact on the ability of experimental animals to learn the task.

4.3.4.4 *Spatial reference memory retention*

Following probe trials, % time spent in each quadrant of the maze was analysed. A significant effect of quadrant was found at both the short term (10 mins) [F(3,48) = 44.996, $p < 0.001$] (Fig. 4.6D) and long term time points (24 hours) [F(3,48) = 22.903, $p < 0.001$] (Fig. 4.6E). No significant group effect was found (10mins: [F(1,16) = 0.105, p = 0.75]; 24 hours: [F(1,16) = 1.8, p = 0.199]). There was no significant group x quadrant interaction (10 min: [F(3,48) = 0.088, p = 0.97]; 24 hours [F(3,48) = 0.664, p = 0.53].

Compared to chance, both hypoperfused and sham animals spent significantly more time in the training quadrant during each probe trial (10 mins: hypoperfused t = 5.894, $p < 0.001$, df = 8; sham t = 6.56, $p < 0.001$, df = 8; 24 hours: hypoperfused t = 4.131, $p < 0.003$, df = 8; sham t = 4.70, $p < 0.002$, df = 8) Fig. 4.6 D&E.

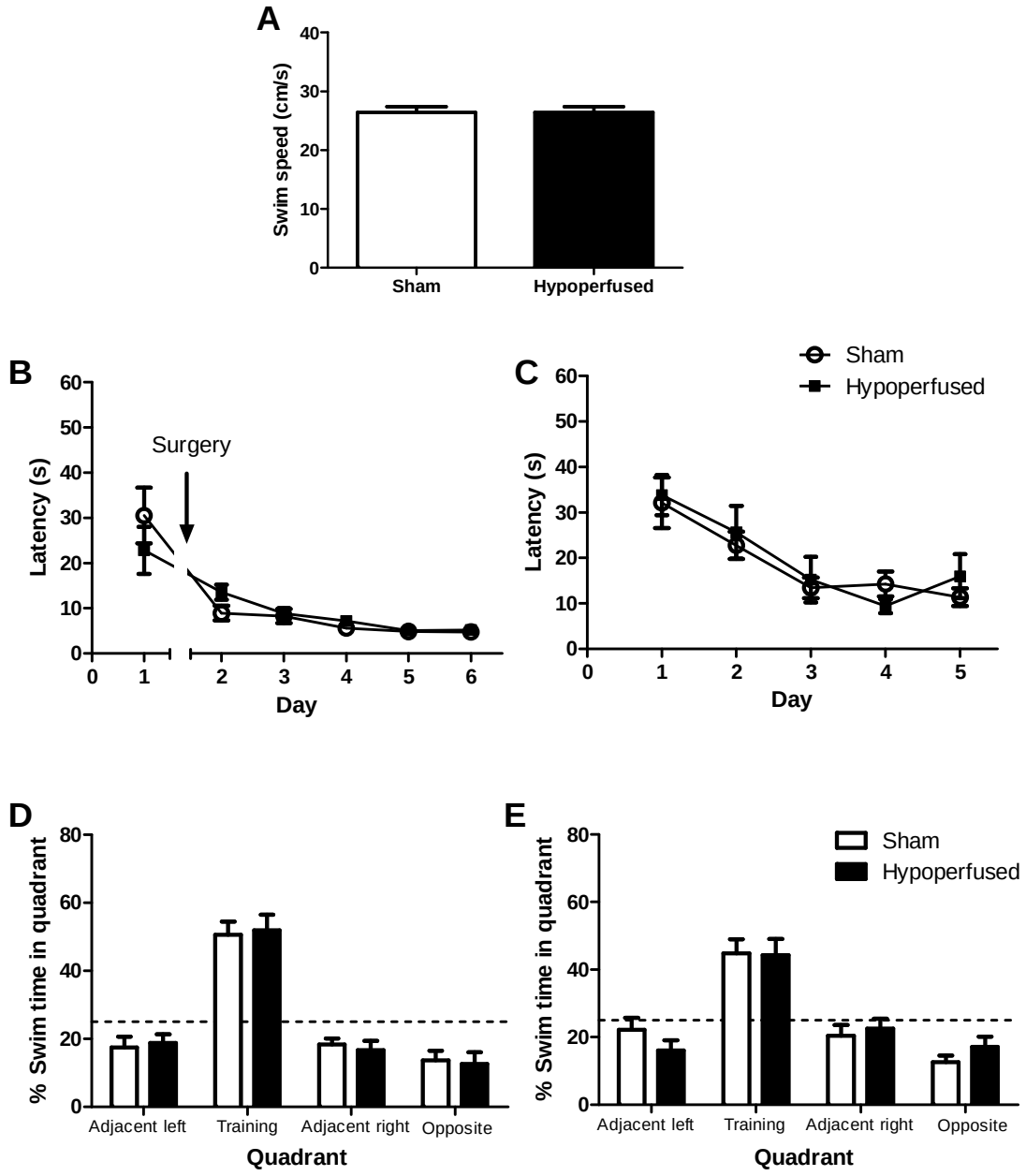

Figure 4.3 Spatial reference memory testing in the water maze

Data are expressed ± SEM. Sham n = 9; hypoperfused n = 9 (A) Swim speeds did not differ between sham and hypoperfused animals (p = 0.981 mean values- sham= 26.41 ± 0.97cm/s, hypoperfused= *26.44 ± 0.93cm/s); two-tailed Student's t-test. (B) Performance of both groups on the cued task improved significantly over training days (p < 0.001). Hypoperfused animals performed as well as shams (p = 0.97); two-way ANOVA. (C) Spatial reference learning was unaffected by hypoperfusion (p = 0.66), the performance of both groups improved significantly across days (p < 0.001); two-way ANOVA. Sham and hypoperfused animals performed equally well during probe tests conducted at (D) 10 mins. (p = 0.75) and (E) 24 hours (p = 0.199) following spatial reference learning; two-way ANOVA. In both probe tests sham and hypoperfused animals spent significantly more time in the training quadrant compared to chance (dashed line); 10 mins. (p < 0.001); 24 hours (p < 0.002); one sample Student's t-test.*

4.3.4.5 *Assessment of serial spatial learning and memory*

Of the 27 (n = 12 sham/15 hypoperfused) animals in cohort two which underwent behavioural testing, 6 animals in total were excluded from analysis of behaviour based on the exclusion criteria described in section 4.3.2 (n = 1 sham/5 hypoperfusion). This gave final group numbers of n = 11 sham/ 10 hypoperfusion.

4.3.4.6 *Cued task*

All mice were able to complete the cued navigation task. Average swim speed for sham animals was 25.25 ± 1.04cm/s (average ± SEM) whilst hypoperfused animals averaged 26.44 ± 0.76 cm/s. Swim speeds did not differ significantly between sham and hypoperfused animals $|t| = 0.901$, $df = 19$, $p = 0.379$ (Fig. 4.7A). A repeated measures ANOVA of the latency to reach the platform across days for sham and hypoperfused animals revealed a significant difference over days [$F(4,76) = 34.538$, $p < 0.001$], but no significant difference between groups [$F(1,19) = 0.054$, $p = 0.82$] (Fig 4.7B). There was no significant group x day interaction [$F(4,76) = 0.16$, $p = 0.958$]. By the last day of the task (day 5), escape latencies averaged less than 10 seconds for animals from both groups.

4.3.4.7 *Serial spatial learning and memory*

A repeated measures ANOVA across the first 5 platform locations revealed the number of trials to learn the platform location to criterion did not change across the first five tasks [$F(4,76) = 1.57$, $p = 0.192$] and also that hypoperfusion did not impact on rate of learning across the tasks [$F(1,19) = 0.04$, $p = 0.853$] (Fig 4.7C). Neither was there a significant group x task interaction [$F(4,76) = 0.52$, $p = 0.718$].

Analysis of % time spent in the training quadrant in the probe tests at 10 mins and 3 hours for the first five platform locations revealed that there was no difference in the amount of time that sham and hypoperfused animals spent in the training quadrant; 10 mins [$F(1,18) = 0.02$, $p = 0.894$] Fig. 4.7D; 3 hours [$F(1,19) = 0.15$, $p = 0.702$] (Fig. 4.7E). Sham and hypoperfused animals were able to learn the same number of platform locations over the first ten days of testing ($|t| = 0.756$, $df = 18$, $p = 0.459$) (Fig. 4.7F).

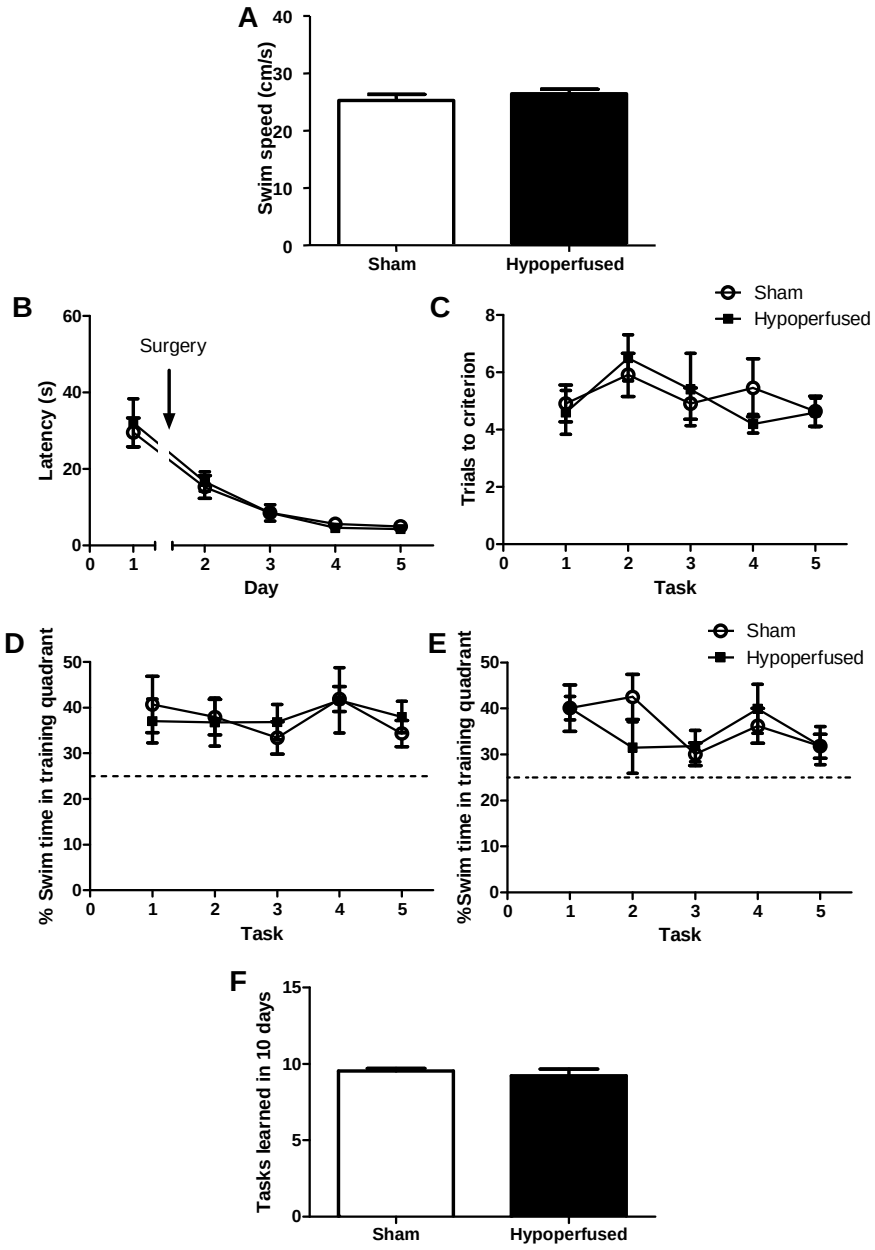

Figure 4.4 Serial spatial reference memory testing in the water maze

Data are expressed ± SEM. Sham n=11; Hypoperfused n=10 (A) Swim speeds did not differ between sham and hypoperfused animals (p = 0.379 mean values- sham= 25.25 ± 1.04cm/s, hypoperfused= 26.44 ± *0.76cm/s); two-way Student's t-test. (B) Both groups improved significantly on the cued task over training days (p<0.001). Hypoperfused animals performed as well as shams (p=0.82). (C) Serial spatial reference learning was unaffected by hypoperfusion (p=0.853), there was no change in number of trials to learn platform location across tasks (p=0.192). Sham and hypoperfused animals performed equally well during probe tests conducted at (D) 10 mins. (p=0.894) and (E) 24 hours (p=0.702) following spatial reference learning; two-way ANOVA. In both probe tests sham and hypoperfused animals spent significantly more time in the training quadrant compared to chance (dashed line). (F) There was no difference in the number of platform locations learned across the first 10 days between sham and hypoperfused animals (p=0.459 mean values- sham= 9.55* ± 0.16 tasks, hypoperfused= 9.22 ± *0.43 tasks); two-way student's t-test.*

4.3.4.8 *Assessment of spatial working memory in the radial arm maze*

Of the 22 (n = 10 sham/12 hypoperfused) animals in cohort three which underwent behavioural testing, 9 hypoperfused animals were excluded from analysis of behaviour based on the exclusion criteria described in section 4.3.2. This gave final group numbers of n=10 sham/ 3 hypoperfusion.

In the radial arm maze task, hypoperfused mice made significantly more working memory (revisiting) errors as compared to sham operated controls [$F(1,11) = 7.93$; $p = 0.017$; Fig. 3.3A]. The number of errors committed per trial by both sham and hypoperfused animals diminished across the training period [$F(7,77) = 8.94$; $p < 0.001$] (Fig. 4.8A). The number of novel arm entries made in the first eight entries did not differ between sham and hypoperfused animals [$F(1,11) = 1.74$; $p = 0.213$]. Over the training period the number of novel arm entries in the first eight entries improved significantly for both groups [$F(7,77) = 2.58$; $p= 0.019$] (Fig. 4.8B).

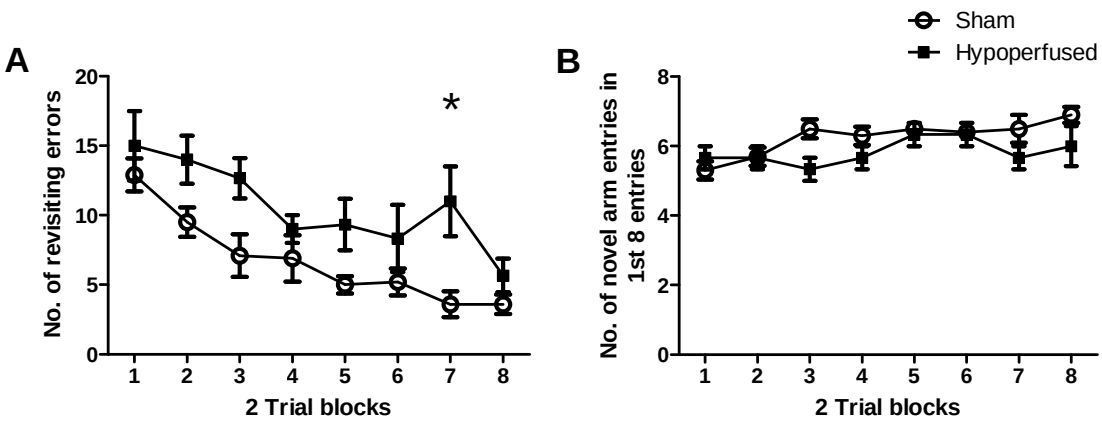

Figure 4.5 Spatial working memory testing in the 8-arm radial arm maze

Data are expressed ± SEM. Sham n=10; Hypoperfused n=3 (A) Sham and hypoperfused animals made significantly fewer revisiting errors across trials ($p<0.0001$). Hypoperfused animals made significantly more revisiting errors as compared to shams ($p=0.017$); two-way ANOVA. (B) Sham and hypoperfused animals made significantly more novel arm entries in the first 8 entries as training progressed ($p=0.019$), the number of novel arm entries made in the first eight entries did not differ between sham and hypoperfused animals ($p=0.213$); two-way ANOVA.

4.3.4.9 *Assessment of behaviour in animals displaying evidence of ischaemic neuronal damage*

Latterly, analysis of behavioural data was conducted to compare animals where evidence of ischaemic neuronal damage was observed with sham and hypoperfused animals displaying only selective white matter damage. All figures relating to this analysis are contained within appendix two. In the spatial reference memory and trials to criterion tasks swim speeds did not differ between any of the 3 cohorts ($p = 0.576$ and $p = 0.227$ respectively; one-way ANOVA; Figs. A2.1A, & A2.2A). In both water maze tasks a repeated measures ANOVA of the latency to reach the platform across days for all 3 cohorts revealed a significant difference over days (SRM- [$F(5,85) = 9.29$, $p < 0.001$], Fig A2.1B; TTC- [$F(4,88) = 37.5$, $p < 0.001$], Fig. A2.2B) and also a significant difference between the groups where ischaemic animals performed significantly worse as compared to the other groups (SRM- [$F(2,85) = 7.11$, $p = 0.006$]; TTC- [$F(2,88) = 3.86$, $p = 0.037$]). There was no significant group x day interaction. In each case however, by the last day of the task, escape latencies averaged less than 10 seconds for all animals.

In the spatial reference learning task a repeated measures ANOVA to compare latencies over the five training days showed a significant effect of day [$F(4,68) = 4.33$, $p = 0.004$] but no significant effect of group [$F(2,68) = 1.49$, $p = 0.254$] (Fig. A2.1C). There was no significant group x day interaction. Following probe trials a significant effect of quadrant was found at both the short term (10 mins [$F(3,51) = 32.81$ $p < 0.001$]) and long term time points (24 hours [$F(3,51) = 11.05$, $p < 0.001$]). No significant group effect was found (10 mins: [$F(2,51) = 0.81$, $p = 0.459$]; 24

hours: [$F(2,51) = 0.67$, $p = 0.526$]). There was no significant group x quadrant interaction. Compared to chance, all animals spent significantly more time in the training quadrant during each probe trial (10 mins: hypoperfused $t = 5.894$, $p < 0.001$, $df = 8$; sham $t = 6.56$, $p < 0.001$, $df = 8$; 24 hours: hypoperfused $t = 4.131$, $p < 0.003$, $df = 8$; sham $t = 4.70$, $p < 0.002$, $df = 8$) (Figs. A2.1 D&E).

In the trials to criterion task a repeated measureas ANOVA across the first 5 platform locations revealed that animals displaying evidence of ischaemic damage took significantly more trials to learn the platform location across the first five tasks [$F(4,88) = 4.41$, $p = 0.003$] and also that ischaemic animals did not learn at the same rate as animals in the other two cohorts [$F(2,88) = 4.07$, $p = 0.031$] (Fig. A2.2C). There was no significant group x task interaction [$F(8,88) = 1.37$, $p = 0.222$]. Analysis of time spent in the training quadrant in the probe tests at 10 mins and 3 hours for the first five platform locations revealed that there was no difference in the amount of time that animals from any cohort spent in the training quadrant; 10 mins [$F(2,84) = 0.03$, $p = 0.973$] (Fig. A2.2D); 3 hours [$F(2,88) = 0.99$, $p = 0.386$] (Fig. A2.2E). Animals with ischaemic neuronal damamge learned fewer tasks in the first ten days than animals from the other two cohorts ($p = 0.013$; Fig. A2.2F); one-way ANOVA with Tukey's multiple comparison post-test.

In the radial arm maze task, as well as hypoperfused animals, ischaemic animals also made significantly more working memory (revisiting) errors as compared to shams [$F(2,119) = 10.61$, $p = 0.001$]. The number of errors committed per trial by all 3 groups diminished across the period [$F(7,119) = 11.18$, $p < 0.001$] (Fig. A2.3A).

Animals from the ischaemic group also made significantly fewer novel arm entries in the first eight as compared to animals from the sham and hypoperfused groups [$F(2,119) = 4.06$, $p = 0.036$]. Over the training period the number of novel arm entries in the first eight entries improved significantly for all three groups [$F(7,119) = 3.63$, $p = 0.001$](Fig. A2.3B).

4.4 Discussion

The results from the study presented in this chapter support the hypothesis that chronic cerebral hypoperfusion results in the development of diffuse white matter pathology and that hypoperfusion is associated with the development of cognitive changes. More specifically, hypoperfusion results in a selective deficit in working memory whilst spatial reference learning and memory and episodic memory remain intact. Analysis of data gathered from animals displaying evidence of ischaemic damage revealed neuronal cell damage within the hippocampus appeared to impact on serial spatial reference learning.

This is the first study to assess behaviour and pathology in the same cohort of animals following hypoperfusion. This parallel assessment accounts for the main difference between the present study and that of Shibata et al (2007). The fact that Shibata et al did not do this precludes the definite attribution of any cognitive changes observed to the presence of white matter pathology alone. The importance of this is highlighted when the number of animals from the RAM study reported in this chapter displaying evidence of ischaemic damage to neuronal perikarya is considered. In the present study 75% of hypoperfused animals which underwent RAM testing displayed evidence of ischaemic damage and so were excluded from

the study, leaving only n = 3 animals for behavioural/pathological analysis. Even so a behavioural deficit was observed thus demonstrating the robustness of this finding. This finding has been replicated several times since within the Horsburgh group. One reason as to why experimental animals from the RAM study displayed a higher incidence of ischaemic damage as compared to the other two cohorts examined may have been due to food deprivation (required for the RAM task; see section 2.3.2.1). Several hypoperfused animals displayed evidence of seizure activity during the RAM task and also in the animal housing facility. Food deprivation is known to lead to altered nutritional status and can lead to abnormally low glucose levels and potentially hypoglycaemia. Hypoglycaemia has been linked to seizure activity and in some cases, to the development of ischaemic neuronal cell death in both animals (Auer et al., 1984) and humans (Auer, 1986) and also the development of deficits in some aspects of spatial memory (Hershey et al., 2005). This highlights the failure of Shibata et al to make a parallel assessment of pathology and behaviour in the same animals as a major limitation.

In addition to their behavioural findings Shibata et al reported that rarefaction of the white matter and glial activation had occurred at 30 days following hypoperfusion (Shibata et al., 2004; Shibata et al., 2007). As discussed in chapter 3, one of the advantages conferred by the present study over that of Shibata et al is the detail with which white matter pathology was examined i.e. via immunohistochemical as opposed to histological examination. In the present study this advantage is further extended through the use of additional antibodies (dMBP and Iba-1). These provide further information as to the components of white matter impacted by hypoperfusion. In agreement with the findings of Shibata et al

hypoperfusion was associated with an upregulated inflammatory response as evidenced by the infiltration of activated microglia to regions of interest examined. Also, as reported in chapter 3 and by others (Holland et al., 2010), immunohistochemical analysis of white matter cellular components confirmed that a key pathological feature of this model is myelin damage and a loss of myelin integrity, as evidenced by dMBP and MAG immunostaining respectively.

It is well established that a correlation exists between hippocampal integrity and intact spatial reference memory (Pappas et al., 1997; D'Hooge and De Deyn, 2001). In the present study selective white matter pathology was found to be present in animals which displayed an impairment in spatial working memory, however, spatial reference learning and memory were unaffected in animals displaying the same levels of pathology. This finding is consistent with that of Shibata et al. (2007). More recently a study was conducted (Miki et al., 2009) utilising a modified version of this model, where BCAS was induced by placing a 0.18mm dia microcoil on one common carotid artery and a 0.16mm dia. microcoil on the other, to investigate the impact of hypoperfusion on the development of white matter pathology and the subsequent impact on cognition. In contrast to the present study, Miki et al. (2009) reported a spatial reference memory deficit in hypoperfused animals as tested using the same watermaze task described in this chapter. This was in conjunction with relatively severe myelin pathology, axonal pathology and accompanying astroglial and microglial upregulation. However they also reported increased levels of ischaemic damage to neuronal perikarya in the hippocampus in a majority of hypoperfused animals. Miki et al. (2009) also reported that hypoperfused animals exhibited less anxiety in an open field test and those

hypoperfused animals exhibiting the most severe CBF reductions (< 30% of baseline levels at day 6 following surgery) displayed evidence of sensorimotor dysfunction when assessed with a rotorod test. The authors attributed this to infarction in the motor and somatosensory cortex although no conclusive pathological evidence was produced in support of this.

In a study (Nishio et al., 2010) designed to investigate longer term pathological and cognitive changes in this model, Nishio et al (2010) found a spatial reference memory deficit using a Barnes maze test at 6 months following hypoperfusion, they also reported working memory deficits similar to those reported in this chapter following 5 months of hypoperfusion. Histological and immunohistochemical examination of pathology in experimental animals following 8 months of hypoperfusion revealed apoptotic neuronal cell death had occurred in both the hippocampus (CA1 & CA3 sub regions) and cortex.

Whilst both of the studies described above (Miki et al., 2009; Nishio et al., 2010) reported a spatial reference memory deficit in response to hypoperfusion, unlike the study described in this chapter, damage to hippocampal neuronal perikarya was found in the majority of experimental animals. This is of interest given that animals displaying evidence of ischaemic neuronal cell loss in the hippocampus in the present study were able to complete the SRM task as successfully as both hypoperfused and sham animals. Of further interest is the fact that in the more challenging serial spatial reference memory task (TTC) ischaemic animals performed significantly worse than sham and hypoperfused animals; taking more trials to learn the platform location across the first five tasks, their rate of learning was slower and they learned fewer tasks over the first ten days of training. The likely reason for this

is due to the added complexity of the TTC task as compared to the SRM task (discussed below). It is well known that the hippocampus plays a major role in spatial memory formation and retention and that hippocampal damage can cause spatial memory impairment (D'Hooge et. al. 2001). It may be that the levels of ischaemic damage observed in animals was not severe enough to impact on spatial reference memory but was severe enough to cause a serial spatial memory impairment. An alternative reason as to why no impairment was found in spatial learning and memory in the animals displaying evidence of ischaemic damage may be due to group size (n=2) and high levels of variance in the data (see appendix A2). In order to investigate this fully, further work using a larger cohort needs to be undertaken.

Deficits in episodic memory and task switching are recognised as an early feature of dementia in humans and have been linked to a loss of white matter integrity (Deary, 2003; Bucur et al., 2008). The trials to criterion protocol utilised by the present study is designed to measure serial spatial learning and memory in mice and is considered a measure of 'episodic like memory' (Chen et al., 2000). This task requires a degree of memory flexibility as successful task performance relies on the ability of animals to constantly update successive platform locations in relation to fixed visual cues in their environment and also to recall the platform location relevant to the current trial (as opposed to previous platform locations). Whilst it has been shown that hippocampal integrity is required for intact episodic memory (Dickerson and Eichenbaum, 2009) and therefore successful completion of this task, the contribution of white matter is unknown. Results from the current study indicate that a loss of white matter integrity did not impact on spatial memory

flexibility, memory retention or learning capacity as hypoperfused animals performed equally well as compared to shams. This suggests that hypoperfusion had no impact on episodic memory in the animals tested, or, alternatively the task is not sensitive/ challenging enough to detect subtle changes which may occur as a result of the diffuse pathology observed.

In the present study it has been demonstrated that selective myelin pathology is associated with a deficit in spatial working memory whilst other elements of spatial memory- spatial reference memory and serial spatial memory remain intact. The underlying reason for this may lie in the degree of behavioural flexibility required for successful performance in different behavioural tasks and also the neuroanatomical basis for these different aspects of cognition.

In the RAM task utilised by the present study and also Shibata et al (2007) a greater degree of memory flexibility is required than in either the spatial reference memory or the trials to criterion water maze tasks. To perform effectively in the spatial reference memory task, animals need to learn only one platform location, whilst platform location in the trials to criterion task needs updating only daily. However, in the RAM task a greater degree of memory flexibility is required as animals are required to constantly update their memory (during the task) with information as to which arms food has been retrieved from. This frequent updating and retrieval of information is likely to require input from many different, anatomically discrete, brain regions and so will rely heavily on intact white matter pathways for successful integration of information (Bucur et al., 2008). A further point of interest is that animals displaying evidence of ischaemic damage performed significantly worse than sham animals in the RAM task, it could be argued that this

would be expected given that white matter damage in this group was likely more severe than in hypoperfused animals where no ischaemic damage had occurred (based on the findings presented in chapter 3). Additionally, animals wth ischaemic damage made fewer novel arm entries in the first 8, in order to ascertain whether this is due to the more severe levels of myelin damage observed in this group or to ischaemic neuronal cell damage, further studies need to be conducted.

Pathology results from this study and also chapter 3 have demonstrated that myelin pathology following hypoperfusion is widespread and diffuse in nature, affecting all regions assessed. This prevents the working memory deficit described in this chapter being attributed to damage in a specific anatomical region. It is unknown exactly which or how many brain regions underlie functional spatial working memory. However, evidence from research conducted suggests that the neuroanatomical basis for functional working memory is considerably more complex than other components of spatial memory and is dependent on a number of distinct regions and their communication with one another. These include, fronto-cortical circuitry, in particular, subsets of neurons within the prefrontal cortex (Fuster, 1973; Funahashi, 2006), posterior parietal and occipital areas (Ricciardi et al., 2006), the CA3 sub region of the hippocampus (Kesner, 2007) and also parahippocampal areas (Hodges, 1996). If this is correct then the underlying cause of the working memory deficit demonstrated by RAM testing as described above may be attributed to the observed loss of myelin integrity and subsequent disconnection of these regions. This is supported by work conducted in models of myelin loss e.g. the plp over-expressing mouse (Kagawa et al., 1994), where working memory deficits have been linked to decreased conduction velocities (Tanaka et al., 2009) and also imaging

studies where increased fractional anisotropy (the physiological correlate of which is thought to be increased myelination and axonal diameter) has been observed within the corpus callosum in individuals following training in a working memory task (Takeuchi et al., 2010).

It could be argued that a potential limitation of the study presented in this chapter and also the previous chapter was failure to measure CBF as a means to providing evidence of hypoperfusion following BCAS had occurred. However, published data exist (Shibata et al., 2004; Shibata et al., 2007) which demonstrates hypoperfusion following BCAS occurs in this model, furthermore, the presence of ischaemic damage to neuronal perikarya in some BCAS operated animals in the present study suggests a reduction in CBF is present following coil placement. A further limitation of this study is that no other physiological correlates of learning and memory were examined following induction of hypoperfusion. These may have included synaptic no., acetylcholine levels/ acetylcholine receptor no., NMDA receptor no. or conduction speed of action potentials, failure to do so means that the deficits in working memory observed following hypoperfusion described above cannot unequivocally be attributed to the white matter pathology observed.

Nonetheless, the findings presented in this chapter represent one of the first studies to conduct a parallel assessment of behaviour and pathology in the same animals following BCAS induced hypoperfusion. This has allowed the identification of cellular components of white matter which are selectively vulnerable to hypoperfusion and to additionally show that modest levels of hypoperfusion, in isolation, can be sufficient to induce deficits in spatial working memory, whilst other components of spatial memory (spatial reference memory and

serial spatial memory) remain intact. Whilst the mechanisms underlying the development of white matter damage following hypoperfusion remain unknown it seems likely that this damage directly contributes to the working memory deficit observed, possibly through disruption of flow of electrical information and signal integration (due to a loss of myelin integrity) as neurons in anatomically distinct brain regions communicate with one another. These findings are clinically relevant in that they demonstrate that hypoperfusion alone may precipitate the development of white matter damage and changes in cognition in the absence of other confounding factors which are often present in elderly individuals presenting with cognitive impairment e.g. hypertension, diabetes and atherosclerosis. The results of the study presented in this chapter have now been published (Coltman et al., 2010).

Once the model of hypoperfusion had been established and characterised the next aim was to study the impact of hypoperfusion on white matter pathology and amyloid levels in a mouse model of Alzheimer's disease.

Chapter 5: The impact of hypoperfusion of varying severities on the extent of white matter and Aβ pathology in a mouse model of AD

5.1 Introduction

A large body of evidence exists linking vascular risk factors which underlie the development of chronic cerebral hypoperfusion and the development of AD in later life (for reviews see (de la Torre, 2002; de la Torre, 2004; de la Torre and Alireza, 2009). These risk factors include hypertension, atherosclerosis and heart failure. Furthermore, recent advances in neuroimaging technology (e.g. SPECT scanning) have identified specific patterns of cerebral hypoperfusion which have been shown to precede the development of clinical AD symptoms (Matsuda, 2007). Another feature which has been recognised as an early event occurring prior to the emergence of clinical symptoms in AD is a loss of white matter integrity (de la Monte, 1989; Bartzokis et al., 2003). Additionally, at *post-mortem*, white matter abnormalities have been shown to exist in the brains of at least 66% of AD patients (Roher et al., 2002). These changes in cerebral perfusion and white matter, in some cases, may occur decades prior to AD diagnosis; however, their contribution to disease onset remains unclear.

At the outset of this thesis studies investigating CBF and white matter abnormalities in transgenic models of AD had been conducted however very few have investigated the link between the two.

This study investigates the hypothesis that hypoperfusion will exacerbate white matter pathology in 3xTg-AD mice. Also, hypoperfusion will induce the development of elevated levels of intraneuronal amyloid pathology and will precipitate the development of extracellular plaque pathology.

5.1.1 *Aims of study*

This study sought to investigate how chronic cerebral hypoperfusion of varying severities, induced using 0.18mm dia. and 0.16mm dia. microcoils, may impact on grey and white matter and intraneuronal amyloid in 3xTg-AD mice.

5.2 Methods

5.2.1 *Animals and experimental design*

Two cohorts of male 3xTg-AD mice (aged 3-4 months) were studied (table 5.1a). Hypoperfusion was induced as described in section 2.2. In cohort 1, hypoperfusion was induced for a period of one month using 0.18mm diameter microcoils. In cohort 2, a more severe level of hypoperfusion was induced for a period of one month using 0.16mm diameter microcoils. Sham animals from each cohort underwent an identical procedure except that microcoils were not applied. Circle of Willis anatomy was compared between C57Bl/6J and 3xTg-AD mice in the absence of any surgery in a third cohort of animals (table 5.1b) as described in section 2.8.

Table 5.1a Initial cohort sizes

Treatment / Cohort	Sham	Hypoperfusion
1 (0.18mm dia. coil one month)	n=12	n=13
2 (0.16mm dia. coil one month)	n=7	n=14

Table 5.1b Cohort size for comparison of Circle of Willis anatomy

Strain / Cohort	C57Bl/6J	3xTg-AD
3 (Comparison of Circle of Willis anatomy)	n=6	n=7

5.2.2 *Pathological analysis*

5.2.2.1 *Histological assessment of gray matter pathology*

Haematoxylin and eosin (H&E) staining, as described in section 2.5, was used to identify areas of ischaemic damage to neuronal perikarya.

5.2.2.2 *Immunohistochemical assessment of white matter pathology*

MAG immunostaining was used to investigate changes in myelin integrity in response to hypoperfusion. APP immunostaining was used to investigate levels of axonal pathology in response to hypoperfusion. Iba-1 immunostaining was used to investigate microglial upregulation in response to hypoperfusion. 4G8 immunostaining was used to investigate changes in white matter Aβ levels in response to hypoperfusion. Immunostaining and quantification was conducted as described in section 2.6 other than for quantification of microglial activation where a grading scale (0-3) was used. The scale was as follows; 0- no activated microglia, 1- baseline activation, few sparsely distributed activated cells, 2- marked upregulation, many activated cells present throughout region, 3- very dense patches of many activated cells. APP and 4G8 immunostaining was conducted by the author, MAG and Iba-1 immunostaining was conducted by Mrs Fiona Scott and Mr Tommy Dingwall.

5.2.2.3 *Immunohistochemical assessment of intraneuronal APP and Aβ levels*

APP immunostaining was used to investigate changes in intraneuronal levels of APP in response to hypoperfusion. 4G8 immunostaining was used to investigate changes in intraneuronal Aβ levels in response to hypoperfusion. Immunostaining was conducted as described in section 2.5 and analysed using image analysis as described in section 2.6. For regions of interest see Fig. 5.1.

5.2.2.4 *Regions of interest*

In this study hemi brain sections were stained and analysed. White matter regions of interest examined were external capsule, internal capsule, hippocampal fimbria, and white matter fibre bundles of the striatum. Intraneuronal APP and Aβ levels were examined in the hippocampal and cortical pyramidal neurons (Fig. 5.1).

5.2.3 *Western blot assay of whole brain homogenate*

Protein extracts were prepared from frozen hemi brains and their concentrations assessed. Samples were separated via SDS-gel electrophoresis and subject to Western blot analysis to investigate protein levels as described in section 2.7. For antibodies and concentrations used see table 2.3.

5.2.4 *Comparison of Circle of Willis anatomy*

A further study was conducted as part of this chapter to compare Circle of Willis (CoW) anatomy between C57Bl/6J and 3xTg-AD mice as described in section 2.8. This was done following pathological analysis to investigate whether strain

specific differences in CoW architecture might underlie the more robust response of 3xTg-AD mice as compared to C57Bl/6J mice to BCAS.

5.2.5 *Statistical analysis*

Results for image analysis of intraneuronal APP, intraneuronal Aβ and Western blot analysis were analysed by Student's t-test. Scores following analysis of MAG, APP and Iba-1 immunostaining were analysed as described in chapters 2, 3 and 4. Results were considered significant when $p < 0.05$.

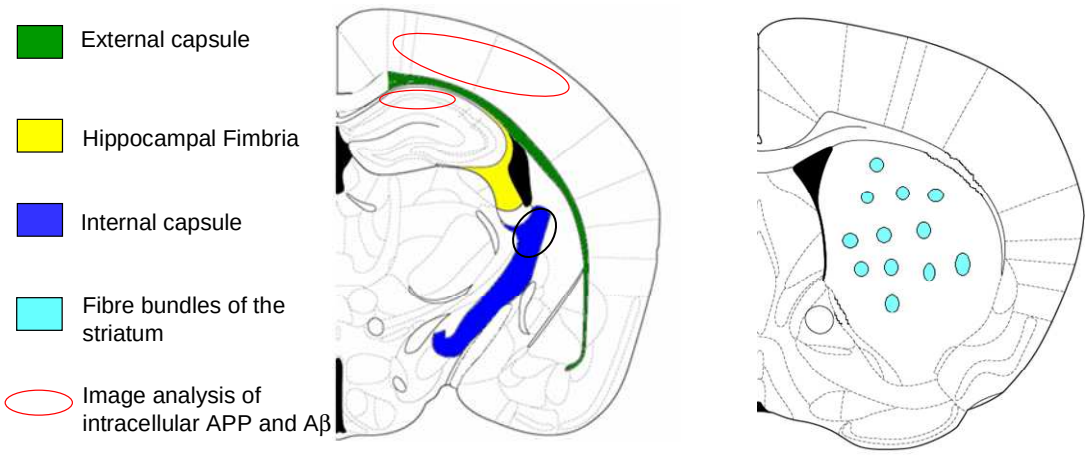

Figure 5.1 White and grey matter regions of interest
White matter regions of interest were the external capsule, internal capsule (area assessed circled, hippocampal fimbria, and white matter fibre bundles of the striatum. Grey matter regions of interest were the CA1 hippocampal subregion and layer IV/ V pyramidal neurons in the cortex. Images adapted from Franklin and Paxinos (1997)

5.3 *Results*

5.3.1 *Recovery from surgery*

All animals recovered well from surgery with the exception of one hypoperfused animal from cohort one and six hypoperfused animals from cohort two, which were culled due to poor recovery. See table 5.2 for final group sizes.

Table 5.2 Final cohort sizes

Treatment / Cohort	Sham	Hypoperfusion
1 (0.18mm dia. coil one month)	n=12	n=12
2 (0.16mm dia. coil one month)	n=7	n=8

5.3.2 Histological examination of grey matter following hypoperfusion

No sham animals from either cohort displayed any evidence of ischaemic damage to neuronal perikarya (as defined in section 2.5.3). In cohort 1, in which BCAS was induced by 0.18mm dia. coils, there was no ischaemic damage to neuronal perikarya. In cohort 2, where animals were subjected to a more severe level of stenosis using 0.16mm dia. microcoils, ischaemic damage was seen in six of eight hypoperfused animals. Five of these animals showed evidence of ischaemic damage in the striatum, three of these also had ischaemic damage in the cortex and one displayed evidence of ischaemic damage in the CA1 and CA3 hippocampal subregions, the sixth animal displayed evidence of ischaemic damage in the cortex

only. Where cortical damage had occurred this was limited to neurons in the upper cortical layers (I, II & III).

5.3.3 *Immunohistochemical analysis of white matter pathology following hypoperfusion*

5.3.3.1 *Assessment of myelin integrity following hypoperfusion*

The probability of a loss of myelin integrity following hypoperfusion induced using 0.18mm diameter microcoils was not increased ($p = 1.000$; Fig 5.2A, B, D), Fisher's exact test. In cohort 1, there were no alterations in myelin integrity in the majority of sham and hypoperfused animals (Fig. 5.2A, B), however in a small subset of animals, 4 sham and 5 hypoperfused animals, minimal myelin damage was observed. This was manifest as disorganisation of myelinated fibres, deposition of myelin debris and vacuolation as described in chapters two, three and four of this thesis. In animals where myelin damage was evident it was widespread and diffuse in nature. Overall myelin integrity did not differ between sham and hypoperfused animals in this cohort (Fig 5.2D; $p = 0.764$) Mann Whitney-U test.

The probability of a loss of myelin integrity following hypoperfusion induced using 0.16mm diameter microcoils was significantly increased ($p = 0.026$; Fig 5.2A,C,E), Fisher's exact test. In cohort 2, most sham animals displayed no evidence of myelin pathology, in those where pathology was evident (3 of 7) it was mild to moderate. A spectrum of pathology was seen across all hypoperfused animals from cohort 2 (Fig 5.2C). Despite there being a higher probability of damage to myelin occurring following BCAS induced using 0.16mm diameter microcoils, overall, the extent of myelin damage was not significantly increased in hypoperfused animals as

compared to shams (Fig 5.2E; $p = 0.159$) Mann-Whitney-U test. In the majority of hypoperfused animals where ischaemic damage had occurred, damage to myelinated fibres was markedly increased (Fig. 5.E highlighted red).

5.3.3.2 *Assessment of axonal pathology following hypoperfusion*

In all animals, modest APP immunostaining was observed in oligodendrocytes in white matter regions, this was accompanied by a subtle axonal pathology (small swellings/axonal bulbs). This was particularly prominent in the hippocampal fimbria, internal capsule and fibre bundles of the striatum.

The probability of axonal damage occurring following hypoperfusion induced using 0.18mm diameter microcoils was not increased ($p = 0.626$; Fig 5.2F, G, I), Fisher's exact test. In cohort 1 hypoperfusion did not exacerbate axonal pathology as compared to shams (Fig. 5.2F, G, I; $p = 0.626$) Mann-Whitney-U test; however in one hypoperfused animal more severe axonal pathology (large axonal bulbs/swellings) was observed in the hippocampal fimbria.

The probability of axonal damage occurring following hypoperfusion induced using 0.16mm diameter microcoils was not increased ($p = 0.214$; Fig 5.2F, H, J), Fisher's exact test. In cohort 2, similarly, hypoperfusion did not exacerbate axonal pathology (Fig. 5.2 F, H, J; $p = 0.284$) Mann-Whitney-U test. However, in 5 of 6 animals from this cohort, where areas of ischaemic damage were observed, localised patches of moderate to severe axonal pathology (denoted by frequently occurring large axonal bulbs/ swellings) was also evident in white matter (inset Fig. 5.2H). This was observed in the striatum of 5 animals, in 3 of these moderate to severe

axonal pathology was also observed in areas within the internal capsule, and in one of these, severe axonal pathology was also evident in the hippocampal fimbria.

5.3.3.3 *Assessment of microglial activation following hypoperfusion*

The presence of activated microglia was evident in all animals, both sham and hypoperfused in both grey and white matter. Generally, more activated microglia were present in hypoperfused animals as compared to shams in each cohort examined, however, inter animal variability was high and there was no significant difference between sham and hypoperfused mice (Fig. 5.2 K, L, M, N, O; cohort 1, $p = 0.652$; cohort 2, $p = 0.11$). Additionally, microglial activation tended to be higher in hypoperfused animals where a more severe level of stenosis had been induced (cohort 2) and was highest in those where evidence of ischaemic damage was identified (Fig. 5.2O). In animals where there was evidence of localised areas of severe myelin disruption, moderate to severe axonal pathology or altered Aβ levels; dense, localised patches of activated microglia were also visible (Fig. 5.2M, inset).

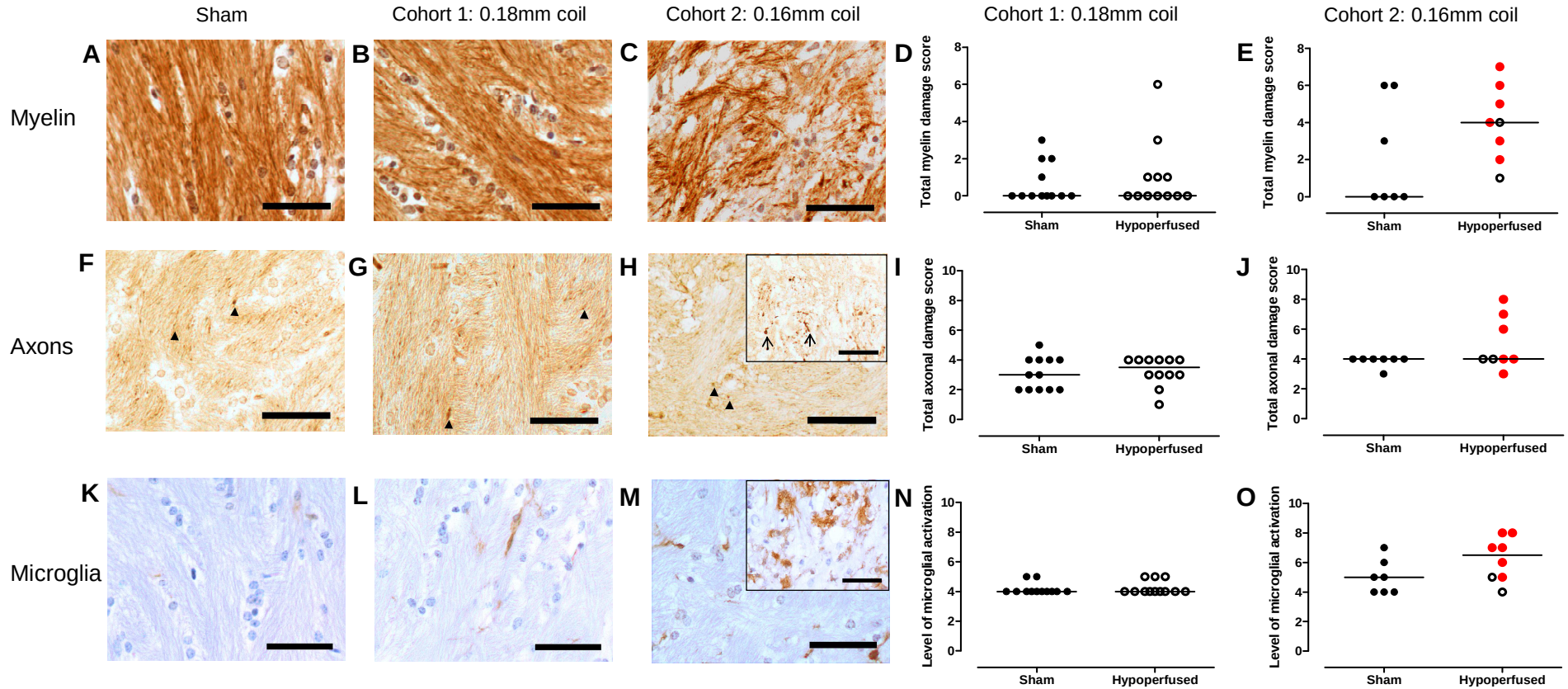

Figure 5.2 Immunohistochemical examination of white matter following hypoperfusion

Representative images from the internal capsule of sham (A, D, G) and hypoperfused animals; cohort 1 (n=12 sham, 12 hypoperfused B, E, H) and cohort 2 (n=7 sham, 8 hypoperfused C, E, I,). The probability of myelin damage occurring was increased following hypoperfusion induced using 0.16mm but not 0.18mm diameter micricoils (p= 0.026 and p= 1.000 respectively. The probability of axonal damage occurring following hypoperfusion was not increased (cohort 1, p=0.626, I; cohort 2, p=0.214) Fisher's exact test. Animals where ischaemic damage to neuronal perikarya was observed in cohort 2 are highlighted in red (E, J, O). MAG immunostaining (A, B, C) revealed no significant difference in levels of myelin damage between sham and hypoperfused animals in cohort 1 (p=0.764, median values- sham = 0, hypoperfused=0, D), or cohort 2 (p= 0.159, median values- sham = 0, hypoperfused=4) Mann Whitney-U test. APP immunostaining revealed that in all animals, axonal pathology was present (arrowheads D,E,F). Overall axonal pathology was not increased following hypoperfusion (cohort 1, (p=0.626 median values- sham=3, hypoperfused=3.5), I; cohort 2, (p=0.284 median values- sham=3, hypoperfused=3), J) Mann Whitney-U test. In some animals subject to more a more severe level of stenosis, localised areas of severe axonal pathology were observed (inset F, open arrowheads). Iba-1 immunostaining (G, H, I) revealed microglial activation was not increased following hypoperfusion (cohort 1, p=0.652 median values- sham=4, hypoperfused=4, N; cohort 2, p=0.11, O median values- sham=5, hypoperfused=6). In some animals, subject to a more severe level of stenosis, patches of densely upregulated microglia were observed. Mann-Whitney-U test. Scale bars = 50μm.

5.3.3.4 *Investigation of white matter Aβ levels following hypoperfusion*

In all animals 4G8 immunostaining revealed low level Aβ expression was evident in oligodendrocytes in white matter regions. There was no change in levels of white matter Aβ in any region of any sham animal or any hypoperfused animal from cohort 1 (Fig. 5.3A, B).

In cohort 2 Aβ levels remained unaltered in most regions in the majority of animals (Fig 5.3C), however, in 4 of 8 hypoperfused animals, consistent with the location of moderate to severe axonal pathology, localised patches of altered Aβ levels were also observed. This was manifest as what appeared to be axonal accumulation of Aβ and was of similar appearance to the axonal swellings seen in APP stained sections, indicative of axonal pathology (inset Fig. 5.3C). Evidence of altered white matter Aβ levels was observed in the internal capsule of one animal, the striatum of another, a third animal displayed evidence of altered Aβ levels in both of these regions whilst abnormal staining was seen in the hippocampal fimbria of the fourth animal.

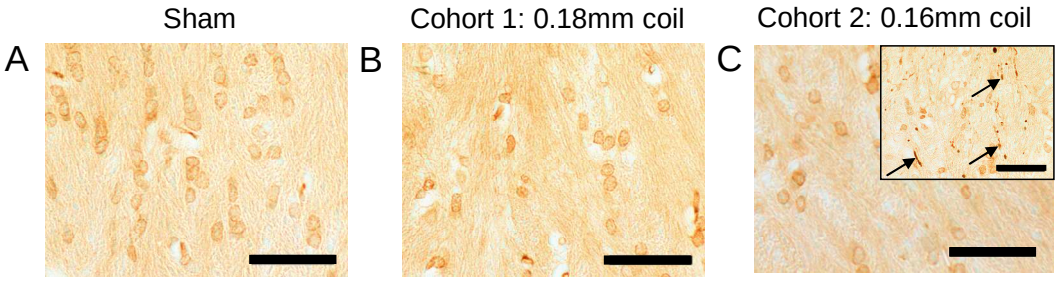

Figure 5.3 White matter Aβ levels following hypoperfusion

Representative images of 4G8 immunostaining in the internal capsule of sham (A) and hypoperfused animals from cohort 1 (B) and cohort 2 (C). White matter Aβ levels were unchanged in response to hypoperfusion, other than in 4 of 8 animals in cohort 2 (inset (C), where a more severe level of hypoperfusion had been induced. Areas where accumulations of Aβ (arrows, inset C) were present were consistent with focal areas of severe axonal pathology. Scale bar= 50μm.

5.3.4 *Western blot analysis of white matter protein levels following hypoperfusion*

5.3.4.1 *MBP Western blotting*

Western blot analysis of MBP levels in whole brain homogenate detected no change between sham and hypoperfused animals in cohort 1 (p = 0.483, Fig. 5.4 B). In cohort 2, MBP levels were significantly reduced in hypoperfused animals as compared to shams (p = 0.005, Fig. 5.4 C).

5.3.4.2 *CNPase Western blotting*

Western blot analysis of CNPase levels in whole brain homogenate detected no change in response to hypoperfusion between sham and experimental animals in either of the cohorts examined; cohort 1 (p = 0.412, Fig 5.5 B); cohort 2 (p = 0.817, Fig. 5.5 C).

5.3.4.3 *MAG Western blotting*

Western blot analysis of MAG levels in whole brain homogenate detected no change in response to hypoperfusion between sham and experimental animals in either of the cohorts examined; cohort 1 (p = 0.697, Fig. 5.6 B); cohort 2 (p = 0.283, Fig. 5.6C).

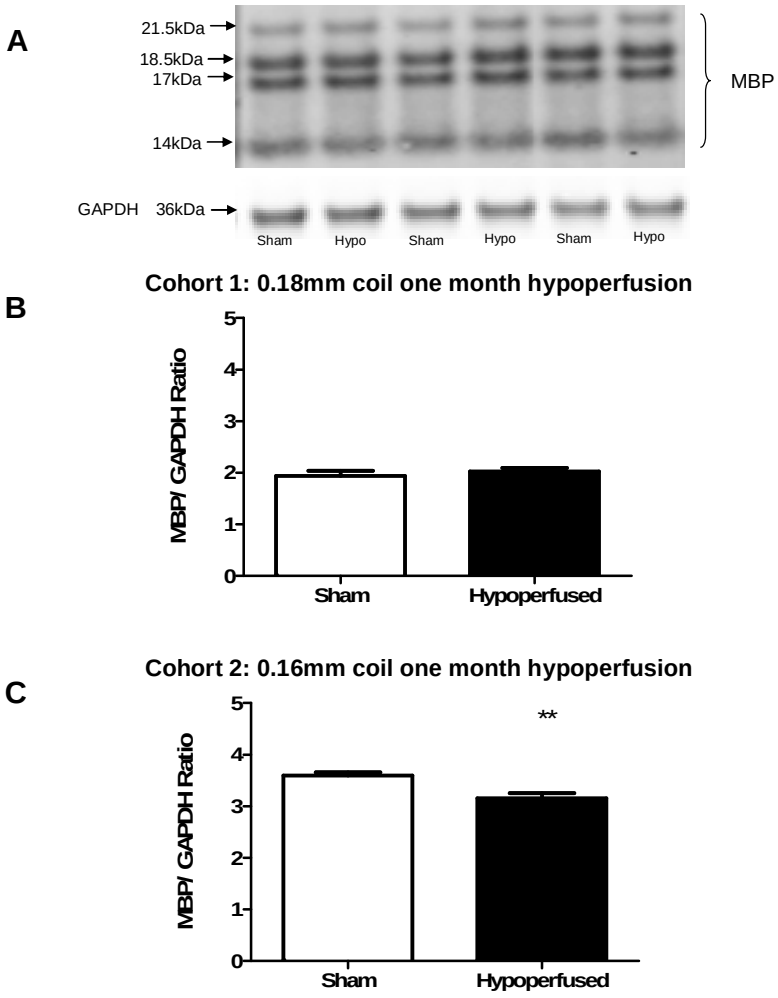

Figure 5.4 MBP levels are reduced in response to severe levels of hypoperfusion

Representative image of Western blot of MBP and GAPDH (A). Data are expressed as mean MBP/ GAPDH ± SEM. Cohort 1, n=12 sham/ n=12 hypoperfused; cohort 2, n=7 sham and 8 hypoperfused. No difference was detected in MBP levels between sham and hypoperfused animals in cohort 1 (p=0.483, mean values- sham= 1.94 ±0.09 hypoperfused= 2.02 ± 0.25, B). In cohort 2, MBP levels were significantly reduced in experimental animals as compared to shams (p=0.005, mean values- sham= 3.6 ± 0.06 hypoperfused= 3.15 ± 0.1 C). Two–tailed Student's t-test.

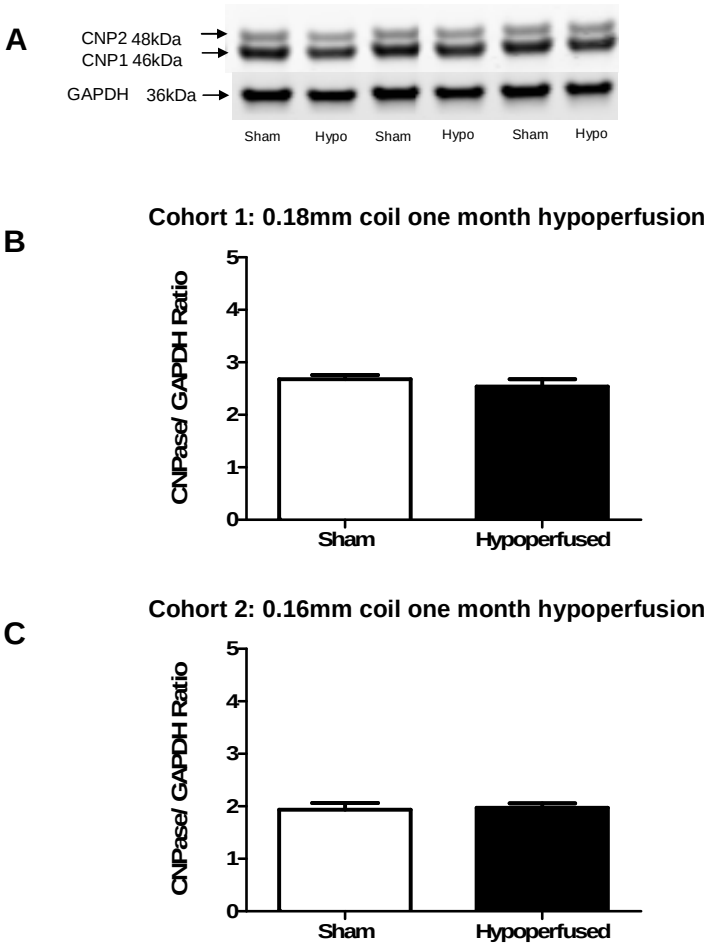

Figure 5.5 CNPase levels are unchanged in response to hypoperfusion

Representative image of Western blot of CNPase and GAPDH (A). Data are expressed as mean CNPase/ GAPDH ± SEM. Cohort 1, n=12 sham/ n=12 hypoperfused; cohort 2, n=7 sham and 8 hypoperfused. No difference was detected in CNPase levels between sham and experimental animals in either of the cohorts; cohort 1, (p=0.412, mean values- sham= 2.68 ± 0.08 hypoperfused= 2.54 ± 0.14 B), cohort 2, (p=0.817, mean values- sham= 1.94 ± 0.13 hypoperfused= 1.97 ± 0.09 C). Two-tailed Student's t-test.

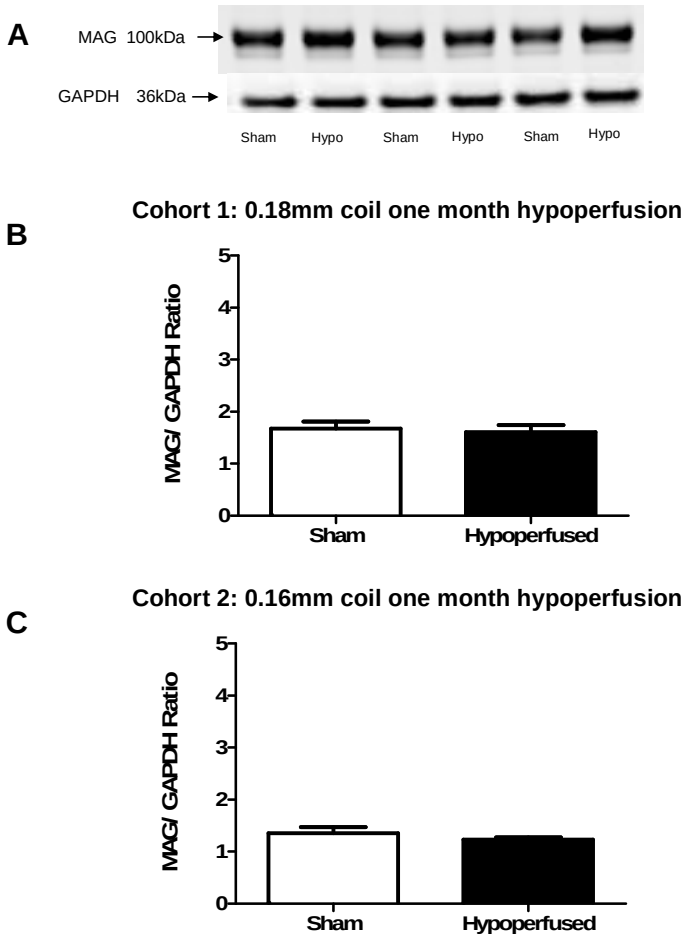

Figure 5.6 MAG levels are unchanged in response to hypoperfusion

Representative image of Western blot of MAG and GAPDH (A). Data are expressed as mean MAG/ GAPDH ± SEM. Cohort 1, n=12 sham/ n=12 hypoperfused; cohort 2, n=7 sham and 8 hypoperfused. No difference was detected in MAG levels between sham and experimental animals in either of the cohorts; cohort 1, (p=0.697, mean values- sham= 1.68 ± 0.13 hypoperfused= 1.60 ± 0.13 B), cohort 2, (p=0.283, , mean values- sham= 1.35 ± 0.28 hypoperfused= 1.23 ± 0.04 C). Two-tailed student's t-test.

5.3.5 *Image analysis of intraneuronal APP levels following hypoperfusion*

Strong cytoplasmic APP expression was observed in layer IV & V pyramidal neurons in the cortex and within neurons in the CA1, CA2 and CA3 subregions of the hippocampus in all mice. The pattern of APP immunostaining was not altered in response to hypoperfusion. There was no significant difference in intraneuronal APP staining in the CA1 region between shams (Fig. 5.4A) and hypoperfused (Fig. 5.4B) mice in cohort 1 (p = 0.200, Fig. 5.4I) or cohort 2, (p = 0.215, Fig. 5.4C, J). Similar results were obtained from analysis of cortical APP expression (appendix 1). In cohort 2, where ischaemic damage to neuronal perikarya was observed intraneuronal APP expression was reduced (Fig 5.4D)

5.3.6 *Image analysis of intraneuronal Aβ expression following hypoperfusion*

Intraneuronal Aβ was clearly visible in CA1 hippocampal pyramidal neurons and layer IV & V cortical pyramidal neurons of all mice. Staining was confined to cell bodies with no extracellular staining present in either region. There was no significant difference in intraneuronal Aβ staining in the CA1 region between sham (Fig. 5.4E) and hypoperfused (Fig. 5.4F) mice in cohort 1 (p = 0.876, Fig. 5.4K), or cohort 2 (p = 0.918, Fig. 5.4G, L). Similar results were obtained from image analysis of cortical Aβ expression (appendix 2). In cohort 2 where ischaemic damage to neuronal perikarya was observed, intraneuronal Aβ expression was reduced (Fig 5.4H).

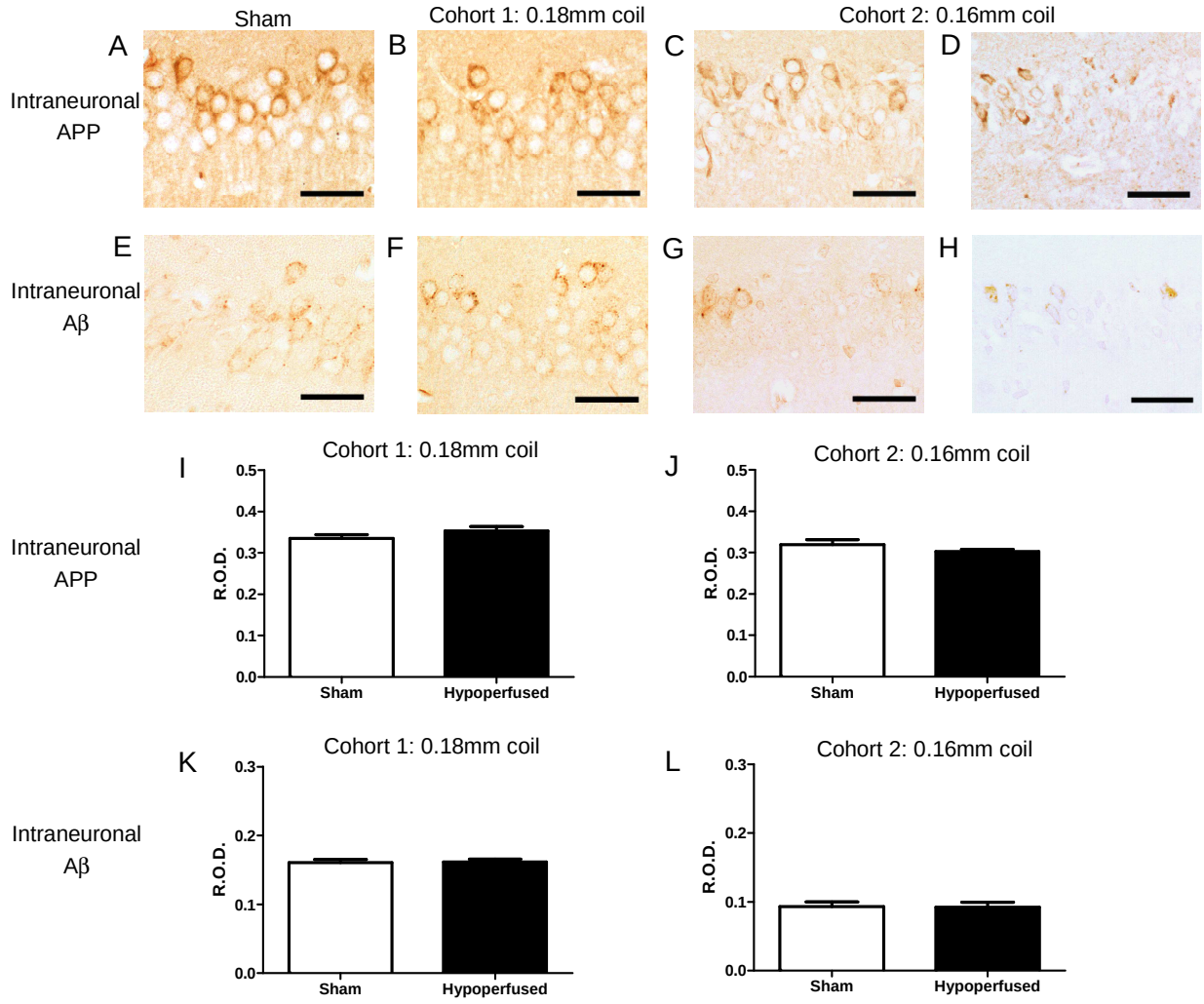

Figure 5.7 Intraneuronal APP and Aβ levels are unchanged in response to hypoperfusion

Representative images of CA1 neurons from sections immunostained for APP (A, B, C, D) and Aβ (E, F, G, H). Data are expressed as R.O.D. ± SEM. Cohort 1, n=12 sham/ n=12 hypoperfused; cohort 2, n=7 sham/ n=8 hypoperfused. Image analysis detected no difference in intraneuronal APP levels between sham and hypoperfused animals in either of the cohorts; cohort 1 (p=0.200, mean values- sham= 0.34 ± 0.01 hypoperfused= 0.35 ± *0.01 I), cohort 2 (p=0.215, , mean values- sham = 0.32 ± 0.13 hypoperfused=* 0.30 ± *0.01 J). Neither was there a difference in levels of intraneuronal Aβ between sham and hypoperfused animals in cohort 1 (p=0.876, , mean values- sham= 0.16 ± 0.01 hypoperfused=* 0.16 ± *0.01 K), or cohort 2 (p=0.918, , mean values- sham= 0.09 ± 0.01 hypoperfused=* 0.09 ± *0.01 F). Two-tailed Student's t-test. In animals from cohort 2 where ischaemic damage to neuronal perikarya was observed, intraneuronal APP and Aβ levels were reduced (D, H). Scale bar = 50μm.*

5.3.7 *Western blot analysis of APP levels following hypoperfusion*

Western blot analysis of APP levels in whole brain homogenate detected no change between sham and hypoperfused animals in either cohort 1, (p = 0.072, Fig. 5.8B), or cohort 2 (p = 0.530, Fig. 5.8C).

5.3.8 *Western blot analysis of APP C-terminal fragment levels following hypoperfusion*

There was no difference in levels of APP C-terminal fragment C99 between sham and hypoperfused animals in either cohort 1 (p = 0.664, Fig. 5.9B), or cohort 2, (p = 0.386, Fig. 5.9D). Similarly there was no difference in levels of C-terminal fragment C83 between sham and hypoperfused animals in either cohort 1 (p = 0.304 Fig.5.9C), or cohort 2 (p = 0.365, Fig. 5.9E). There was no change in the C83/C99 ratio between sham and hypoperfused animals from either cohort (appendix 3).

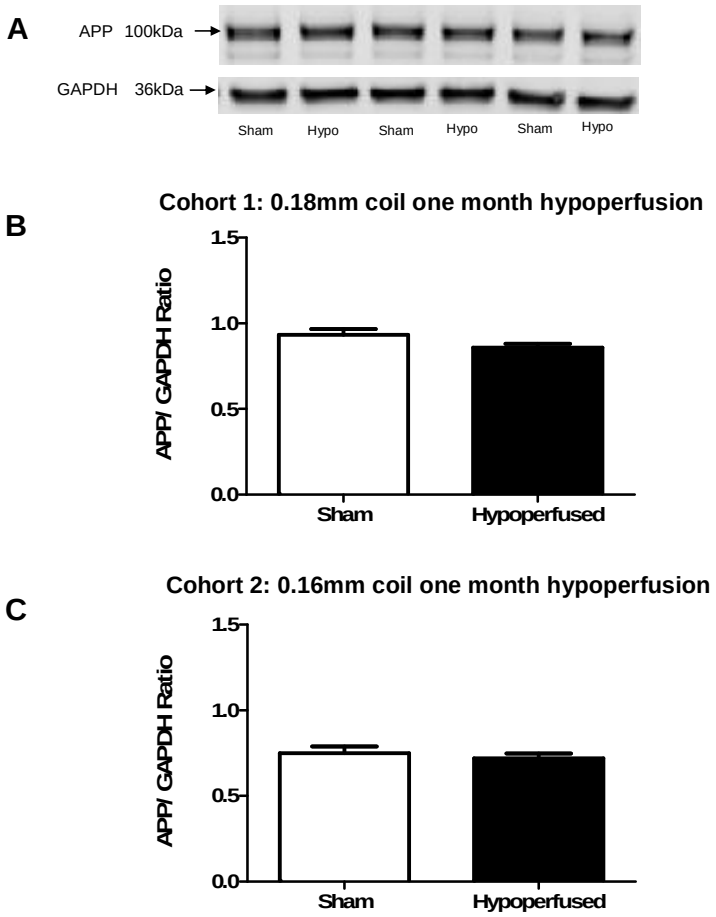

Figure 5.8 APP levels are unchanged in response to hypoperfusion

Representative image of Western blot of APP and GAPDH (A). Data are expressed as mean APP/ GAPDH ± SEM. Cohort 1, n=12 sham/ n=12 hypoperfused; cohort 2, n=7 sham/ n=8 hypoperfused. No difference was detected in APP levels between sham and experimental animals in either of the cohorts; cohort 1 (p=0.072, mean values- sham= 0.93 ± 0.03 hypoperfused= 0.86 ± 0.02 B), cohort 2 (p=0.530, , mean values- sham= 0.75 ± 0.04 hypoperfused= 0.72 ± 0.03 C). Two-tailed Student's t-test.

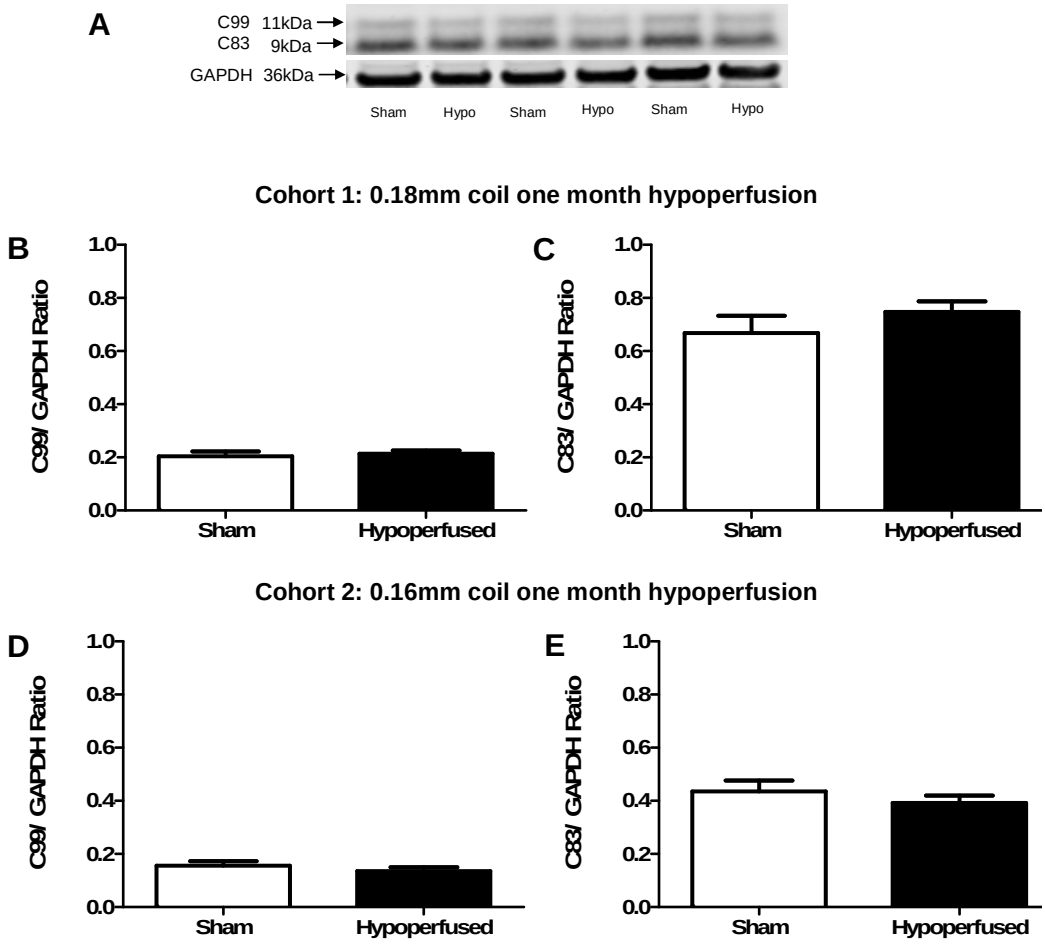

Figure 5.9 APP processing is unaffected following hypoperfusion

Representative images of Western blot of APP C-terminal fragments C83 and C99 and GAPDH (A). Data are expressed as mean C terminal fragment/ GAPDH ± SEM. Cohort 1, n=12 sham/ n=12 hypoperfused; cohort 2, n=7 sham/ n=8 hypoperfused. No difference was detected in levels of C-terminal fragments C99 or C83 between sham and experimental either of the cohorts, ***C99****- cohort 1(p=0.664, , mean values- sham= 0.2 ± 0.0.02 hypoperfused=* 0.21 ± *0.01 B), cohort 2 (p=0.386, , mean values- sham= 0.67 ± 0.07 hypoperfused= 0.75 ± 0.04 D),* ***C83****- cohort 1 (p=0.304, , mean values- sham= 0.16 ± 0.02 hypoperfused= 0.14 ± 0.0.01 C), cohort 2 (p=0.365, , mean values- sham= 0.44 ± 0.04 hypoperfused= 0.39 ± 0.03 E). Two-tai led Student's t-test.*

5.3.9 Comparison of Circle of Willis anatomy

Circle of Willis anatomy was compared between C57Bl/6J and 3xTg-AD mice as described in section 2.8. In C57Bl/6J mice (n = 6), three mice were deficient of both posterior communicating arteries (PcomA), in the three remaining mice from this group only one PcomA was present. In 3xTg-AD mice (n = 7), no animals were deficient of both PcomAs, in four animals the Circle of Willis was complete, in two animals only one PcomA was present and one animal had two PcomAs present on the same side. Thus none of the C57Bl/6J mice had a complete Circle of Willis whilst four of seven 3xTg-AD mice examined did (Table 5.3). Comparison between groups by Fisher's exact test revealed that this difference was not statistically significant ($p = 0.07$). This was verified by another observer.

Table 5.3 Comparison of Circle of Willis anatomy

Strain / No. of PcomAs	C57Bl/6J (n=6)	3xTg-AD (n=7)
2	0	4
1	3	3
0	3	0

5.4 *Discussion*

Results from the present study demonstrate that chronic cerebral hypoperfusion, induced using 0.18mm dia. microcoils in 3xTg-AD mice aged 4-5 months, does not exacerbate white matter pathology; however, carotid stenosis induced with smaller coils causes more extensive white matter pathology (axonal damage, myelin disruption/ loss and inflammation) and a greater extent of ischaemic

neuronal damage. Additionally, a more severe level of hypoperfusion is sufficient to induce subtle alterations to white matter Aβ levels in some animals. Contrary to the initial hypothesis, hypoperfusion does not impact on APP processing or on intraneuronal levels of APP or Aβ in pyramidal neurons in the hippocampus or cortex, other than in the presence of ischaemic damage to neuronal perikarya, when levels are reduced.

At the outset of this thesis no studies had been conducted to investigate how hypoperfusion may impact on the development of white matter and amyloid pathology in mouse models of AD. Subsequently there have been three of note (Kitaguchi et al., 2009; Koike et al., 2010; Yamada et al., 2011).

Kitaguchi et al. (2009) utilised the same model of hypoperfusion described in this chapter in J9 $APP^{Swd/Ind}$ (Hsia et al., 1999) mice where they found, using 0.18mm diameter coils to induce stenosis, that white matter rarefaction and gliosis had occurred following coil placement. This was in conjunction with an overall increase in extracellular levels of fibrillar Aβ and the number of cortical neurons staining immunopositive for intraneuronal $Aβ_{1–42}$. They also reported the presence of Aβ in white matter fibres in regions of interest examined, however this was not altered following hypoperfusion. These findings are in contrast to those of the present study where exacerbated white matter pathology was not observed in 3xTg-AD mice subject to the same level of stenosis, neither were there changes in intraneuronal levels of Aβ. One reason for this difference may be due to the age of animals studied 4-5 months in the present study vs 12 months in the study by Kitaguchi et al.; this is discussed below and addressed in the following chapter. An alternative

reason as to why results of the present study do not concur with those of Kitaguchi et al. may be due to strain specific differences in cerebrovascular architecture.

A further reason for the disparity between the results of Kitaguchi et al. (2009) and those presented here may be variation in methodology. A potential limitation of the present study is the use of an antibody (4G8) which does not differentiate between different forms of Aβ, furthermore recent evidence has been published demonstrating cross-reactivity occurring between 4G8 and APP (Winton et al., 2011). Kitaguchi et al only reported an increase in the number of $A\beta_{1-42}$ positive neurons not $A\beta_{1-40}$. As well as the possibility of causing a false positive result, the use of 4G8 may have masked any subtle alterations in the $A\beta_{1-40}/A\beta_{1-42}$ ratio which would have been detected had antibodies specific to each form been employed. An alternative and more sensitive method of detecting alterations in Aβ levels in response to hypoperfusion would have been to use an ELISA. This would also have allowed differences in the $A\beta_{1-40}/ A\beta_{1-42}$ ratio to be examined.

Yamada et al (2011) also utilised the BCAS model of hypoperfusion in J20 $APP^{Swd/Ind}$ (Mucke et al., 2000) to investigate the impact of hypoperfusion on cognitive function and Aβ metabolism. Yamada et al. (2011) found that overall, levels of extracellular soluble Aβ were increased in response to BCAS, this was in conjunction with decreased levels of Aβ deposition and cored plaque formation thus implying, in accordance with the findings of Kitaguchi et al. and in contrast to the findings of the present study, that Aβ metabolism is altered in response to hypoperfusion. This finding is also of interest because it lends weight to the hypothesis that extracellular amyloid plaques in AD may be broken down following upregulation of the inflammatory response as is typically seen in ischaemia

(Akiyama and McGeer, 2004). Furthermore, results from Yamada et al. demonstrated a reference memory impairment which may have been due to the increased levels of soluble Aβ, or, alternatively due to neuronal cell loss, which was observed in the hippocampus in BCAS operated transgenic mice.

Koike et al (2010) investigated the impact of mild hypoperfusion in 3xTg-AD mice utilising a different model to that described in this chapter. In their study, hypoperfusion was induced via complete ligation of the common carotid artery for a period of four minutes and the effects were studied 48 hours, three weeks and three months later. Changes to Aβ levels and levels of normal tau and phosphorylated tau were recorded acutely, however these had returned to baseline by three months. White matter changes in response to hypoperfusion were not assessed. Although findings from this study clearly indicate a link between a CBF reduction and AD pathology, it could be argued that the method of induction and duration of hypoperfusion when compared to those utilised by the present study, model less accurately the longer term, chronic changes in blood flow associated with ageing and vascular risk factors linked to AD occurrence in later life.

In the present study, exacerbated white matter pathology was only observed in animals where a more severe level of stenosis had been induced using 0.16mm diameter microcoils, furthermore this was only in animals where ischaemic damage to neuronal perikarya had occurred (75% of surviving animals). Also of note is the proportion of animals (~50%) from this cohort which had to be culled following poor recovery from surgery. Whilst no pathological study was undertaken following termination of these animals, all displayed an ischaemic phenotype (hunched, circling and ptosis) accompanied by a drop in body temperature and body weight

prior to culling. The fact that some 3xTg-AD mice were able to withstand this level of hypoperfusion suggests that collateral circulation in this strain may be more robust than in C57Bl/6J mice (discussed below).

As stated above, almost all animals which were subject to BCAS using 0.16mm dia. microcoils in the present study displayed evidence of ischaemic damage and focal areas of severe white matter pathology. Of interest, is that in animals where no ischaemic damage was observed, levels of myelin damage, axonal pathology and inflammation did not appear to be increased as compared to shams (Fig 5.3). Axonal pathology has previously been reported in transgenic models of AD (Song et al., 2004; Stokin et al., 2005; Sun et al., 2005; Wirths et al., 2006), as has damage to myelinated fibres (Games et al., 1995; Wirths et al., 2006; Desai et al., 2009; Desai et al., 2010) and also elevated levels of inflammatory cells (Games et al., 1995). Both axonal pathology and elevated levels of microglial activation have been linked with increased susceptibility to the development of ischaemia in APP transgenics (Zhang et al., 1997; Koistinaho et al., 2002). The presence of axonal pathology and also intraneuronal Aβ in the AD brain has been demonstrated to cause elevated levels of inflammation and therefore increased metabolic demand. Conversely CBF reductions have been observed in the brains of both human AD patients and transgenic AD models, in particular, and of note the 3xTg-AD mouse model has been demonstrated to have reduced cerebrovascular volume (Bourasset et al., 2009) and altered regional cerebral glucose uptake (Nicholson et al., 2009) as compared to age matched non-Tg controls. This is possibly due to the presence of Aβ, which as well as being synaptotoxic, has been shown to impact negatively on cerebrovascular reactivity (Zhang et al., 1997) and endothelial cellular function

(Thomas et al., 1996). Additionally 3xTg-AD mice have been demonstrated to have higher resting intraneuronal Ca^{2+} levels as compared to non-transgenic controls (Lopez et al., 2008). Taking these points into account, it could be argued that the AD brain is sensitised to the development of ischaemic damage following any vascular insult due to an already altered metabolism. This may be the reason why no intermediate group exists where exacerbated white matter pathology is seen in the absence of ischaemic damage following induction of stenosis using 0.16mm dia. microcoils.

Findings reported in this chapter also demonstrate that, in response to a more severe level of stenosis, MBP levels in experimental animals were reduced. A possible reason for this is myelin loss following the development of ischaemic damage (as seen in 6 of 8 surviving experimental animals). MBP levels have been shown to be altered following hypoperfusion in experimental animal models where CBF reductions are severe enough such that ischaemic damage to neuronal perikarya is observed (Kurumatani et al., 1998; Cho et al., 2006). This raises the question as to why reductions were not observed in levels of the other myelin proteins investigated, CNPase and MAG. One potential reason and one which highlights a limitation of the present study is that Western Blotting was conducted in whole brain homogenate for all proteins investigated. The abundance of CNPase and MAG is relatively low in whole brain homogenate therefore any subtle changes in these proteins may be masked due to their relatively low concentrations. Retrospectively, a more robust measure of white matter protein quantification would have been to micro-dissect out the visible white matter tracts and conduct Western blotting using this tissue instead. Also, when examining sections following MAG immunostaining, a loss of MAG was not observed as such, rather, a cellular redistribution of protein

which was evident as accumulations of myelin debris. Attempts were made to measure both MAG and MBP levels in immunostained sections using image analysis (data not reported); however no differences were found between sham and hypoperfused animals in either cohort examined. In the case of MAG this is most likely due to the reason outlined above i.e. cellular redistribution of protein. In the case of MBP this is possibly due to the sheer abundance of MBP in white matter tracts masking any detectable loss, alternatively it may be due to methodological differences. Whilst Western blotting gives a global representation of alterations in protein levels, image analysis of immunostaining only allows selected regions to be examined. It may simply be the case that regions where white matter damage had occurred were not present in sections examined.

Nonetheless the fact that MBP levels were altered raises the question of whether myelin repair is occurring in animals following hypoperfusion. Whilst there is no direct evidence for this, an interesting point to consider is the ratio of MBP isoform expression in 3xTg-AD mice. As stated in section 1.1.2.1 of this thesis the two MBP isoforms preferentially expressed in the adult mouse are 18.5 and 14kDa (Staugaitis et al., 1990) which play a role in compaction of the myelin sheath (Roach et al., 1985). However, in the 3xTg-AD mice utilised in the present study it is the 18.5kDa and 17kDa isoforms which are most abundant (Fig. 5.4). The upregulated expression of the 17kDa isoform, which is thought to play a role in myelination/remyelination (Pedraza et al., 1997) may be indicative of a repair process. It seems unlikely that this is in response to the hypoperfusion itself as other studies conducted within the Horsburgh group have shown that MBP isoform expression is normal in hypoperfused C57Bl/6J mice (Scullion, unpublished data). More importantly, isoform expression did not differ between sham and hypoperfused

animals. This differential MBP isoform expression may instead be linked to the presence of Aβ or the expression of human AD related transgenes. This hypothesis is supported by work published by (Desai et al., 2009; Desai et al., 2010), who demonstrated that region specific abnormalities in brain myelination exist in 3xTg-AD mice, possibly due to the presence of $A\beta_{1-42}$. Furthermore, a proteomics study conducted recently (Martin et al., 2008) demonstrated that MBP gene expression was upregulated in 3xTg-AD mice as compared to age matched controls. Clearly further work is required to substantiate this. However, this in itself highlights a limitation of this study; the lack of a non-transgenic control (discussed below).

Severe cerebrovascular challenges such as stroke have been identified as one of the leading risk factors for the development of AD in later life. Studies conducted in animals models of stroke have demonstrated that following an acute ischaemic insult, levels of amyloid precursor protein (APP) and Aβ are elevated (Kalaria et al., 1993; Pluta et al., 1994) and that this occurs in conjunction with the development of white matter pathology (Wakita et al., 2002).

In the study described in this chapter, changes to white matter Aβ levels were only observed in areas where moderate to severe axonal pathology (grading score 2 or 3) was evident. The impairment of axonal transport and accumulation of APP, due to disruption of the cytoskeleton in damaged axons is a common feature often seen following brain injury. In addition to stroke, this has also been observed following traumatic brain injury (McKenzie et al., 1996; Spain et al., 2010). Some studies have reported that APP is co-transported via kinesin I mediated transport along axons with the secretases (β & γ) required for its cleavage to produce Aβ (Kamal et al., 2000; Kamal et al., 2001) although evidence contrary to this has also

been published (Lazarov et al., 2005). Nonetheless it is accepted that APP containing vesicles accumulate along with amyloidogenic secretases (and other organelles) at sites of axonal injury (Stokin et al., 2005). Taking this into account, it is possible that the altered Aβ levels seen following hypoperfusion in the present study are a result of amyloidogenic APP processing at sites of axonal injury.

Contrary to the initial hypothesis set out at the beginning of this chapter, hypoperfusion did not impact on overall intraneuronal APP or Aβ levels, nor did hypoperfusion precipitate the development of amyloid plaque pathology. However, in pyramidal neurons where ischaemic damage had occurred, APP and Aβ levels were reduced, this was in conjunction with marked microglial upregulation. Microglia have been shown to express receptors which, early in AD pathogenesis promote the phagocytosis and clearance of Aβ (Hickman et al., 2008). Therefore the marked microglial upregulation in areas where ischaemic damage to neuronal perikarya was observed may account for reductions in levels of intraneuronal APP/ Aβ.

Microglial activation may also account for why overall levels of intraneuronal Aβ were unchanged. Given the considerably higher baseline levels of activated microglia observed in 3xTg-AD mice as compared to the C57Bl/6J mice utilised in chapters 3 and 4, it is possible that microglia mediated Aβ clearance is sufficient, in 3xTg-AD mice (aged 4-5 months) to prevent excess Aβ accumulation, even following the induction of hypoperfusion. Alternatively, given that hypoperfusion did not impact on the APP processing pathway, as evidenced by no change to APP C-terminal fragment levels, it is possible that hypoperfusion does not contribute to increased levels of AD pathology. Given the amount of

epidemiological evidence to the contrary, this is contentious, however based on results presented above this point cannot be dismissed. An alternative explanation may be that hypoperfusion was not present for a sufficient length of time to impact on Aβ levels.

Work conducted within this laboratory (Kelly et al., 2001) and by others (Fujii et al., 1997; Yang et al., 1997; Kitagawa et al., 1998; Maeda et al., 1998) has demonstrated that variability in cerebrovascular architecture exists between different inbred strains of laboratory mice and that this likely underlies varying susceptibility to reductions in CBF. To date, no studies have been published which have investigated cerebrovascular architecture in 3xTg-AD mice. The study presented in this chapter, to compare Circle of Willis anatomy between C57Bl/6J and 3xTg-AD mice found notable strain related differences; specifically regarding the presence of the PcomA.

Previous studies to examine the cerebrovascular architecture of C57Bl/6J wild type mice, the background strain upon which $APP^{Swe/Ind}$ transgenics are bred, and SV-129 mice (3xTg-AD mice are bred on a C57Bl/6J x SV129 background), have revealed strain specific differences in Circle of Willis anatomy (Fujii et al., 1997; Wellons et al., 2000) similar to those reported here, between C57Bl/6J and 3xTg-AD mice. Although differences in Circle of Willis anatomy between the two strains in the present study were not statistically significant, observations made suggest that 3xTg-AD mice may have a more robust collateral circulation than C57Bl/6J mice. This difference may explain the more robust response of 3xTg-AD mice to BCAS and the disparity between the present study and those of Kitaguchi et

al. (2009) and Yamada et al. (2011). This also highlights the failure to measure CBF as a limitation of the current study.

As pointed out above, a further limitation of the current study is the lack of a non-transgenic control. The reason no non-transgenic controls were included in the study described in this chapter is due to a lack of availability. The founder animals used to establish the 3xTg-AD mouse colony, from which all experimental animals described in this study were derived, were homozygous for the human AD related transgenes. This precluded the generation of non-transgenic animals for use as controls. In light of this, and taking into consideration the differences in cerebrovascular architecture between C57Bl/6J and 3xTg-AD mice discussed above, were this study to be repeated the use of an alternative AD mouse model may be more appropriate i.e. one where transgenes are expressed on a C57Bl/6J background e.g. the J9 or J20 strain (Hsiao et al., 1996; Mucke et al., 2000) or the Tg2576 strain.

In summary evidence presented in this chapter demonstrates that BCAS, as induced using 0.18mm dia. microcoils for a period of one month, is insufficient to influence the development of AD pathology, or to exacerbate pre-existing white matter pathology in 3xTg-AD mice. However, a more severe level of stenosis, as induced using 0.16mm dia. microcoils, is sufficient to cause the development of focal areas of severe white matter pathology and ischaemic damage to neuronal perikarya in a majority of experimental 3xTg-AD animals. In some animals where severe white matter pathology is present altered white matter Aβ levels may be observed, possibly due to amyloidogenic APP processing at sites of axonal injury.

As discussed above a factor which must be considered when interpreting the findings outlined in this chapter is the age of animals studied (4-5 months). When

considered retrospectively this may be considered one of the biggest limitations of the present study. In younger animals Aβ clearance mechanisms may be robust enough such that Aβ deposits (both intra and extracellular) do not accumulate, this has been demonstrated recently in Tg2576 mice (Hawkes et al., 2011). Where perivascular drainage, thought to be a major clearance route for Aβ (Bell and Zlokovic, 2009; Weller et al., 2009) was shown to be intact in animals as old as 7 months. Similarly, in younger animals the vessels of the cerebrovasculature may be plastic enough such that they are able to compensate for BCAS as induced via 0.18mm dia. microcoils, thus precluding the exacerbation of white matter pathology. With this in mind, the following chapter will investigate how white matter protein levels change with ageing in 3xTg-AD mice and also whether ageing confers increased vulnerability to the development of white matter damage following BCAS.

Chapter 6: Does ageing impact on white matter protein levels or confer increased vulnerability to hypoperfusion in 3xTg-AD mice?

6.1 *Introduction*

Results from numerous neuroimaging studies have shown that a reduction in brain white matter volume (Guttmann et al., 1998; Resnick et al., 2000) and myelin sheath integrity (Peters, 2002, 2009) are characteristic of normal ageing. This is supported by evidence from *post-mortem* stereological studies conducted on non-demented elderly subjects (Pakkenberg and Gundersen, 1997; Tang et al., 1997) and is consistent across several species including the rhesus monkey (Wisco et al., 2008) and the rat (Yang et al., 2009). In AD patients, white matter loss and damage to the myelin sheath have been shown to be exacerbated (Salat et al., 2009). Despite this, few studies have been conducted to examine alterations in white matter component proteins with normal ageing, or in AD.

Reductions in cerebral blood flow are known to occur with normal ageing and these have been shown to correlate with increased levels of white matter damage (Kawamura et al., 1991). Several factors have been proposed as an underlying cause for this age related development of hypoperfusion, including changes to endothelial cells which lead to decreased vascular reactivity (Farkas et al., 2006) and also microvascular changes within the capillary network (de Jong, 1991; Brown and Thore, 2011). These changes are thought to confer increased vulnerability to cerebrovascular insults predisposing individuals to further reductions in cerebral blood flow, which may occur as a result of the development of an age related disease state e.g. hypertension or atherosclerosis.

Whilst much work has been successfully conducted to characterise how the cerebrovasculature changes with normal ageing and also how age related disorders such as hypertension may accelerate these changes (Farkas et al., 2000), the degree to which these changes may augment damage to white matter following further CBF reductions remains to be fully elucidated.

This study investigated the hypothesis that ageing impacts on white matter protein levels in 3xTg-AD mice and that aged animals will show increased vulnerability to hypoperfusion and the subsequent development of white matter damage.

6.1.1 *Aims of study*

The aims of this study were to investigate the impact of ageing on white matter protein composition in young and old sham and hypoperfused 3xTg-AD mice and to investigate, through the utilisation of the hypoperfusion model previously described, the impact of hypoperfusion on white matter integrity in a cohort of aged 3xTg-AD mice.

6.2 *Materials and Methods*

6.2.1 *Mice and group sizes*

Two cohorts of male 3xTg-AD mice were used (table 6.1). Hypoperfusion was induced in experimental animals from each cohort using 0.18mm diameter microcoils for a period of one month. In cohort 1, young animals aged 3-4 months at time of surgery were studied (these were the same animals referred to as cohort 1 in chapter 5). The second cohort consisted of older animals aged 13-14 months at time of surgery. Even though greater levels of damage were observed following hypoperfusion using a 0.16mm diameter coil in the preceding chapter, hypoperfusion was induced using a 0.18mm diameter coil in the present study as there was a concern following the relatively high mortality rate observed in young animals following BCAS with the narrower coil, that aged animals would be even less able to tolerate the CBF reduction due to age related changes in cerebrovascular integrity.

Table 6.1 Initial cohort sizes

Age / Treatment	Cohort 1	Cohort 2
Sham	n=12	n=6
Hypoperfusion	n=13	n=12

6.2.2 *Western blotting*

Protein extracts were prepared from frozen hemi brains and their concentrations assessed. Samples (5µg) were separated via SDS-gel electrophoresis and subject to Western blot analysis to investigate protein levels as described in section 2.7. For antibodies and concentrations used see table 2.3.

6.2.3 *Pathological analysis*

6.2.3.1 *Histological assessment of gray matter pathology*

Haematoxylin and eosin (H&E) staining, as described in section 2.5, was used to identify areas of ischaemic damage to neuronal perikarya.

6.2.3.1 *Immunohistochemical assessment of white matter pathology*

MAG immunostaining was used to investigate changes in myelin integrity in response to hypoperfusion. APP immunostaining was used to investigate levels of axonal pathology in response to hypoperfusion. Iba-1 immunostaining was used to investigate microglial upregulation in response to hypoperfusion. 4G8 immunostaining was used to investigate changes in white matter Aβ levels in response to hypoperfusion. Immunostaining and quantification was conducted as described in section 2.6. other than for quantification of microglial activation where a grading scale (0-3) was used. The scale was as follows; 0- no activated microglia, 1- baseline activation, few sparsely distributed activated cells, 2- marked upregulation, many activated cells present throughout region, 3- very dense patches of many activated cells. APP and 4G8 immunostaining was conducted by the author, MAG and Iba-1 immunostaining was conducted by Mrs Fiona Scott and Mr Tommy Dingwall.

6.2.4 *Regions of interest*

In this study hemi brain sections were stained and analysed. As in chapter 5, white matter regions of interest examined were external capsule, internal capsule, hippocampal fimbria, and white matter fibre bundles of the striatum (Fig. 6.1).

6.2.5 *Statistical analysis*

Results for Western blot analysis were analysed by Student's t-test. Pathology was analysed in the same manner as chapters 3, 4 and 5. Initially Fisher's exact test was used to determine whether the probability of damage ocurring to white matter components was increased higher following hypoperfusion. Mann-Whitney U tests were used to compare loss of myelin integrity, levels of axonal pathology and levels of degraded myelin between sham and hypoperfused animals. Results were considered significant when $p < 0.05$.

6.3 *Results*

6.3.1 *Recovery from surgery*

As reported in chapter 5, all animals from the cohort of animals aged 3-4 months recovered well from surgery with the exception of one hypoperfused animal which was culled following poor recovery. All animals from the aged cohort recovered well from surgery. See table 6.2 for final cohort sizes.

Table 6.2 Final cohort sizes

Age / Treatment	Cohort 1	Cohort 2
Sham	n=12	n=6
Hypoperfusion	n=12	n=12

6.3.2 *Western blotting*

6.3.2.1 *Western blot analysis of MBP levels in young vs old 3xTg-AD sham and hypoperfused mice*

MBP levels were found to be significantly increased in old sham animals as compared to young sham animals ($p<0.001$, Fig. 6.1A). A similar result was seen when levels of MBP were compared in old and young hypoperfused animals ($p < 0.001$, Fig. 6.1B).

6.3.2.2 *Western blot analysis of CNPase levels in young vs old 3xTg-AD sham and hypoperfused mice*

CNPase levels were found to be significantly increased in old sham animals as compared to young ($p < 0.001$, Fig. 6.2A). A similar result was seen when comparing CNPase in old and young hypoperfused animals ($p < 0.001$, Fig. 6.2B).

6.3.2.3 *Western blot analysis of MAG levels in young vs old 3xTg-AD sham and hypoperfused mice*

MAG levels were found to be significantly reduced in old sham animals as compared to young sham animals ($p = 0.036$, Fig. 6.3A). A similar result was seen when MAG levels in young and old hypoperfused animals were compared ($p = 0.011$, Fig. 6.3B).

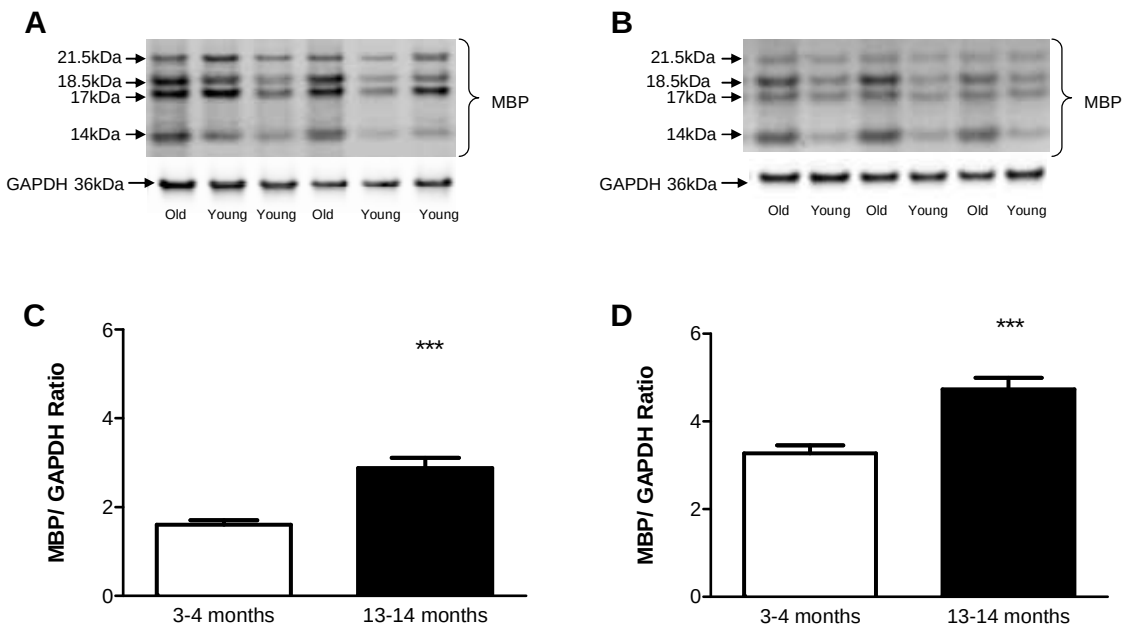

Figure 6.1 MBP levels are increased with ageing

Representative images of Western blot of MBP and GAPDH (A, B). Data are expressed as mean MBP/ GAPDH ± SEM. Young vs old sham animals n=12 young/ n=6 old; young vs old hypoperfused animals n=12 young/ n= 12 old. MBP levels were significantly increased in old as compared to young sham (p<0.001; mean values- sham= 1.60 ± 0.09 hypoperfused= 2.88 *± 0.23 A, C) and hypoperfused animals (p=0.001; mean values- sham= 3.23 ± 0.18 hypoperfused=* 4.73 *± 0.26 B, D). Two tailed Student's t-test.*

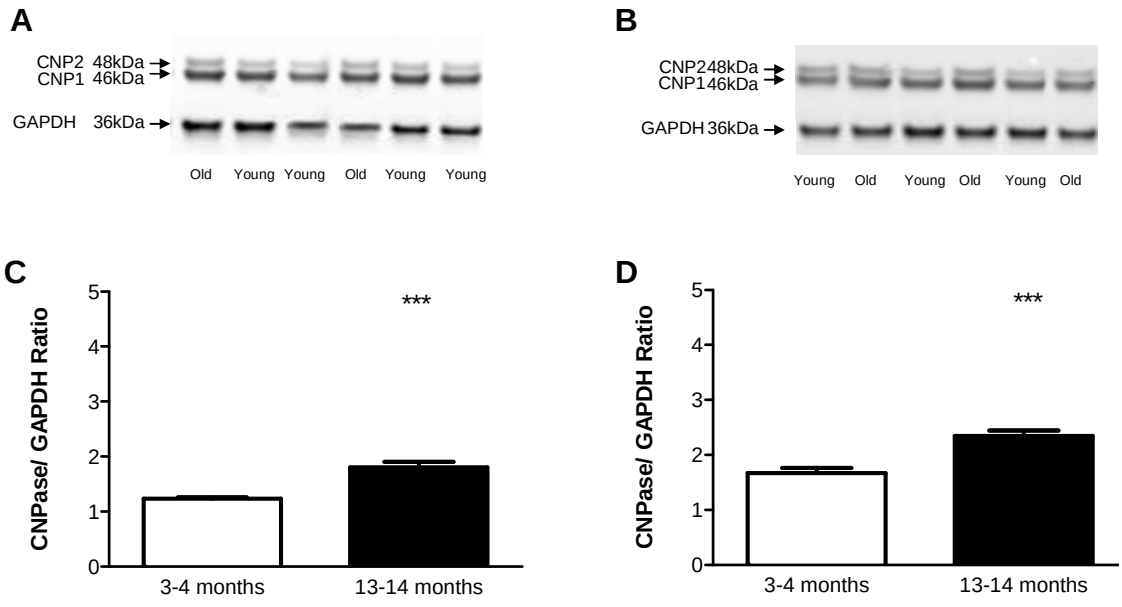

Figure 6.2 CNPase levels are increased with ageing

Representative images of Western blot of CNPase and GAPDH (A, B). Data are expressed as mean CNPase/ GAPDH ± SEM. Young vs old sham animals n=12 young/ n=6 old; young vs old hypoperfused animals n=12 young/ n= 12 old. CNPase levels were significantly increased in old as compared to young sham ($p<0.001$; mean values- sham= 1.24 ± 0.02 hypoperfused= 1.80 ± 0.09 A, C) and hypoperfused ($p<0.001$; mean values- sham= 1.67 ± 0.09 hypoperfused= 2.35 ± 0.09 B, D) animals. Two tailed Student's t-test.

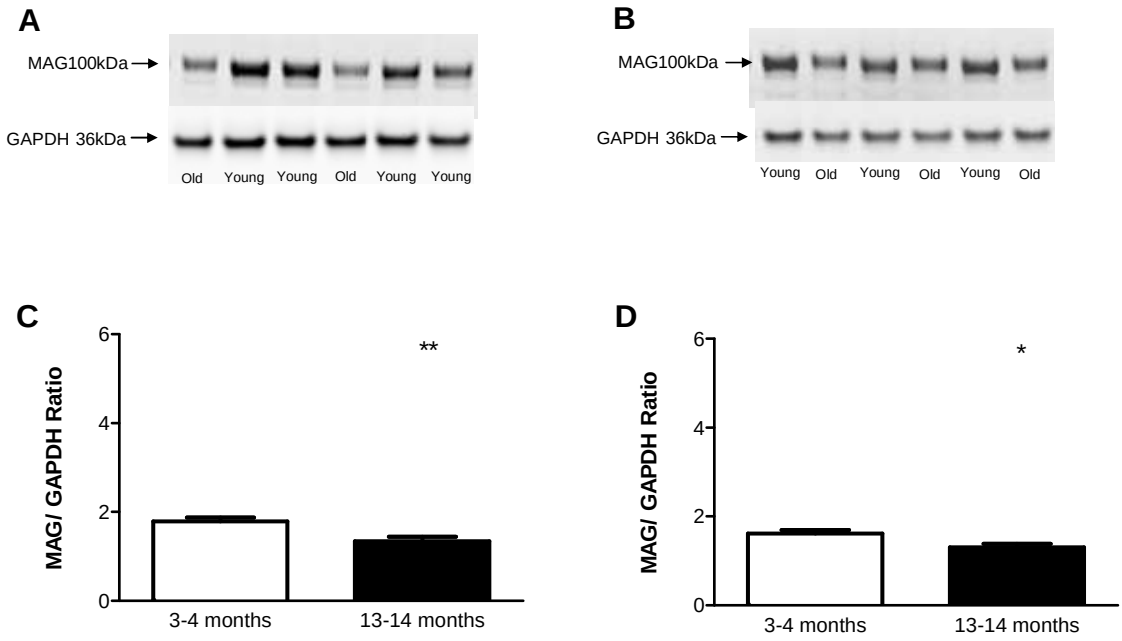

Figure 6.3 MAG levels are reduced with ageing

Representative images of Western blot of MAG and GAPDH (A, B). Data are expressed as MAG/ GAPDH ± SEM. Young vs old sham animals n=12 young/ n=6 old; young vs old hypoperfused animals n=12 young/ n= 12 old. MAG levels were significantly reduced in young and old sham (p=0.036; mean values- sham= 1.79 ± 0.08 hypoperfused= 1.34 ± 0.10 A, C) and young and old hypoperfused (p=0.011; mean values- sham= 1.62 ± 0.08 hypoperfused= 1.30 ± 0.08 B, D) animals. Two tailed Student's t-test.

6.3.2.4 *Western blot analysis of protein levels in response to hypoperfusion in aged 3xTg-AD mice*

Western blotting was also employed to investigate how hypoperfusion might impact on APP, MAG, CNPase and MBP levels in the aged cohort of animals described in this study. No changes were detected in the levels of any of these proteins following one month of hypoperfusion induced using 0.18mm diameter microcoils (appendix 4).

6.3.3 *Histological examination of grey matter following hypoperfusion in aged 3xTg-AD mice*

H&E sections were examined for evidence of ischaemic damage to neuronal perikarya as described in section 2.5.3. One hypoperfused animal displayed evidence of neuronal perikaryal damage. This was observed in the striatum, the hippocampus and the upper layers of the cortex. Areas of damage were bordered by normal appearing healthy cells. No aged sham 3xTg-AD mice displayed any evidence of ischaemic damage.

6.3.4 *Evaluation of white matter pathology in aged 3xTg-AD mice following hypoperfusion*

6.3.4.1 *Assessment of myelin integrity following hypoperfusion*

The probability of a loss of myelin integrity following hypoperfusion was not increased in aged animals ($p = 0.600$; Fig 6.4A, B, C), Fisher's exact test. There were no alterations in myelin integrity in the majority of aged sham or hypoperfused 3xTg-AD mice, however in a small subset of animals, 1 sham and 5 hypoperfused animals, minimal myelin damage was observed. Overall myelin integrity did not

differ between sham and hypoperfused animals in this cohort (Fig. 6.4 A, B, C; p = 0.402) Mann Whitney-U test. In the animal where ischaemic damage to neuronal perikarya was observed, highlighted in red (Fig. 6.4C), areas of severe myelin pathology, were present.

6.3.4.2 *Assessment of axonal pathology following hypoperfusion*

As described in chapter 5, low level APP expression was observed in oligodendrocytes. A baseline level of axonal pathology was also present, however in aged 3xTg-AD mice this was more pronounced than in the younger animals examined in chapter 5. Accumulations of APP in axonal swellings/ bulbs were present with greater frequency and were larger in size. The probability of axonal damage occurring following hypoperfusion was not increased (Fig. 6.4D, E, F; p = 0.634) Fisher's exact test. Hypoperfusion did not exacerbate axonal pathology as compared to shams in aged 3xTg-AD mice (Fig. 6.4 D, E, F; p = 0.634). In the animal where ischaemic damage to neuronal perikarya was observed, highlighted in red (Fig. 6.4F), areas of moderate to severe axonal pathology were also present.

6.3.4.3 *Assessment of microglial activation following hypoperfusion*

The presence of activated microglia was evident in all regions of all animals examined. In aged 3xTg-AD mice microglial activation was markedly more pronounced, in all brain regions, than in the younger 3xTg-AD animals examined in chapter 5. Analysis of microglial activation in the aged cohort revealed that there was no difference in levels of microglial activation following hypoperfusion (p = 0.122; Fig. 6.4G, H, I). In the hypoperfused animal where evidence of ischaemic damage was observed (marked in red; Fig. 6.4I), dense patches of activated microglia

were observed in areas corresponding to those where ischaemic damage to neuronal perikarya was evident.

6.3.4.4 *Investigation of white matter Aβ levels following hypoperfusion*

Hypoperfusion had no impact on white matter Aβ levels, other than in the hypoperfused animal in which ischaemic damage was observed. In this animal altered Aβ levels were visible in the white matter fibre bundles of the striatum consistent with the location of severe axonal pathology. No animals displayed any evidence of extracellular plaque pathology.

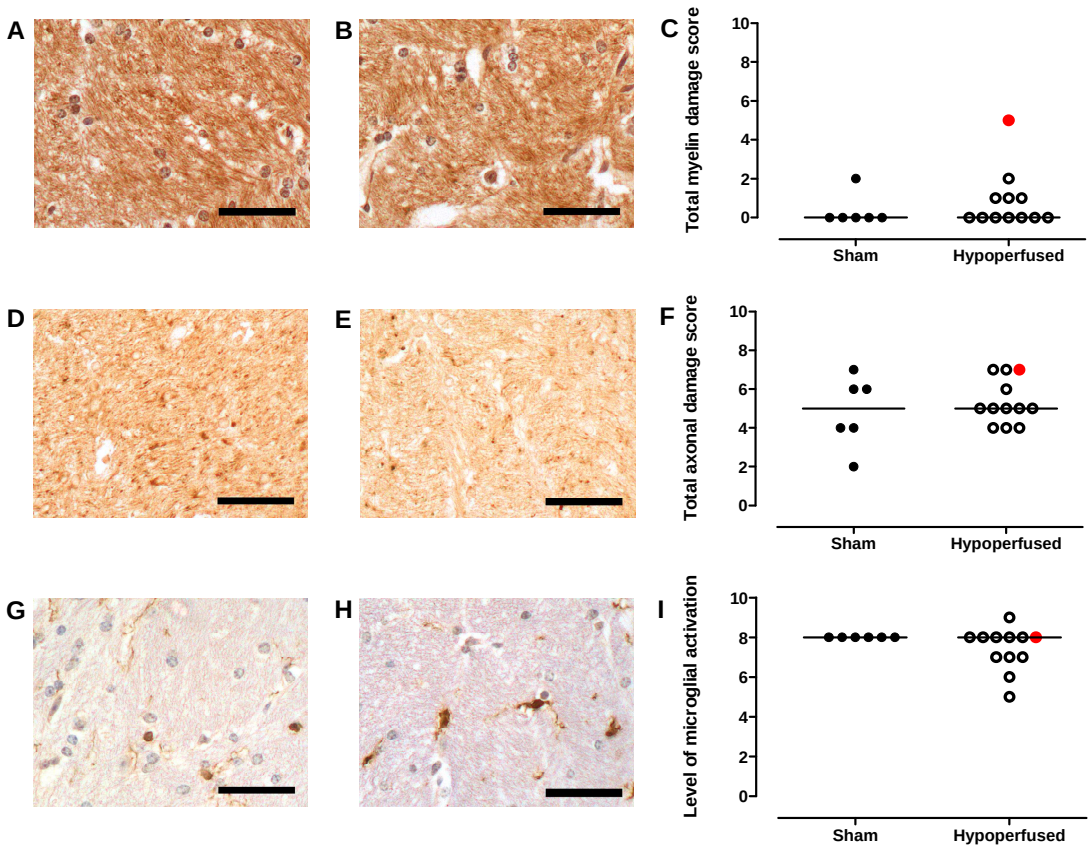

Figure 6.4 Immunohistochemical examination of white matter in aged 3xTg-AD mice following hypoperfusion

Representative images of MAG, APP and Iba-1 immunostaining in the internal capsule of aged 3xTg-AD sham (A, D, G) and hypoperfused (B, E, H) mice. The probability of myelin damage occurring was not increased following hypoperfusion (p= 0.600). Neither was the probability of axonal damage occurring following hypoperfusion (p=0.634) Fisher's exact test. The hypoperfused animal displaying evidence of ischaemic damage is highlighted in red (C, F, I). Hypoperfusion did not impact on myelin integrity in aged animals (p=0.402, median values- sham= 0, hypoperfused= 0, C). Axonal pathology (black arrows) was present in all animals examined but was not exacerbated following hypoperfusion (p=0.634, median values- sham=5, hypoperfused= 5, F)). There was no difference in levels of microglial activation in aged 3xTg-AD hypoperfused mice as compared to shams (p=0.122, median values- sham=8, hypoperfused=8, I) Mann Whitney-U test. Scale bar = 50μm.

6.4 *Discussion*

Results from the present study demonstrate that white matter protein composition is differentially altered in 3xTg-AD mice with normal ageing, levels of MBP and CNPase are increased in conjunction with a decrease in levels of MAG. However, contrary to the original hypothesis there was no strong evidence that ageing increased susceptibility of white matter to hypoperfusion in 3xTg-AD mice.

Whilst the majority of published data regarding white matter changes with ageing and AD has been gathered from studies conducted in either humans or non-human primates, the study presented in this chapter is one of the first to investigate how levels of the white matter proteins, MBP, CNPase and MAG change with ageing in 3xTg-AD mice. Desai et al. (2009) compared MBP and CNPase levels in 2 month and 6 month old 3xTg-AD mice and also non-transgenic controls. In contrast to the results presented in this chapter, they reported reductions in MBP and CNPase levels in 6 month old 3xTg-AD mice as compared to younger and control animals. One reason for this discrepancy may be due to methodological differences. The present study examined protein levels in whole brain homogenate; Desai et al. conducted their Western blot analysis in microdissected tissue samples from the entorhinal cortex and hippocampus. However, it was only following subregion specific immunohistochemical analysis that a statistical difference in protein levels was observed. This was in the CA1 subregion of the hippocampus and layer II/ III of the entorhinal cortex. These are both areas associated with the early development of pathology in AD, and possibly where one might expect to see reductions in myelin protein levels due to increased levels of Aβ prior to the development of overt plaque pathology (discussed below).

Previous studies conducted to examine how white matter changes with normal ageing and in patients with AD, have reported that overall white matter volume decreases with advancing age and that this is exacerbated in AD (Guttmann et al., 1998; Bartzokis et al., 2003). This has been attributed mainly to a loss of myelin lipid as opposed to proteins (Stommel et al., 1989; Svennerholm et al., 1991); however, myelin protein composition has also been shown to change (Sloane et al., 2003; Hinman et al., 2008). In accordance with results from the present study, findings presented by Sloane et al. (2003) demonstrate a loss of MAG in conjunction with increased levels of CNPase in a cohort of ageing rhesus monkeys as compared to young controls. These findings were in part, recapitulated by Hinman et al. (2008) who also reported an increase in CNPase levels with ageing in the rhesus monkey. Several studies have investigated MBP levels in ageing animals however results are conflicting, some report no change (Sloane et al., 2003), some report a decrease (Ansari and Loch, 1975), whilst the present study, reports an increase. One possible reason for this may be sampling of different brain areas in different studies. Irrespective of this, a large range of studies support the hypothesis that in addition to overall white matter loss with ageing, the protein profile of white matter also changes.

Reductions in levels of MAG, have also been reported in studies investigating pathological conditions such as hypoxia/ ischaemia (Aboul-Enein et al., 2003) where MAG is one of the first myelin proteins to be lost, and also MS (Gendelman et al., 1985) where, in certain types of lesion, MAG loss is prominent. Furthermore, previous work in MAG null mice has shown that reductions in MAG may precede the loss of myelin or changes in expression of other myelin proteins (Loers et al., 2004). It has been suggested that loss of MAG with normal ageing may be an

indicator of damage to oligodendrocytes (Sloane et al., 2003). As well as playing an important role in axo-glial trophic signalling, MAG is thought to play a role in the adherence of the myelin sheath to the axon (see section 1.1). If this trophic signalling/ anchoring mechanism is lost, either as a result of age related myelin damage, or, in AD, Aβ mediated toxicity, then a loss of normal axonal function (e.g. disruption of axonal transport) and the development of axonal pathology might occur. The over production of other myelin proteins e.g. CNPase and MBP is possibly due to some compensatory remyelination mechanism attempting to correct for this (Peters, 2002; Peters and Sethares, 2002). Alternatively, increases in CNPase and MBP may be due to increased proliferation of oligodendrocytes following age related oligodendrocyte degeneration/ loss (Peters, 2009). A further reason which could explain increased levels of MBP and CNPase with ageing is the production of 'redundant' myelin. This has been described in the rhesus monkey (Peters and Sethares, 2002), the toad (Rosenbluth, 1966) and also the mouse (Sturrock, 1976). In aged animals the thickness of the myelin sheath has been demonstrated to increase; this tends to occur in sheaths which envelope small diameter axons however why this occurs is unknown (Peters, 2009). Finally, ultrastructural analysis has shown that in ageing animals, myelin malformations are present in many myelin sheaths. These can appear as fluid filled cavities, termed balloons, which require the production of excess myelin by the parent oligodendrocyte. It has been suggested that the formation of myelin balloons is degenerative (Peters, 2009) as, in addition to ageing, they are observed following application of agents known to cause demyelination e.g. cuprizone (Ludwin, 1978)

or chronic copper poisoning (Howell et al., 1974) and also in severe diabetes (Tamura and Parry, 1994).

In addition to investigating alterations in white matter protein levels with ageing, a further aim of the present study was to examine whether age would confer increased vulnerability of white matter to hypoperfusion. Other studies attempting to investigate the impact of hypoperfusion on the development of white matter damage have examined pathological changes in young animals (as in previous chapters). It could be argued that one of the drawbacks of using young animals in studies such as these is that they do not accurately model the aged brain, where a degree of hypoperfusion may already be present due to age related changes to the cerebrovasculature (Leenders et al., 1990; Farkas et al., 2006). Thus creating a situation where white matter is rendered even more vulnerable to further reductions in CBF.

Findings from the present study, contrary to the initial hypothesis, indicate that white matter pathology (myelin disruption, axonal pathology, microglial activation) was not exacerbated in response to hypoperfusion in aged 3xTg-AD mice. One possible reason for this may be, as postulated in chapter 5, that hypoperfusion as induced using 0.18mm diameter microcoils may be insufficient to induce white matter pathology, even in older animals, due to Circle of Willis architecture. Alternatively, it may be possible that age related changes to the cerebrovasculature may not have begun to occur in the 3xTg-AD mice examined, at least not to the point where the animals had become vulnerable to the level of hypoperfusion induced. This theory is supported by work in the rat, where age related deterioration of the cerebrovasculature was not observed until animals were aged 16 months (de Jong,

1991) other than in the presence of an additional confounding factor, hypertension, when pathology was observed from ~12 months (Farkas et al., 2000).

Although unchanged in response to hypoperfusion, axonal pathology was observed to increase with ageing in 3xTg-AD mice (as compared to animals examined in chapter 5). Age related increases in axonal pathology have been observed and reported in other transgenic mouse models of AD in the absence of overt plaque pathology. The presence of intraneuronal amyloid pathology, similar to that observed in 3xTg-AD mice utilised in this thesis, has been proposed as a possible causative factor for this (Wirths et al., 2007). Higher levels of microglial activation were also observed in aged 3xTg-AD mice as compared to the younger animals utilised in the previous chapter. Microglial activation is a common feature seen in early Alzheimer's disease where it has been shown to increase with disease progression (Mastrangelo and Bowers, 2008) and also normal ageing (Peters, 2002).

Aβ toxicity has been proposed as a mechanism by which white matter is lost in AD. Work to examine protein levels in human AD brains has shown that levels of CNPase (Vlkolinský et al., 2001) and MBP were reduced in conjunction with elevated white matter levels of Aβ (Roher et al., 2002). Again, these results differ from those presented in this chapter, where levels of MBP and CNPase were shown to be increased. One reason for this may be due to the lack of Aβ pathology present in the 3xTg-AD animals utilised in the present study. Several studies have shown that Aβ is toxic to oligodendrocytes and myelin (Jantaratnotai et al., 2003; Roth et al., 2005). Furthermore white matter changes have been reported as an early event occurring in several AD mouse models (Stokin et al., 2005; Wirths et al., 2006; Desai et al., 2009; Desai et al., 2010) and in some cases, Aβ mediated toxicity has

been demonstrated to underlie this (Desai et al., 2010). However in the aged 3xTg-AD mice utilised by the present study, Aβ levels were relatively low (compared to levels previously reported (Oddo et al., 2003a) as evidenced by the lack of plaque pathology which was expected to be present in most animals from 12 months of age. Why levels of Aβ pathology in 3xTg-AD animals examined in this chapter were lower than expected is unknown however this finding is not novel and has been reported by others (Hirata-Fukae et al., 2008; Mastrangelo and Bowers, 2008). Possible reasons may be due to a loss of phenotype related to successive breeding, founder effects between colonies, or altered expression of transgenes (Kwang-Jin Oh, 2010).

Were this study to be repeated, a remedy to this, and also possibly the relatively low levels of Aβ pathology observed, would be to either induce a more severe level of stenosis as described in chapter 5, using 0.16mm diameter microcoils or, alternatively, as suggested in chapter 5, utilise an AD model which is more vulnerable to reductions in CBF. As suggested above, the use of an alternative AD model would also allow for the inclusion of non-transgenic animals, potentially providing a clearer understanding as to why white matter protein levels were altered with ageing in the present study.

Including non-transgenic controls would also be advantageous because this would allow the attribution of the observed axonal pathology to either the expression of AD related mutant transgenes or ageing in 3xTg-AD mice. Additionally, transgene expression cannot be discounted as a reason for the observed changes in white matter protein levels. Several recent studies have implicated a role for BACE-1 and γ-secretase in the regulation of myelination and myelin thickness (Hu et al.,

2008; Bartzokis, 2009). The mutant APP^{Swe} gene which is expressed in 3xTgAD mice is known to alter BACE-1 activity (Haass et al., 1995). Similarly the mutant $PS1^{M146V}$ which is also expressed in 3xTg-AD animals is known to alter γ-secretase activity. Expression of these mutant transgenes, in addition to altering APP processing, may also impact on other processing/ signalling pathways in which they play a role; including myelination/ remyelination and in turn levels of white matter proteins (Bartzokis, 2009).

Results presented in this chapter demonstrate that with normal ageing, alterations in white matter protein levels occur in 3xTg-AD mice. Whilst the reasons for this remain unclear, a point of interest is how they may impact on cognitive function. Taking into account the results presented in chapter 4, it seems possible a loss of axo-glial integrity due to a reduction in levels of MAG, may impact negatively on normal cognitive function. Additionally formation of sheaths of redundant myelin or any alterations in the thickness of the myelin sheath may cause altered conduction speed of nerve impulses (Peters, 2002; Bartzokis, 2004; Peters, 2009). This could potentially lead to disruption of neuronal circuits and may play a role in the development of any age related cognitive deficits. Clearly further work is required to substantiate this.

Chapter 7: General Discussion

7.1 Summary

The findings of this thesis clearly demonstrate that chronic cerebral hypoperfusion impacts detrimentally on white matter, causing a loss of myelin integrity, and that this is associated with a deficit in spatial working memory. Additionally, the work conducted in 3xTg-AD mice has shown that hypoperfusion does not impact on levels of intraneuronal Aβ pathology, nor does it exacerbate white matter pathology in this strain. It has also been demonstrated that levels of some white matter proteins change with ageing in 3xTg-AD mice.

7.2 Limitations and further work

Whilst several studies described in this body of work have yielded positive results which may be considered novel findings, there are limitations, raised briefly in the previous chapters which warrant, further discussion here.

In addition to the numerous methodological alterations which could be made to improve studies e.g. micro-dissection of white matter tracts for use in Western blotting experiments or use of an ELISA as a method to quantify changes in Aβ levels as mentioned in chapter 5, two major caveats stand out. The first of these relates to the use of the antibody 4G8 as a marker for Aβ whilst the second relates to the 3xTg-AD mouse strain utilised in chapters 5 and 6.

Since completion of this body of work results of a study conducted in 3xTg-AD mice have demonstrated cross-reactivity between antibody 4G8 and full length APP (Winton et al., 2011) furthermore the authors concluded that what had previously been described as intracellular Aβ in cortical and pyramidal neurons in

3xTg-AD brain tissue was in fact intracellular APP. As suggested in chapter 5, were this work to be repeated, then the use of multiple methods of Aβ quantification would need to be employed to avoid mis-interpretation of results and also to demonstrate in a more robust fashion any changes which might occur in Aβ levels following hypoperfusion.

Given the findings of Winton et. al. (2011) which suggest that what was initially thought to be intracellular amyloid is in fact APP and also that pathology in the 3xTg-AD strain utilised was different to that first reported i.e. was not present, even in older animals, further work investigating the impact of hypoperfusion on Aβ levels would best be conducted in a different strain e.g PDAPP (Games et al., 1995), Tg2576 (Hsiao et al., 1996) or J9 (Hsia et al., 1999). These strains are better characterised in terms of age of onset of pathology. Furthermore, they may also be back crossed onto the C57Bl/6J strain, thus avoiding the potential issues surrounding strain specific differences in response to hypoperfusion due to variations in cerebrovascular architecture as described in chapter 5. Finally, future studies should be conducted in older animals, where amyloid pathology has already begun to develop, with hindsight, the age of animals used; especially in chapter 5 was too young. As discussed, younger animals are less likely to have developed amyloid pathology; additionally their Aβ clearance mechanisms are likely to be functionally robust as compared to aged animals, thus even if hypoperfusion does impact on amyloid pathology development/ metabolism, in younger animals this may not be detectable.

Follow up studies to those described in this body of work might include an investigation as to whether the white matter damage observed following hypoperfusion causes a functional deficit. This could be done using electrophysiology to measure conduction velocity and/ or field potentials, particularly within the frontal cortex and hippocampus. Other studies might include an electron microscopy study to investigate myelin integrity at the ultra-structural level, or alternatively a study utilising con-focal microscopy to image, myelin integrity, amyloid deposition or integrity of the cerebrovasculature.

7.3 White matter pathology and the development of cognitive deficits following hypoperfusion

In the mouse model of chronic cerebral hypoperfusion described in this thesis, hypoperfusion was modelled in a 'pure' form i.e. hypoperfusion in the absence of any other co-morbidities or confounding factors such as ageing, diabetes or hypertension. For this reason, it may considered an appropriate model of hypoperfusion with ageing in humans, where CBF has been shown to be reduced by up to 20% by the age of 65 as compared to age 20 (Leenders et al., 1990). Whilst other models of chronic cerebral hypoperfusion are available, none are able to recapitulate with the same success as the model utilised here, the subtle reductions in cerebral blood flow which are seen to occur with ageing in humans.

Findings presented in chapters 3 and 4 demonstrate that chronic cerebral hypoperfusion is sufficient to cause damage to the myelin component of white matter, resulting in a loss of myelin integrity and potential disruption of neuronal communication. Although this damage is relatively subtle, compared, for example, to the characteristic white matter lesions of leukoaraiosis (Fazekas et al., 1993;

O'Sullivan, 2008) or to that caused by more severe cerebrovascular challenges such as stroke (Moskowitz et al., 2010), it is sufficient to produce a deficit in spatial working memory. This is possibly due to its diffuse and widespread nature resulting from the global reduction in CBF, and the reliance of intact working memory on unbroken communication between many distinct brain regions including the posterior parietal and occipital areas, and the prefrontal cortex (Ricciardi et al., 2006). In order to confirm that the myelin damage observed following hypoperfusion leads to a functional deficit, electrophysiological studies could be conducted to investigate conduction velocity via intracellular recording (e.g. (Crawford et al., 2009) and or signal strength by measuring field inputs (e.g. (Stephanova et al., 2005).

In addition to myelin damage another feature of the hypoperfusion model is an upregulation of microglial activation, indicative of an inflammatory response. This inflammatory response in itself may cause further damage to white matter, possibly leading to subsequent axonal and neuronal injury, initiating a self perpetuating cycle of pathology which, over time, could impact on other aspects of cognition. This hypothesis is supported by results from another study conducted within the Horsburgh group, where, following six months of hypoperfusion, a loss of white and grey matter integrity was observed, in conjunction with breakdown of the penetrating arterioles and fibrinoid necrosis. At six months the working memory deficit was found to be more prominent than at two months and deficits in spatial reference memory were also observed (Holland et al, in preparation). Although work is ongoing to examine white matter pathology in these animals the development of a deficit in spatial reference memory suggests the presence of a more severe pathology than that seen at one month. This may be axonal; previous work in

this lab has demonstrated an association between axonal injury following TBI and spatial reference memory deficits (Spain et al., 2010). Taken together, these findings suggest that hypoperfusion initiates a progressive white matter pathology that also leads to vascular disturbances and that these pathologies impact detrimentally on cognition.

7.4 Chronic cerebral hypoperfusion, white matter damage and the development of AD

A large body of evidence exists linking chronic cerebral hypoperfusion resulting from vascular disorders with the development of AD in later life e.g. (Breteler et al., 1994; Breteler, 2000; Launer et al., 2000; de la Torre, 2002; Altman and Rutledge, 2011). Furthermore specific patterns of regional hypoperfusion have been identified as strong predictors of conversion from mild cognitive impairment to AD (Matsuda, 2007; Yoshiura et al., 2009; Hu et al., 2010; Kume et al., 2011). The findings presented in chapter 5 demonstrated that, in animals where hypoperfusion was sufficient to cause focal areas of severe white matter pathology, subtle alterations in white matter Aβ levels were also observed. As discussed this was possibly due to amyloidogenic APP processing at the site of axonal injury. In the absence of severe white matter damage, levels of Aβ remained unchanged. These findings are in contrast to other studies conducted in animal models of AD which have reported altered levels of AD pathology following less severe levels of BCAS induced cerebral hypoperfusion (e.g. Kitaguchi et al. (2009); Koike et al. (2010); Yamada et. al (2011)). Whilst the reason for this, as discussed in chapter 5, may have been due to strain related differences in cerebrovascular architecture, this

highlights an interesting point regarding the validity of animal models which must be considered when attempting to utilise them in the study of human disease.

Currently available transgenic models of AD are reliant on expression of transgenes which underlie the development of the familial form of the disease. Bearing in mind that familial AD accounts for less than 1% of cases, the question must be asked, how pertinent are these models to the sporadic form of the disease? Whilst animal models allow investigation into the factors which may influence AD pathology e.g. in the context of this work, hypoperfusion, they have limitations when used to investigate the underlying causes of AD. This is because transgene expression will ultimately lead to all animals developing pathology. This precludes their use in the identification of environmental factors which may cause AD development.

Finally, when considering the mechanisms underlying the development of sporadic AD, it is important to bear in mind that it is considered to be a multifactorial disorder of which there are, arguably, several different phenotypes (Ryan and Rossor, 2010). Many risk factors e.g. stroke, traumatic brain injury, hypertension have been identified as being associated with its development however none, as yet in isolation, have been identified as a cause. The reason for this is possibly that in order for disease onset to occur, multiple risk factors need to be present for a significant length of time (Small and Duff, 2008).

7.5 Current strategies for white matter repair

Clinical treatment strategies for risk factors associated with the development of hypoperfusion already exist (discussed below). However investigations into the repair/ prevention of white matter damage in general, remain at the preclinical stage.

This is, at least in part, due to a lack of understanding of the underlying mechanisms involved.

Currently the majority of studies investigating white matter repair strategies are focused on remyelination following demyelination in demyelinating diseases (Franklin and ffrench-Constant, 2008). These diseases include inherited genetic disorders (leukodystrophies) and also multiple sclerosis where demyelination occurs due to aberrant inflammation (Compston and Coles, 2002). Two main approaches to remyelination are currently being investigated. These are, cell replacement via cell transplant e.g. stem cell therapy and promotion of repair by the endogenous stem and precursor cell populations (Franklin and ffrench-Constant, 2008). Whilst cell replacement therapy may be appropriate where demyelination has occurred, given the type of white matter pathology observed following hypoperfusion this strategy seems inappropriate. Results presented in this thesis do not demonstrate demyelination as a pathological feature occurring following hypoperfusion; instead hypoperfusion is associated with a more subtle myelin disruption, where some myelin components were identified as being more susceptible to hypoperfusion than others e.g. MAG.

7.6 Is MAG a critical mediator in the development of white matter damage and associated cognitive decline in ageing and following hypoperfusion?

In addition to vulnerability to hypoperfusion, work in this thesis has also demonstrated that MAG levels are reduced with ageing in 3xTg-AD mice. This finding has also been observed in other aged animal models (Sloane et al., 2003). As yet however, no data has been published concerning MAG levels in aged humans. The reason MAG levels are reduced with ageing remains to be elucidated, one possible explanation may be as a result of age related hypoperfusion, or alternatively age related damage to oligodendrocytes possibly due to increased levels of oxidative stress (Squier, 2001; Floyd and Hensley, 2002).

Why MAG is vulnerable to ageing and hypoperfusion is unclear however one reason may be due to its cellular location at the periaxonal membrane (Sloane et al., 2003). If normal cellular function becomes impaired due to an imbalance in energy delivery or demand, it seems possible that the proteins and cellular functions most vulnerable will be those most distally located in relation to the cell body. Other work conducted within the Horsburgh group has demonstrated that changes in MAG and some paranodal proteins can be detected as early as three days following hypoperfusion (Reimer et al, in preparation). Other studies have also shown that MAG is one of the first proteins lost following hypoxia/ ischaemia (Aboul-Enein et al., 2003) and also in some MS lesions (Gendelman et al., 1985; Lassmann, 2003).

As previously discussed, MAG is thought to play a role in the maintenance of axon-glial integrity. Specifically axon-glia or glia-glia signal transduction and adhesion and also myelin maintenance and stabilisation of paranodal loops (Erb et al., 2006). If myelin sheath adherence to the axon is lost then cell-cell signalling between oligodendrocytes and axons will be disrupted and action potential

propagation will most likely be impacted (Hinman et al., 2006). Furthermore, loss of oligodendrocyte trophic signalling could be the initiating factor in the development of axonal pathology eventually leading to neuronal cell loss (Pan et al., 2005; Fancy et al., 2010). Taking this into account, loss of MAG function through protein loss or cellular redistribution as a result of hypoperfusion and/ or ageing may be the initiating factor underlying the development of associated cognitive changes. One way to investigate this would be to generate a line of MAG over-expressing transgenic mice. Providing MAG over expression did not impact phenotypically, chronic cerebral hypoperfusion could be induced in these animals to investigate if MAG over expression would prevent the development of a cognitive deficit. If a study such as this were successful then follow up biochemical studies might include attempts to elucidate the signalling pathways involved in maintaining the MAG mediated axon-glial connection. An understanding as to how this becomes disrupted with ageing and/ or hypoperfusion may present novel therapeutic opportunities.

7.7 Inflammation as a potential therapeutic target

In addition to further mechanistic insight into the link between hypoperfusion and the development of white matter pathology the BCAS mouse model of hypoperfusion may also be applied to investigating how myelin damage following hypoperfusion may be reversed or repaired. As stated above cell replacement/ proliferation therapy may not be the most appropriate treatment strategy for the type of subtle damage observed following the development of modest levels of hypoperfusion. However, one pathological feature of the model which does represent an interesting target is the upregulated inflammatory response.

Cytokines released by activated microglia have been shown to impact negatively on oligodendrocytes and myelin causing damage (Schmitz and Chew, 2008). Thus attenuation of the inflammatory response following hypoperfusion may reduce or even prevent damage to myelin and subsequent cognitive changes. A study such as this would be relatively easy to conduct with many compounds which display anti inflammatory properties being currently available e.g. non-steroidal anti inflammatory drugs.

Alternatively, compounds which have previously been demonstrated to attenuate white matter damage following ischaemia e.g. melatonin could be investigated. Melatonin has been shown to attenuate damage to white matter following ischaemia in neonatal (Olivier et al., 2009) and adult rats (Lee et al., 2007). It is thought that melatonin impacts negatively on pro inflammatory signalling and additionally accelerates oligodendrocyte maturation from oligodendrocyte progenitor cells (Pappolla et al., 1998; Escames, 2010). Interestingly, and of note melatonin has also been demonstrated to improve pathological outcome in animal models of AD (Pappolla et al., 2000).

7.8 Current clinical intervention strategies for the treatment of hypoperfusion

When considering the impact of chronic cerebral hypoperfusion clinically, it is important to bear in mind that the development of chronic cerebral hypoperfusion does not always lead to the development of white matter damage, nor does the presence of abnormalities in brain white matter automatically predispose the patient to the development of cognitive deficits. However, when the findings presented in this body of work are considered alongside that of the wider scientific community, a

picture begins to emerge which paints chronic cerebral hypoperfusion as a major risk factor for the development of white matter damage and cognitive decline, potentially leading to more severe forms of dementia such as AD.

The current clinical implications of this body of work are clear. In the majority of humans, chronic cerebral hypoperfusion occurs as part of the ageing process (Leenders et al., 1990; Brown and Thore, 2011). This may be exacerbated in the presence of age associated vascular risk factors (de Jong, 1991), leading to the development of white matter damage and initially subtle changes in cognition which may eventually progress to full blown dementia. However, it has been demonstrated that many individuals remain asymptomatic for years prior to the onset of detectable cognitive changes (Drzezga, 2009; Bendlin et al., 2010). For this reason, intervention strategies should be focused on preventing or delaying the onset of hypoperfusion if possible, or, endeavouring to slow the progression of hypoperfusion at an earlier stage, instead of attempting to treat it once hypoperfusion is established and cognitive changes are detectable.

In agreement with the above, early intervention strategies have already been suggested to identify and treat vascular risk factors, in an attempt to reduce the incidence of those most at risk going on to develop severe forms of dementia such as AD. Recently a two tier screening system was proposed (de la Torre, 2010) (Fig. 7.1) comprising a series of primary screens employed to identify those at risk of developing dementia due to the presence of vascular risk factors. Following primary screening, individuals identified as ‘at risk’ then undergo a further series of secondary screens including neuroimaging and cognitive testing to assess current cognitive status. The appropriate medical treatment to attempt to slow/ prevent the onset of cognitive decline may then be prescribed. This system offers a number of benefits; the primary screening

techniques are cost effective, easy to perform, and non-invasive, also during primary screening a number of other deleterious conditions may be identified (de la Torre, 2010).

Currently the appropriate treatment for hypoperfusion very much depends upon the risk factor underlying its development. For example, to promote healthier ageing and thereby minimise the probability of developing a risk factor associated with hypoperfusion in later life, a number of lifestyle factors may be modified. These include smoking cessation, moderation of alcohol intake, under taking regular exercise and eating healthily (Flicker, 2010). Clinical treatment tends to be risk factor dependent also, although this is not aimed at alleviating hypoperfusion as such, rather at managing the underlying cause of hypoperfusion e.g. treatment of hypercholesterolemia with lipid lowering drugs such as statins (Witztum, 1989), the appropriate management of diabetes with insulin therapy or treatment of hypertension with angiotensin converting enzyme (ACE) inhibitors (Rubin, 1978).

Implementation of a screening treatment system such as the one outlined above and in Fig. 7.1, which could be conducted regularly in patients (say every 3-5 years, from 35 years of age onwards), in conjunction with the appropriate treatment strategies, would almost certainly decrease the incidence of those with vascular risk factors developing dementia.

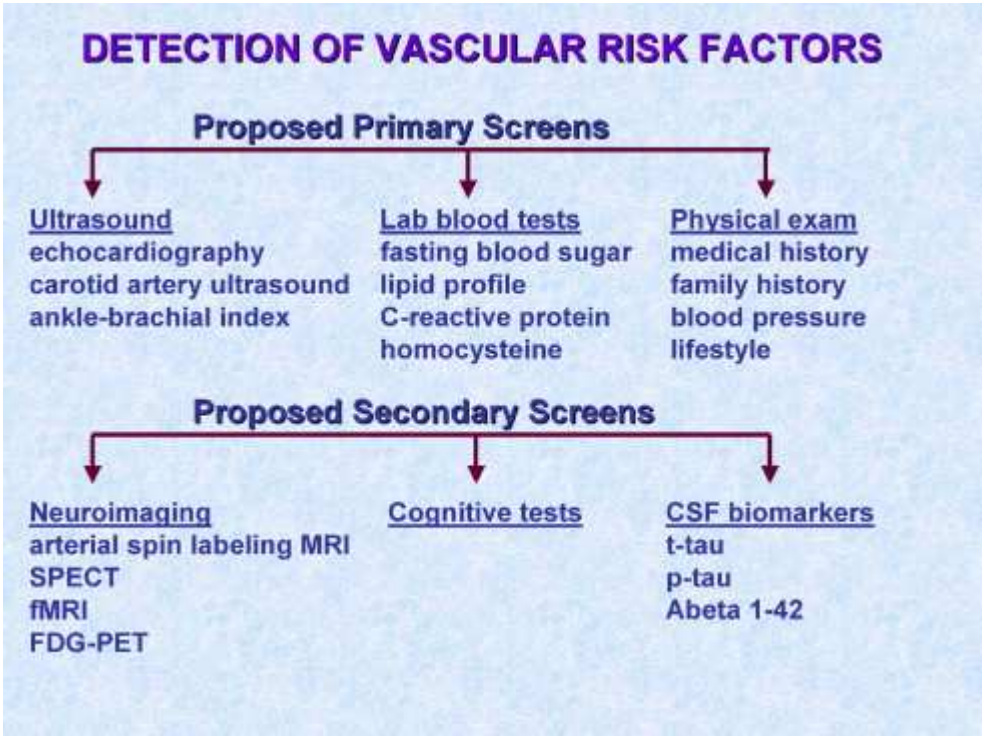

Figure 7.1 Proposed screening system for vascular risk factors

Patients undergo a series of cost, effective, non-invasive, easily conducted procedures as part of a primary screen. Those displaying vascular risk factors undergo a series of in depth secondary screens to assess cognitive status prior to commencing an appropriate treatment regime. (Image taken from de la Torre (2010))

7.9 Concluding remarks

Based on evidence from work presented in this thesis and elsewhere, the development of chronic cerebral hypoperfusion is a major risk factor associated with brain white matter damage and cognitive decline. Further work, using the model of hypoperfusion utilised in studies presented in this thesis may help to elucidate whether hypoperfusion associated white matter damage may be prevented or even repaired. Work such as this may impact in a significantly positive manner not only in dementia research but other clinical areas where white matter is also of relevance.

References

Aboul-Enein F, Rauschka H, Kornek B, Stadelmann C, Stefferl A, BrÃœCk W, Lucchinetti C, Schmidbauer M, Jellinger K, Lassmann H (2003) Preferential Loss of Myelin-Associated Glycoprotein Reflects Hypoxia-Like White Matter Damage in Stroke and Inflammatory Brain Diseases. Journal of Neuropathology & Experimental Neurology 62:25-33.

Airey DC, Lu L, Williams RW (2001) Genetic Control of the Mouse Cerebellum: Identification of Quantitative Trait Loci Modulating Size and Architecture. J Neurosci 21:5099-5109.

Akiguchi I, Tomimoto H, Wakita H, Kawamoto Y, Matsuo A, Ohnishi K, Watanabe T, Budka H (2004) Topographical and cytopathological lesion analysis of the white matter in Binswanger's disease brains. Acta Neuropathologica 107:563-570.

Akiyama H, McGeer PL (2004) Specificity of mechanisms for plaque removal after A[beta] immunotherapy for Alzheimer disease. Nat Med 10:117-118.

Alonso A, Zaidi T, Novak M, Grundke-Iqbal I, Iqbal K (2001) Hyperphosphorylation induces self-assembly of tau into tangles of paired helical filaments/straight filaments. Proc Natl Acad Sci U S A 98:6923 - 6928.

Altman R, Rutledge JC (2011) The vascular contribution to Alzheimer's disease. Clinical Science 119:407-421.

Ansari KA, Loch J (1975) Decreased myelin basic protein content of the aged human brain. Neurology 25:1045.

Arriagada PV, Growdon JH, Hedley-Whyte ET, Hyman BT (1992) Neurofibrillary tangles but not senile plaques parallel duration and severity of Alzheimer's disease. Neurology 42:631-.

Auer RN (1986) Progress review: hypoglycemic brain damage. Stroke 17:699-708.

Auer RN, Olsson Y, Siesja BK (1984) Hypoglycemic brain injury in the rat. Correlation of density of brain damage with the EEG isoelectric time: a quantitative study. Diabetes 33:1090-1098.

Ballatore C, Lee VMY, Trojanowski JQ (2007) Tau-mediated neurodegeneration in Alzheimer's disease and related disorders. Nat Rev Neurosci 8:663-672.

Bartzokis G (2004) Age-related myelin breakdown: a developmental model of cognitive decline and Alzheimer's disease. Neurobiology of Aging 25:5-18.

Bartzokis G (2009) Alzheimer's disease as homeostatic responses to age-related myelin breakdown. Neurobiology of Aging In Press, Corrected Proof.

Bartzokis G, Cummings JL, Sultzer D, Henderson VW, Nuechterlein KH, Mintz J (2003) White Matter Structural Integrity in Healthy Aging Adults and Patients With Alzheimer Disease: A Magnetic Resonance Imaging Study. Arch Neurol 60:393-398.

Baumann N, Pham-Dinh D (2001) Biology of Oligodendrocyte and Myelin in the Mammalian Central Nervous System. Physiol Rev 81:871-927.

Bell KFS, Ducatenzeiler A, Ribeiro-da-Silva A, Duff K, Bennett DA, Claudio Cuello A (2006) The amyloid pathology progresses in a neurotransmitter-specific manner. Neurobiology of Aging 27:1644-1657.

Bell R, Zlokovic B (2009) Neurovascular mechanisms and blood–brain barrier disorder in Alzheimer's disease. Acta Neuropathologica 118:103-113.

Bendlin BB, Ries ML, Canu E, Sodhi A, Lazar M, Alexander AL, Carlsson CM, Sager MA, Asthana S, Johnson SC (2010) White matter is altered with parental family history of Alzheimer's disease. Alzheimer's and Dementia 6:394-403.

Berzin TM, Zipser BD, Rafii MS, Kuo--Leblanc V, Yancopoulos GD, Glass DJ, Fallon JR, Stopa EG (2000) Agrin and microvascular damage in Alzheimer's disease. Neurobiology of Aging 21:349-355.

Bifulco M, Laezza C, Aloj SM, Garbi C (1993) Mevalonate controls cytoskeleton organization and cell morphology in thyroid epithelial cells. Journal of Cellular Physiology 155:340-348.

Billings LM, Oddo S, Green KN, McGaugh JL, LaFerla FM (2005) Intraneuronal Abeta causes the onset of early Alzheimer's disease-related cognitive deficits in transgenic mice. Neuron 45:675 - 688.

Blass JP, Hoyer S, Nitsch R (1991) A Translation of Otto Binswanger's Article, 'The Delineation of the Generalized Progressive Paralyses'. Arch Neurol 48:961-972.

Bourasset F, Ouellet M, Tremblay C, Julien C, Do TM, Oddo S, LaFerla F, Calon F (2009) Reduction of the cerebrovascular volume in a transgenic mouse model of Alzheimer's disease. Neuropharmacology 56:808-813.

Brain RW (1993) Brain's Diseases of the Nervous System, 10th Edition. New York: Oxford University Press.

Breteler MM (2000) Vascular Involvement in Cognitive Decline and Dementia: Epidemiologic Evidence from the Rotterdam Study and the Rotterdam Scan Study. Annals of the New York Academy of Sciences 903:457-465.

Breteler MMB, van Swieten JC, Bots ML, Grobbee DE, Claus JJ, van den Hout JHW, van Harskamp F, Tanghe HLJ, de Jong PTVM, van Gijn J, Hofman A (1994) Cerebral white matter lesions, vascular risk factors, and cognitive function in a population based study. Neurology 44:1246.

Brown WR, Thore CR (2011) Review: Cerebral microvascular pathology in ageing and neurodegeneration. Neuropathology and Applied Neurobiology 37:56-74.

Brun A, Englund E (1986) Brain changes in dementia of Alzheimer's type relevant to new imaging diagnostic methods. Progress in Neuro-Psychopharmacology and Biological Psychiatry 10:297-308.

Bucur B, Madden DJ, Spaniol J, Provenzale JM, Cabeza R, White LE, Huettel SA (2008) Age-related slowing of memory retrieval: Contributions of perceptual speed and cerebral white matter integrity. Neurobiology of Aging 29:1070-1079.

Butt AM, Ibrahim M, Ruge FM, Berry M (1995) Biochemical subtypes of oligodendrocyte in the anterior medullary velum of the rat as revealed by the monoclonal antibody rip. Glia 14:185-197.

Campagnoni A, Macklin W (1988) Cellular and molecular aspects of myelin protein gene expression. Molecular Neurobiology 2:41-89.

Capello E, Voskuhl RR, McFarland HF, Raine CS (1997) Multiple sclerosis: Re-expression of a developmental gene in chronic lesions correlates with remyelination. Annals of Neurology 41:797-805.

Caplan LR (2005) Dilatative arteriopathy (dolichoectasia): What is known and not known. Annals of Neurology 57:469-471.

Caroni P (1997) Overexpression of growth-associated proteins in the neurons of adult transgenic mice. Journal of Neuroscience Methods 71:3-9.

Caspersen C, Wang N, Yao J, Sosunov A, Chen X, Lustbader JW, Xu HW, Stern D, McKhann G, Yan SD (2005) Mitochondrial Aβετα: a potential focal point for neuronal metabolic dysfunction in AlzheimerÂ's disease. The FASEB Journal 19:2040-2041.

Castellani RJ, Rolston RK, Smith MA (2010) Alzheimer Disease. Disease-a-Month 56:484-546.

Chandler S, Coates R, Gearing A, Lury J, Wells G, Bone E (1995) Matrix metalloproteinases degrade myelin basic protein. Neuroscience Letters 201:223-226.

Chen G, Chen KS, Knox J, Inglis J, Bernard A, Martin SJ, Justice A, McConlogue L, Games D, Freedman SB, Morris RGM (2000) A learning deficit related to age and [beta]-amyloid plaques in a mouse model of Alzheimer's disease. Nature 408:975-979.

Cho K-O, La HO, Cho Y-J, Sung K-W, Kim SY (2006) Minocycline attenuates white matter damage in a rat model of chronic cerebral hypoperfusion. Journal of Neuroscience Research 83:285-291.

Choy M, Ganesan V, Thomas DL, Thornton JS, Proctor E, King MD, van der Weerd L, Gadian DG, Lythgoe MF (2006) The chronic vascular and haemodynamic response after permanent bilateral common carotid occlusion in newborn and adult rats. J Cereb Blood Flow Metab 26:1066-1075.

Chung Y-A, Hyun O J, Kim J-Y, Kim K-J, Ahn K-J (2009) Hypoperfusion and Ischemia in Cerebral Amyloid Angiopathy Documented by 99mTc-ECD Brain Perfusion SPECT. J Nucl Med 50:1969-1974.

Cizas P, Budvytyte R, Morkuniene R, Moldovan R, Broccio M, Lösche M, Niaura G, Valincius G, Borutaite V (2010) Size-dependent neurotoxicity of [beta]-amyloid oligomers. Archives of Biochemistry and Biophysics 496:84-92.

Clarkson A (2007) Anesthetic-mediated protection/preconditioning during cerebral ischemia. Life Sciences 80:1157-1175.

Coltman R, Spain A, Tsenkina Y, Fowler JH, Smith J, Scullion G, Allerhand M, Scott F, Kalaria RN, Ihara M, Daumas S, Deary IJ, Wood E, McCulloch J, Horsburgh K (2010) Selective white matter pathology induces a specific impairment in spatial working memory. Neurobiology of Aging In Press, Corrected Proof.

Compston A, Coles A (2002) Multiple sclerosis. The Lancet 359:1221-1231.

Cotman C, Anderson A (1995) A potential role for apoptosis in neurodegeneration and Alzheimer's disease. Molecular Neurobiology 10:19-45.

Crawford DK, Mangiardi M, Xia X, López-Valdés HE, Tiwari-Woodruff SK (2009) Functional recovery of callosal axons following demyelination: a critical window. Neuroscience 164:1407-1421.

D'Hooge R, De Deyn PP (2001) Applications of the Morris water maze in the study of learning and memory. Brain Research Reviews 36:60-90.

Danton GH, Dietrich WD (2003) Inflammatory Mechanisms after Ischemia and Stroke. Journal of Neuropathology & Experimental Neurology 62:127-136.

de Jong G, Jansen AS, Horvath E, Gispen WH, Luiten PG. (1991) Nimodipine effects on cerebral microvessels and sciatic nerve in aging rats. Neurobiology of Ageing 13:8.

de la Monte SM (1989) Quantitation of cerebral atrophy in preclinical and end-stage alzheimer's disease. Annals of Neurology 25:450-459.

de la Torre JC (2002) Vascular Basis of Alzheimer's Pathogenesis. Annals of the New York Academy of Sciences 977:196-215.

de la Torre JC (2004) Is Alzheimer's disease a neurodegenerative or a vascular disorder? Data, dogma, and dialectics. The Lancet Neurology 3:184-190.

de la Torre JC (2010) Vascular risk factor detection and control may prevent Alzheimer's disease. Ageing Research Reviews 9:218-225.

de la Torre JC, Alireza M (2009) Chapter 3 Cerebrovascular and Cardiovascular Pathology in Alzheimer's Disease. In: International Review of Neurobiology, pp 35-48: Academic Press.

de Reuck J (1971) The Human Periventricular Arterial Blood Supply and the Anatomy of Cerebral Infarctions. European Neurology 5:321-334.

Deary IJ, Bastin ME, Pattie A, Clayden JD, Whalley LJ, Starr JM, Wardlaw JM (2006) White matter integrity and cognition in childhood and old age. Neurology 66:505-512.

Deary IJ, Leaper S A, Murray A D, Staff R T, Whalley L J (2003) Cerebral white matter abnormalities and lifetime cognitive change: A 67-year follow-up of the Scottish Mental Survey of 1932. Psychology and Aging:140-148.

DeCarli C, Miller BL, Swan GE, Reed T, Wolf PA, Carmelli D (2001) Cerebrovascular and Brain Morphologic Correlates of Mild Cognitive Impairment in the National Heart, Lung, and Blood Institute Twin Study. Arch Neurol 58:643-647.

Derdeyn CP, Videen TO, Yundt KD, Fritsch SM, Carpenter DA, Grubb RL, Powers WJ (2002) Variability of cerebral blood volume and oxygen extraction: stages of cerebral haemodynamic impairment revisited. Brain 125:595-607.

Desai MK, Sudol KL, Janelsins MC, Mastrangelo MA, Frazer ME, Bowers WJ (2009) Triple-transgenic Alzheimer's disease mice exhibit region-specific abnormalities in brain myelination patterns prior to appearance of amyloid and tau pathology. Glia 57:54-65.

Desai MK, Mastrangelo MA, Ryan DA, Sudol KL, Narrow WC, Bowers WJ (2010) Early Oligodendrocyte/Myelin Pathology in Alzheimer's Disease Mice Constitutes a Novel Therapeutic Target. The American Journal of Pathology 177:1422-1435.

deToledo-Morrell L, Stoub TR, Wang C, Helen ES (2007) Hippocampal atrophy and disconnection in incipient and mild Alzheimer's disease. In: Progress in Brain Research, pp 741-753, 823: Elsevier.

Di Paola M, Di Iulio F, Cherubini A, Blundo C, Casini AR, Sancesario G, Passafiume D, Caltagirone C, Spalletta G (2010) When, where, and how the corpus callosum changes in MCI and AD. Neurology 74:1136-1142.

Dickerson BC, Eichenbaum H (2009) The Episodic Memory System: Neurocircuitry and Disorders. Neuropsychopharmacology 35:86-104.

Dodel RC, Du Y, Bales KR, Gao F, Eastwood B, Glazier B, Zimmer R, Cordell B, Hake A, Evans R, Gallagher-Thompson D, Thompson LW, Tinklenberg JR, Pfefferbaum A, Sullivan EV, Yesavage J, Altstiel L, Gasser T, Farlow MR, Murphy

GM, Paul SM (2000) Î±2 Macroglobulin and the risk of Alzheimerâ€™s disease. Neurology 54:438.

Drzezga A (2009) Diagnosis of Alzheimer's disease with [18F]PET in mild and asymptomatic stages. Behavioural Neurology 21:101-115.

Duan J-H, Wang H-Q, Xu J, Lin X, Chen S-Q, Kang Z, Yao Z-B (2006) White matter damage of patients with Alzheimer’s disease correlated with the decreased cognitive function. Surgical and Radiologic Anatomy 28:150-156.

Duff K, Eckman C, Zehr C, Yu X, Prada C-M, Perez-tur J, Hutton M, Buee L, Harigaya Y, Yager D, Morgan D, Gordon MN, Holcomb L, Refolo L, Zenk B, Hardy J, Younkin S (1996) Increased amyloid-[beta]42(43) in brains of mice expressing mutant presenilin 1. Nature 383:710-713.

Eckman EA, Reed DK, Eckman CB (2001) Degradation of the Alzheimer's Amyloid Î² Peptide by Endothelin-converting Enzyme. Journal of Biological Chemistry 276:24540-24548.

Eckman EA, Watson M, Marlow L, Sambamurti K, Eckman CB (2003) Alzheimer's Disease Î²-Amyloid Peptide Is Increased in Mice Deficient in Endothelin-converting Enzyme. Journal of Biological Chemistry 278:2081-2084.

Edgar JM, Nave K-A (2009) The role of CNS glia in preserving axon function. Current Opinion in Neurobiology 19:498-504.

Edvznsson MET, McCulloch J. (1993) Cerebral blood flow and metabolism. New York: Raven.
Elder GA, Gama Sosa MA, De Gasperi R (2010) Transgenic Mouse Models of Alzheimer's Disease. Mount Sinai Journal of Medicine: A Journal of Translational and Personalized Medicine 77:69-81.

Elesber AA, Bonetti PO, Woodrum JE, Zhu X-Y, Lerman LO, Younkin SG, Lerman A (2006) Bosentan preserves endothelial function in mice overexpressing APP. Neurobiology of Aging 27:446-450.

Enzinger C, Smith S, Fazekas F, Drevin G, Ropele S, Nichols T, Behrens T, Schmidt R, Matthews P (2006) Lesion probability maps of white matter hyperintensities in elderly individuals. Journal of Neurology 253:1064-1070.

Erb M, Flueck B, Kern F, Erne B, Steck AJ, Schaeren-Wiemers N (2006) Unraveling the differential expression of the two isoforms of myelin-associated glycoprotein in a mouse expressing GFP-tagged S-MAG specifically regulated and targeted into the different myelin compartments. Molecular and Cellular Neuroscience 31:613-627.

Escames G, Lopez A., Garcia JA, .Garcia L., Acuna-Castroviejo D., Garcia JJ, Lopez L. (2010) The Role of Mitochondria in Brain Aging and the Effects of Melatonin. Current Neuropharmacology 8:182-193.

Evans M (1994) Transgenic rodents. Animals with novel genes. Cambridge: Cambridge University Press.

Fancy SPJ, Kotter MR, Harrington EP, Huang JK, Zhao C, Rowitch DH, Franklin RJM (2010) Overcoming remyelination failure in multiple sclerosis and other myelin disorders. Experimental Neurology 225:18-23.

Farkas E, Luiten PGM (2001) Cerebral microvascular pathology in aging and Alzheimer's disease. Progress in Neurobiology 64:575-611.

Farkas E, Luiten PGM, Bari F (2007) Permanent, bilateral common carotid artery occlusion in the rat: A model for chronic cerebral hypoperfusion-related neurodegenerative diseases. Brain Research Reviews 54:162-180.

Farkas E, De Jong GI, Apró E, Keuker JIH, Luiten PGM (2000) Calcium antagonists decrease capillary wall damage in aging hypertensive rat brain. Neurobiology of Aging 22:299-309.

Farkas E, de Vos R, Donka G, Jansen Steur E, Mihály A, Luiten P (2006) Age-related microvascular degeneration in the human cerebral periventricular white matter. Acta Neuropathologica 111:150-157.

Fazekas F, Kleinert R, Offenbacher H, Schmidt R, Kleinert G, Payer F, Radner H, Lechner H (1993) Pathologic correlates of incidental MRI white matter signal hyperintensities. Neurology 43:1683.

Fernando MS, O'Brien JT, Perry RH, English P, Forster G, McMeekin W, Slade JY, Golkhar A, Matthews FE, Barber R, Kalaria RN, Ince PG, Neuropathology Group of MC (2004) Comparison of the pathology of cerebral white matter with post-mortem magnetic resonance imaging (MRI) in the elderly brain. Neuropathology and Applied Neurobiology 30:385-395.

Fernando MS, Simpson JE, Matthews F, Brayne C, Lewis CE, Barber R, Kalaria RN, Forster G, Esteves F, Wharton SB, Shaw PJ, O'Brien JT, Ince PG, on behalf of the MRCCFaANSG (2006) White Matter Lesions in an Unselected Cohort of the Elderly: Molecular Pathology Suggests Origin From Chronic Hypoperfusion Injury * Annex - Supplemental Online-Only Content. Stroke 37:1391-1398.

Fields RD (2008) White matter in learning, cognition and psychiatric disorders. Trends in Neurosciences 31:361-370.

Flicker L (2010) Modifiable Lifestyle Risk Factors for Alzheimer's Disease. Journal of Alzheimer's Disease 20:803-811.

Floyd RA, Hensley K (2002) Oxidative stress in brain aging: Implications for therapeutics of neurodegenerative diseases. Neurobiology of Aging 23:795-807.

Fox NC, Warrington EK, Seiffer AL, Agnew SK, Rossor MN (1998) Presymptomatic cognitive deficits in individuals at risk of familial Alzheimer's disease. A longitudinal prospective study. Brain 121:1631-1639.

Franklin RJM, ffrench-Constant C (2008) Remyelination in the CNS: from biology to therapy. Nat Rev Neurosci 9:839-855.

Fujii M, Hara H, Meng W, Vonsattel JP, Huang Z, Moskowitz MA (1997) Strain-Related Differences in Susceptibility to Transient Forebrain Ischemia in SV-129 and C57Black/6 Mice. Stroke 28:1805-1811.

Funahashi S (2006) Prefrontal cortex and working memory processes. Neuroscience 139:251-261.

Fuster JM (1973) Unit activity in prefrontal cortex during delayed-response performance: neuronal correlates of transient memory. J Neurophysiol 36:61-78.

Games D, Adams D, Alessandrini R, Barbour R, Borthelette P, Blackwell C, Carr T, Clemens J, Donaldson T, Gillespie F, Guido T, Hagopian S, Johnson-Wood K, Khan K, Lee M, Leibowitz P, Lieberburg I, Little S, Masliah E, McConlogue L, Montoya-Zavala M, Mucke L, Paganini L, Penniman E, Power M, Schenk D, Seubert P, Snyder B, Soriano F, Tan H, Vitale J, Wadsworth S, Wolozin B, Zhao J (1995) Alzheimer-type neuropathology in transgenic mice overexpressing V717F [beta]-amyloid precursor protein. Nature 373:523-527.

Garden G, Möller T (2006) Microglia Biology in Health and Disease. Journal of Neuroimmune Pharmacology 1:127-137.

Gendelman HE, Pezeshkpour GH, Pressman NJ, Wolinsky JS, Quarles RH, Dobersen MJ, Trapp BD, Kitt CA, Aksamit A, Johnson RT (1985) A quantitation of myelin-associated glycoprotein and myelin basic protein loss in different demyelinating disease. Annals of Neurology 18:324-328.

Giannakopoulos P, Herrmann FR, BussiÃ¨re T, Bouras C, Kavari E, Perl DP, Morrison JH, Gold G, Hof PR (2003) Tangle and neuron numbers, but not amyloid load, predict cognitive status in Alzheimer's disease. Neurology 60:1495-1500.

Gibbs JM, Leenders KL, Wise RJS, Jones T (1984) EVALUATION OF CEREBRAL PERFUSION RESERVE IN PATIENTS WITH CAROTID-ARTERY OCCLUSION. The Lancet 323:310-314.

Glenner GG, Wong CW (1984a) Alzheimer's disease: Initial report of the purification and characterization of a novel cerebrovascular amyloid protein. Biochemical and Biophysical Research Communications 120:885-890.

Glenner GG, Wong CW (1984b) Alzheimer's disease and Down's syndrome: Sharing of a unique cerebrovascular amyloid fibril protein. Biochemical and Biophysical Research Communications 122:1131-1135.

Goate A, Chartier-Harlin M-C, Mullan M, Brown J, Crawford F, Fidani L, Giuffra L, Haynes A, Irving N, James L, Mant R, Newton P, Rooke K, Roques P, Talbot C, Pericak-Vance M, Roses A, Williamson R, Rossor M, Owen M, Hardy J (1991)

Segregation of a missense mutation in the amyloid precursor protein gene with familial Alzheimer's disease. Nature 349:704-706.

Gorelick PB, Scuteri A, Black SE, DeCarli C, Greenberg SM, Iadecola C, Launer LJ, Laurent S, Lopez OL, Nyenhuis D, Petersen RC, Schneider JA, Tzourio C, Arnett DK, Bennett DA, Chui HC, Higashida RT, Lindquist R, Nilsson PM, Roman GC, Sellke FW, Seshadri S (2011) Vascular Contributions to Cognitive Impairment and Dementia. Stroke 42:2672-2713.

Gotz J, Chen F, Barmettler R, Nitsch RM (2001) Tau filament formation in transgenic mice expressing P301L tau. J Biol Chem 276:529 - 534.
Gralle M, Ferreira ST (2007) Structure and functions of the human amyloid precursor protein: The whole is more than the sum of its parts. Progress in Neurobiology 82:11-32.

Grammas P, Yamada M, Zlokovic B (2002) The cerebromicrovasculature: A key player in the pathogenesis of Alzheimer's disease Journal of Alzheimer's Disease 4:217-223.

Gravel M, Peterson J, Yong VW, Kottis V, Trapp B, Braun PE (1996) Overexpression of 2',3'-Cyclic Nucleotide 3'-Phosphodiesterase in Transgenic Mice Alters Oligodendrocyte Development and Produces Aberrant Myelination. Molecular and Cellular Neuroscience 7:453-466.

Griffin TWS, Sheng JG, Roberts GW, Mrak RE (1995) Interleukin-1 Expression in Different Plaque Types in Alzheimer's Disease: Significance in Plaque Evalution. Journal of Neuropathology & Experimental Neurology 54:276-281.

Guela C, Wu C-K, Saroff D, Lorenzo A, Yuan M, Yankner BA (1998) Aging renders the brain vulnerable to amyloid [beta]-protein neurotoxicity. Nat Med 4:827-831.

Guttmann CRG, Jolesz FA, Kikinis R, Killiany RJ, Moss MB, Sandor T, Albert MS (1998) White matter changes with normal aging. Neurology 50:972-978.

Haass C, Lemere CA, Capell A, Citron M, Seubert P, Schenk D, Lannfelt L, Selkoe DJ (1995) The Swedish mutation causes early-onset Alzheimer's disease by beta-secretase cleavage within the secretory pathway. Nat Med 1:1291 - 1296.

Hakak Y, Walker JR, Li C, Wong WH, Davis KL, Buxbaum JD, Haroutunian V, Fienberg AA (2001) Genome-wide expression analysis reveals dysregulation of myelination-related genes in chronic schizophrenia. Proceedings of the National Academy of Sciences of the United States of America 98:4746-4751.

Haley SM, Osberg JS (1989) Kappa Coefficient Calculation Using Multiple Ratings Per Subject: A Special Communication. Physical Therapy 69:970-974.

Hardy J (2009) The amyloid hypothesis for Alzheimer’s disease: a critical reappraisal. Journal of Neurochemistry 110:1129-1134.

Hardy J, Allsop D (1991) Amyloid deposition as the central event in the aetiology of Alzheimer's disease. Trends in Pharmacological Sciences 12:383-388.

Hardy J, Selkoe DJ (2002) The Amyloid Hypothesis of Alzheimer's Disease: Progress and Problems on the Road to Therapeutics. Science 297:353-356.
Harrison MJ (1989) Influence of haematocrit in the cerebral circulation Cerebrovascular and Brain Metabolism Reviews 1:55-67.

Hattori H, Takeda M, Kudo T, Nishimura T, Hashimoto S (1992) Cumulative white matter changes in the gerbil brain under chronic cerebral hypoperfusion. Acta Neuropathologica 84:437-442.

Hawkes C, HÃ¤rtig W, Kacza J, Schliebs R, Weller R, Nicoll J, Carare R (2011) Perivascular drainage of solutes is impaired in the ageing mouse brain and in the presence of cerebral amyloid angiopathy. Acta Neuropathologica 121:431-443.

Hershey T, Perantie DC, Warren SL, Zimmerman EC, Sadler M, White NH (2005) Frequency and Timing of Severe Hypoglycemia Affects Spatial Memory in Children With Type 1 Diabetes. Diabetes Care 28:2372-2377.

Hickman SE, Allison EK, El Khoury J (2008) Microglial Dysfunction and Defective {beta}-Amyloid Clearance Pathways in Aging Alzheimer's Disease Mice. J Neurosci 28:8354-8360.

Hinman JD, Chen CD, Oh SY, Hollander W, Abraham CR (2008) Age-dependent accumulation of ubiquitinated 2′,3′-cyclic nucleotide 3′-phosphodiesterase in myelin lipid rafts. Glia 56:118-133.

Hinman JD, Peters A, Cabral H, Rosene DL, Hollander W, Rasband MN, Abraham CR (2006) Age-related molecular reorganization at the node of Ranvier. The Journal of Comparative Neurology 495:351-362.

Hirao K, Ohnishi T, Hirata Y, Yamashita F, Mori T, Moriguchi Y, Matsuda H, Nemoto K, Imabayashi E, Yamada M, Iwamoto T, Arima K, Asada T (2005) The prediction of rapid conversion to Alzheimer's disease in mild cognitive impairment using regional cerebral blood flow SPECT. NeuroImage 28:1014-1021.

Hirata-Fukae C, Li H-F, Hoe H-S, Gray AJ, Minami SS, Hamada K, Niikura T, Hua F, Tsukagoshi-Nagai H, Horikoshi-Sakuraba Y, Mughal M, Rebeck GW, LaFerla FM, Mattson MP, Iwata N, Saido TC, Klein WL, Duff KE, Aisen PS, Matsuoka Y (2008) Females exhibit more extensive amyloid, but not tau, pathology in an Alzheimer transgenic model. Brain Research 1216:92-103.

Hodges H (1996) Maze procedures: the radial-arm and water maze compared. Cognitive Brain Research 3:167-181.

Holcomb L, Gordon MN, McGowan E, Yu X, Benkovic S, Jantzen P, Wright K, Saad I, Mueller R, Morgan D, Sanders S, Zehr C, O'Campo K, Hardy J, Prada C-M, Eckman C, Younkin S, Hsiao K, Duff K (1998) Accelerated Alzheimer-type

phenotype in transgenic mice carrying both mutant amyloid precursor protein and presenilin 1 transgenes. Nat Med 4:97-100.

Holland PR, Bastin ME, Jansen MA, Merrifield GD, Coltman RB, Scott F, Nowers H, Khallout K, Marshall I, Wardlaw JM, Deary IJ, McCulloch J, Horsburgh K (2010) MRI is a sensitive marker of subtle white matter pathology in hypoperfused mice. Neurobiology of Aging In Press, Corrected Proof.

Hope T, Keene J, Fairburn C, McShane R, Jacoby R (1997) Behaviour changes in dementia 2: Are there behavioural syndromes? International Journal of Geriatric Psychiatry 12:1074-1078.

Howell JM, Blakemore WF, Gopinath C, Hall GA, Parker JH (1974) Chronic copper poisoning and changes in the central nervous system of sheep. Acta Neuropathologica 29:9-24.

Hsia AY, Masliah E, McConlogue L, Yu G-Q, Tatsuno G, Hu K, Kholodenko D, Malenka RC, Nicoll RA, Mucke L (1999) Plaque-independent disruption of neural circuits in Alzheimer's disease mouse models. Proceedings of the National Academy of Sciences of the United States of America 96:3228-3233.

Hsiao K, Chapman P, Nilsen S, Eckman C, Harigaya Y, Younkin S, Yang F, Cole G (1996) Correlative Memory Deficits, Abeta Elevation, and Amyloid Plaques in Transgenic Mice. Science 274:99-103.

Hsu M-J, Sheu J-R, Lin C-H, Shen M-Y, Hsu CY (2010) Mitochondrial mechanisms in amyloid beta peptide-induced cerebrovascular degeneration. Biochimica et Biophysica Acta (BBA) - General Subjects 1800:290-296.

Hsu SM, Raine L, Fanger H (1981) Use of avidin-biotin-peroxidase complex (ABC) in immunoperoxidase techniques: a comparison between ABC and unlabeled antibody (PAP) procedures. J Histochem Cytochem 29:577-580.

Hu WT, Wang Z, Lee VMY, Trojanowski JQ, Detre JA, Grossman M (2010) Distinct cerebral perfusion patterns in FTLD and AD. Neurology 75:881-888.

Hu X, He W, Diaconu C, Tang X, Kidd GJ, Macklin WB, Trapp BD, Yan R (2008) Genetic deletion of BACE1 in mice affects remyelination of sciatic nerves. The FASEB Journal 22:2970-2980.

Huang H-M, Ou H-C, Hsueh S-J (1998) Amyloid [beta] peptide enhanced bradykinin-mediated inositol (1,4,5)trisphosphate formation and cytosolic free calcium. Life Sciences 63:195-203.

Hutton M, Lendon CL, Rizzu P, Baker M, Froelich S, Houlden H, Pickering-Brown S, Chakraverty S, Isaacs A, Grover A, Hackett J, Adamson J, Lincoln S, Dickson D, Davies P, Petersen RC, Stevens M, de Graaff E, Wauters E, van Baren J, Hillebrand M, Joosse M, Kwon JM, Nowotny P, Che LK, Norton J, Morris JC, Reed LA, Trojanowski J, Basun H, Lannfelt L, Neystat M, Fahn S, Dark F, Tannenberg T,

Dodd PR, Hayward N, Kwok JBJ, Schofield PR, Andreadis A, Snowden J, Craufurd D, Neary D, Owen F, Oostra BA, Hardy J, Goate A, van Swieten J, Mann D, Lynch T, Heutink P (1998) Association of missense and 5[prime]-splice-site mutations in tau with the inherited dementia FTDP-17. Nature 393:702-705.

Iadecola C (2010) The overlap between neurodegenerative and vascular factors in the pathogenesis of dementia. Acta Neuropathologica 120:287-296.

Iadecola C, Zhang F, Niwa K, Eckman C, Turner SK, Fischer E, Younkin S, Borchelt DR, Hsiao KK, Carlson GA (1999) SOD1 rescues cerebral endothelial dysfunction in mice overexpressing amyloid precursor protein. Nat Neurosci 2:157-161.

Ihara M, Polvikoski T, Hall R, Slade J, Perry R, Oakley A, Englund E, O'Brien J, Ince P, Kalaria R (2010) Quantification of myelin loss in frontal lobe white matter in vascular dementia, Alzheimer's disease, and dementia with Lewy bodies. Acta Neuropathologica 119:579-589.

Iqbal K, Grundke-Iqbal I (2008) Alzheimer Review Series: Alzheimer neurofibrillary degeneration: significance, etiopathogenesis, therapeutics and prevention. Journal of Cellular and Molecular Medicine 12:38-55.

Jankowsky JL, Younkin LH, Gonzales V, Fadale DJ, Slunt HH, Lester HA, Younkin SG, Borchelt DR (2007) Rodent Aβ Modulates the Solubility and Distribution of Amyloid Deposits in Transgenic Mice. Journal of Biological Chemistry 282:22707-22720.

Jantaratnotai N, Ryu JK, Kim SU, McLarnon JG (2003) Amyloid [beta] peptide-induced corpus callosum damage and glial activation in vivo. NeuroReport 14:1429-1433.

Jarrett JT, Berger EP, Lansbury PT (1993) The carboxy terminus of the .beta. amyloid protein is critical for the seeding of amyloid formation: Implications for the pathogenesis of Alzheimer's disease. Biochemistry 32:4693-4697.

Jones TH, Morawetz RB, Crowell RM, Marcoux FW, FitzGibbon SJ, DeGirolami U, Ojemann RG (1981) Thresholds of focal cerebral ischemia in awake monkeys. Journal of Neurosurgery 54:773-782.

Jonsson L, Wimo A (2009) The Cost of Dementia in Europe: A Review of the Evidence, and Methodological Considerations. PharmacoEconomics 27:391-403
Junque C, Pujol J, Vendrell P, Bruna O, Jodar M, Ribas JC, Vinas J, Capdevila A, Marti-Vilalta JL (1990) Leuko-Araiosis on Magnetic Resonance Imaging and Speed of Mental Processing. Arch Neurol 47:151-156.

Kagawa T, Ikenaka K, Inoue Y, Kuriyama S, Tsujii T, Nakao J, Nakajima K, Aruga J, Okano H, Mikoshiba K (1994) Glial cell degeneration and hypomyelination caused by overexpression of myelin proteolipid protein gene. Neuron 13:427-442.

Kalaria RN, Pax AB (1995) Increased collagen content of cerebral microvessels in Alzheimer's disease. Brain Research 705:349-352.

Kalaria RN, Bhatti SU, Lust WD, Perry G (1993) The Amyloid Precursor Protein in Ischemic Brain Injury and Chronic Hypoperfusiona. Annals of the New York Academy of Sciences 695:190-193.

Kalback WE, Chera; Castaño, Eduardo; Rahman, Afroza; Kokjohn, Tyler; Luehrs, Dean; Sue, Lucia; Cisneros, Raquel; Gerber, Francoise; Richardson, Claudia; Bohrmann, Bernd; Walker, Douglas; Beach, Thomas; Roher, Alex (2004) Atherosclerosis, vascular amyloidosis and brain hypoperfusion in the pathogenesis of sporadic Alzheimer's disease. Neurological Research 26:525-539.

Kamal A, Stokin GB, Yang Z, Xia C-H, Goldstein LSB (2000) Axonal Transport of Amyloid Precursor Protein Is Mediated by Direct Binding to the Kinesin Light Chain Subunit of Kinesin-I. Neuron 28:449-459.

Kamal A, Almenar-Queralt A, LeBlanc JF, Roberts EA, Goldstein LSB (2001) Kinesin-mediated axonal transport of a membrane compartment containing [beta]-secretase and presenilin-1 requires APP. Nature 414:643-648.

Kang J, Lemaire H-G, Unterbeck A, Salbaum JM, Masters CL, Grzeschik K-H, Multhaup G, Beyreuther K, Muller-Hill B (1987) The precursor of Alzheimer's disease amyloid A4 protein resembles a cell-surface receptor. Nature 325:733-736.

Kato H, Kogure K (1990) Neuronal damage following non-lethal but repeated cerebral ischemia in the gerbil. Acta Neuropathologica 79:494-500.

Kawamura J, Meyer JS, Terayama Y, Weathers S (1991) Leukoaraiosis correlates with cerebral hypoperfusion in vascular dementia. Stroke 22:609-614.

Kelly S, McCulloch J, Horsburgh K (2001) Minimal ischaemic neuronal damage and HSP70 expression in MF1 strain mice following bilateral common carotid artery occlusion. Brain Research 914:185-195.

Kennedy KM, Raz N (2009) Aging white matter and cognition: Differential effects of regional variations in diffusion properties on memory, executive functions, and speed. Neuropsychologia 47:916-927.

Kesner RP (2007) Behavioral functions of the CA3 subregion of the hippocampus. Learning & Memory 14:771-781.

Kim T, Pfeiffer SE (1999) Myelin glycosphingolipid/cholesterol-enriched microdomains selectively sequester the non-compact myelin proteins CNP and MOG. Journal of Neurocytology 28:281-293.

Kitagawa K, Matsumoto M, Yang G, Mabuchi T, Yagita Y, Hori M, Yanagihara T (1998) Cerebral Ischemia After Bilateral Carotid Artery Occlusion and Intraluminal

Suture Occlusion in Mice: Evaluation of the Patency of the Posterior Communicating Artery. J Cereb Blood Flow Metab 18:570-579.

Kitaguchi H, Tomimoto H, Ihara M, Shibata M, Uemura K, Kalaria RN, Kihara T, Asada-Utsugi M, Kinoshita A, Takahashi R (2009) Chronic cerebral hypoperfusion accelerates amyloid [beta] deposition in APPSwInd transgenic mice. Brain Research 1294:202-210.

Kitano H, Kirsch JR, Hurn PD, Murphy SJ (2006) Inhalational anesthetics as neuroprotectants or chemical preconditioning agents in ischemic brain. J Cereb Blood Flow Metab 27:1108-1128.

Kluver H, Barrera E (1953) A Method for the Combined Staining of Cells and Fibers in the Nervous System *. Journal of Neuropathology & Experimental Neurology 12:400-403.

Koike MA, Green KN, Blurton-Jones M, LaFerla FM (2010) Oligemic Hypoperfusion Differentially Affects Tau and Amyloid-{beta}. Am J Pathol 177:300-310.

Koistinaho M, Kettunen MI, Goldsteins G, KeinÃ¤nen R, Salminen A, Ort M, Bures J, Liu D, Kauppinen RA, Higgins LS, Koistinaho J (2002) β-Amyloid precursor protein transgenic mice that harbor diffuse Aβ deposits but do not form plaques show increased ischemic vulnerability: Role of inflammation. Proceedings of the National Academy of Sciences of the United States of America 99:1610-1615.

Kudo T, Takeda M, Tanimukai S, Nishimura T (1993) Neuropathologic changes in the gerbil brain after chronic hypoperfusion. Stroke 24:259-264.

Kume K, Hanyu H, Sato T, Hirao K, Shimizu S, Kanetaka H, Sakurai H, Iwamoto T (2011) Vascular risk factors are associated with faster decline of Alzheimer disease: a longitudinal SPECT study. Journal of Neurology:1-9.

Kurihara T, Tsukada Y (1967) THE REGIONAL AND SUBCELLULAR DISTRIBUTION OF 2′,3′-CYCLIC NUCLEOTIDE 3′-PHOSPHOHYDROLASE IN THE CENTRAL NERVOUS SYSTEM. Journal of Neurochemistry 14:1167-1174.

Kurumatani T, Kudo T, Ikura Y, Takeda M, Kontos HA (1998) White Matter Changes in the Gerbil Brain Under Chronic Cerebral Hypoperfusion • Editorial Comment. Stroke 29:1058-1062.

Kwang-Jin Oh SEP, Sarita Lagalwar, Laurel Vana, Lester Binder, and Elliott J. Mufson, (2010) Staging of Alzheimer's Pathology in Triple Transgenic Mice: A Light and Electron Microscopic Analysis. International Journal of Alzheimer's Disease 2010.

LaFerla FM, Green KN, Oddo S (2007a) Intracellular amyloid-[beta] in Alzheimer's disease. Nat Rev Neurosci 8:499-509.

LaFerla FM, Green KN, Oddo S (2007b) Intracellular amyloid-beta in Alzheimer's disease. Nat Rev Neurosci 8:499 - 509.

Lambert J-C, Heath S, Even G, Campion D, Sleegers K, Hiltunen M, Combarros O, Zelenika D, Bullido MJ, Tavernier B, Letenneur L, Bettens K, Berr C, Pasquier F, Fievet N, Barberger-Gateau P, Engelborghs S, De Deyn P, Mateo I, Franck A, Helisalmi S, Porcellini E, Hanon O, de Pancorbo MM, Lendon C, Dufouil C, Jaillard C, Leveillard T, Alvarez V, Bosco P, Mancuso M, Panza F, Nacmias B, Bossu P, Piccardi P, Annoni G, Seripa D, Galimberti D, Hannequin D, Licastro F, Soininen H, Ritchie K, Blanche H, Dartigues J-F, Tzourio C, Gut I, Van Broeckhoven C, Alperovitch A, Lathrop M, Amouyel P (2009) Genome-wide association study identifies variants at CLU and CR1 associated with Alzheimer's disease. Nat Genet 41:1094-1099.

Landis J, Koch, GG. (1977) The measurement of observer agreement for categorical data. Biometrics:16.

Lane RD, Laukes C, Marcus FI, Chesney MA, Sechrest L, Gear K, Fort CL, Priori SG, Schwartz PJ, Steptoe A (2005) Psychological Stress Preceding Idiopathic Ventricular Fibrillation. Psychosom Med 67:359-365.

Lasarzik I, Noppens Rd, Wolf T, Bauer H, Luh C, Werner C, Engelhard K, Thal S (2011) Dose-Dependent Influence of Sevoflurane Anesthesia on Neuronal Survival and Cognitive Outcome After Transient Forebrain Ischemia in Sprague-Dawley Rats. Neurocritical Care:1-8.

Lassmann H (2003) Hypoxia-like tissue injury as a component of multiple sclerosis lesions. Journal of the Neurological Sciences 206:187-191.

Lassmann H, Bartsch U, Montag D, Schachner M (1997) Dying-back oligodendrogliopathy: A late sequel of myelin-associated glycoprotein deficiency. Glia 19:104-110.

Lau T-L, Ambroggio EE, Tew DJ, Cappai R, Masters CL, Fidelio GD, Barnham KJ, Separovic F (2006) Amyloid-[beta] Peptide Disruption of Lipid Membranes and the Effect of Metal Ions. Journal of Molecular Biology 356:759-770.

Launer LJ, Ross GW, Petrovitch H, Masaki K, Foley D, White LR, Havlik RJ (2000) Midlife blood pressure and dementia: the Honolulu-Asia aging study. Neurobiology of aging 21:49-55.

Lazarov O, Morfini GA, Lee EB, Farah MH, Szodorai A, DeBoer SR, Koliatsos VE, Kins S, Lee VMY, Wong PC, Price DL, Brady ST, Sisodia SS (2005) Axonal Transport, Amyloid Precursor Protein, Kinesin-1, and the Processing Apparatus: Revisited. J Neurosci 25:2386-2395.

Lazic S (2009) Statistical evaluation of methods for quantifying gene expression by autoradiography in histological sections. BMC Neuroscience 10:5.

Lee J-T, Xu J, Lee J-M, Ku G, Han X, Yang D-I, Chen S, Hsu CY (2004) Amyloid-β peptide induces oligodendrocyte death by activating the neutral sphingomyelinaseâ€“ceramide pathway. The Journal of Cell Biology 164:123-131.

Lee M-Y, Kuan Y-H, Chen H-Y, Chen T-Y, Chen S-T, Huang C-C, Yang IP, Hsu Y-S, Wu T-S, Lee EJ (2007) Intravenous administration of melatonin reduces the intracerebral cellular inflammatory response following transient focal cerebral ischemia in rats. Journal of Pineal Research 42:297-309.

Leenders KL, Perani D, Lammertsma AA, Heather JD, Buckingham P, Jones T, Healy MJR, Gibbs JM, Wise RJS, Hatazawa J, Herold S, Beaney RP, Brooks DJ, Spinks T, Rhodes C, Frackowiak RSJ (1990) CEREBRAL BLOOD FLOW, BLOOD VOLUME AND OXYGEN UTILIZATION. Brain 113:27-47.

Lesne S, Koh MT, Kotilinek L, Kayed R, Glabe CG, Yang A, Gallagher M, Ashe KH (2006) A specific amyloid-[beta] protein assembly in the brain impairs memory. Nature 440:352-357.

Levy-Lahad E, Wijsman EM, Nemens E, Anderson L, Goddard KA, Weber JL, Bird TD, Schellenberg GD (1995b) A familial Alzheimer's disease locus on chromosome 1. Science 269:970-973.

Levy-Lahad E, Wasco W, Poorkaj P, Romano DM, Oshima J, Pettingell WH, Yu CE, Jondro PD, Schmidt SD, Wang K, al e (1995a) Candidate gene for the chromosome 1 familial Alzheimer's disease locus. Science 269:973-977.

Levy E, Carman MD, Fernandez-Madrid IJ, Power MD, Lieberburg I, van Duinen SG, Bots GT, Luyendijk W, Frangione B (1990) Mutation of the Alzheimer's disease amyloid gene in hereditary cerebral hemorrhage, Dutch type. Science 248:1124-1126.

Lewis J, Dickson DW, Lin W-L, Chisholm L, Corral A, Jones G, Yen S-H, Sahara N, Skipper L, Yager D, Eckman C, Hardy J, Hutton M, McGowan E (2001) Enhanced Neurofibrillary Degeneration in Transgenic Mice Expressing Mutant Tau and APP. Science 293:1487-1491.

Lewis J, McGowan E, Rockwood J, Melrose H, Nacharaju P, Van Slegtenhorst M, Gwinn-Hardy K, Murphy MP, Baker M, Yu X, Duff K, Hardy J, Corral A, Lin W-L, Yen S-H, Dickson DW, Davies P, Hutton M (2000) Neurofibrillary tangles, amyotrophy and progressive motor disturbance in mice expressing mutant (P301L) tau protein. Nat Genet 25:402-405.

Li Y-J, Oliveira SA, Xu P, Martin ER, Stenger JE, Scherzer CR, Hauser MA, Scott WK, Small GW, Nance MA, Watts RL, Hubble JP, Koller WC, Pahwa R, Stern MB, Hiner BC, Jankovic J, Goetz CG, Mastaglia F, Middleton LT, Roses AD, Saunders AM, Schmechel DE, Gullans SR, Haines JL, Gilbert JR, Vance JM, Pericak-Vance

MA (2003) Glutathione S-transferase omega-1 modifies age-at-onset of Alzheimer disease and Parkinson disease. Human Molecular Genetics 12:3259-3267.

Liebeskind DS (2003) Collateral Circulation. Stroke 34:2279-2284.

Lin S-Z, Chiou T-L, Chiang Y-H, Song W-S (1995) Hemodilution Accelerates the Passage of Plasma (Not Red Cells) Through Cerebral Microvessels in Rats. Stroke 26:2166-2171.

Little DMJ (1959) Hypothermia. Anesthesiology 20:842-877.

Loers G, Aboul-Enein F, Bartsch U, Lassmann H, Schachner M (2004) Comparison of myelin, axon, lipid, and immunopathology in the central nervous system of differentially myelin-compromised mutant mice: a morphological and biochemical study. Molecular and Cellular Neuroscience 27:175-189.

Lopez JR, Lyckman A, Oddo S, LaFerla FM, Querfurth HW, Shtifman A (2008) Increased intraneuronal resting [Ca2+] in adult Alzheimer's disease mice. Journal of Neurochemistry 105:262-271.

Luckhaus C, Flüß MO, Wittsack H-J, Grass-Kapanke B, Jänner M, Khalili-Amiri R, Friedrich W, Supprian T, Gaebel W, Mödder U, Cohnen M (2008) Detection of changed regional cerebral blood flow in mild cognitive impairment and early Alzheimer's dementia by perfusion-weighted magnetic resonance imaging. NeuroImage 40:495-503.

Ludwin S (1978) Central nervous system demyelination and remyelination in the mouse: an ultrastructural study of cuprizone toxicity. Journal of laboratory investigation 39:15.

Lycette RM, Danforth WF, Koppel JL, Olwin JH (1970) The Binding of Luxol Fast Blue Arn by Various Biological Lipids. Biotechnic & Histochemistry 45:155-160.

Lye TC, Shores EA (2000) Traumatic Brain Injury as a Risk Factor for Alzheimer's Disease: A Review. Neuropsychology Review 10:115-129.

Maeda K, Hata R, Hossmann K-A (1998) Differences in the cerebrovascular anatomy of C57Black/6 and SV129 mice. NeuroReport 9:1317-1319.

Marner L, Nyengaard JR, Tang Y, Pakkenberg B (2003) Marked loss of myelinated nerve fibers in the human brain with age. The Journal of Comparative Neurology 462:144-152.

Martin B, Brenneman R, Becker KG, Gucek M, Cole RN, Maudsley S (2008) iTRAQ Analysis of Complex Proteome Alterations in 3xTgAD Alzheimer's Mice: Understanding the Interface between Physiology and Disease. PLoS ONE 3:e2750.

Mastrangelo M, Bowers W (2008) Detailed immunohistochemical characterization of temporal and spatial progression of Alzheimer's disease-related pathologies in male triple-transgenic mice. BMC Neuroscience 9:81.

Matsuda H (2007) Role of Neuroimaging in Alzheimer's Disease, with Emphasis on Brain Perfusion SPECT. J Nucl Med 48:1289-1300.

McKenzie KJ, McLellan DR, Gentleman SM, Maxwell WL, Gennarelli TA, Graham DI (1996) Is β-APP a marker of axonal damage in short-surviving head injury? Acta Neuropathologica 92:608-613.

McKerracher L, David S, Jackson DL, Kottis V, Dunn RJ, Braun PE (1994) Identification of myelin-associated glycoprotein as a major myelin-derived inhibitor of neurite growth. Neuron 13:805-811.

Metcalfe MJ, Figueiredo-Pereira ME (2010) Relationship Between Tau Pathology and Neuroinflammation in Alzheimer's Disease. Mount Sinai Journal of Medicine: A Journal of Translational and Personalized Medicine 77:50-58.

Miki K, Ishibashi S, Sun L, Xu H, Ohashi W, Kuroiwa T, Mizusawa H (2009) Intensity of chronic cerebral hypoperfusion determines white/gray matter injury and cognitive/motor dysfunction in mice. Journal of Neuroscience Research 87:1270-1281.

Miller RH, Raff MC (1984) Fibrous and protoplasmic astrocytes are biochemically and developmentally distinct. J Neurosci 4:585-592.

Moskowitz MA, Lo EH, Iadecola C (2010) The Science of Stroke: Mechanisms in Search of Treatments. Neuron 67:181-198.

Mucke L, Masliah E, Yu G-Q, Mallory M, Rockenstein EM, Tatsuno G, Hu K, Kholodenko D, Johnson-Wood K, McConlogue L (2000) High-Level Neuronal Expression of Abeta 1-42 in Wild-Type Human Amyloid Protein Precursor Transgenic Mice: Synaptotoxicity without Plaque Formation. J Neurosci 20:4050-4058.

Naggara O, Oppenheim C, Rieu D, Raoux N, Rodrigo S, Dalla Barba G, Meder J-F (2006) Diffusion tensor imaging in early Alzheimer's disease. Psychiatry Research: Neuroimaging 146:243-249.

Nakaji K, Ihara M, Takahashi C, Itohara S, Noda M, Takahashi R, Tomimoto H (2006) Matrix Metalloproteinase-2 Plays a Critical Role in the Pathogenesis of White Matter Lesions After Chronic Cerebral Hypoperfusion in Rodents. Stroke 37:2816-2823.

Nicholson RM, Kusne Y, Nowak LA, LaFerla FM, Reiman EM, Valla J (2009) Regional cerebral glucose uptake in the 3xTG model of Alzheimer's disease highlights common regional vulnerability across AD mouse models. Brain Research 1347:179-185.

Nishio K, Ihara M, Yamasaki N, Kalaria RN, Maki T, Fujita Y, Ito H, Oishi N, Fukuyama H, Miyakawa T, Takahashi R, Tomimoto H (2010) A Mouse Model Characterizing Features of Vascular Dementia With Hippocampal Atrophy * Supplemental Methods. Stroke 41:1278-1284.

Niwa K, Kazama K, Younkin SG, Carlson GA, Iadecola C (2002) Alterations in Cerebral Blood Flow and Glucose Utilization in Mice Overexpressing the Amyloid Precursor Protein. Neurobiology of Disease 9:61-68.

Niwa K, Porter VA, Kazama K, Cornfield D, Carlson GA, Iadecola C (2001) Abeta - peptides enhance vasoconstriction in cerebral circulation. Am J Physiol Heart Circ Physiol 281:H2417-2424.

Niwa K, Younkin L, Ebeling C, Turner SK, Westaway D, Younkin S, Ashe KH, Carlson GA, Iadecola C (2000) Aβ 40-related reduction in functional hyperemia in mouse neocortex during somatosensory activation. Proceedings of the National Academy of Sciences of the United States of America 97:9735-9740.

O'Donnell KA, Rapp PR, Hof PR (1999) Preservation of Prefrontal Cortical Volume in Behaviorally Characterized Aged Macaque Monkeys. Experimental Neurology 160:300-310.

O'Sullivan M (2008) Leukoaraiosis. Practical Neurology 8:26-38.

O'Sullivan M, Jones DK, Summers PE, Morris RG, Williams SCR, Markus HS (2001) Evidence for cortical "disconnection" as a mechanism of age-related cognitive decline. Neurology 57:632-638.

Oddo S, Caccamo A, Kitazawa M, Tseng BP, LaFerla FM (2003a) Amyloid deposition precedes tangle formation in a triple transgenic model of Alzheimer's disease. Neurobiol Aging 24:1063 - 1070.

Oddo S, Billings L, Kesslak JP, Cribbs DH, LaFerla FM (2004) A[beta] Immunotherapy Leads to Clearance of Early, but Not Late, Hyperphosphorylated Tau Aggregates via the Proteasome. Neuron 43:321-332.

Oddo S, Caccamo A, Shepherd JD, Murphy MP, Golde TE, Kayed R, Metherate R, Mattson MP, Akbari Y, LaFerla FM (2003b) Triple-Transgenic Model of Alzheimer's Disease with Plaques and Tangles: Intracellular A[beta] and Synaptic Dysfunction. Neuron 39:409-421.

Ogata J, Fujishima M, Tamaki K, Nakatomi Y, Ishitsuka T, Omae T (1982) Stroke-prone spontaneously hypertensive rats as an experimental model of malignant hypertension. Virchows Archiv 394:185-194.

Okamoto K, Yamori, Y. (1973) Spontaneous hypertension in rats versus essential hypertension in man. Singapore medical journal 14:393-394.

Olivier P, Fontaine RH, Loron G, Van Steenwinckel J, Biran Vr, Massonneau Vr, Kaindl A, Dalous J, Charriaut-Marlangue C, Aigrot M-Sp, Pansiot J, Verney C, Gressens P, Baud O (2009) Melatonin Promotes Oligodendroglial Maturation of Injured White Matter in Neonatal Rats. PLoS ONE 4:e7128.

Pakkenberg B, Gundersen HJG (1997) Neocortical neuron number in humans: Effect of sex and age. The Journal of Comparative Neurology 384:312-320.

Pakkenberg B, Pelvig D, Marner L, Bundgaard MJ, Gundersen HJG, Nyengaard JR, Regeur L (2003) Aging and the human neocortex. Experimental Gerontology 38:95-99.

Palmer JC, Kehoe PG, Love S (2010) Endothelin-converting enzyme-1 in Alzheimer's disease and vascular dementia. Neuropathology and Applied Neurobiology 36:487-497.

Palmer JC, Baig S, Kehoe PG, Love S (2009) Endothelin-Converting Enzyme-2 Is Increased in Alzheimerâ€™s Disease and Up-Regulated by AÎ². The American Journal of Pathology 175:262-270.

Pan B, Fromholt SE, Hess EJ, Crawford TO, Griffin JW, Sheikh KA, Schnaar RL (2005) Myelin-associated glycoprotein and complementary axonal ligands, gangliosides, mediate axon stability in the CNS and PNS: Neuropathology and behavioral deficits in single- and double-null mice. Experimental Neurology 195:208-217.

Pantoni L, Garcia JH (1997) Pathogenesis of Leukoaraiosis : A Review. Stroke 28:652-659.

Pantoni L, Garcia JH, Gutierrez JA, Rosenblum WI (1996) Cerebral White Matter Is Highly Vulnerable to Ischemia. Stroke 27:1641-1647.

Pappas BA, Davidson CM, Bennett SAL, de la Torre JC, Fortin T, Tenniswood MPR (1997) Chronic Ischemia: Memory Impairment And Neural Pathology in the Rata. Annals of the New York Academy of Sciences 826:498-501.

Pappolla M, Bozner P, Soto C, Shao H, Robakis NK, Zagorski M, Frangione B, Ghiso J (1998) Inhibition of Alzheimer a beta-Fibrillogenesis by Melatonin. Journal of Biological Chemistry 273:7185-7188.

Pappolla MA, Chyan YJ, Poeggeler B, Frangione B, Wilson G, Ghiso J, Reiter RJ (2000) An assessment of the antioxidant and the antiamyloidogenic properties of melatonin: implications for Alzheimer's disease. Journal of Neural Transmission 107:203-231.

Pardon M-C, Kendall DA, Pérez-Diaz F, Duxon MS, Marsden CA (2004) Repeated sensory contact with aggressive mice rapidly leads to an anticipatory increase in core body temperature and physical activity that precedes the onset of aversive responding. European Journal of Neuroscience 20:1033-1050.

Pedraza L, Fidler L, Staugaitis SM, Colman DR (1997) The Active Transport of Myelin Basic Protein into the Nucleus Suggests a Regulatory Role in Myelination. Neuron 18:579-589.

Perry VH, Nicoll JAR, Holmes C (2010) Microglia in neurodegenerative disease. Nat Rev Neurol 6:193-201.

Peters A (2002) The effects of normal aging on myelin and nerve fibers: A review. Journal of Neurocytology 31:581-593.

Peters A (2009) The effects of normal aging on myelinated nerve fibers in monkey central nervous system. Frontiers in Neuroanatomy 4:12.

Peters A, Sethares C (2002) Aging and the myelinated fibers in prefrontal cortex and corpus callosum of the monkey. The Journal of Comparative Neurology 442:277-291.

Peters APS, Webster H de F (1991) The Fine Structure of the Nervous System: the Neuron and the Supporting Cells. Oxford: Oxford University Press.

Pimplikar SW (2009) Reassessing the amyloid cascade hypothesis of Alzheimer's disease. The International Journal of Biochemistry & Cell Biology 41:1261-1268.

Pluta R, Kida E, Lossinsky AS, Golabek AA, Mossakowski MJ, Wisniewski HM (1994) Complete cerebral ischemia with short-term survival in rats induced by cardiac arrest. I. Extracellular accumulation of Alzheimer's [beta]-amyloid protein precursor in the brain. Brain Research 649:323-328.

Privat A, Jacque C, Bourre JM, Dupouey P, Baumann N (1979) Absence of the major dense line in myelin of the mutant mouse [`]shiverer'. Neuroscience Letters 12:107-112.

Prohovnik I, Mayeux R, Sackeim HA, Smith G, Stern Y, Alderson PO (1988) Cerebral perfusion as a diagnostic marker of early Alzheimer's disease. Neurology 38:931-.

Qiu C, De Ronchi, D. and Fratiglioni, L (2007) The epidemiology of the dementias: an update. Current Opinion in Psychiatry 20:6.

Quarles RH (2007) Myelin-associated glycoprotein (MAG): past, present and beyond. Journal of Neurochemistry 100:1431-1448.

Quarles RH, Everly JL, Brady RO (1973) EVIDENCE FOR THE CLOSE ASSOCIATION OF A GLYCOPROTEIN WITH MYELIN IN RAT BRAIN. Journal of Neurochemistry 21:1177-1191.

Quarles RH, Macklin W.B., Morrell P (2006) Basic Neurochemistry: Molecular, Cellular, and Medical Aspects. New York: Elsevier Inc.

Querfurth HW, LaFerla FM (2010) Alzheimer's Disease. New England Journal of Medicine 362:329-344.

Rasband MN, Tayler J, Kaga Y, Yang Y, Lappe-Siefke C, Nave KA, Bansal R (2005) CNP is required for maintenance of axon–glia interactions at nodes of Ranvier in the CNS. Glia 50:86-90.

Raz N, Rodrigue KM, Kennedy KM, Acker JD (2007) Vascular Health and Longitudinal Changes in Brain and Cognition in Middle-Aged and Older Adults. [Article].

Resnick SM, Goldszal AF, Davatzikos C, Golski S, Kraut MA, Metter EJ, Bryan RN, Zonderman AB (2000) One-year Age Changes in MRI Brain Volumes in Older Adults. Cerebral Cortex 10:464-472.

Ricciardi E, Bonino D, Gentili C, Sani L, Pietrini P, Vecchi T (2006) Neural correlates of spatial working memory in humans: A functional magnetic resonance imaging study comparing visual and tactile processes. Neuroscience 139:339-349.

Riekse RG, Leverenz JB, McCormick W, Bowen JD, Teri L, Nochlin D, Simpson K, Eugenio C, Larson EB, Tsuang D (2004) Effect of Vascular Lesions on Cognition in Alzheimer's Disease: A Community-Based Study. Journal of the American Geriatrics Society 52:1442-1448.

Roach A, Takahashi N, Pravtcheva D, Ruddle F, Hood L (1985) Chromosomal mapping of mouse myelin basic protein gene and structure and transcription of the partially deleted gene in shiverer mutant mice. Cell 42:149-155.

Rogaev EI, Sherrington R, Rogaeva EA, Levesque G, Ikeda M, Liang Y, Chi H, Lin C, Holman K, Tsuda T, Mar L, Sorbi S, Nacmias B, Piacentini S, Amaducci L, Chumakov I, Cohen D, Lannfelt L, Fraser PE, Rommens JM, George-Hyslop PHS (1995) Familial Alzheimer's disease in kindreds with missense mutations in a gene on chromosome 1 related to the Alzheimer's disease type 3 gene. Nature 376:775-778.

Rogaeva E, Meng Y, Lee JH, Gu Y, Kawarai T, Zou F, Katayama T, Baldwin CT, Cheng R, Hasegawa H, Chen F, Shibata N, Lunetta KL, Pardossi-Piquard R, Bohm C, Wakutani Y, Cupples LA, Cuenco KT, Green RC, Pinessi L, Rainero I, Sorbi S, Bruni A, Duara R, Friedland RP, Inzelberg R, Hampe W, Bujo H, Song Y-Q, Andersen OM, Willnow TE, Graff-Radford N, Petersen RC, Dickson D, Der SD, Fraser PE, Schmitt-Ulms G, Younkin S, Mayeux R, Farrer LA, St George-Hyslop P (2007) The neuronal sortilin-related receptor SORL1 is genetically associated with Alzheimer disease. Nat Genet 39:168-177.

Rogers J, Strohmeyer R, Kovelowski C, Li R (2002) Microglia and inflammatory mechanisms in the clearance of amyloid β peptide. Glia 40:260-269.

Roher AE, Weiss N, Kokjohn TA, Kuo Y-M, Kalback W, Anthony J, Watson D, Luehrs DC, Sue L, Walker D, Emmerling M, Goux W, Beach T (2002) Increased Aβ Peptides and Reduced Cholesterol and Myelin Proteins Characterize White Matter Degeneration in Alzheimer's Disease Biochemistry 41:11080-11090.

Rombouts SARB, Goekoop R, Stam CJ, Barkhof F, Scheltens P (2005) Delayed rather than decreased BOLD response as a marker for early Alzheimer's disease. NeuroImage 26:1078-1085.

Rosenberg GA, Kornfeld M, Stovring J, Bicknell JM (1979) Subcortical arteriosclerotic encephalopathy (Binswanger). Neurology 29:1102.

Rosenberg GA, Sullivan N, Esiri MM, Sobel RA (2001) White Matter Damage Is Associated With Matrix Metalloproteinases in Vascular Dementia Editorial Comment : Matrix Metalloproteinases and Diffuse White Matter Injury. Stroke 32:1162-1168.

Rosenbluth J (1966) REDUNDANT MYELIN SHEATHS AND OTHER ULTRASTRUCTURAL FEATURES OF THE TOAD CEREBELLUM. The Journal of Cell Biology 28:73-93.

Roth AD, RamÍRez G, AlarcÓN R, Von Bernhardi R (2005) Oligodendrocytes damage in Alzheimer's disease: Beta amyloid toxicity and inflammation. Biological Research 38:381-387.

Rowbotham GF, Little E (1965) Circulations of the cerebral hemispheres. British Journal of Surgery 52:8-21.

Roy S, Zhang B, Lee VMY, Trojanowski JQ (2005) Axonal transport defects: a common theme in neurodegenerative diseases. Acta Neuropathologica 109:5-13.

Rubin BAM, Horovitz ZP. (1978) Captopril (SQ 14,225) (D-3-mercapto-2-methylpropranoyl-L-proline): a novel orally active inhibitor of angiotensin-converting enzyme and antihypertensive agent. Progress in Cardiovascular Discovery 21:12.

Ruitenberg A, den Heijer T, Bakker SLM, van Swieten JC, Koudstaal PJ, Hofman A, Breteler MMB (2005) Cerebral hypoperfusion and clinical onset of dementia: The Rotterdam study. Annals of Neurology 57:789-794.

Ryan NS, Rossor MN (2010) Correlating familial Alzheimers disease gene mutations with clinical phenotype. Biomarkers in Medicine 4:99-112.

Salat DH, Greve DN, Pacheco JL, Quinn BT, Helmer KG, Buckner RL, Fischl B (2009) Regional white matter volume differences in nondemented aging and Alzheimer's disease. NeuroImage 44:1247-1258.

Salthouse TN (1962) Luxol Fast Blue Arn: A New Solvent Azo Dye with Improved Staining Qualities for Myelin and Phospholipids. Biotechnic and Histochemistry 37:313 - 316.

Salzer JL, Holmes WP, Colman DR (1987) The amino acid sequences of the myelin-associated glycoproteins: homology to the immunoglobulin gene superfamily. The Journal of Cell Biology 104:957-965.

Sarti C, Pantoni L, Bartolini L, Inzitari D (2002) Cognitive impairment and chronic cerebral hypoperfusion: What can be learned from experimental models. Journal of the Neurological Sciences 203-204:263-266.
Scheinberg P (1988) Dementia due to vascular disease--a multifactorial disorder. Stroke 19:1291-1299.

Schenk F, Morris RGM (1985) Dissociation between components of spatial memory in rats after recovery from the effects of retrohippocampal lesions. Experimental Brain Research 58:11-28.

Scheuner D, Eckman C, Jensen M, Song X, Citron M, Suzuki N, Bird TD, Hardy J, Hutton M, Kukull W, Larson E, Levy-Lahad L, Viitanen M, Peskind E, Poorkaj P, Schellenberg G, Tanzi R, Wasco W, Lannfelt L, Selkoe D, Younkin S (1996) Secreted amyloid [beta]-protein similar to that in the senile plaques of Alzheimer's disease is increased in vivo by the presenilin 1 and 2 and APP mutations linked to familial Alzheimer's disease. Nat Med 2:864-870.

Schmid-Schonbein H (1983) Macrorheology and Microrheology of Blood in Cerebrovascular Insufficiency. European Neurology 22:2-22.

Schmitz T, Chew L-J (2008) Cytokines and Myelination in the Central Nervous System. TheScientificWorldJOURNAL 8:1119-1147.

Selkoe DJ (1991) The molecular pathology of Alzheimer's disease. Neuron 6:487-498.

Selkoe DJ, Podlisny MB (2002) DECIPHERING THE GENETIC BASIS OF ALZHEIMER'S DISEASE. Annual Review of Genomics and Human Genetics 3:67-99.

Selkoe DJ, Podlisny MB, Joachim CL, Vickers EA, Lee G, Fritz LC, Oltersdorf T (1988) Beta-amyloid precursor protein of Alzheimer disease occurs as 110- to 135-kilodalton membrane-associated proteins in neural and nonneural tissues. Proceedings of the National Academy of Sciences of the United States of America 85:7341-7345.

Shankar GM, Li S, Mehta TH, Garcia-Munoz A, Shepardson NE, Smith I, Brett FM, Farrell MA, Rowan MJ, Lemere CA, Regan CM, Walsh DM, Sabatini BL, Selkoe DJ (2008) Amyloid-[beta] protein dimers isolated directly from Alzheimer's brains impair synaptic plasticity and memory. Nat Med 14:837-842.

Sherrington R, Rogaev EI, Liang Y, Rogaeva EA, Levesque G, Ikeda M, Chi H, Lin C, Li G, Holman K, Tsuda T, Mar L, Foncin JF, Bruni AC, Montesi MP, Sorbi S, Rainero I, Pinessi L, Nee L, Chumakov I, Pollen D, Brookes A, Sanseau P, Polinsky RJ, Wasco W, Da Silva HAR, Haines JL, Pericak-Vance MA, Tanzi RE, Roses AD, Fraser PE, Rommens JM, St George-Hyslop PH (1995) Cloning of a gene bearing missense mutations in early-onset familial Alzheimer's disease. Nature 375:754-760.

Shibata M, Ohtani R, Ihara M, Tomimoto H (2004) White Matter Lesions and Glial Activation in a Novel Mouse Model of Chronic Cerebral Hypoperfusion. Stroke 35:2598-2603.

Shibata M, Yamasaki N, Miyakawa T, Kalaria RN, Fujita Y, Ohtani R, Ihara M, Takahashi R, Tomimoto H (2007) Selective Impairment of Working Memory in a Mouse Model of Chronic Cerebral Hypoperfusion. Stroke 38:2826-2832.

Simpson JE, Fernando MS, Clark L, Ince PG, Matthews F, Forster G, O'Brien JT, Barber R, Kalaria RN, Brayne C, Shaw PJ, Lewis CE, Wharton SB, Group MRCCFaANS (2007a) White matter lesions in an unselected cohort of the elderly: astrocytic, microglial and oligodendrocyte precursor cell responses. Neuropathology and Applied Neurobiology 33:410-419.

Simpson JE, Ince PG, Higham CE, Gelsthorpe CH, Fernando MS, Matthews F, Forster G, O'Brien JT, Barber R, Kalaria RN, Brayne C, Shaw PJ, Stoeber K, Williams GH, Lewis CE, Wharton SB, the MRCCFaANSG (2007b) Microglial activation in white matter lesions and nonlesional white matter of ageing brains. Neuropathology and Applied Neurobiology 33:670-683.

Skaper S, Evans N, Soden P, Rosin C, Facci L, Richardson J (2009) Oligodendrocytes are a Novel Source of Amyloid Peptide Generation. Neurochemical Research 34:2243-2250.

Sloane JA, Hinman JD, Lubonia M, Hollander W, Abraham CR (2003) Age-dependent myelin degeneration and proteolysis of oligodendrocyte proteins is associated with the activation of calpain-1 in the rhesus monkey. Journal of Neurochemistry 84:157-168.

Small SA, Duff K (2008) Linking A[beta] and Tau in Late-Onset Alzheimer's Disease: A Dual Pathway Hypothesis. Neuron 60:534-542.

Song S-K, Kim JH, Lin S-J, Brendza RP, Holtzman DM (2004) Diffusion tensor imaging detects age-dependent white matter changes in a transgenic mouse model with amyloid deposition. Neurobiology of Disease 15:640-647.

Spain A, Daumas S, Lifshitz J, Rhodes J, Andrews PJD, Horsburgh K, Fowler JH (2010) Mild Fluid Percussion Injury in Mice Produces Evolving Selective Axonal Pathology and Cognitive Deficits Relevant to Human Brain Injury. Journal of Neurotrauma 27:1429-1438.

Squier TC (2001) Oxidative stress and protein aggregation during biological aging. Experimental Gerontology 36:1539-1550.

St George-Hyslop PH (2000) Genetic Factors in the Genesis of Alzheimer's Disease. Annals of the New York Academy of Sciences 924:1-7.

Staugaitis SM, Smith PR, Colman DR (1990) Expression of myelin basic protein isoforms in nonglial cells. The Journal of Cell Biology 110:1719-1727.

Stephanova DI, Daskalova M, Alexandrov AS (2005) Differences in potentials and excitability properties in simulated cases of demyelinating neuropathies. Part I. Clinical Neurophysiology 116:1153-1158.

Sternlicht MD, Werb Z (2001) HOW MATRIX METALLOPROTEINASES REGULATE CELL BEHAVIOR. Annual Review of Cell and Developmental Biology 17:463-516.

Stokin GB, Lillo C, Falzone TL, Brusch RG, Rockenstein E, Mount SL, Raman R, Davies P, Masliah E, Williams DS, Goldstein LSB (2005) Axonopathy and Transport Deficits Early in the Pathogenesis of Alzheimer's Disease. Science 307:1282-1288.

Stommel A, Berlet HH, Debuch H (1989) Buoyant density and lipid composition of purified myelin of aging human brain. Mechanisms of Ageing and Development 48:1-14.

Stout JC, Jernigan TL, Archibald SL, Salmon DP (1996) Association of Dementia Severity With Cortical Gray Matter and Abnormal White Matter Volumes in Dementia of the Alzheimer Type. Arch Neurol 53:742-749.

Strittmatter WJ, Saunders AM, Schmechel D, Pericak-Vance M, Enghild J, Salvesen GS, Roses AD (1993) Apolipoprotein E: high-avidity binding to beta-amyloid and increased frequency of type 4 allele in late-onset familial Alzheimer disease. Proceedings of the National Academy of Sciences of the United States of America 90:1977-1981.

Sturrock RR (1976) Changes in Neuroglia and Myelination in the White Matter of Aging Mice. Journal of Gerontology 31:513-522.

Sun S-W, Song S-K, Harms MP, Lin S-J, Holtzman DM, Merchant KM, Kotyk JJ (2005) Detection of age-dependent brain injury in a mouse model of brain amyloidosis associated with Alzheimer's disease using magnetic resonance diffusion tensor imaging. Experimental Neurology 191:77-85.

Svennerholm L, Boström K, Helander CG, Jungbjer B (1991) Membrane Lipids in the Aging Human Brain. Journal of Neurochemistry 56:2051-2059.

Takeuchi H, Sekiguchi A, Taki Y, Yokoyama S, Yomogida Y, Komuro N, Yamanouchi T, Suzuki S, Kawashima R (2010) Training of Working Memory Impacts Structural Connectivity. The Journal of Neuroscience 30:3297-3303.

Tamura E, Parry GJ (1994) Severe radicular pathology in rats with longstanding diabetes. Journal of the Neurological Sciences 127:29-35.

Tanaka H, Ma J, Tanaka KF, Takao K, Komada M, Tanda K, Suzuki A, Ishibashi T, Baba H, Isa T, Shigemoto R, Ono K, Miyakawa T, Ikenaka K (2009) Mice with Altered Myelin Proteolipid Protein Gene Expression Display Cognitive Deficits Accompanied by Abnormal Neuronâ€“Glia Interactions and Decreased Conduction Velocities. The Journal of Neuroscience 29:8363-8371.

Tang Y, Nyengaard JR, Pakkenberg B, Gundersen HJG (1997) Age-Induced White Matter Changes in the Human Brain: A Stereological Investigation. Neurobiology of Aging 18:609-615.

Tanzi RE, Moir RD, Wagner SL (2004) Clearance of Alzheimer's A[beta] Peptide: The Many Roads to Perdition. Neuron 43:605-608.

Thomas DJ, Marshall J, Russell RWR, Wetherley-Mein G, Boulay GHD, Pearson TC, Symon L, Zilkha E (1977) EFFECT OF HÆMATOCRIT ON CEREBRAL BLOOD-FLOW IN MAN. The Lancet 310:941-943.

Thomas T, Thomas G, McLendon C, Sutton T, Mullan M (1996) [beta]-Amyloid-mediated vasoactivity and vascular endothelial damage. Nature 380:168-171.

Tiehuis A, Vincken K, van den Berg E, Hendrikse J, Manschot S, Mali W, Kappelle L, Biessels G (2008) Cerebral perfusion in relation to cognitive function and type 2 diabetes. Diabetologia 51:1321-1326.

Tkachev D, Mimmack ML, Ryan MM, Wayland M, Freeman T, Jones PB, Starkey M, Webster MJ, Yolken RH, Bahn S (2003) Oligodendrocyte dysfunction in schizophrenia and bipolar disorder. The Lancet 362:798-805.

Trapp BD, Bernier L, Andrews SB, Colman DR (1988) Cellular and Subcellular Distribution of 2′,3′-Cyclic Nucleotide 3′-Phosphodiesterase and Its mRNA in the Rat Central Nervous System. Journal of Neurochemistry 51:859-868.

Trudel X, Brisson C, Milot A (2010) Job Strain and Masked Hypertension. Psychosom Med 72:786-793.

Turner PR, O'Connor K, Tate WP, Abraham WC (2003) Roles of amyloid precursor protein and its fragments in regulating neural activity, plasticity and memory. Progress in Neurobiology 70:1-32.

Ukmar M, Makuc E, Onor M, Garbin G, Trevisiol M, Cova M (2008) Evaluation of white matter damage in patients with Alzheimer’s disease and in patients with mild

cognitive impairment by using diffusion tensor imaging. La Radiologia Medica 113:915-922.

Van Den Bergh R, Van Der Eecken H, Luyendijk W (1968) Anatomy and Embryology of Cerebral Circulation. In: Progress in Brain Research, pp 1-25: Elsevier.

van Dijk EJ, Breteler MMB, Schmidt R, Berger K, Nilsson L-G, Oudkerk M, Pajak A, Sans S, de Ridder M, Dufouil C, Fuhrer R, Giampaoli S, Launer LJ, Hofman A, for the CC (2004) The Association Between Blood Pressure, Hypertension, and Cerebral White Matter Lesions: Cardiovascular Determinants of Dementia Study. Hypertension 44:625-630.

Vlkolinský R, Cairns N, Fountoulakis M, Lubec G (2001) Decreased brain levels of 2',3'-cyclic nucleotide-3'-phosphodiesterase in Down syndrome and Alzheimer's disease. Neurobiology of Aging 22:547-553.

Vogel US, Thompson RJ (1988) Molecular Structure, Localization, and Possible Functions of the Myelin-Associated Enzyme 2′,3′-Cyclic Nucleotide 3′-Phosphodiesterase. Journal of Neurochemistry 50:1667-1677.

Von Bernhardi R, Tichauer JE, Eugenín J (2010) Aging-dependent changes of microglial cells and their relevance for neurodegenerative disorders. Journal of Neurochemistry 112:1099-1114.

Wakita H, Tomimoto H, Akiguchi I, Kimura J (1994) Glial activation and white matter changes in the rat brain induced by chronic cerebral hypoperfusion: an immunohistochemical study. Acta Neuropathologica 87:484-492.

Wakita H, Tomimoto H, Akiguchi I, Matsuo A, Lin J-X, Ihara M, McGeer P-L (2002) Axonal damage and demyelination in the white matter after chronic cerebral hypoperfusion in the rat. Brain Research 924:63-70.

Walsh DM, Klyubin I, Fadeeva JV, Cullen WK, Anwyl R, Wolfe MS, Rowan MJ, Selkoe DJ (2002) Naturally secreted oligomers of amyloid [beta] protein potently inhibit hippocampal long-term potentiation in vivo. Nature 416:535-539.

Weidensteiner C, Metzger F, Bohrmann ABB, Kuennecke B, von Kienlin M (2009) Cortical hypoperfusion in the B6.PS2APP mouse model for Alzheimer's disease: Comprehensive phenotyping of vascular and tissular parameters by MRI. Magnetic Resonance in Medicine 62:35-45.

Weller R, Preston S, Subash M, Carare R (2009) Cerebral amyloid angiopathy in the aetiology and immunotherapy of Alzheimer disease. Alzheimer's Research & Therapy 1:6.

Wellons JC, Sheng H, Laskowitz DT, Burkhard Mackensen G, Pearlstein RD, Warner DS (2000) A comparison of strain-related susceptibility in two murine recovery models of global cerebral ischemia. Brain Research 868:14-21.

Winton MJ, Lee EB, Sun E, Wong MM, Leight S, Zhang B, Trojanowski JQ, Lee VMY (2011) Intraneuronal APP, Not Free AÎ² Peptides in 3xTg-AD Mice: Implications for Tau versus AÎ²-Mediated Alzheimer Neurodegeneration. The Journal of Neuroscience 31:7691-7699.

Wirths O, Weis J, Szczygielski J, Multhaup G, Bayer T (2006) Axonopathy in an APP/PS1 transgenic mouse model of Alzheimer's disease. Acta Neuropathologica 111:312-319.

Wirths O, Weis J, Kayed R, Saido TC, Bayer TA (2007) Age-dependent axonal degeneration in an Alzheimer mouse model. Neurobiology of Aging 28:1689-1699.

Wisco JJ, Killiany RJ, Guttmann CRG, Warfield SK, Moss MB, Rosene DL (2008) An MRI study of age-related white and gray matter volume changes in the rhesus monkey. Neurobiology of Aging 29:1563-1575.

Witztum JL (1989) Current approaches to drug therapy for the hypercholesterolemic patient. Circulation 80:1101-1114.

Wu EX, Tang H, Asai T, Yan SD (2004) Regional cerebral blood volume reduction in transgenic mutant APP (V717F, K670N/M671L) mice. Neuroscience Letters 365:223-227.

Wu Z, Guo H, Chow N, Sallstrom J, Bell RD, Deane R, Brooks AI, Kanagala S, Rubio A, Sagare A, Liu D, Li F, Armstrong D, Gasiewicz T, Zidovetzki R, Song X, Hofman F, Zlokovic BV (2005) Role of the MEOX2 homeobox gene in neurovascular dysfunction in Alzheimer disease. Nat Med 11:959-965.

Xia W, Zhang J, Kholodenko D, Citron M, Podlisny MB, Teplow DB, Haass C, Seubert P, Koo EH, Selkoe DJ (1997) Enhanced Production and Oligomerization of the 42-residue Amyloid Î²-Protein by Chinese Hamster Ovary Cells Stably Expressing Mutant Presenilins. Journal of Biological Chemistry 272:7977-7982.

Xu J, Chen S, Ahmed SH, Chen H, Ku G, Goldberg MP, Hsu CY (2001) Amyloid-{beta} Peptides Are Cytotoxic to Oligodendrocytes. J Neurosci 21:118RC-.

Yamada M, Ihara M, Okamoto Y, Maki T, Washida K, Kitamura A, Hase Y, Ito H, Takao K, Miyakawa T, Kalaria RN, Tomimoto H, Takahashi R (2011) The Influence of Chronic Cerebral Hypoperfusion on Cognitive Function and Amyloid Î² Metabolism in APP Overexpressing Mice. PLoS ONE 6:e16567.

Yang G, Kitagawa K, Matsushita K, Mabuchi T, Yagita Y, Yanagihara T, Matsumoto M (1997) C57BL/6 strain is most susceptible to cerebral ischemia following bilateral common carotid occlusion among seven mouse strains: selective neuronal death in the murine transient forebrain ischemia. Brain Research 752:209-218.

Yang S, Li C, Lu W, Zhang W, Wang W, Tang Y (2009) The myelinated fiber changes in the white matter of aged female Long-Evans rats. Journal of Neuroscience Research 87:1582-1590.

Yoshiura T, Hiwatashi A, Noguchi T, Yamashita K, Ohyagi Y, Monji A, Nagao E, Kamano H, Togao O, Honda H (2009) Arterial spin labelling at 3-T MR imaging for detection of individuals with Alzheimer's disease. European Radiology 19:2819-2825.

Zhang F, Eckman C, Younkin S, Hsiao KK, Iadecola C (1997) Increased Susceptibility to Ischemic Brain Damage in Transgenic Mice Overexpressing the Amyloid Precursor Protein. J Neurosci 17:7655-7661.

Appendix 1: dMBP immunostaining

Degraded myelin was assessed using anti-dMBP antibody. Anti-dMBP antibody positively immunostains degraded myelin (Ihara et al., 2010). The grading scale was as follows; no degraded myelin present (grade 0), minimal degraded myelin (grade 1), moderate areas of degraded myelin grade (2) and extensive areas of degraded myelin (grade 3). Sections were examined and graded by Dr Karen Horsburgh. Data were analysed by the author.

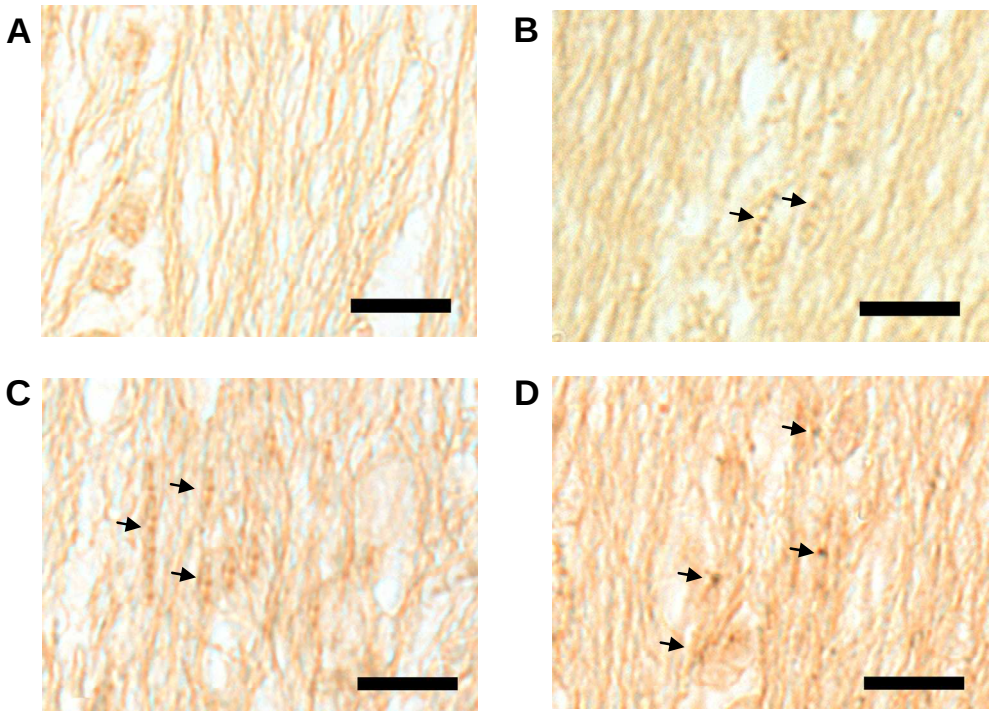

Figure A1 dMBP immunostaining grading scale

Individual brain regions were scored as (A) no degraded myelin present (grade 0), (B) minimal degraded myelin (grade 1); arrows identify small punctuate accumulations of dMBP, (C) moderate areas of degraded myelin (grade 2); arrows identify myelinated fibres positively stained for dMBP, (D) extensive areas of degraded myelin (grade 3); arrows identify larger fibres densely stained for dMBP. Images taken from the internal capsule. Scale bar = 12.5μm.

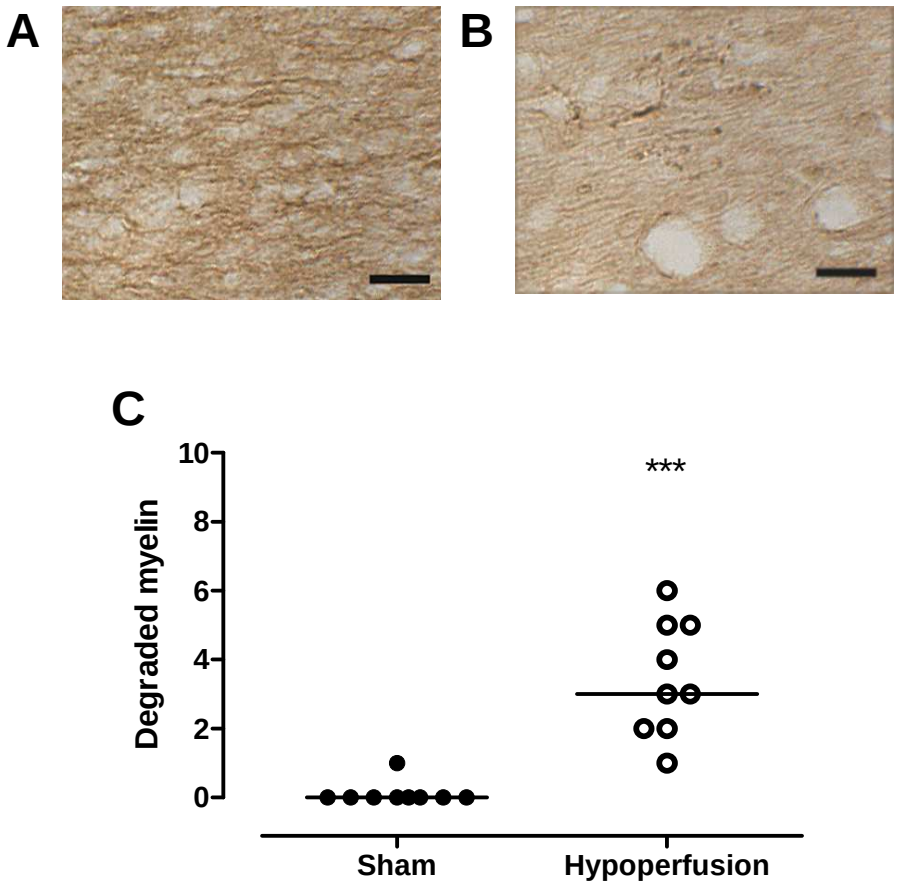

Figure A1.2 Assessment of dMBP immunostaining

The probability of myelin damage occurring following hypoperfusion was increased ($p < 0.001$; A,B,C) Fisher's exact test. n=9 sham/ n=9 hypoperfused There was a significant increase in levels of degraded myelin in hypoperfused mice as compared to shams (Fig. A2C; $p < 0.001$, median values- sham= hyopperfused= 3) Mann Whitney-U test.

Appendix 2: Analysis of behavioural tasks including animals with ischaemic neuronal damage

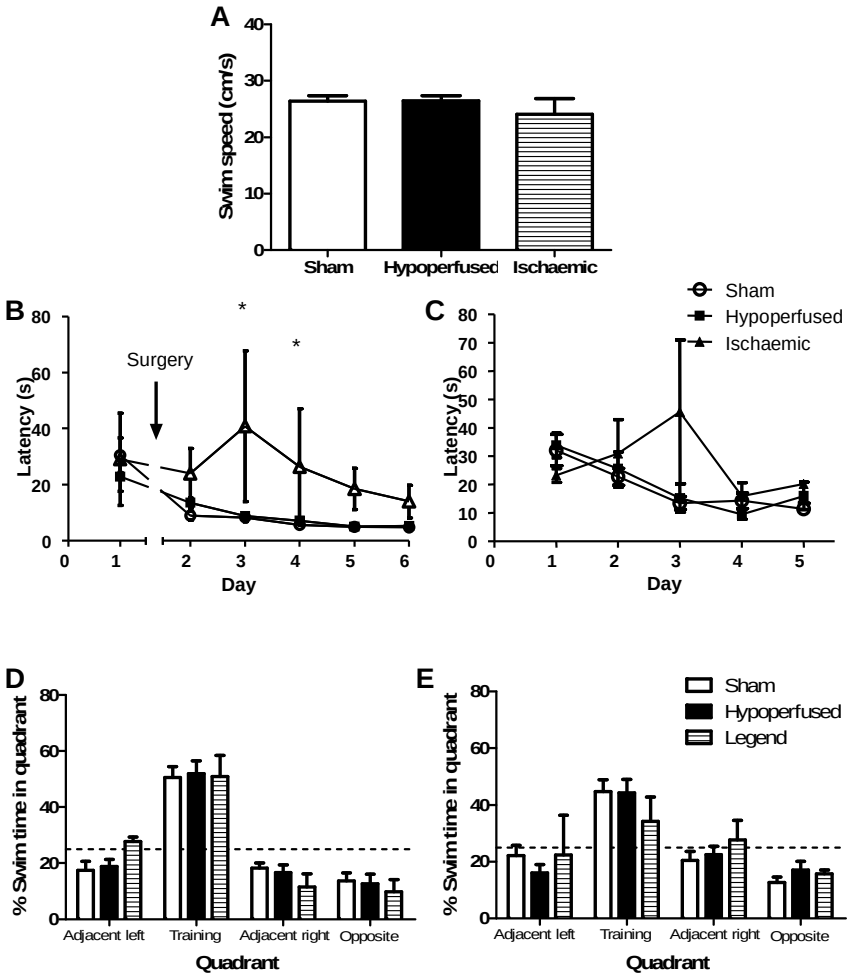

Figure A2.1 Spatial referencece memory testing in the water maze

Data are expressed ± SEM. Sham n = 9; hypoperfused n = 9; ischaemic n=2 (A) Swim speeds did not differ between the groups (p = 0.576 mean values- sham= 26.41 ± 0.97cm/s, hypoperfused= *26.44 ± 0.93cm/s, ischaemic*=24.09 ± 2.75cm/s*); one-way ANOVA. (B) Performance of groups on the cued task improved significantly over training days (p < 0.001). Hypoperfused animals performed as well as shams whilst ischaemic animals performed significantly worse than shams (p = 0.005); two-way ANOVA with Bonferroni post test. (C) Spatial reference learning was unaffected by hypoperfusion (p = 0.254), the performance of all groups improved significantly across days (p < 0.001); two-way ANOVA. All groups performed equally well during probe tests conducted at (D) 10 mins. (p = 0.459) and (E) 24 hours (p = 0.526) following spatial reference learning; two-way ANOVA. In both probe tests all animals spent significantly more time in the training quadrant compared to chance (dashed line); 10 mins. (p < 0.001); 24 hours (p < 0.001); two-way ANOVA.*

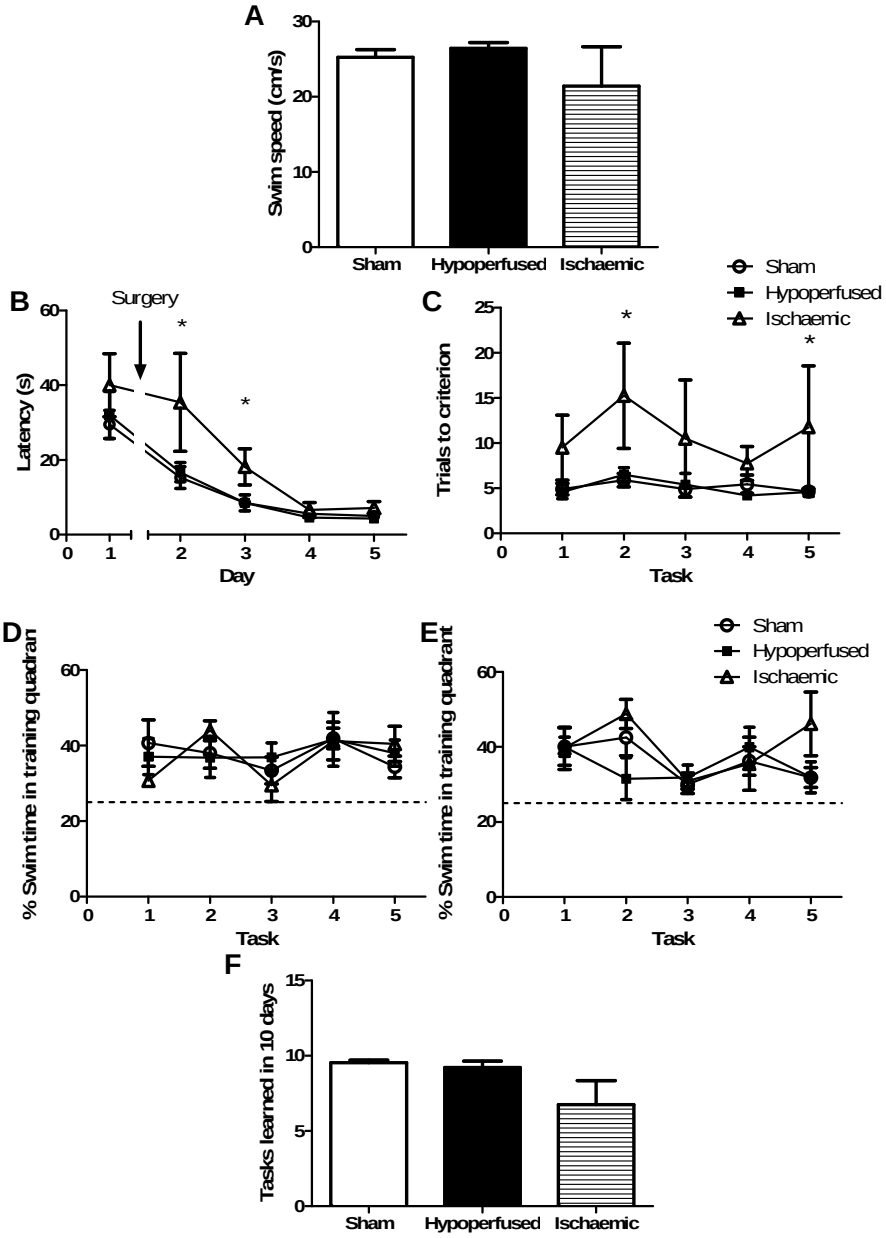

Figure A2.2 Serial spatial reference memory testing in the water maze

Data are expressed ± SEM. Sham n=11; Hypoperfused n=10, Ischaemic n=4 (A) Swim speeds did not differ between groups (p = 0.227 mean values- sham= 25.25 ± 1.04cm/s, hypoperfused= 26.44 ± 0.76cm/s, ischaemic= 21.43 ± 5.24cm/s one-way ANOVA. (B) All groups improved significantly on the cued task over training days (p<0.001). Animals with ischaemic damage performed significantly worse on the cued version of the watermaze task as compared to sham and hypoperfused animals (p=0.037) two-way Anova with Bonferroni's post test. (C) Animals with ischaemic neuronal damage showed impaired serial spatial reference learning (p=0.031), animals with ischaemic damage took significantly more trials to learn platform locations across tasks (p=0.003). All animals performed equally well during probe tests conducted at (D) 10 mins. (p=0.973) and (E) 24 hours (p=0.386) following spatial reference learning; two-way ANOVA. In both probe tests all animals spent significantly more time in the training quadrant compared to chance (dashed line). (F) Ischaemic animals learned significantly fewer platform locations as compared to sham and hypoperfused animals across the first 10 days (p=0.013) mean values- sham= 9.55 ± 0.16 tasks, hypoperfused= 9.22 ± 0.43 tasks, ischaemic=6.75 ± 1.60); one-way ANOVA with Tukeys multiple comparison..

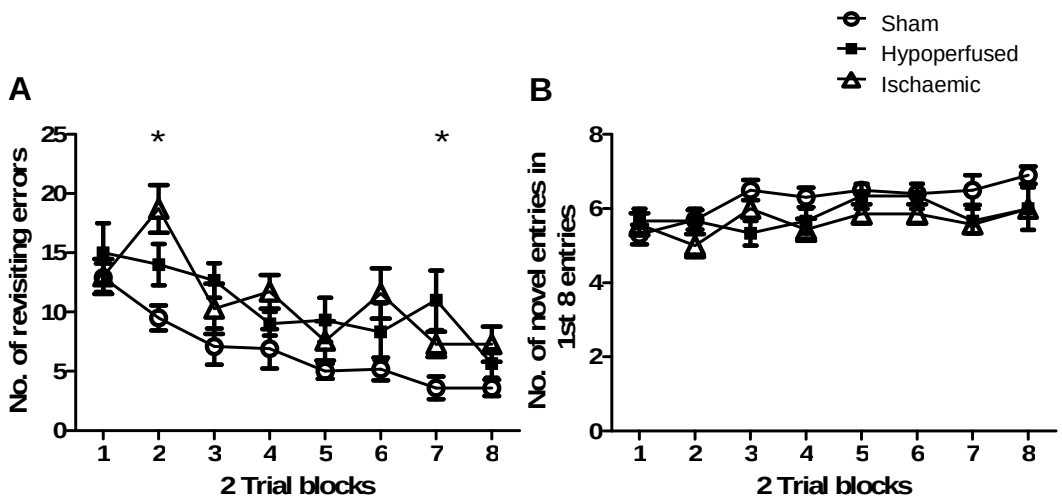

Figure A2.3 Spatial working memory testing in the 8-arm radial arm maze

Data are expressed ± SEM. Sham n=10; Hypoperfused n=3, Ischaemic n=7 (A) all animals made significantly fewer revisiting errors across trials ($p<0.0001$). Both ischaemic and hypoperfused animals made significantly more revisiting errors as compared to shams ($p=0.001$); two-way ANOVA with Bonferroni's post test. (B) All animals made significantly more novel arm entries in the first 8 entries as training progressed ($p=0.019$), ischaemic animals made significantly fewer novel arm entries made in the first eight entries as compared to sham and hypoperfused animals animals ($p=0.036$); two-way ANOVA.

Appendix 3: Cortical intracellular APP levels in 3xTg-AD mice following hypoperfusion

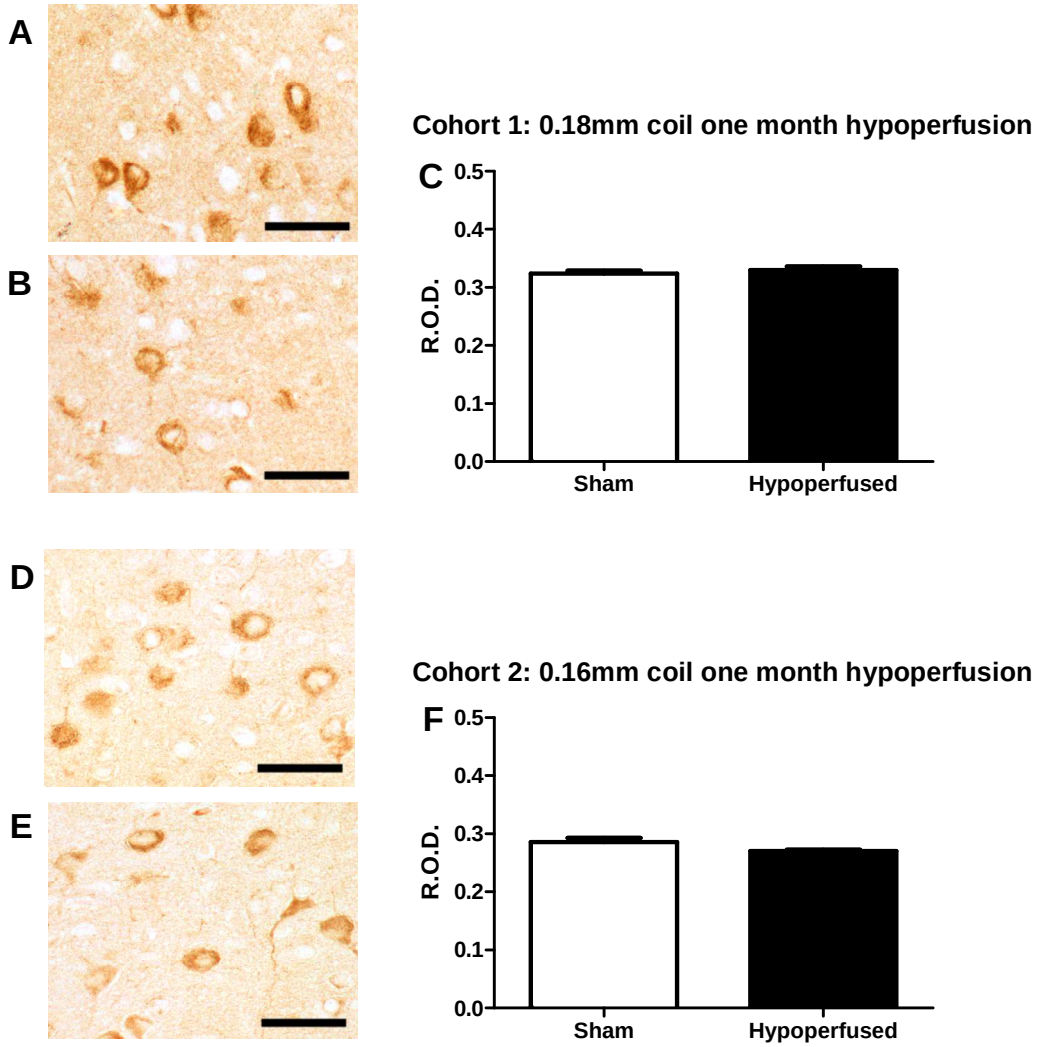

Figure A3 Image analysis of intracellular APP expression in cortical neurons
Data are expressed as mean R.O.D. ± SEM. Cohort 1, n=12 sham/ n=12 hypoperfused; cohort 2, n=7 sham and 8 hypoperfused. Image analysis of intracellular APP levels in layer IV/ V cortical, pyramidal neurons yielded results similar to those obtained from analysis of intracellular hippocampal APP expression. Intracellular APP levels did not differ between sham (A, D) and experimental animals (B, E) from either group examined; cohort 1 (0.18mm coil; p=0.399, mean values- sham= 0.32 ± 0.01 hypoperfused= 0.33 ± 0.01 C); cohort 2 (0.16mm coil; p=0.053, mean values- sham= 0.29 ± 0.01 hypoperfused= 0.27 ± 0.01 F). Student's two-tailed t-test. Scale bar = 50μm

Appendix 4: Cortical intracellular Aβ levels in 3xTg-AD mice following hypoperfusion

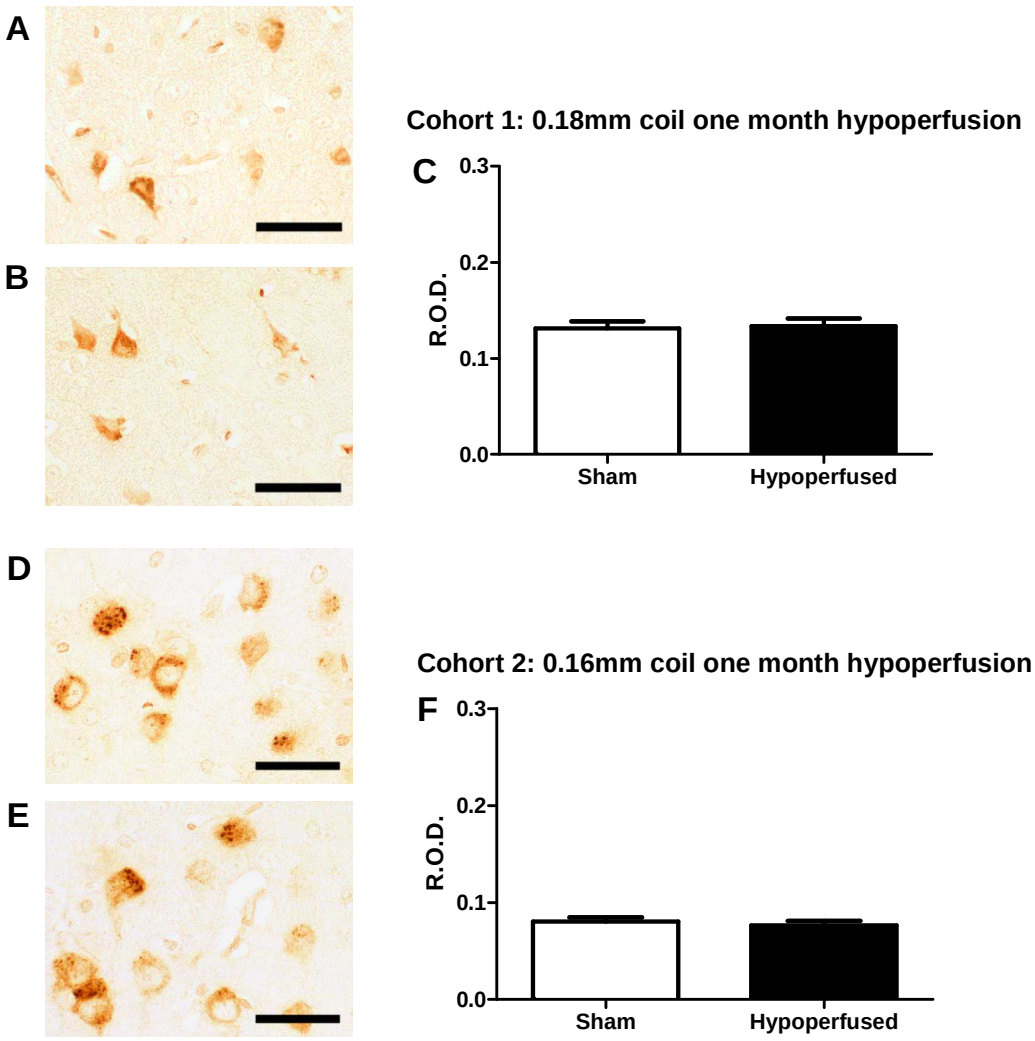

Figure A4 Image analysis of intracellular Aβ expression in cortical neurons
Data are expressed as mean R.O.D. ± SEM. Cohort 1, n=12 sham/ n=12 hypoperfused; cohort 2, n=7 sham and 8 hypoperfused. Image analysis of intracellular Aβ levels in layer IV/ V cortical, pyramidal neurons yielded results similar to those obtained from analysis of intracellular hippocampal Aβ expression. Intracellular Aβ levels did not differ between sham (A, D) and experimental animals (B, E) from either cohort examined; cohort 1 (0.18mm coil; p=0.822, mean values- sham= 0.13 ± 0.01 hypoperfused= 0.13 ± 0.01 C); cohort 2 (0.16mm coil; p=0.536, mean values- sham= 0.08 ± 0.01 hypoperfused= 0.07 ± 0.01 F). Student's two-tailed t-test. Scale bar = 50μm

Appendix 5: C99/C83 c-terminal fragment ratios in 3xTg-AD mice following hypoperfusion

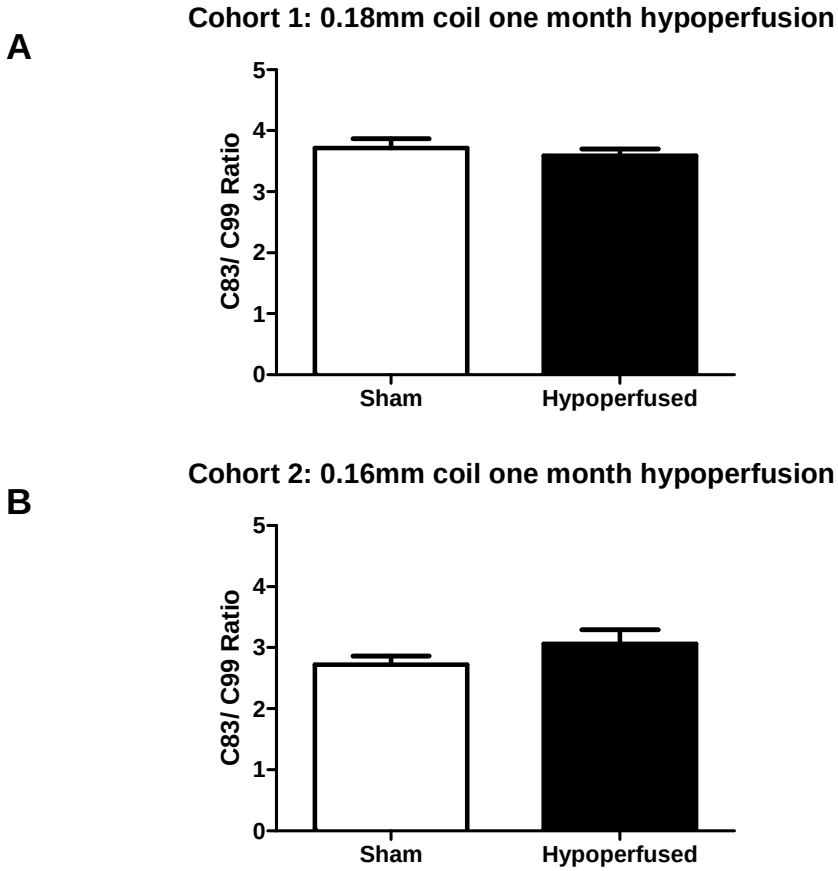

Figure A5 Comparison of the C83/ C99 fragment ratio between sham and hypoperfused mice

Data are expressed as mean C83/ C99 Ratio ± SEM. Cohort 1, n=12 sham/ n=12 hypoperfused; cohort 2, n=7 sham and 8 hypoperfused. There was no change in the C83/ C99 fragment ratio between sham and hypoperfused animals in either of the cohorts tested; cohort 1 (0.18mm coil; p=0.526, mean values- sham= 3.71 ± 0.15 hypoperfused= 3.59 ± 0.11 A), cohort 2 (0.16mm coil; p=0.243, mean values- sham= 2.72 ±0.14 hypoperfused= 3.06 ±0.23 B). Student's two tailed t-test.

Appendix 6: White matter protein levels in aged 3xTg-AD mice following hypoperfusion

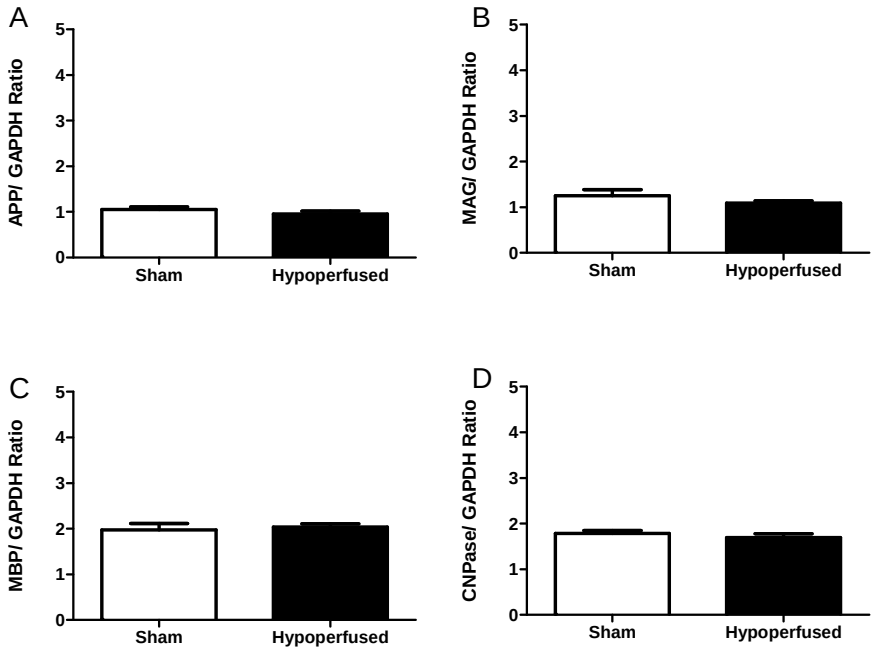

Figure A6 White matter protein levels in aged 3xTg-AD mice following hypoperfusion

There was no change in levels of any white matter proteins examined between aged sham and hypoperfused animals; APP (p=0.320, mean values- sham= 1.05 ± 0.06 hypoperfused= 0.96 ± 0.05 A4 A), MAG (p=0.0.194, mean values- sham= 1.25 ± 0.13 hypoperfused= 1.09 ± 0.05 A4 B); MBP (p=0.0.656, mean values- sham= 1.98 ± 0.14 hypoperfused= 2.04 ± 0.07 A4 C); CNPase (p=0.502, mean values- sham= 1.79 ± 0.07 hypoperfused= 1.69 ± 0.09 A4 D).

Appendix 7: Publications

Papers

Coltman R, Spain A, Tsenkina Y, Fowler JH, Smith J, Scullion G, Allerhand M, Scott F, Kalaria RN, Ihara M, Daumas S, Deary IJ, Wood E, McCulloch J, Horsburgh K (2010) Selective white matter pathology induces a specific impairment in spatial working memory. Neurobiology of Aging. In Press, Corrected Proof.

Holland, P. R., Bastin, M. E., Jansen, M. A., Merrifield, G. D., Coltman, R., Scott, F., Nowers, H., Khallout, K., Marshall, I., Wardlaw, J. M., Deary, I. J., McCulloch, J., Horsburgh, K. (2010). MRI is a sensitive marker of subtle white matter pathology in hypoperfused mice. Neurobiology of Aging. In Press, Corrected Proof.

Abstracts

Coltman R, Spain A, Tsenkina Y, Smith J, Fowler JH, Ihara M, Kalaria RN, Daumas S, Kelly P, Deary IJ, Wood E, McCulloch J, Horsburgh K. (2009). Chronic cerebral hypoperfusion causes myelin damage and is associated with a selective impairment in working memory. *International Conference on Alzheimer's Disease.* Vienna, Austria, July

Coltman, R., Kalaria, R., Ihara, M., Deary, I.J., McCulloch, J., Fowler, J., Horsburgh, K. (2009) Varying severities of chronic hypoperfusion on the development of Alzheimer's disease pathology *Research into Ageing Grantholders' Conference*. Birmingham, UK, September

Coltman, R., Spain, A., Fowler, J., Ihara, M., Kalaria, R., Daumas, S., Wood, E., Kelly, P., Deary, I. J., McCulloch, J., Horsburgh, K. (2008). White matter integrity is compromised in response to chronic cerebral hypoperfusion and may impact on cognition in ageing. *Research into Ageing Grantholders' Conference*. Birmingham, UK, September

Horsburgh, K., Bastin, M. E., Jansen, M. A., Merrifield, G. D., Coltman, R. B., Spain, A., Tsenkina, Y., Scullion, G., Scott, F., Marshall, I., Wardlaw, J., Wood, E., Deary, I. J., McCulloch, J., Holland, P. R. (2010). In vivo evaluation of diffusion tensor and magnetization transfer imaging in a mouse model of selective white matter pathology. *Society for Neuroscience. San Diego, USA. November*.

Scullion, G., Fowler, J. H., Karali, K., Coltman, R., Green, G., Smith, C., Horsburgh, K. (2010). Increased accumulation of amyloid in white matter in Alzheimer's disease brains and transgenic models. *13th International Conference on Alzheimer's Disease and related diseases.* Honolulu, USA, July.

Scullion, G., Coltman, R., Fowler, J. H., Horsburgh, K. (2010). The influence of chronic cerebral hypoperfusion on Alzheimer's disease-like pathology in 3xTg mice. *13th International Conference on Alzheimer's Disease and related diseases.* Honolulu, USA, July.

Holland, P. R., Bastin, M. E., Coltman, R., Khallout, K., Scott, F., Dingwall, T., Jansen, M. A., Merrifield, G. D., Marshall, I., McCulloch, J., Horsburgh, K. (2009). Imaging White Matter Pathology in a Mouse Model of Chronic Cerebral Hypoperfusion. *Research into Ageing Grantholders' Conference*. Birmingham, UK, September.